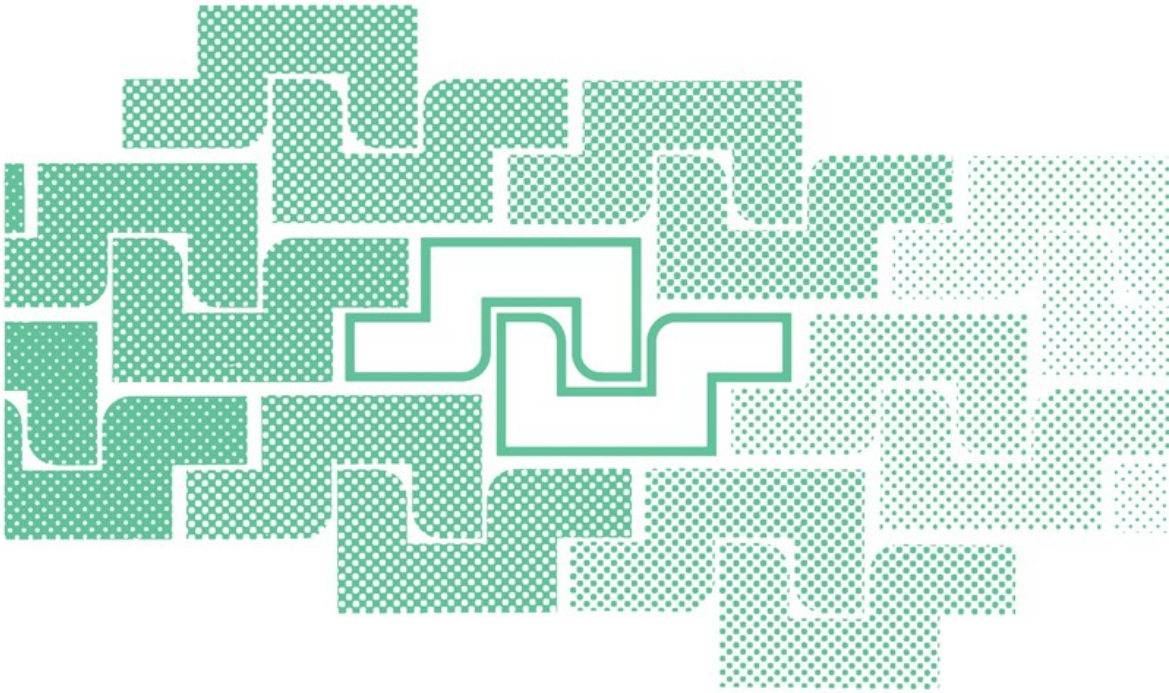

Riverbank Filtration Hydrology

Impacts on System Capacity and Water Quality

Edited by

Stephen A. Hubbs

NATO Science Series

IV. Earth and Environmental Sciences – Vol. 60

Riverbank Filtration Hydrology

NATO Science Series

A Series presenting the results of scientific meetings supported under the NATO Science Programme.

The Series is published by IOS Press, Amsterdam, and Springer (formerly Kluwer Academic Publishers) in conjunction with the NATO Public Diplomacy Division.

Sub-Series

I. Life and Behavioural Sciences	IOS Press
II. Mathematics, Physics and Chemistry	Springer (formerly Kluwer Academic Publishers)
III. Computer and Systems Science	IOS Press
IV. Earth and Environmental Sciences	Springer (formerly Kluwer Academic Publishers)

The NATO Science Series continues the series of books published formerly as the NATO ASI Series.

The NATO Science Programme offers support for collaboration in civil science between scientists of countries of the Euro-Atlantic Partnership Council. The types of scientific meeting generally supported are "Advanced Study Institutes" and "Advanced Research Workshops", and the NATO Science Series collects together the results of these meetings. The meetings are co-organized by scientists from NATO countries and scientists from NATO's Partner countries — countries of the CIS and Central and Eastern Europe.

Advanced Study Institutes are high-level tutorial courses offering in-depth study of latest advances in a field.
Advanced Research Workshops are expert meetings aimed at critical assessment of a field, and identification of directions for future action.

As a consequence of the restructuring of the NATO Science Programme in 1999, the NATO Science Series was re-organized to the four sub-series noted above. Please consult the following web sites for information on previous volumes published in the Series.

http://www.nato.int/science
http://www.springeronline.com
http://www.iospress.nl

Series IV: Earth and Environmental Sciences – Vol. 60

Riverbank Filtration Hydrology

edited by

Stephen A. Hubbs
WaterAdvice Associates,
Louisville, KY, U.S.A.

Published in cooperation with NATO Public Diplomacy Division

Proceedings of the NATO Advanced Research Workshop on
Riverbank Filtration Hydrology
Bratislava, Slovakia
September 2004

A C.I.P. Catalogue record for this book is available from the Library of Congress.

ISBN-10 1-4020-3937-9 (PB)
ISBN-13 978-1-4020-3937-9 (PB)
ISBN-10 1-4020-3936-0 (HB)
ISBN-13 978-1-4020-3936-2 (HB)
ISBN-10 1-4020-3938-7 (e-book)
ISBN-13 978-1-4020-3938-6 (e-book)

Published by Springer,
P.O. Box 17, 3300 AA Dordrecht, The Netherlands.

www.springer.com

Printed on acid-free paper

Printed in the Netherlands.

Dedication

This book is dedicated to our meeting hosts in Bratislava, Slovak Republic, who provided warm hospitality and excellent facilities for this workshop.

Contents

Contributing Authors

Ľubomír Banský, GROUND WATER Consulting, Ltd. Kolískova 1, 84105 Bratislava 4, Slovak Republic, SK

Tiffany Caldwell, University of Louisville, Louisville Kentucky USA

Jim Constantz, USGS, Menlo Park, California USA

Peter Engesgaard Geological Institute, University of Copenhagen, Denmark

T. Grischek, Institute for Water Sciences, University of Applied Sciences Dresden, 01069 Dresden, F.-List-Platz 1, Germany

Christine Hatch, University of California, Santa Cruz, CA 95064

Paulo Herrera., Department of Earth and Ocean Sciences, The University of British Columbia, Canada

Zoltán Hlavatý, GROUND WATER Consulting, Ltd. Kolískova 1, 84105 Bratislava 4, Slovak Republic, SK

Stephen A. Hubbs, WaterAdvice Associates PLLC, 3715 Hughes Road Louisville, KY USA

W. Macheleidt, Institute for Water Sciences, University of Applied Sciences Dresden, 01069 Dresden, F.-List-Platz 1, Germany

Jordi Martín-Alonso, Barcelona's Water Company (Agbar), Barcelona, Spain

Igor Mucha, GROUND WATER Consulting, Ltd. Kolískova 1, 84105 Bratislava 4, Slovak Republic, SK

W. Nestler, Institute for Water Sciences, University of Applied Sciences Dresden, 01069 Dresden, F.-List-Platz 1, Germany

Henning Prommer, Utrecht University, The Netherlands

Chittaranjan Ray, University of Hawaii at Manoa, Honolulu, Hawaii, USA

Dalibor Rodák, GROUND WATER Consulting, Ltd. Kolískova 1, 84105 Bratislava 4, Slovak Republic, SK

Dave C. Schafer, David Schafer & Associates White Pine Road, North Oaks, Minnesota 55127, USA

Jürgen Schubert, Dürener Str. 38, Düsseldorf, Germany

Dorte Seifert, Environment & Resources DTU, Technical University of Denmark

Grace W. Su, Lawrence Berkeley National Laboratory, Berkeley, CA 94720

Bernhardt Wett, Institute of Environmental Engineering, University of Innsbruck, Austria

Acknowledgements

The book is a compilation of contributions from an Advanced Research Workshop on Riverbank Filtration Hydrology, held in Bratislava, Slovakia in September, 2004. The contributions were reviewed by workshop participants, which strengthened the scientific content of the compilation as a whole. The efforts of the authors and reviewers are greatly appreciated. Appreciation is also expressed to Jen Lair, who assisted in the editing of this book.

The workshop and the compilation of this book was funded by the Public Diplomacy Division NATO's Collaborative Programs Section. The participants benefited not only from the scientific exchange, but also from the opportunity to establish friendships across cultural barriers.

Preface

The workshop from which this book is taken was held to share knowledge from the US and Europe on the science of riverbank filtration hydrology. Participants at the workshop represented all known elements of science that impact the hydrology of riverbank filtration: surface water hydrology, particle filtration, biological processes, and geochemical processes.

Those unfamiliar with the science of Riverbank Filtration might want to start with Chapter Fourteen, which includes some of the basic concepts of riverbank filtration hydrology. This chapter was written with the RBF novice in mind. It also includes extensive site data from RBF facilities in Europe and the US.

The first four chapters cover the basic hydrology of riverbank filtration, with a focus on those factors impacting system capacity and water quality through the clogging processes. Chapters Five and Six evaluate the impacts of biological and geochemical processes, and their impacts on flow and water quality. Chapters Seven and Eight provide examples of how modelling is used to predict yield and water quality in RBF facilities.

Chapters Nine through Thirteen document case studies from RBF facilities in Europe and the US. Chapter Six also contains extensive data on the many RBF sites located in the Netherlands. These chapters provide valuable practical experience from managers and scientists of RBF facilities across Europe and the US which should be helpful to those considering RBF as a water supply.

Chapter Fourteen was written after the workshop, and provides a listing of key measures developed during the workshop to be considered when designing RBF facilities. This chapter was written to provide a compilation of data from successful RBF sites to gain better insight into future sites being considered for RBF facilities. Data from many Riverbank Filtration sites are provided for these key measures.

Discussion from this workshop indicated that further research is needed into the impact of gas bubble formation on the flow through riverbeds, and through porous media in general. Several of the workshop participants had observed the formation of gas in laboratory settings, and outgassing has been observed in at least two field sites. This is an area warranting further work.

SIGNIFICANCE OF HYDROLOGIC ASPECTS ON RBF PERFORMANCE

Everything is linked to everything else

Jürgen Schubert
Dürener Str. 38, Düsseldorf, Germany

Abstract: Clogging of the riverbed is still an important factor causing uncertainness in the planning stage of riverbank filtration plants. Several attempts have been made to develop tools, which are suitable to predict this process. But up till now, these tools are only a slight help for the engineering of riverbank filtration plants. On the other hand there exists a lot of experience about clogging from the operation of riverbank filtration plants. But to utilize this experience for a new plant, the hydrological and morphological aspects of the river and the aquifer have to be analyzed carefully to create a basis for the transfer of available knowledge. This paper deals with the relevant properties of rivers, concerning riverbank filtration: the runoff regime and the runoff dynamics, the river-aquifer interactions, the stream processes – erosion, transport and deposition – and the progress of the clogging process itself.

Key words: Characteristics of rivers concerning RBF: runoff regime and runoff dynamics, river morphology, erosion, bed load transport, deposition, structure of the riverbed, river-aquifer interaction, the clogging process.

1. INTRODUCTION

Clogging is caused by the continual percolation of water, which contains suspended matter. This process will appear in impounded basins, artificial groundwater recharge and riverbank filtration (RBF). Clogging in impounded basins is sometimes a desired process to reduce water losses. The upper layer in basins for artificial groundwater recharge is removed and cleaned at regular intervals. A first lesson to be learned from artificial

Stephen A. Hubbs (ed.), Riverbank Filtration Hydrology, 1–20.

groundwater recharge is that the so-called “Schmutzdecke” is essential for the purification of the percolated water.

Mechanical clogging of parts of the riverbed during long-term operation of RBF wells is principally unavoidable. The main task during the planning of RBF plants is to choose a suitable site for the plant near the river and to determine the type and the site arrangement of the wells.

The planning process of a groundwater plant is opened with a careful and very detailed site catchment area analysis, based on the geologic situation, the properties of the aquifer, the regional hydrology and the existing as well as possible future risks for contamination. The results of this investigation are used to determine type, size and location of the wells, to estimate long-term quantity and quality of the abstracted ground water and to check the necessity of protective measures for sustainable groundwater quality.

The step from planning groundwater plants to riverbank filtration (RBF) plants involves a significant expansion of the total catchment area, usually including the whole upstream drainage basin of the river and in detail the regions of the river upstream and downstream the location of the wells. Of particular importance for sustainable yield of the RBF wells is the unavoidable clogging process in the infiltration area. The decrease of the hydraulic conductivity of the riverbed by clogging will emerge in several steps and finally be balanced out between the position and shape of the cone of depression of the wells and the self-cleaning power of the river.

Based on a detailed site catchment area analysis, completed by pumping tests, all tools are available to predict the long-term behavior of groundwater wells very precisely. This is quite different with RBF wells due to the difficult assessment of the clogging process. Several attempts have been made to overcome this problem by theoretical and experimental means (Riesen, 1975). But the clogging process as a result of the dynamic river-aquifer interaction is rather complex and, up till now, this process cannot be calculated in advance employing some formula.

RBF is employed since more than 130 years along European rivers and a lot of experience on RBF well arrangement and operation is available (Hunt et al., 2002). This experience may be linked to relevant characteristics of the river to utilize it as a tool not only for the estimation of the clogging process but also for the optimal arrangement of RBF wells. This chapter will focus the attention on river characteristics and the mechanical clogging process.

1.1 Safe Drinking Water – A Reason to Utilize RBF

The legal definition of drinking water quality is a negative definition worldwide: Threshold limit values are limits for substances and microorganisms found in water. Values based on toxicological data have

been derived to safeguard health on the basis of lifelong consumption. When looking at carcinogenesis and mutagenesis as non-threshold phenomena, other principles are applied in addition: Threshold limit values defined by precautionary aspects for preventing adverse affects of a general nature. Threshold limit values for aesthetic parameters are provided to prevent unpleasant changes, such as in taste, color and odor. Any water, which complies with these threshold limit values, can be classified and supplied as drinking water (WHO, 2004).

But the definition of a high quality drinking water is a quite different matter. The hydrologic cycle is an approved method of nature to provide high quality drinking water. A positive definition of a high quality drinking water is therefore based on pure groundwater without any contamination with reference to the hydrologic cycle. Such a definition can be found for example in DIN 2000, a Technical Standard in Germany (DIN 2000, 2000).

The preference of groundwater for water supply or, if not available, of a natural (riverbank filtration) or artificial (infiltration, groundwater recharge) subsoil passage of river water is a result of the conclusions drawn from the early outbreak of epidemic cholera in Hamburg, Germany (1892), caused by drinking water drawn from the Elbe River. This preference is now reflected in the concept of the DIN 2000.

To focus the attention on water quality aspects, it is expedient to vary the virtual point of raw water extraction. There are two important purification steps in the hydrologic cycle of nature. One step is evaporation, which separates H_2O from natural substances, chiefly salts, and all impurities. This step needs too much energy to be employed in urban water supply and this step creates totally demineralized water, which is not convenient for water supply. A second more interesting purification step is infiltration and subsoil passage of water. This step incorporates the physicochemical and biological processes to treat water and to balance out the physical (e.g. temperature), chemical (e.g. carbonate balance), and biological (e.g. low assimilable organic carbon concentration (AOC)) properties of the water.

The most advantageous water supply is to extract raw water after infiltration and subsoil passage from suitable aquifers (groundwater) regarding water quality aspects. The next most advantageous water supply is riverbank filtered water and replenished groundwater. Both types of raw water utilize the benefits of the powerful natural purification step:

- Removal of particles and turbidity
- Removal of bacteria, viruses, parasites
- Biodegradation of micro-pollutants, NOM, THM-precursors
- Reduction of mutagenic activity
- Smoothing out variations in temperature and concentration
- Compensation for peaks and shock loads.

The quality of surface water depends on several influences, e.g. contamination by sewage water, by fertilizers and pesticides from agriculture, by industrial chemicals in the case of accidents, from traffic on the surface water, etc. Usually the source water quality decreases from lakes over reservoirs to rivers. While surface water from lakes and reservoirs may be extracted by direct intake with only low risks, the direct intake from river water is always accompanied with higher risks (e.g. parasites, micro-pollutants) regarding the aim to produce safe drinking water. Therefore the potential of the natural purification steps of infiltration and subsoil passage should be utilized where possible.

2. CHARACTERISTICS OF THE RIVER

2.1 The Runoff Regime

The aerial extent, structural diversity, and altitudes in the headwater regions of the drainage basin associated with the regional and seasonal distribution of precipitation create the runoff regime of natural rivers. The runoff regime is characterized by amount, frequency, length, time and rate of change of runoff conditions. Runoff dynamics and runoff volumes are important factors when looking at the river and channel morphology, the transport of solids, the modification of the riverbed and the interactions with the groundwater (Leibundgut and Hildebrand, 1999).

Human impact on streams – e.g. for flood control, hydropower generation and improved navigation – changes the natural runoff regime. Dams dramatically alter the flow characteristics of rivers; particularly, the transport and deposition of solids, the erosion of the riverbed, and the interactions with the groundwater may be severely affected by dams.

The runoff regime of a river may initially be characterized by the average monthly discharge, developed from daily data over several decades. Figure 1, as an example, shows the result for the Rhine River at Lobith (near the German/Netherlands border) and Basel (near the Switzerland/German border), the Aare River (one of the headwaters) and the Mosel River (one of the tributaries). Compared to other European rivers, the Rhine River with a drainage basin of approximately 224.000 km^2 and a total length of 1320 km is not among the largest rivers. But the Rhine River is one of the most important European rivers and one of the busiest waterways due to its abundance of water and balanced runoff regime.

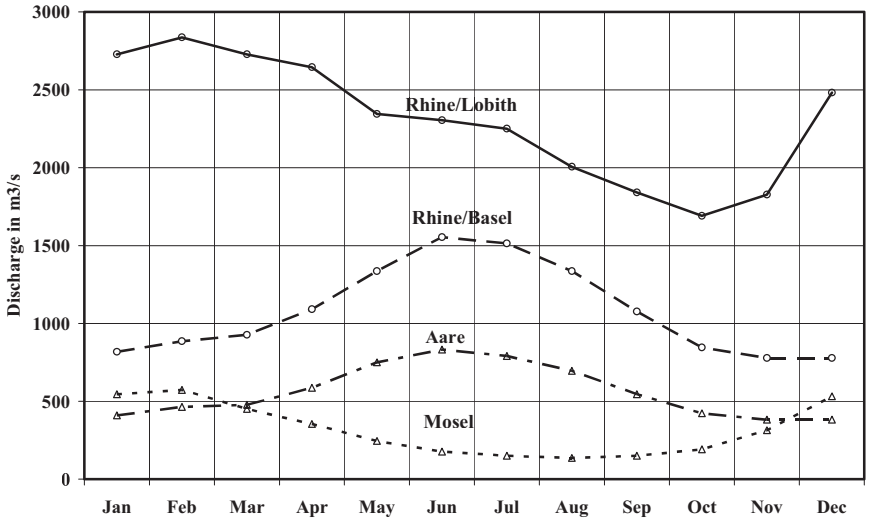

Figure 1. Average monthly discharge of the Rhine River at Lobith and at Basel, the Aare and the Mosel River.

The main sources of the Rhine River are the snow and glacier regions in the Swiss Alps with an average annual precipitation up to more than 2,500 mm. The headwater region is drained by the rivers Aare and the Alpine Rhine. Both rivers show the typical characteristics of high mountain range rivers with maximum runoff in the thawing season between May and July. The smoothing effects by lakes near the fringe of the mountain range (Lac Leman and Lake of Constance) are included in the runoff regime of both rivers. The rivers Aare and Alpine Rhine contribute approximately 50 % to the total runoff of the Rhine River.

The Mosel River is a typical low mountain range river with low runoff in the summer season and high runoff during the rainy season between November and March, and is typical of most of the other tributaries of the Rhine River The average annual precipitation in the drainage basin of the Mosel River and likewise in the regions of the other low mountain range rivers is approximately 800 mm.

Averaging discharge or level data is helpful to understand the basic properties of the runoff regime. But only unaltered original data give insight into the runoff dynamics of a river. Figure 2 shows a clip-out (500 days) of the stage hydrograph of the Rhine River near Düsseldorf (River km 744.2). Though the Rhine River with its dams in the Upper Rhine region is not spared from human impacts, the runoff dynamics in the downstream region approach to the properties of a natural river.

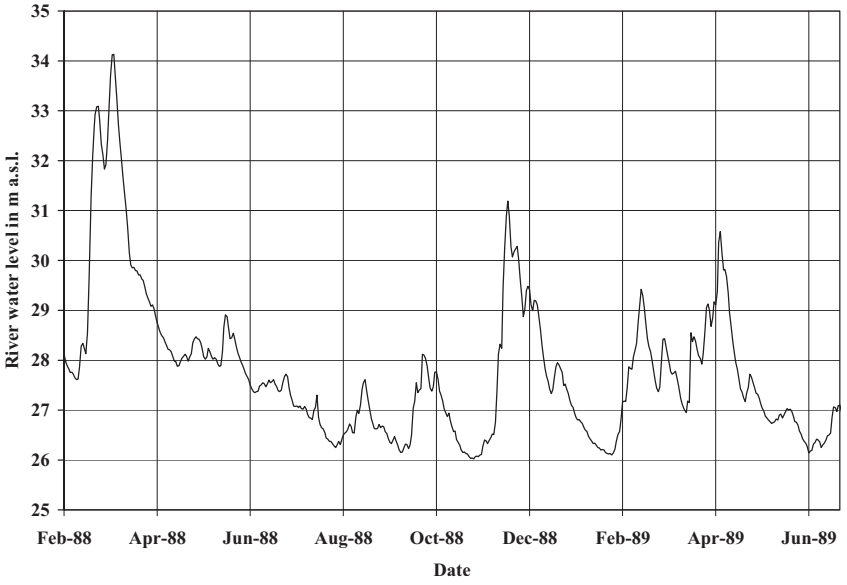

Figure 2. Stage hydrograph of the Rhine River near Düsseldorf (km 744.2).

This is quite different at the dam-regulated Ohio River. Figure 3 shows a clip-out (600 days) of the stage hydrograph of the Ohio River near Louisville, KY, indicating greatly dampened runoff dynamics.

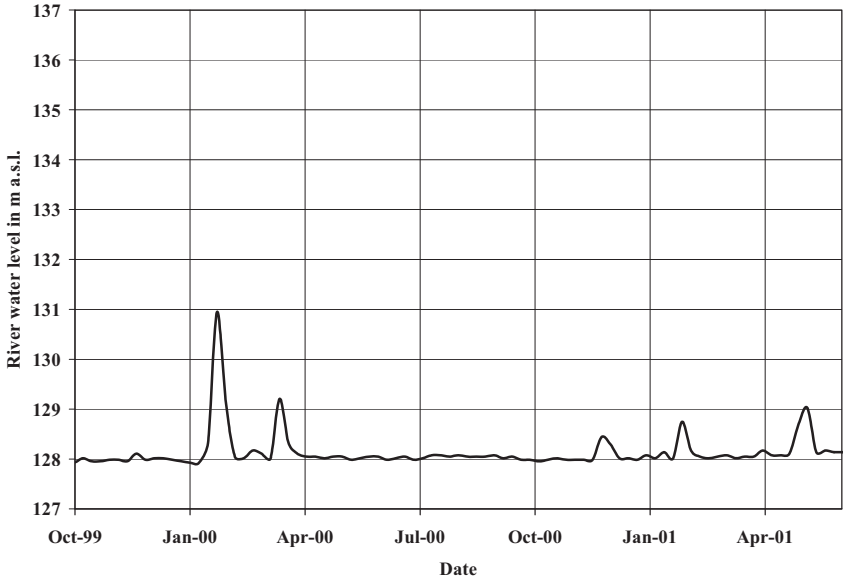

Figure 3. Stage hydrograph of the Ohio River near Louisville (Hubbs, 2003).

2.2 Bank Storage

The stage hydrograph represents the runoff dynamics of the river and controls natural river-aquifer interactions. Typical river-aquifer interactions during a flood wave were investigated in the Neuwieder Becken, a section of the Middle Rhine region near Koblenz, Germany (Ubell, 1987a,b). The adjacent aquifer, composed of fluvial sediments based on tertiary layer, is characterized by a hydraulic conductivity between $2*10^{-2}$ and $4*10^{-3}$ m/s, a porosity of 0.2 and a thickness of 10 to 15 m.

The aim of the investigation was to understand and to quantify the bank storage process, which occurs by the passage of a flood wave: groundwater runoff into the river is interrupted and bank filtrate is temporarily stored in the adjacent aquifer. A gallery of seven monitoring wells (U01 – U07) was installed perpendicular to the 300 m wide river at river km 602.4 to collect data of the groundwater level. Based on the gauge observations – including the river level and relevant data of the aquifer – a time series of the specific volume of bank storage and infiltration/exfiltration rates was determined.

Figure 4 shows the level of the Rhine River during a flood wave with a rise of about 5 m at river km 602.4.

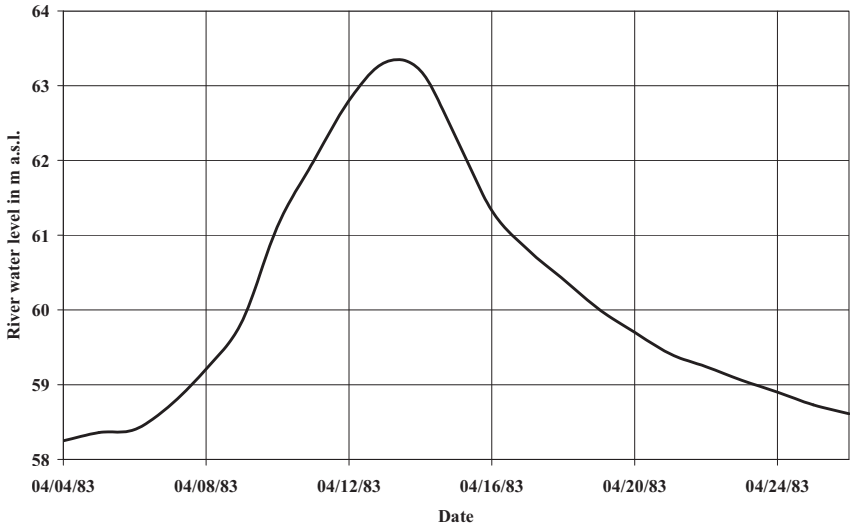

Figure 4. River level of the Rhine River at river km 602.4 during a flood wave.

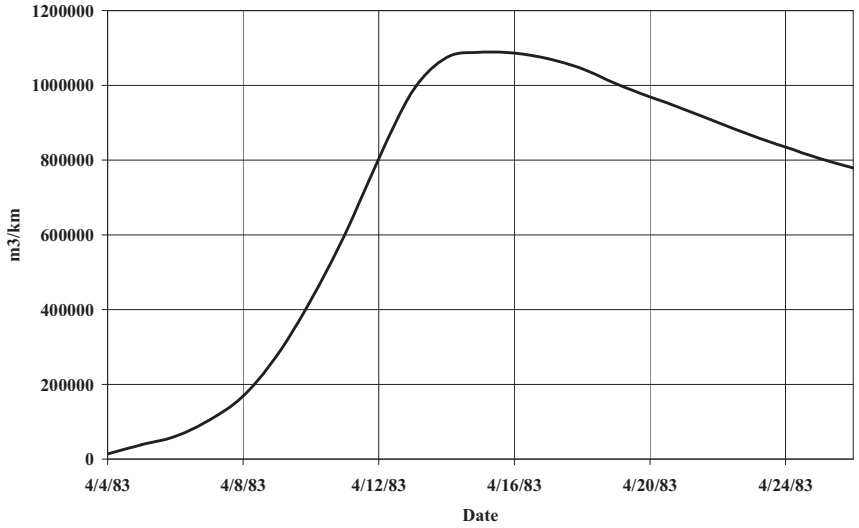

Figure 5. Changes in volume of bank storage during the passage of a flood wave.

The cumulative specific volume of bank storage during the flood event is shown in Figure 5. More than 1 million cubic meters of bank-filtered water

entered the left side part of the aquifer in a few days along a riverbed length of 1 km!

Figure 6 shows the quantitative part of the river-aquifer interaction by the rates of infiltration and exfiltration. The maximum infiltration rate into the aquifer of approximately 2,400 l/s km is about three to five times higher than the infiltration rates of existing RBF plants! The flow direction at the river-aquifer border changes about four days after the maximum infiltration rate of bank-filtered water to exfiltration of bank filtered water and groundwater into the river. A significant amount of bank-filtered water is stored in the aquifer for weeks or months (see Fig. 5). Bank-filtered water penetrated about 300 m into the adjacent aquifer during this event. Even smaller flood events significantly increase the volume of bank storage and the depth of penetration.

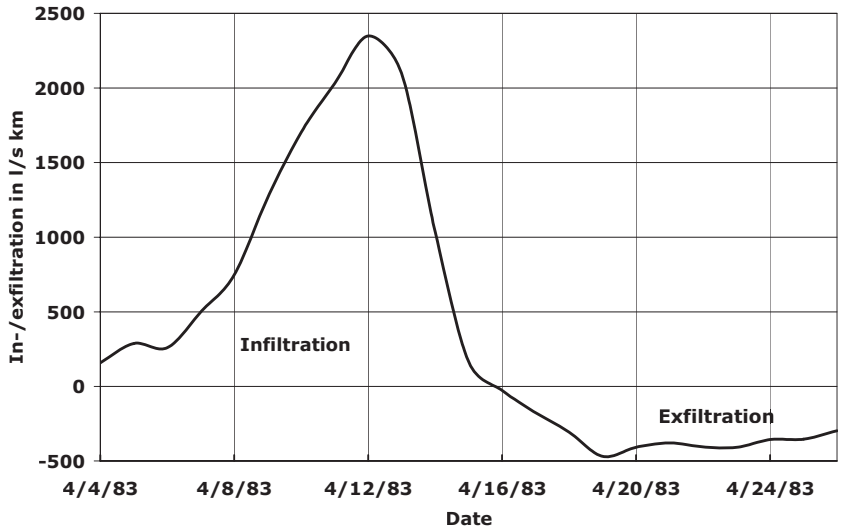

Figure 6. Infiltration and exfiltration rates during a flood wave.

One aspect concerning the clogging process should be mentioned in advance, based on the investigations of the bank storage effect of a flood wave. In the gallery of the seven monitoring wells along the cross section at river km 602.4 monitoring well U01 is situated close to the bank of the river. This allows, the estimation of possible variations of the hydraulic conductivity of the infiltration area due to clogging when combined with the infiltration rates. These data indicate that during this short time of infiltration (about 12 days) no significant decrease of the hydraulic conductivity could be found. This result corresponds with experience and may by supported by

a later discussion of the sequences of the clogging process during the early stage of RBF operation.

2.3 Runoff Dynamics and Transport of Suspended Matter

Flood waves cause an increase in the transport of suspended matter and bed load. The increase of suspended matter originates from the coincidence of matter from soils washed up by heavy rainfall, direct runoff from sewage water treatment plants (overflow), erosion of the riverbed and banks, and re-suspension of suspended matter e.g. upstream of dams. This load of suspended matter rises nearly exponentially with the discharge of the river up to a maximum and relapses quickly as the discharge begins to decrease. In the infiltration area of RBF plants high concentrations of suspended matter decrease the hydraulic conductivity of the riverbed significantly and may protect the silt layer against erosion in clogged areas by increased differential pressure into the riverbed.

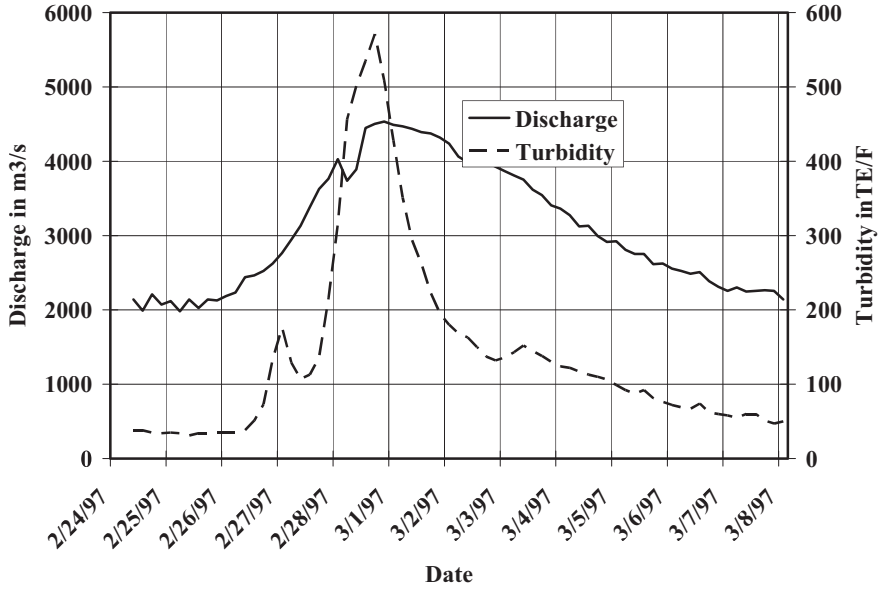

Figure 7. Turbidity during a flood event in 1997 in the Rhine River at Koblenz.

Figure 7 shows the regime of suspended matter during a flood wave (Breitung, 1999). The concentration of suspended matter is represented by Formacine turbidity units (TE/F), which tend to underestimate the influence of coarser particles (sand and gravel). The maximum concentration of

suspended matter (340 g/m^3 corresponding with 575 TE/F) is reached just before the maximum runoff (4.610 m^3/s) occurs. The turbidity during steady state conditions is in the range of 40 TE/F.

2.4 Stream Processes

The runoff regime alters the profile and the bed of a river by erosion, transport of sediments, and deposition and in the long run creates landforms. The critical erosion velocity varies with the size of particles. Fundamental research in the field of the critical velocities for erosion, transport, and sedimentation over a spectrum of grain sizes between clay and stone has been carried out and published by Hjulström (Hjulström, 1935).

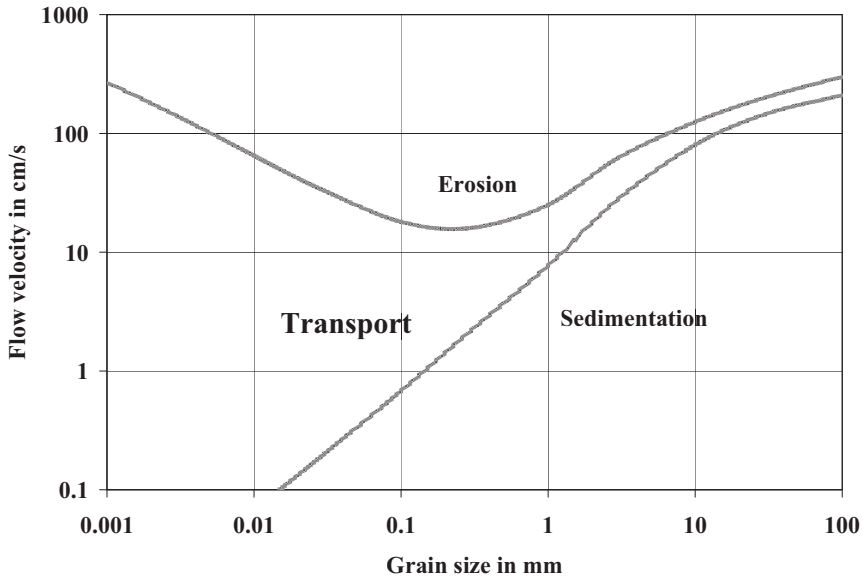

Figure 8. Hjulström diagram: Conditions for erosion, transport and sedimentation.

Figure 8 shows the slightly modified Hjulström diagram, which in this form is valid for uniform grain size only. The critical velocity for the beginning of erosion has a minimum at the grain size of fine sand, which confirms the common experience with stream processes. For clay and for stones the critical erosion velocity is about ten times higher! If the grain size is mixed, the tendency for bed material to be moved will increase.

Of particular importance for bed load transport are temporary water rolls (vortex) with horizontal axes, which occur prevalently during rising river

water level. Due to the vertical distribution of the flow velocity in a river channel ground rolls are created, rotating contrary to the flow direction along the riverbed (Wundt, 1953). Those ground rolls contribute in loosening the sediments at the riverbed and feed the transport. These rolls create forceful transport effects that result in sediment transport greater than that, which would be expected from the increase in flow rate and stream velocity alone.

Regarding the energy transformation between two adjacent cross sections of a river with approximately the same shape and area during steady state conditions, the discharge and the average flow velocity don't change. That means, that the kinetic energy of the river flow will be conserved. Only the potential energy, depending on the hydraulic gradient of the river, is completely consumed by internal friction (turbulence, vortex) and friction along the riverbed (Louis, 1961). During the rise of the river level (unsteady state conditions), caused by a flood wave, there occurs a temporary increase in the hydraulic gradient and a temporary difference in discharge between two adjacent cross sections. This means that additional potential and kinetic energy is available during the passage of the front of even smaller flood waves to be transformed into friction. Figure 7 may be interpreted as an image of this process. This supports observations that the runoff dynamics are an essential factor for the self-cleaning potential of a river.

2.5 The Profile of a River

The profile of a river is permanently exposed to the stream processes. Erosion is the dominating process in the headwater regions. Sediments are transported downstream and are deposited when the stream velocity falls below their settling velocities. In the mid-reach section of a river deposition and erosion may be regarded as alternating processes due to the runoff dynamics. Where a river approaches base level, water slows and deposition is the dominating process, which creates depositional landforms, such as deltas.

The general shape of the profile of a river shows a high gradient in the headwater region, a gradually waning gradient in the mid-reaches and a small gradient approaching base level (e.g. the mouth of the river). Figure 9 shows the profile of the Rhine River as an example. Altogether three base levels characterize the profile of the Rhine River. The Lake of Constance accumulates the coarse sediments from the Alpine Rhine River. After this first base level the gradient starts with a steep rise again and reaches low values at the hard rocks of the Nackenheimer Schwelle, which forms the second base level. The third base level is the mouth of the river into the North Sea.

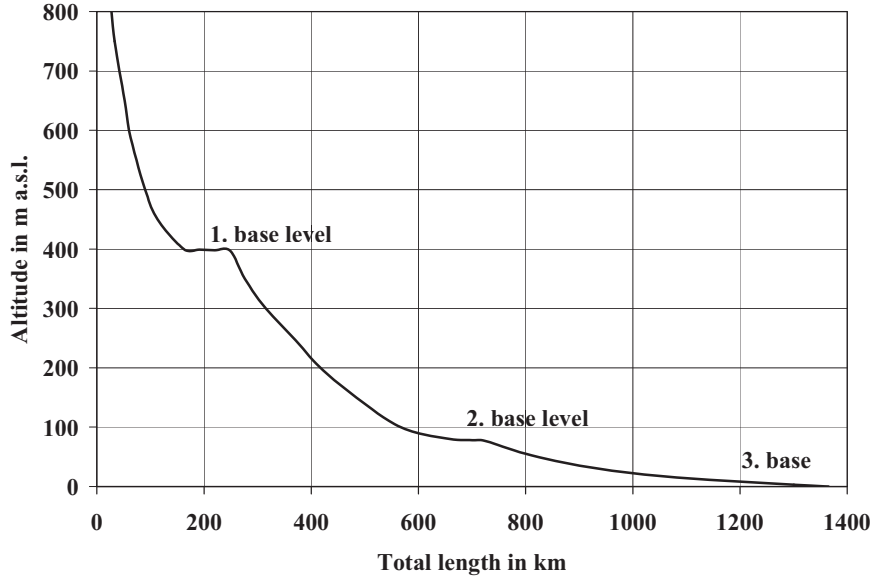

Figure 9. Profile of the Rhine River.

RBF along the Rhine River is not employed upstream of the first base level due to the coarse material in the adjacent aquifers. Between the first and second base level there can only be found a few RBF plants. RBF would be possible but is not typical for this region because the depth of several 100 m and the width of the alluvial deposits are more suitable for groundwater extraction.

An agglomeration of RBF plants exists in the alluvial deposits of the Lower Rhine region between the second and third base level of the river (Schubert, 2002). It may be helpful to consider the characteristic data of this region between Rhine-km 660 and Rhine-km 789 concerning RBF (Der Bundesminister für Verkehr, 1987):

Average hydraulic gradient	0.21 – 0.18 m/km
Average flow velocity	1.4 – 1.0 m/s
Average shear stress on the riverbed (MQ)	Approximately 10 N/m^2
Mean grain size diameter of the bed load	13 mm at km 660
	8 mm at km 780
Mean grain size diameter in the riverbed	33 mm at km 640
	26 mm at km 730
	10 mm at km 860
Hydraulic conductivity of the adjacent aquifer	$k_f = 2.2 \times 10^{-2}$ to 3.3×10^{-3} m/s.

These conditions have supported RBF operation for more than 130 years.

When the slope of the river and the flow velocity decreases, the channel begins to meander. The development of meanders is a natural phenomenon of river channels caused by the inertia of the flow. In meanders or bends the maximum flow velocity occurs towards the outside of the bend. This outside border is washed out by erosion and the riverbed is deepened, creating an asymmetric cross section of the riverbed (Schubert, 2002). In this dynamic process the larger fraction of the riverbed material that resists erosion – e.g. stones – accumulate and may cause a paved bed along the outside bend. The resulting riverbed is immobile even during the passage of flood waves. In regions near the inside border of the bend the flow velocity is low and deposition occurs; the riverbed material remains movable.

Meanders of the river channel are preferred sites for RBF plants; inside the loop of a meander the natural cross flow between the upstream and the downstream side of the loop augments the proportion of bank-filtered water in the extracted well water. An additional advantage is the movable riverbed along the inside border of the river channel, which supports the self-cleaning process of clogged areas.

3. THE CLOGGING PROCESS

River-aquifer interactions are governed by the fluctuating water level of the river. The resulting gradients between the quickly changing river level and the gradual adaptation of the groundwater table in the adjacent aquifer control flow and transport of the infiltrated river water. The runoff dynamics are not only relevant for clogging processes and flow velocities in the subsoil, but can also affect the water quality of the well water by fluctuating removal efficiency, e.g. due to varying residence times.

Infiltration of river water to an aquifer is a natural phenomenon at the upstream side of river bends, due to the hydraulic gradient of the river, and during rising river levels, without any wells near the riverbank (natural bank storage). These natural infiltration processes don't cause clogging because they are temporary and are over and over interrupted by groundwater exfiltration into the river. This natural variation of the flow direction prevents clogging of the riverbed.

Clogging is caused by the continuous infiltration of river water due to well pumpage. Clogging of parts of the riverbed during long-term operation of RBF wells is principally unavoidable.

The progress of the clogging process from the beginning of pump operation shows some important details. During the first phase of clogging two competing processes are involved:

- Clogging of the riverbed: Correlative to the distribution of the infiltration rate a spatially different clogged layer will be formed in the region of the cone of depression of the wells. Within the infiltration area a permanent equalization between regions of different permeability leads gradually to an adaptation of different specific infiltration rates. The distribution of infiltration rates is more uniform at the end of the first phase without significant reduction of the permeability of the riverbed.
- Suffosion in the pore channels of the adjacent aquifer: Suffosion means a hydro-mechanical deformation phenomenon of natural aquifers caused by the motion of water through a porous medium. With the operation of RBF wells the natural variations of the flow direction between the wells and the river are stopped. Governed by the uniform flow direction the transport and displacement of fine fractions in the pores of the aquifer gets started. The skeleton of the non-uniform grain structure is not altered during this process, but the pore channels are smoothed with a positive effect on the hydraulic conductivity. This type of inside suffosion is a temporary process. Once the fine particles are displaced due to the flow conditions, the process runs out.

Both processes together in the early stage of RBF operation, which may reach for several months, are generically characterized by small fluctuations, but no significant decrease of the water yield! Therefore predictions on the long-term behavior of the system cannot be drawn from the data of the first phase.

The second phase of the clogging process is characterized by a significant reduction of permeability in the whole infiltration area and a reduction of the water yield. The self-regulating system tries to find the balance between the ongoing clogging process and the self-cleaning processes of the river, chiefly governed by the runoff dynamics. Compensation by intensification of the depression cone, to stabilize the water yield, may introduce a third phase of the clogging process.

The third phase of the clogging process is characterized by the spread out of an unsaturated zone beyond the riverbed. The zone where the direct contact between the aquifer and the riverbed will be interrupted spreads out. At the same time, caused by deepening of the depression cone, additional infiltration areas will be developed with lower driving head and may be in regions of the riverbed with higher flow velocities. The reduction of permeability in the infiltration area and the reduction of water yield are going on, but on a lower level.

A forth and final phase of the clogging process is characterized by the total interruption between the cone of depression and the riverbed near the well site. This situation often means the end of RBF operation.

Based on the data of the Louisville RBF well at the Ohio River (Hubbs, 2003) phase one to three of the clogging process may be visualized. Figure 10 shows the original data of the river water level, the well water level, and the pumping rate from the beginning of RBF operation over a period of nearly 200 weeks.

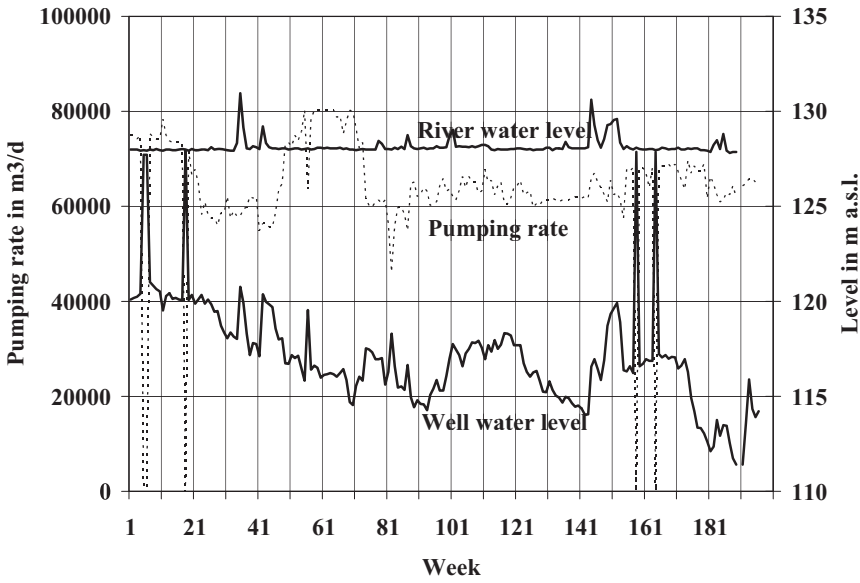

Figure 10. Pumping results of the RBF facility on the bank of Ohio River at River Mile 592 (Louisville Water Company).

From the beginning of pump operation to about week 20 the driving head is less then 8 m during an average pumping rate of about 74,000 m^3/d. A driving head of about 12 m is reached in week 60 during a pumping rate of about 80.000 m^3/d. At the end of the observation period (week 188) the driving head is about 16 m during an average pumping rate of 64,000 m^3/d. This sequence indicates severe clogging. But to quantify the clogging process, also the influence of the water temperature and respectively the viscosity of the water on the yield have to be considered. Figure 11 shows the temperature of the river water and the well water.

The seasonal fluctuation of the river water temperature is between 30 degree Celsius and 2 degree Celsius. The water temperature of the well water is smoothed by riverbank filtration and fluctuates between 26 and 11

degree Celsius. The resulting viscosity varies significantly from 0.8 to 1.66 m^2/s in the river water and 0.88 to 1.27 m^2/s in the well water.

To normalize the data of the pumping rate from the influence of varying water temperatures, a representative water temperature has to be determined. For this purpose a fictitious water temperature in the aquifer has been introduced as an average value between the river water temperature and the well water temperature regarding the time lag of four till five weeks between both temperatures.

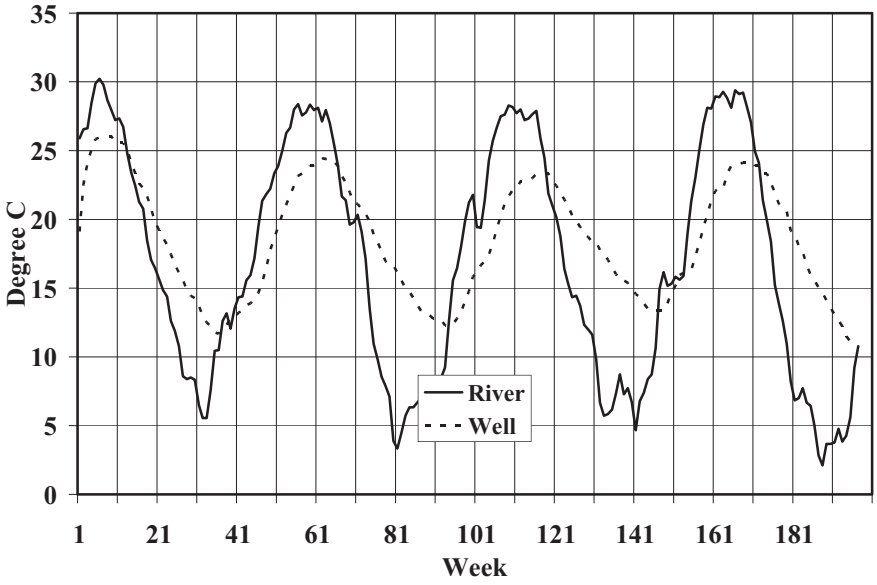

Figure 11. Water temperature of the river water and the well water.

Two different approaches have been employed, to visualize the pattern of the clogging process and its interrelation with the flow dynamics of the river. One approach is the time series of the specific capacity. The specific capacity is based on the temperature-corrected pumping rate Q' in m^3/s and the driving head in m. The other approach is based on the analytical methods for groundwater flow towards a ditch and towards a well. Both approaches lead to corresponding results due to the simplified analytical methods and allow acceptable insight into the general pattern of the clogging process. Figure 12 shows the result with the specific capacity $m^3/s/m$.

Three different segments can be extracted from the sequence of the specific capacity:

- First phase of the clogging process: Between the beginning of pump operation and about week 23 are smaller variations but no decrease of the specific capacity.

- Second phase of the clogging process: A significant drop of the specific capacity occurs between week 23 and week 61.
- Third phase of the clogging process: Between week 61 and the end of the observation period in week 188 the decrease of the specific capacity proceeds slowly.

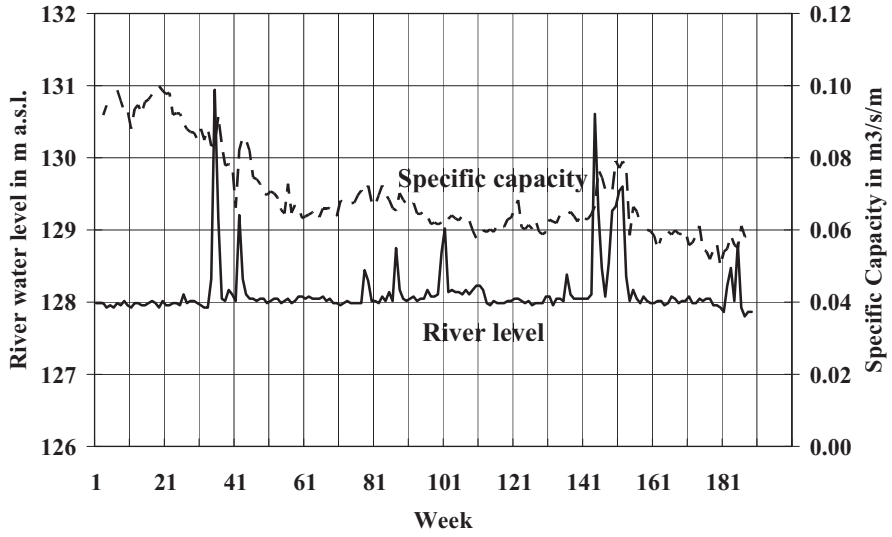

Figure 12. Pattern of the clogging process.

Even minor variations in the river level of less than 1 m (in week 78, 87, 101 and 136) are able to cause temporary improvements of the specific capacity. A real jump is caused by a flood wave with an amplitude of 2.6 m in week 144 and two flood waves during phase two (3 m in week 35 and 1.2 m in week 42). But the time series of the specific capacity through week 185 also show that the position and size of the cone of depression is not yet balanced out with the self-cleaning potential of the river.

4. CONCLUSIONS

The runoff regime, characterized by amount, frequency, length, time and rate of change of runoff conditions, determines the self-cleaning potential of a river. As this is the main process limiting clogging of the riverbed during RBF operation, the properties of the river must be considered when

predicting specific capacity for a RBF design and when determining the operation parameters (well discharge) of the RBF wells.

The European philosophy for the design and operation of RBF wells is based on the aim of safe quality of the well water and long-term operation of the plant. Adequate safe well water quality means an average retention time of the bank-filtered water in the subsoil of minimal three weeks. This time seems to be necessary for the removal of bacteria, viruses, and cysts of parasites, it is helpful to balance out fluctuating temperatures, concentrations and shock loads and it improves biodegradation of more resistant organic compounds. The consideration of this principle – retention time in the subsoil - is sufficient, in general, for the optimal design of the RBF arrangement, particularly the distance of the wells from the riverbank and the pumping rate. The second principle for long-term operation may be verified by the position of the drawdown curve relative to the riverbed. The steeper inner part of the drawdown curve should be completely in the aquifer outside the bank and only the flat outer part beyond the riverbed, thus limiting the driving head and reducing the pressure on the clogged areas. The suitable driving head correlated to the middle discharge line (MQ) depends on the local conditions of the aquifer and the river (runoff regime and river water quality); in the Lower Rhine region a relevant driving head of less than 1 m at the MQ-line has proven effective.

REFERENCES

Breitung, Vera, 1999, Organische Schadstoffbelastung in Schwebstoffen des Rheins während Hochwasserwellen (Organic micropollutants in suspended matter in the River Rhine during flood events), Hydrologie und Wasserwirtschaft 43, 1999, H.1; pp. 17 –22.

Der Bundesminister für Verkehr, Abteilung Binnenschiffahrt und Wasserstraßen, 1987, Untersuchung der Abfluss- und Geschiebeverhältnisse des Rheins (Investigation of discharge and bed load transport of the Rhine River). Bonn.

DIN 2000: Zentrale Trinkwasserversorgung: Leitsätze für Anforderungen an Trinkwasser; Planung, Bau, Betrieb und Instandhaltung der Versorgungsanlagen (Public Water Supply: Guidelines for Drinking Water; Design, Construction, Operation and Maintenance). Technische Regel des DVGW. Deutsches Institut für Normung, Berlin, 2000.

Hjulström, Filip, 1935, Studies on the morphological activity of rivers. Bull. Geol. Inst. of Upsala 25, pp. 221 – 258.

Hubbs, Steve, 2003, Plugging in Riverbank Filtration Systems: Evaluating Yield-limiting Factors. National Water Research Institute, NWRI-2003-10.

Hunt, Henry, Schubert, Jürgen and Ray, Chittaranjan, Operation and Maintenance Considerations in: Riverbank Filtration –Improving Source-Water Quality, Ch. Ray, G. Melin, R.B. Linsky, Kluwer Academic Publishers, Dordrecht/Boston/London, pp. 61 – 70.

Leibundgut, Christian, Hildebrand, Alexander, 1999, Natural runoff and runoff dynamics. UFZ-Bericht Nr. 31/1999, W. Geller (ed), UFZ Centre of Environmental Research, Leipzig.

Louis, Herbert, 1961, Allgemeine Geomorphologie (General Geomorphology). Walter de Gruiter Verlag, Berlin.

Riesen, Sigurd van, 1975, Uferfiltratverminderung durch Selbstdichtung an Gewässersohlen (Shrinkage of bank filtrate by clogging of the riverbed). Dissertation, Fakultät für Bauingenieur und Vermessungswesen, Universität Karlsruhe.

Schubert, Jürgen, 2002b, German Experience with Riverbank Filtration Systems, in: Riverbank Filtration –Improving Source-Water Quality, Ch. Ray, G. Melin, R.B. Linsky, Kluwer Academic Publishers, Dordrecht/Boston/London, pp. 35 – 48.

Ubell, Karoly, 1987a, Austauschvorgänge zwischen Fluss- und Grundwasser – Teil I (Surface Water and Groundwater Interaction – Part I), Deutsche Gewässerkundliche Mitteilungen 31, 1987, H.4, pp. 119 – 125.

Ubell, Karoly, 1987b, Austauschvorgänge zwischen Fluss- und Grundwasser – Teil II (Surface Water and Groundwater Interaction – Part II), Deutsche Gewässerkundliche Mitteilungen 31, 1987, H.5, pp. 142 – 148.

World Health Organization, 2004: Guidelines for Drinking Water Quality. WHO, Geneva.

Wundt, Walter, 1953, Gewässerkunde (Hydrology). Springer Verlag, Berlin, Göttingen, Heidelberg.

EVALUATING STREAMBED FORCES IMPACTING THE CAPACITY OF RIVERBED FILTRATION SYSTEMS

Stephen A. Hubbs
WaterAdvice Associates, 3715 Hughes Road, Louisville KY stevehubbs@bellsouth.net
Formerly with the Louisville Water Company, Louisville KY

Abstract: The static and dynamic forces at work on a riverbed impact both the clogging processes and the regenerative scouring processes in RBF systems. This chapter reviews shear forces exerted on a riverbed, and considers the additional forces developed under conditions of infiltration with saturated and unsaturated flow. Methods of measuring streambed shear stress are evaluated in relation to streambed scouring, and the relative impact of barge traffic on streambed shear stress is discussed. These measures help to define the suitability of a site for Riverbank Filtration.

Keywords: Riverbank Filtration, RBF, shear, stress, scour

1. INTRODUCTION

The traditional approach to designing high-capacity RBF systems for public water supply involves analyzing hydrogeologic site conditions and performing a pre-construction pump test to predict wellfield capacities. The pump test typically lasts for a period of one to several days, with the results used to design pumps and wellscreen for the final installation. Analysis of the pump test data is used to determine aquifer characteristics of transmissivity, and can yield information on the riverbed conductance at the time of the pump test. Data from the pump test can be adjusted based upon aquifer temperature to give a range for system output capacity.

Stephen A. Hubbs (ed.), Riverbank Filtration Hydrology, 21–42.

This system of design works adequately with smaller capacity systems that impart very low infiltration velocities and minimal stress on the infiltration area of the riverbed. However, practice has shown that for large capacity RBF systems, the wellfield specific capacity decreases with time for a period of several years before reaching a stable sustainable yield. This has been referred to anecdotally as the "settling in" period for such systems, with final system specific capacity decreasing by one-third or more of the original capacity predicted by the pump test. (See Chapter 9: LWC case history.) Without predictive tools to estimate this deterioration in wellfield performance, the water supply manager is left to hope that the wellfield will perform to the designed capacity.

The elements of an RBF system controlling long-term sustainable capacity of a wellfield can be divided into three yield-limiting factors: riverbed conductance; aquifer transmissivity; and wellscreen dynamics (Figure 1). In vertical wellscreen systems, the limited amount of wetted screen and high velocities around the wellscreen are important variables affecting the long-term capacity of a well system. Advances in radial well design, however, have allowed for up to 500 meters of horizontal wellscreen to be developed in formations where vertical wells can accommodate only 20 meters of wellscreen. In many formations, this change has eliminated wellscreen dynamics as the limiting factor in sustainable well capacity.

Recent investigations have indicated that riverbed conductance is likely the capacity-limiting factor in high-capacity RBF systems. However, the impact of riverbed conductance and its change with time on long-term sustainable yield have not been thoroughly evaluated. It has been observed that riverbed conductance varies as a function of time (Hubbs, 2004), which is likely the result of riverbed clogging. This clogging can be caused by mechanical particle impingement, biological growth, or geochemical reactions within the aquifer/riverbed interface. All three of these processes can be impacted by dynamic and static hydraulic forces. However, the impact of these clogging processes on the long-term specific capacity of a wellfield is poorly understood.

This chapter focuses on the mechanical processes of clogging and an evaluation of the hydraulic forces involved in both the clogging and scouring processes.

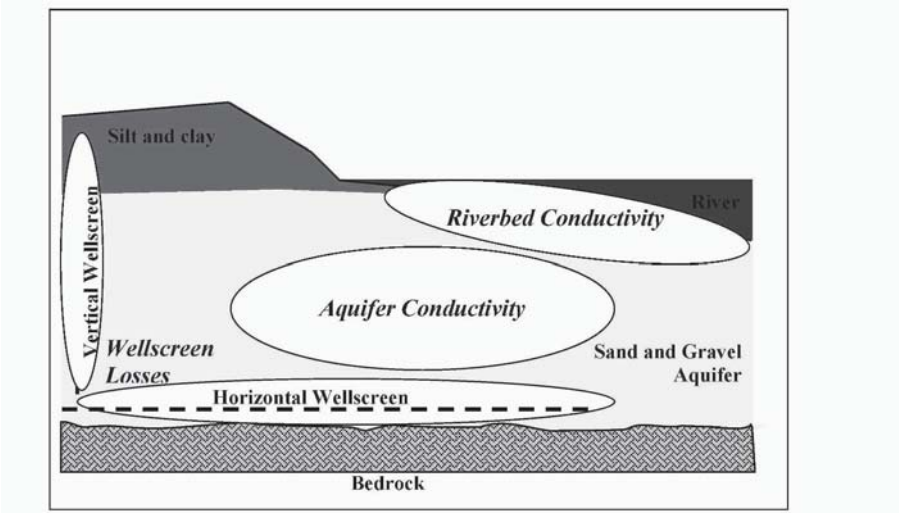

Figure 1. Yield-limiting factors in Riverbank Filtration Systems

2. PARTICLE FORCE DIAGRAM

The hydraulic forces imparted onto an individual particle (sand or gravel) on a riverbottom may be divided into static forces and dynamic forces. In most evaluations of riverbed shear and sediment transport, the dynamic forces are the most obvious, with the moving water imparting laminar and turbulent forces on the particle. Static forces include particle buoyancy and the overall weight of the water column at a given point. Since equal static forces usually are assumed to be exerted on the riverbed particle from all directions, the weight of the water column is not typically considered in the overall evaluation of forces on the particle.

2.1 Forces in Streambeds without Induced Infiltration

Julien (1998) has provided a graphic illustration of these forces presented in Figure 2. This force diagram illustrates the forces required to impart a shear force adequate to cause movement of the particle, which occurs when the lift and drag forces overcome the particle weight and adjacent particle resisting forces. This diagram assumes no velocity gradient

into or out of the riverbed, as would occur whenever a stream is gaining or losing to the adjacent aquifer.

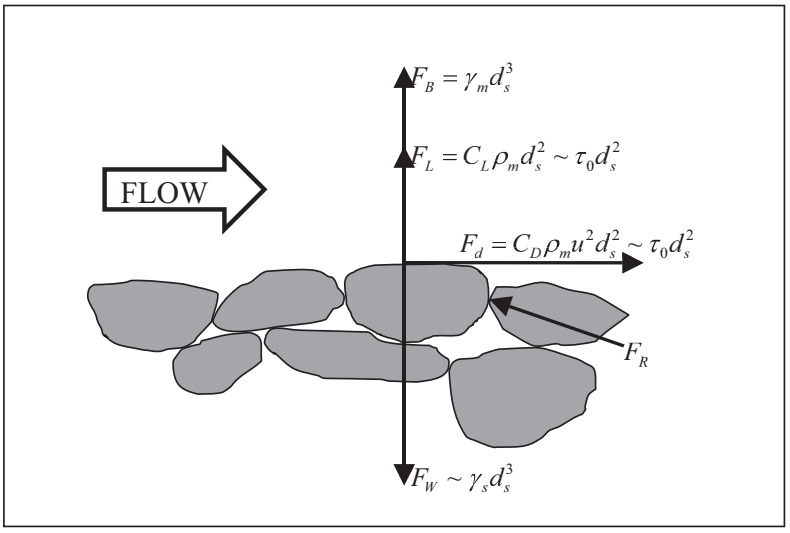

Figure 2. Force Diagram without Infiltration Forces (after Julien, 1998). *F_B is the buoyant force, F_L is the lift force, F_D is the drag force, F_W is the particle weight, and F_R is the resisting force. γ_m is the specific weight of water, γ_s is the specific weight of the sediment particle, d_s is the particle size, d_s^3 represents the particle volume, ρ_m is the fluid density, C_D is a drag coefficient, C_L is the lift coefficient, τ_o is the streambed shear stress, and U is the fluid velocity.*

2.2 Forces Imparted by Infiltration in RBF Systems

To evaluate the relative magnitude of forces that come into play when a velocity gradient is imparted into the riverbed or riverbank, the velocity and viscosity must be considered along with the particle area perpendicular to the flow. The velocity forces become complicated as the water passes into the aquifer; the approach velocity is a fraction of the in-aquifer velocity, which is impacted by the porosity of the formation. For a typical sand aquifer with a porosity of 20%, the velocity within the aquifer is 5 times greater than the approach velocity at the riverbed. The fluid velocity within the aquifer is caused by a hydraulic gradient, and if the aquifer is uniform and not impacted by clogging, the velocity is constant and the head loss increases linearly with distance. This force is shown in Figure 3 as the infiltration force F_I.

Experience has shown, however, that the riverbed/aquifer interface is impacted by various forms of clogging, from simple surface particle impingement, to invasion of smaller particles into the riverbed, to biological growth, to geochemical reactions. As these forms of clogging are highly variable in time and space, analytical approximations have been utilized to assign an overall factor to "riverbed conductance" in a given system. This factor allows computer modeling of riverbed conductivity by assuming a given depth (travel distance) of riverbed, and a hydraulic conductivity for that depth. Traditional modeling techniques arrive at a similar solution by using the technique of "image" wells (see Mucha, Chapter 3).

Until recently, computer models of aquifers hydraulically connected to rivers did not consider the possibility of the aquifer being dewatered under the river itself. This condition has been indicated in the literature (Constantz 2003, Hubbs, Chapter 9 of this book), and leads to a reconsideration of the assumptions regarding the particle force diagram.

It is appropriate at this time to introduce some qualitative information regarding streambed conditions observed in the field at various sites. Prior to initiation of pumping at the RBF facility at the Louisville Water Company, the riverbed immediately adjacent to the wellfield was observed to be soft and easily penetrated. During periods when the piezometric surface in the aquifer is observed to be lower than the riverbed, however, the riverbed surface was observed to be highly resistive to penetration. Under these conditions, a diver had difficulty penetrating the riverbed surface with his knife, but when a sediment sample was removed by prying it from the surface, the sample became non-cohesive and free-flowing. Similar conditions have been observed at other RBF sites under high-pumping conditions, where the riverbed could not be sampled because of the shear resistance of the surface (Golnitz, personal communication). The recharge basins in Sonoma County (California) Water Authority have exhibited similar behavior when under unsaturated conditions, with the flooded sand basins being highly resistive to penetration, but samples were totally non-cohesive when extracted. Similar observations have been made in high-rate filters in surface water treatment plants, when filter headloss exceeds the head over the filter (personal observation).

With this as a background, the force diagram was re-considered with the possibility of unsaturated conditions existing in the aquifer under a clogged riverbed. Under unsaturated conditions, static forces must be added to the overall forces acting on the particle or river surface. This additional force, and the balancing resistive force from the riverbed, is shown in Figure 3.

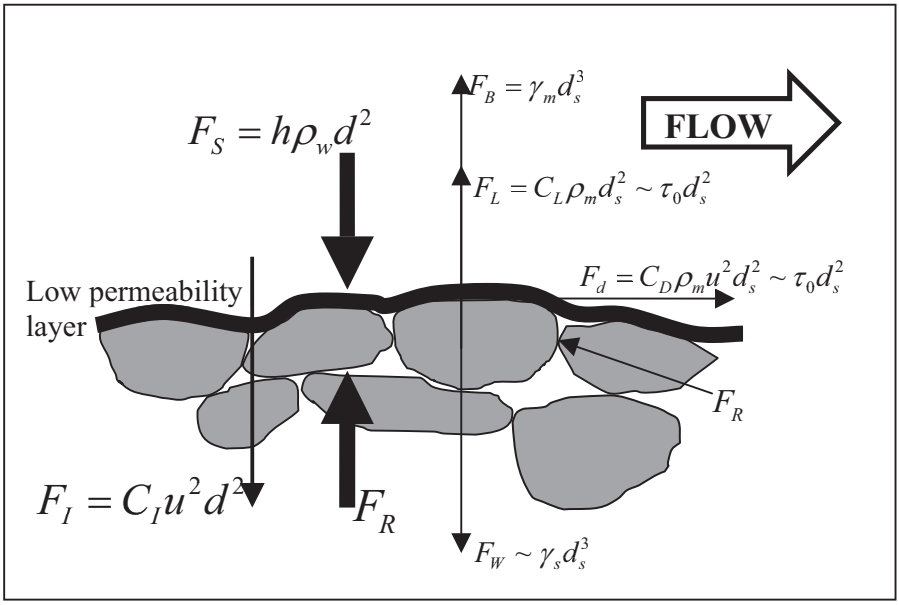

Figure 3. Force Diagram under Unsaturated Conditions with static forces shown. (F_I=infiltration force, C_I=infiltration coefficient, F_s = static force, h=the depth of water column over the riverbed)

The clogging layer in Figure 3 is simplistically shown as a single membrane overlying the riverbed media. It is more likely that the conditions required to develop unsaturated conditions under a riverbed develop over time (years), and include surface deposition, particle invasion into the riverbed media, and biological and geochemical processes. Thus, the saturated clogging layer above the unsaturated portion of the aquifer might be better represented as a zone upon which surrogate hydraulic forces are exerted, as opposed to forces on individual particles. The thickness of the saturated zone has been observed by in-situ piezometers to be less than 0.6 meters at Louisville. Observations from divers at this site indicate that this zone may be as thin as 3 cm.

2.3 Comparative Analysis of Riverbed Forces

To put these forces into perspective, the typical range of each of these forces needs to be calculated. The science of sediment transport was well developed in the 1970's, and typical shear forces on riverbeds have been reported in the range of 1 to 100 N/m^2. Values of 20 N/m^2 are reasonable, as a horizontal force imparted by the moving stream over the riverbed surface.

In a given stream, the viscosity and particle density factors will remain constant regardless of the direction of flow, so that the forces imparted by an infiltration flow of water would differ from the horizontal forces primarily by fluid velocity, although an argument could be made that anisotropic conditions resulting from the sorting of sediment on the riverbed would impact the particle cross sectional area facing the flow vector. Approach velocities (Darcy velocity) in RBF systems have been measured with maximum values in the range of 0.09 meters/hour or 0.00003 meters per second (Wang 2002), compared to typical horizontal stream velocities in the range of 1.5 meters per second and typical velocities at the streambed of 0.15 m/sec. It is thus reasonable to conclude that the forces exerted by the vertical velocity component into the riverbed will be over three orders of magnitude lower than the horizontal shear force. Assuming a porosity of 0.2, the in-aquifer velocities would be roughly 5 times the approach velocity, or 0.00015 meters/second. The forces exerted by the approach velocities and in-aquifer velocities are thus negligible compared to the horizontal shear forces.

It can also be argued that the vertical flow velocity into the streambed will compress the laminar sublayer in the horizontal flow regime, resulting in an increase in the shear forces exerted on the riverbed (Schlichting, 1968). Assuming this sublayer is compressed at a rate comparable to the ratio of the horizontal to vertical velocity at the streambed, this factor would likewise be negligible compared to streambed shear forces.

Finally considering the static forces exerted by a column of water over riverbed over an unsaturated aquifer, the force on the riverbed is the weight of the water column, and the resisting force must be provided by the riverbed itself. This force for a 6 meter column of water is approximately 60,000 N/m^2, or roughly 3000 times greater than any other force exerted on the riverbed. Typical values for these forces are summarized below for comparison:

- Vertical Infiltration forces: 0.002 N/m^2
- Compression of laminar layer: 0.002 N/m^2
- Horizontal shear forces: 20 N/m^2
- **Hydrostatic:** **60,000** N/m^2

The head loss exerted by the aquifer on the flowing stream of water through it must also be considered with the overall system of forces working on and immediately below the riverbed. Head loss in aquifers associated with moving water is impacted by the hydraulic conductivity of the media and the viscosity and velocity of the fluid. Under normal wellfield operation and saturated conditions (Chapter 9), data from Louisville indicates that head loss in the first 0.6 meter of riverbed is approximately 5 meters, while the next 2.1 meters of riverbed exerts approximately 0.03 meters of headloss.

2.4 Hypothesis for Riverbed Clogging under Unsaturated Conditions

The reduction in riverbed conductivity over time has been attributed to particle impingement on the surface, particle invasion into the riverbed matrix, biological clogging, and geochemical clogging. Another possibility is offered: that the riverbed surface mixture of clay, silt, and sand loosely deposited in alluvial processes exhibit relatively high permeability until the aquifer supporting them becomes unsaturated, at which time the forces of the overlying water column compress the loose soil into a structure with much lower hydraulic conductivity.

If unsaturated conditions exist under the riverbed, the entire weight of the water column is supported by the riverbed above the unsaturated zone. It is reasonable to expect that as unsaturated conditions develop, the portion of the aquifer above the unsaturated zone would drain, forcing the headloss of the overlying water column across a thinning upper saturated zone. As this de-saturation progresses, the weight of the overlying column of water is transferred from the entire submerged aquifer to a relatively thin layer of the riverbed. As this proceeds, the conductivity of the riverbed decreases dramatically.

While the thickness of riverbed assuming this load is unknown, it is known to be less than 0.6 meter at Louisville (the location of the pressure probe closest to the riverbed). When a diver successfully penetrated this layer with his knife, he observed it to be less than 2 cm thick and upon penetration substantial flow into the riverbed was observed as the muddied water disappeared into small hole created in the riverbed. Thus, it appears that at this point of observation very near the edge of the unsaturated zone, the thickness of the layer of very low hydraulic conductivity was in the range of 2 cm thick. (See Chapter 9 for data supporting this theory on riverbed clogging under unsaturated conditions.)

This hypothesis is consistent with observations in RBF facilities in Louisville, Sonoma County, and Cincinnati Ohio, where adequate data exist to consider the hypothesis.

Given the potential for a dramatic decrease in riverbed conductance as hypothesized above, the importance of riverbed area, width, and aquifer storage become critical elements in a wellfield design. Systems with wide streams, massive storage and highly transmissive formations may be able to withstand periods of high demand by drawing from aquifer storage without having the piezometric surface dip below the riverbed. However, systems with smaller streams and aquifers closely confined by valley walls and shallow depth to bedrock have a higher reliance on infiltration, and may find that under conditions when capacity is needed the most, riverbed conductance could decrease dramatically as a result unsaturated conditions developing under the riverbed, reducing overall system capacity. This condition is exacerbated under conditions of low water temperature, as the increased viscosity of water drives the piezometric surface even lower for a given flow.

3. MEASURING SHEAR STRESS AS AN INDICATOR OF RIVERBED SCOUR

The process of riverbed clogging can be offset by the regenerative process of streambed scouring. Schubert (2002) has described the hydraulic process of streambed scouring and its importance in the limitation of clogging in RBF systems. Riverbed scouring is the result of shear forces imparted on a riverbed by the motion of the water passing over the riverbed, and the resistance to this motion imparted by the riverbed itself. While there is no practical technique for directly measuring this shear force on a riverbed, it can be estimated by the surface slope of the stream, vertical velocity profiles in the stream, and the sediment in transport on the riverbed. Each of these three techniques is examined, using data from the Ohio River at Louisville, Kentucky as an example.

3.1 Stream Scour and Sediment Transport-basics

The science of erosion and sediment transport was highly developed in the 1970's, driven primarily by the concern for scouring around highway bridges and bridge piers and the sedimentation of reservoirs, and more recently by the concern for the effects of sediment deposition on stream aquatic life. The process of erosion has modified the surface of the earth and sorted the sediments that form many of the alluvial aquifers used for water supply. This process is powered by the energy of falling water, with the rate

controlled by the composition and resistance of the soils and rocks exposed to the flowing water (Leopold, 1964).

The energy potential of a stream can be directly measured by the change of elevation of the stream surface with distance, or the slope of the stream. The energy level in the headwaters of streams is typically high, causing the fine sands and gravels to be carried downstream, leaving large rocks and cobbles in the streambeds. As the energy level decreases with moderate slopes in the mid-reaches of a stream, sands and gravels may be deposited and sorted into highly productive aquifers. If the rates of deposition vary widely with geologic time, distinct zones and layers of media of varying particle size can result in complex aquifers with variable capacity for water supply. As stream slopes decrease near the delta area at the mouth of a stream, finer sands, silts and clays are typically deposited, limiting the conductance between the stream and the adjacent aquifer.

The capacity of a stream for riverbed scour and sediment transport can thus be inferred by considering the slope of the stream through a river profile. River profiles for several streams are presented in Chapter 14 (Caldwell). Although many of these streams support similarly sized RBF systems, the river hydrology and riverbed scouring characteristics vary greatly among the system sites.

Many streams are impacted by control structures (locks and dams) for flood control, navigation, and power supply. The appropriate slope to use for streambed shear stress is the slope within the pool of the dam, which is often a fraction of the natural stream slope. If one is primarily concerned with annual maximum scouring rates, however, and if these control structures are routinely submerged by flood flows, the average stream slope across several pools can be used to provide a rough estimate of average stream bed shear forces under these conditions. The change in elevation of the stream bed or top-of-bank can also be used to estimate annual maximum historical stream slope in the absence of any other data.

The sediment transported by streams is determined by the composition and weathering of rocks and soils within the watershed, and the resuspension of riverbed materials from upstream. Periods of high and consistent flow during glacial periods produced many large, well sorted aquifers with good hydraulic connectivity to the streambeds. Materials in transport today may reflect the continued transport of upstream glacial deposits, or newer gravel, sand, silt and clay from upgradient weathering of rocks and soils. Chalk pebble aquifers have been identified in Ukraine, with wind-blown sand at the surface and a tight chalk-clay layer between. Most productive RBF aquifers seem to have a highly transmissive aquifer overlain with a floodplain of more recently deposited silts and clays.

Sediment particle size profiles for the Ohio River at Louisville are provided in Figure 3 of Chapter 9. This graphic contains data for suspended solids under two flow conditions, and riverbed material taken from various points across the river. It is interesting to note that at Louisville the particle size distribution of the streambed is very similar to the particle size distribution of the adjacent aquifer at a similar elevation. It appears that the annual sorting of bed material in current geologic time has not resulted in a significantly different mix of material from that originally deposited by glaciation.

3.2 Estimating Riverbed Shear Stress with Stream Slope

The shear stress acting on a riverbed manifests itself in several physically observable characteristics of a stream, the most obvious being the surface slope of the stream. The slope of the river surface undisturbed by falls or ripples provides a direct measure of the resistance to flow imparted by a streambed. In a perfectly uniform reach of a river, the stream slope provides a direct measure of riverbed shear forces. However, the presence of bends, bedforms (ripples and dunes on the streambed), and physical obstructions like bridge piers and driftwood also impart a resistance to flow, and the total stream energy loss inferred by stream slope may be as much as twice that exerted by streambed shear forces alone (Leopold, 1992).

Extensive field data on stream surface elevations were collected on the Ohio River in the Louisville area by USGS for a stream modeling program funded by ORSANCO (Wagner, 2001). This project included both field-measured surface elevations and flow-modeled surface elevations from which streambed characteristics may be computed. These data were supplemented with stream slope data gathered by the author from USGS, U.S. Army Corps of Engineers, National Oceanic and Atmospheric Administration, and Louisville Water Company sources for the April 2002 high flow condition experienced in the Ohio River.

These slope data were used to estimate the shear stress on the riverbottom according to the technique described in Julien (1998) as follows:

Shear stress = Slope * Density of water * depth

Available data from three stream flow conditions were evaluated for stream slope and computed shear stress. Between the points of measure there are few bends and no bridges or dams, and thus the calculations were expected to give reasonable estimations of bed shear stress. These calculations are summarized in Table 1.

The **maximum** estimated riverbed shear stress was 9.2 Newtons/m^2. This compares to the **average** shear stress on the Rhine River of 10 N/m^2 as reported by Schubert (2002).

Table 1. Shear Stress Estimated from Slope Calculations

Location (river miles)	Flow m^3/sec	Slope 1/1000	Depth (meters)	Shear Stress (Newton/m^2)
High Flow Conditions				
589.8 to 594.6	10,847	0.043	9.6	4.05
594.6 to 599.5	10,847	0.051	12.3	6.13
599.5 to 604.8	10,847	0.047	13.4	6.16
560 to 600.6	10,818	0.058	11.1	6.31
600.6 to 604.8	10,818	0.036	13.9	4.90
560 to 600.6	13,282	0.084	11.1	9.16
Low Flow Conditions				
589.8 to 594.6	963	0.0031	7.6	0.24
594.6 to 599.5	963	0.0019	10.7	0.20
599.5 to 604.8	963	0.0093	12.2	1.11

3.3 Estimating Riverbed Shear Stress from Stream Velocity Profiles

The shear forces are a function of stream velocity, and may be estimated by various stream velocity measures such as average stream velocity, which is often estimated by stream flow. The one-dimensional average stream velocity is a gross estimate of complex 3-dimentional in-stream velocities. Under ideal conditions, the velocity in a direction of flow perpendicular to the cross-section of the stream will demonstrate a profile versus depth that is logarithmic in shape with zero velocity at the riverbed, (Julien, 1998).

The characteristics of this idealized profile provide an estimate of the shear stress imparted by the stream bed at that point. This technique of estimating shear stress on a streambed requires data on the velocity profile of the stream. Two hypothetical velocity profiles with zero velocity near the riverbed and a logarithmic increase in velocity with depth from the bottom are shown in Figure 4, demonstrating relatively low shear stress from a smooth-bottom stream and higher shear stress from a rougher bottom stream.

A calculated shear velocity, shear stress, and friction slope can be derived from any two points on the velocity profile, according to the following equations (from Julien, 1998):

$$\text{Shear Velocity} = k^* \text{ Ln } (V_2 - V_1)/\text{Ln } (D_2/D_1)$$

Bed shear stress = (density of water)*(bed shear velocity)^2

Friction slope = (shear stress)/(spec wt water*depth from bottom)

In these equations, **V** is the velocity at a given depth, **D** is the depth from the stream bottom, and ***k*** is the von karman constant of 0.4, the density of water is 1000 kg/m^3, and the specific weight of water is 9810 Newtons/ m^3 at 10 degrees Celsius.

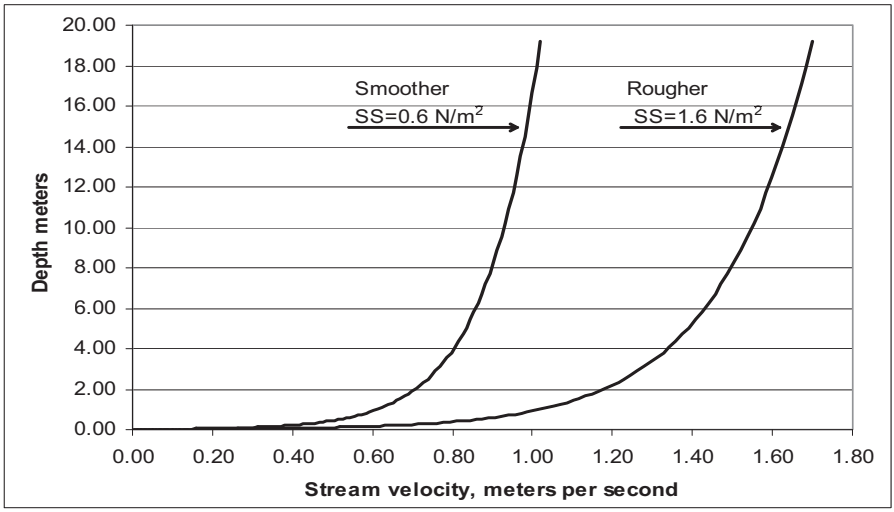

Figure 4. Theoretical Velocity Profiles

Recent advances with in-stream velocity measurement with acoustic doppler current profiler technology have provided huge databases of discrete velocity components across entire river cross-sections. These data allow the estimation of riverbed shear forces at specific locations, based on the velocity profile at that point. Profiler technology suffers from the inability to produce data within one meter of the stream bed and stream surface. The velocity readings near the stream bed are critical in estimating the riverbed shear stress, thus limiting the value of these data in estimating shear stress.

Velocity profiles were measured on the Ohio River in the Louisville area by USGS (Wagner, 2001) using acoustic doppler current profiler technology. Data selected for the particular evaluation in this chapter were

collected at mid-stream at a river flow of 11,000 m^3/sec and are presented in Table 2. These data are instantaneous readings, and are thus subject to the variations caused by eddy currents. Ideally, time-averaged data would be used; however, the profiler data by its nature is instantaneous.

Because of the variability of the data and its departure from the theoretical log profile with zero velocity at the riverbed, some interpretation of the profile is required in order to estimate riverbed shear stress. The profile was fitted to a logarithmic curve using Excel's log estimate regression function, and values for shear velocity, shear stress, and friction slope were calculated. The profile was then modified with a zero velocity boundary and the log-fit curve data was again analyzed for shear velocity, stress, and slope. The various manipulations to the data are shown in Figure 5, and a summary of these calculations for shear velocity, shear stress and friction slope is provided in Table 3.

Table 2. Velocity Profile Data from Acoustic Doppler.

depth	velocity
meters	m/sec
11.44	1.63
10.94	1.69
10.44	1.68
9.94	1.56
9.44	1.70
8.94	1.62
8.44	1.60
7.94	1.50
7.44	1.51
6.94	1.47
6.44	1.42
5.94	1.31
5.44	1.37
4.94	1.29
4.44	1.28
3.94	1.27
3.44	1.27
2.94	1.25
2.44	1.01
1.94	1.03
1.44	0.91
0.003	0.00
AVG	**1.42**

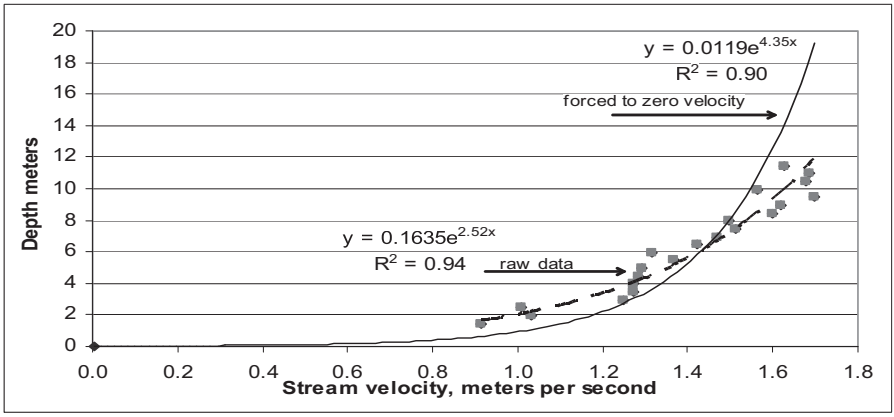

Figure 5. Modifications of the Velocity Profile for Shear Stress Calculations.

Table 3. Shear stress calculations from modifications of velocity profile data.

	Shear velocity m/sec	shear stress N/m^2	friction slope
raw data log-fit	0.15	22	0.0002
raw data plus forced zero	0.08	6.4	0.000056
Bottom 20' plus zero	0.07	4.9	0.000043

The most notable impact of these data manipulations was the assignment of a zero velocity near the stream bottom, which drove a much flatter slope as the velocity profile neared the y axis, compared to the raw data. This creates an assumed condition of a smoother boundary interface, compared to the shape of the profile without a forced zero intercept.

3.4 Estimating Riverbed Shear Stress from Streambed Sediment Transport

One of the more intuitive methods of assessing the shear stresses exerted on a streambed is to evaluate the size of the media that is in transport on the riverbed. While this can be accomplished by capturing media in transport during various flow events, it is also possible to get an indication of these shear stresses by simply observing the media on streambed itself under normal flow conditions.

Streambeds have naturally occurring and predictable variations in shear stress, depending on the stream geometry. It is easy to observe the

impact and variations of shear forces on a stream by looking at a typical stream through a bend, pool, and riffle. Outside bends indicate high shear forces with steep cut walls and deposition of larger stones, or no deposition at all. Insides of bends show a gradation of smaller stones and gravels indicative of the lower velocities and lower shear stresses. Riffles reveal the larger stones that move only during high flow events, while bars show the impact of decreasing shear stresses downstream of bends and as the water levels recede after higher flow events. These patterns are consistent in both small and large streams.

It is also possible to use riverbed media to estimate shear forces resulting from recent flow events, as stones moved recently will be placed randomly on the streambed, thus exposing indications of having being recently moved. In areas where a particular size stone has recently moved, algae growth on both the top and bottom indicates recent movement. A stone with no algae present indicates that the stone moved from below the armor layer of the stream, and was recently placed on the surface. By observing such deposition patterns in conjunction with recent streamflow events and measuring the stones on the riverbed, it is possible to estimate the relative shear stresses at various points in a stream, and with various flows.

An example of this shear stress estimating technique is provided with the Great Miami River in Cincinnati. Following a high flow event of 570 m^3/sec, stones as large as 0.3 meter by 0.1 meter had rolled, as was indicated by algae on both the top and bottom of a stone as it lay in the stream. This stone was taken from a riffle and was typical of those found there (see the photographs in Figure 7). This circumstance would indicate the higher range of shear stresses for the stream for the given flow event. Most of the exposed bars were covered with medium cobble, roughly 0.1 meter by 0.02 meter, indicating moderate or average shear forces for the streambed (see lower picture in Figure 7). The inside bends, conversely, had a wide range of stones on the surface, but only the smaller of these indicated recent movement (0.05 meters and smaller).

Julien (1998) provides a compilation of data from the Highway Research Board, indicating the threshold shear forces required to move granular material in a streambed (Table 4). These values indicate that the larger stones described above reflect shear stresses in the range of 200 N/m^2, while the cobble on the bars reflect shear stresses in the range of 80 N/m^2, and the gravel in the inside bends reflects shear stresses in the range of 40 N/m^2.

Table 4. Approximate Threshold Conditions for Granular Media at 20°C (from Julien).

Class name	d_s (mm)	Critical Shear Stress (N/m^2)
Large cobble	128	111
Small Cobble	64	53
Very Course Gravel	32	26
Course Gravel	16	12
Medium Gravel	8	5.7
Fine Gravel	4	2.7
Very Fine Gravel	2	1.3
Very Course Sand	1	0.47
Course Sand	.5	0.27
Medium Sand	.25	0.19
Fine Sand	.125	0.145
Very Find Sand	.0625	0.110

This technique provides an opportunity to "ground truth" calculated shear stresses based on other estimation techniques, and supports the logical conclusion that the steeper streams with more dramatic flow variation will show higher and more variable shear stresses. This technique also provides information regarding the variation in streambed shear stress as a function of stream geometry within a given reach. This method of estimating riverbed shear stress is more easily applied to streams that provide easy access (streams with low flow depths of 1 meter or less), although sediment samples from deeper streams may be similarly interpreted.

The lower picture in Figure 7 also shows the natural orientation of riverbed media that produces anisotropic conditions in an aquifer. Random flipping of stones on the riverbed during high flow events results in random orientations with respect to resistance to streambed shear forces. Those stones in orientations exhibiting the greatest resistance to shear resist flipping, while stones in other orientations are more likely to flip again and again, until they are positioned in an orientation that resists flipping or are transported to an area of lower shear stress. This selectivity with respect to shear forces results in the pattern of consistent orientation and spacing of the stones on the riverbed as seen in the picture.

Referring again to the sediment data from the Ohio River at Louisville in Chapter 9, the bulk of the riverbed is composed of media with a D_{50} of 0.3 to 0.8 mm, indicating a shear stress at streambed transport of 0.2 to 0.4 N/m^2. The largest media on the streambed is in the range of 10 to 15 mm, indicating shear stresses of 6 to 10 N/m^2. These stones were found in a trough in the vicinity of a flow separation in the stream caused by upstream deposits from a small stream, and thus represent localized shear stresses.

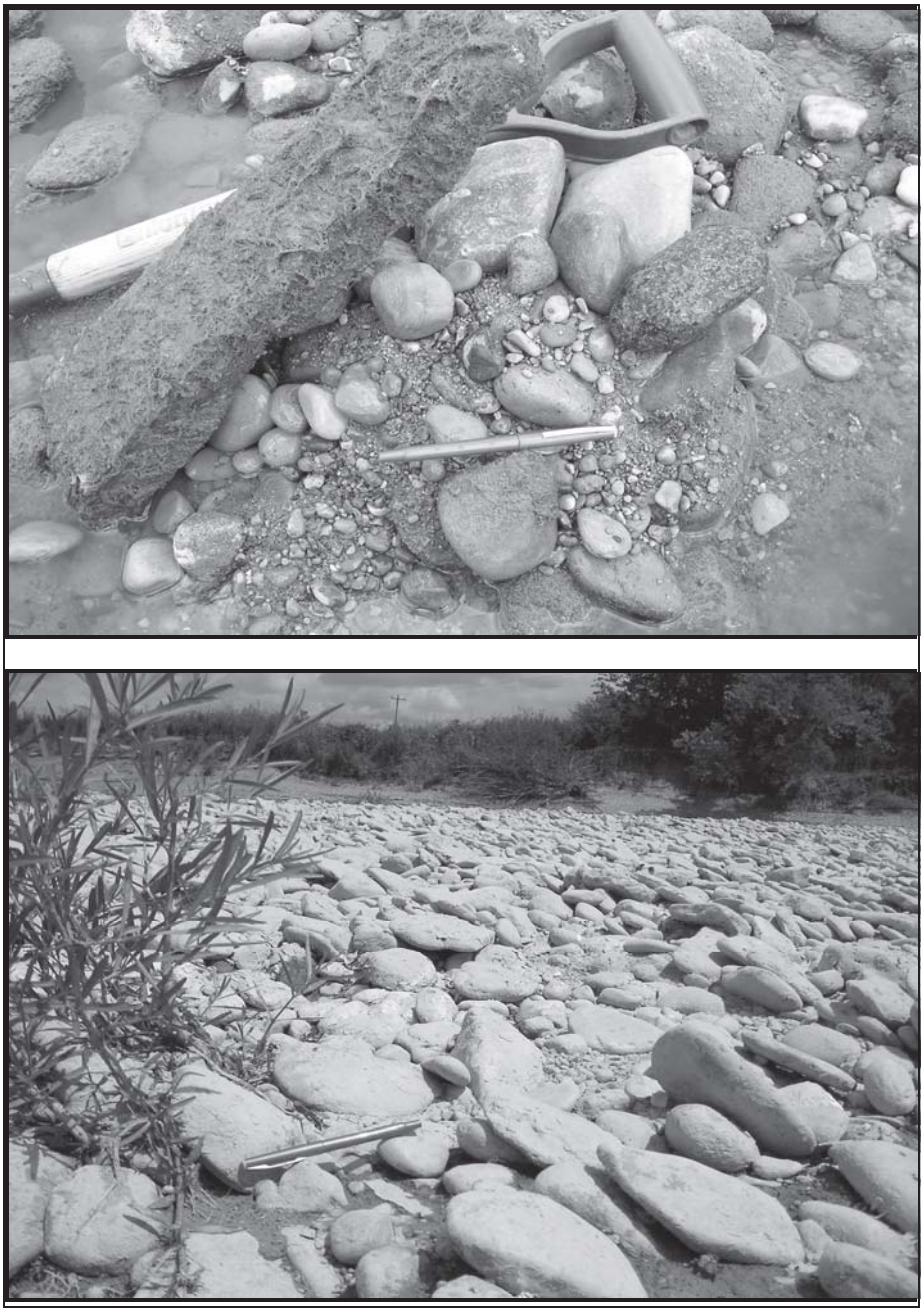

Figure 6. Riverbed Sediment from the Great Miami River.

The data from the Great Miami and Ohio Rivers illustrate how riverbed material analysis can be used to easily categorize the differences in streams with regards to shear stress. These differences are noticeable both within a given stream and between streams in general.

3.5 Estimating Shear Velocities caused by River Traffic

The focus of this chapter has been slanted towards measuring the shear stresses caused by natural streamflow. However, on streams used for commercial transport, the bed shear stresses exerted by a passing vessel can exceed even the highest stresses exerted by natural flow. In regularly traveled streams, this traffic can represent a short-term, high frequency shear stress event that could have a significant impact on mediating the impacts of clogging.

The techniques for measuring the magnitude of shear stress from a passing vessel include direct measurement of velocity near a passing vessel and measurements from scale-models of rivers using simulated vessels. While data from these two techniques are sometimes conflicting, it is obvious that vessels on smaller navigable streams exert significant shear stresses on stream bottoms. (Maynord, 1990 and 2000)

Several elements of vessel passage causing shear stresses have been described in the literature. The first is a reversed-pulse resulting from the headwater immediately in front of the vessel, which leads the vessel by as much as 50 meters. Depending on whether the vessel is traveling upstream or down, the drag force from the vessels can impart a higher or lower velocity on the stream surface. The displacement of water under the vessel can cause significant local changes in stream velocity (up to 1 meter per second), especially when the submerged vessel cross-section is large compared to the stream cross section. Behind the passing vessel, the prop-thrust impact tends to be exerted primarily on the stream surface, with return flow occurring at the streambed.

At the point immediately below the propeller, however, the return flow re-circulating from behind the tow and the upstream flow being accelerated through the propeller meet, creating a significant riverbed stress. At this location, flow directions have been observed to be vertically upward towards the propeller. It is anticipated that this upward flow would result in a highly turbulent flow pattern, and that significant shear stress would be anticipated on the riverbed.

It has also been observed that riverbed shear forces are much greater when vessels are changing directions or starting motion. Shear stresses under these conditions can be much more significant than for a passing vessel at constant velocity.

The published information is augmented with the author's observation of visually noticeable increases in stream turbidity behind a passing vessel on the Ohio River, as observed from the air. During low turbidity river conditions, the area of higher turbidity was sharply defined as a narrow plume approximately the width of the vessel, and was visible for at least one kilometer beyond the passing vessel. It is thus concluded that passing vessels can exert adequate shear forces in their immediate path capable of re-suspending riverbed sediment, and could have an impact in the overall clogging of riverbeds.

4. COMMENTS

An understanding of the forces at work on a streambed aids in interpreting how a streambed responds to hydraulic flows in the stream and aquifer. The combination of flow into the riverbed and particle invasion work together to clog an otherwise highly productive streambed. The regenerative forces of streambed scour tend to restore the conductivity of the streambed. The balance between the degenerative clogging processes and regenerative scouring processes will determine the sustainable yield of the system, assuming biological and geochemical clogging processes are not an issue.

Nevertheless, there remains a need to provide practical measures that will allow design engineers to quantify the clogging and scouring processes, and design systems that reflect the natural capacity of the streambed and aquifer.

4.1 Predicting Riverbed Shear Stresses

Shear stress calculations can be made using an average stream velocity, velocity profiles, or stream slope data. If average values are used, a general stream energy value will be generated. While this energy value is valuable in predicting streambed shear stresses, it does not predict specific conditions that exist at a particular site. The variation of streambed shear stresses as impacted by bathemetry, bends, bedforms, and obstructions can greatly impact streambed hydraulic conductivity at a particular location in a stream cross-section.

It is thus necessary to consider both the general scouring potential of a stream and the site-specific elements of the riverbed when considering a site for riverbank filtration Analyzing riverbed sediments prior to design improves the likelihood of an effective design. Following changes in

riverbed composition after initiation of pumping can provide valuable information for managing the long-term capacity of the system.

4.2 Predicting Unsaturated Conditions

It is critical in the design stage to estimate the maximum pumping conditions allowable for a site that will prevent the aquifer under the recharge area of the riverbed from becoming unsaturated. Techniques for collecting data under streambeds are presented in Chapters 9 (Hubbs) and 11 (Constantz). The piezometric surface under a streambed might be predicted through modeling, given parameters for aquifer and streambed conductivity, stream flow characteristics, and wellfield operation data. This is a research need for modeling; to better predict the piezometric head under a streambed given aquifer and streambed conductivity and available head.

4.3 Aquifer Storage

The volume of storage available in a particular aquifer is also important in RBF systems if the clogging process progresses to the point where riverbed infiltration becomes limited. Decreased flow from the streambed resulting from seasonal clogging or clogging resulting from less frequent events such as drought can be offset by supplemental flow from aquifer storage on a temporary basis, which will be induced by the decreased head in the aquifer. Under these conditions, the point of recharge from the stream will be extended away from the well, either across the width of the stream in very large rivers, or upstream and downstream in narrower streams.

5. ACKNOWLEDGEMENTS

Work described in this project was funded by the Louisville Water Company, with contributions from the American Water Works Association Research Foundation and the United States Geologic Survey.

REFERENCES

Constantz, J. Unsaturated Zone Processes in the Sonoma County Recharge Basins. U.S. EPA /USGS Meeting on Cryptosporidium Removal by Bank Filtration. Reston VA. Sept. 2003.

Gollnitz, W., (personal communication), Cincinnati Water Works, July 2004

Julien, Pierre, *Erosion and Sedimentation*. Cambridge, UK: Cambridge University Press, 1998

Leopold, L.B., and M. Wolman, J. Miller. Fluvial Processes in Geomorphology. Dover Publications, Inc. New York. 1992.

Maynord, S. T., "Velocities Induced by Commercial Navigation", Technical Report HL-90-15, U.S. Army Engineer Research Waterways Experiment Station, Vicksburg, MS. 1990

Maynord, S. T. "Shear Stress on Shallow-Draft Barge Hulls", ENV Report 24, Army Engineer Research Waterways Experiment Station, Vicksburg, MS. 2000

Schlichting, H. *Boundary Layer Theory*. 6th ed., McGraw Hill, New York. 1968

Schubert, J. 2002. Hydraulic aspects of riverbank filtration – field studies. *Journal of Hydrology*. 266(2002) 145-161.

Wang, J. Z. Evaluation of Riverbank Filtration as a Drinking Water Treatment Process, Report 90922, American Water Works Research Foundation. 2002

Wagner,C.R., and D. Mueller, "Calibration and Validation of a Two-Dimensional Hydrodynamic Model of the Ohio River, Jefferson County, Kentucky", USGS Report 01-4091, 2001.

IMPACT OF RIVERBED CLOGGING – COLMATATION – ON GROUND WATER

Igor Mucha, Ľubomír Banský, Zoltán Hlavatý, Dalibor Rodák
GROUND WATER Consulting, Ltd. Kolískova 1, 84105 Bratislava 4, Slovak Republic, SK

Abstract: Clogging in RBF systems is defined in hydrogeologic terms, and analytical methods of measuring reduction in riverbed conductivity are presented. Computer modeling techniques are presented, and a program for estimating the impact of clogging is provided. Water quality of the Danube river is presented in context of impact on infiltrated water.

Key words: River Bank Filtration, RBF, Ground water, colmation, clogging, modeling, water quality, hydrology, Danube River

1. DEFINITION OF CLOGGING

Clogging of a riverbed refers generally to changes in the exchange processes between the river water and ground water. These processes are usually described as infiltration and filtering, and they are accompanied by changes in: flow throughout the riverbed, mechanical filtering or sieving, sorption, chemical oxidation and reduction, and ion exchange.

Clogging affects water flow as an increase of flow resistance between a river and an aquifer. Clogging is time dependent and is a function of various factors, mainly of processes of riverbed sedimentation and erosion, and direction and rate of water flow between a river and an aquifer. This is generally a function of flow velocities, flow rates, content and composition of suspended load and transported bed load material, water level, and biological activity. It is important to understand the changes of flow hydraulics in order to examine clogging.

Stephen A. Hubbs (ed.), Riverbank Filtration Hydrology, 43–72.

Riverbeds and riverbanks are surfaces with equal piezometric head across the river water flow, and therefore the water flow is perpendicular at this surface into the aquifer. Thin layers of finer sediments often cover the riverbed, and some part of the aquifer near the riverbed is clogged to some degree by fine particles that settle inside of aquifer pores during aquifer recharge/infiltration processes. In such an event, there could be two kinds of flow; flow that is impounded (third-order boundary), and/or flow that is not impounded (second-order boundary). (Shestakow V., M., 1977, 1979, Mucha I., Schestakow V., M., 1987). This is illustrated in classical figures by Schestakow (1979) shown in Figure 1.

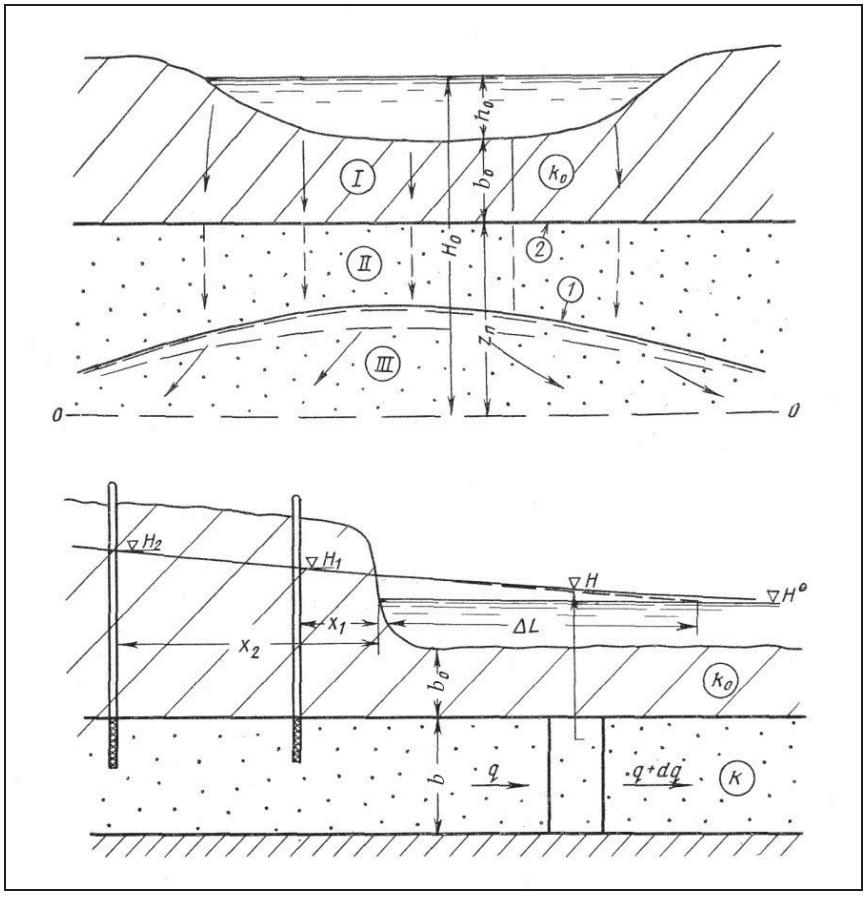

Figure 1. Ground water flow close to reservoir or river (Schestakov 1979). (1) ground water level, (2) resistive layer or clogged river bed sediments. Top – not impounded, free ground water level; bottom – impounded ground water level into clogged sediments.

Flow with impounded ground water flow arises when the piezometric level is above the zone of the clogged riverbed. In the case of a thin clogged layer, the flow is perpendicular to the riverbed and the flow velocity is Figure 2:

$$v = (H^o - H)\, k_o/b_o$$

and in the case without impoundment

$$v = h_o\, k_o/b_o$$

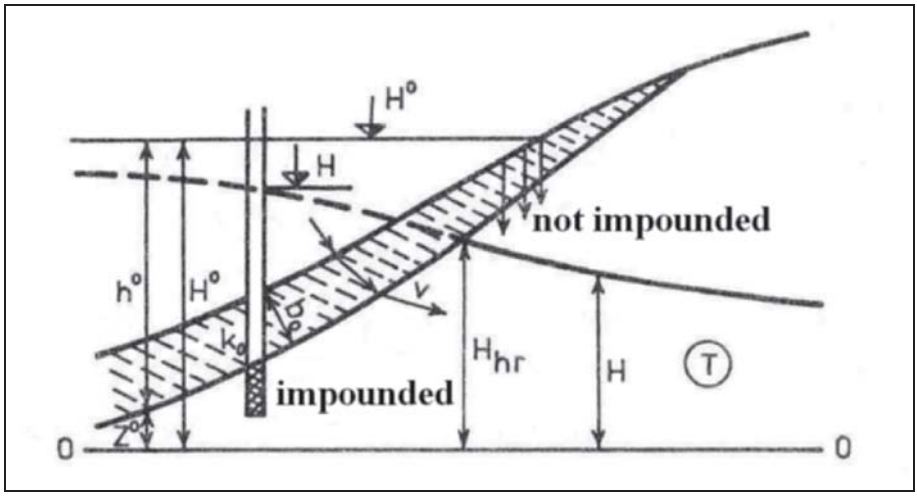

Figure 2. Infiltration via impounded and not impounded parts of riverbed

The ratio k_o/b_o is the clogging characteristic, k_o is hydraulic conductivity of clogging zone, and b_o is its thickness. During the survey, it is usually not possible to estimate separately the values of k_o and b_o. Flow throughout such a riverbed is called riverbed infiltration or recharge, and if pumping is involved, it is called induced infiltration or recharge. For practical computation, flow rate per 1-meter wide vertical cross-section is:

$$q = k_o\, A\, (H^o - H)/b_o = T\, (H^o - H)/\, \Delta L,$$

which means

$$A\,k_o/b_o = T/\Delta L, \quad \text{and} \quad \Delta L = A\,k_o/(b_o\,T)$$

where:
k_o – hydraulic conductivity of clogged river bottom layer, (m/s);
b_o – thickness of the clogged river bottom layer, (m);
A – flow cross section by unit length of the river, (m^2);
H^o – river water head, (m);
h^o – piezometric head on the bottom of the clogged layer, (m);
q – flow rate (discharge), (m^3/s);
ΔL – substituting length of aquifer characterizing clogging, (m);
T – aquifer transmissivity (m^2/s).

ΔL is the general hydraulic resistance parameter equal to the aquifer length, characterizing resistance of the clogged passage of the river bottom. This parameter also includes the partial penetration of the river, anisotropy, and aquifer heterogeneity. *ΔL* refers to generalized characteristics of the river bottom, which determine water level difference and gradient increase between the river and ground water level.

The *ΔL* clogging parameter is time and event dependent. *ΔL* slowly increases during the usual river flow rate and flow velocities as a result of sedimentation processes. During flood events and erosion processes, *ΔL* decreases relatively quickly.

ΔL is originally derived for a boundary condition fully penetrating the aquifer. Therefore, in natural conditions, it also includes hydraulic resistance of a partially penetrating river, and in this case, also hydraulic anisotropy and heterogeneity of the clogged riverbottom and aquifer.

2. PRACTICAL METHOD OF ESTIMATING CLOGGING

2.1 Stationary Groundwater Flow through the Riverbed

The simplest way to estimate *ΔL* is to use a system of observation wells with piezometers, as shown in Figure 1. By plotting river water level and ground water levels against distance, and evaluating ground water level slope, ***ΔL*** could be graphically evaluated directly. While this technique is not very exact, it gives an idea of clogging processes in time and space if there are enough observation wells.

The usual test in for evaluating a site for ground water supply is the pumping test. Stabilization of the cone of depression around a pumping well may occur in the vicinity of a river. Since a river is source of recharge in the pump test, it is possible to replace the well-river system with an "image well" of negative discharge (the method of images), and superpose the Theis equation for this image well into the solution for piezometric surface. A requirement of the pumping test is that it should last long enough to exclude the impact of the water table (delay yield), and when estimating changes of ***ΔL*** in time, the test should be repeated, which is usually not possible. Schestakow (1979) explained the principles of clogging estimation using the pumping test, as illustrated in Figure 3 and explained below.

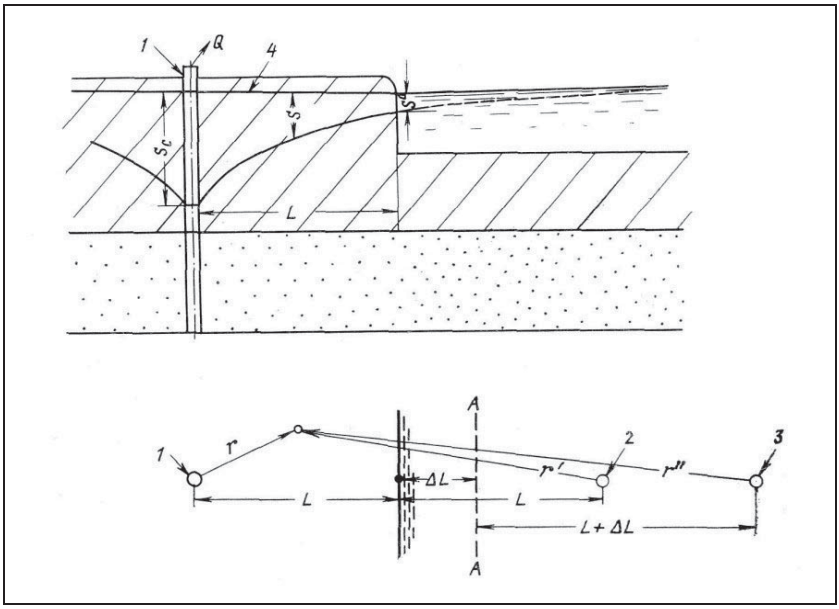

Figure 3. Well near the reservoir or watercourse (1 – well, 2 – image well without clogging, 3 – image well with clogging)

Using the Theis equation, the drawdown in an image well for no clogging is:

$$S = Q/4\pi T\,[W(u)-W(u')]$$

and for clogging is:

$$S = Q/4\pi T\,[W(u)-W(u'')]$$

where:

$u = r^2 S/ (4 T t)$, $u'' = r''^2 S/(4 T t)$

r – radius of image well from observation point (piezometer, well), (m),

r′ – radius of image well from observation point (piezometer, well) without clogging, (m),

r″ – radius of image well from observation point (piezometer, well) including the ΔL , (m),

T – aquifer transmissibility (m^2/s),

S – storage factor (-),

t – time (s)

This equation can be used in the well-known Theis' method by applying bi-logarithmic type curves (Figure 4) or the Jacob simplified semi-logarithmic method (Figure 5).

2.2 Interpretation of *ΔL* using Ground Water Level Fluctuation

Estimation regional and time dependent changes of *ΔL* is best accomplished by using observation wells, continuous surface and ground water level data, and piezometric level fluctuation.

It is necessary to know the development of clogging in time and space when considering: aquifer recharge, ground water level fluctuation, well capacity in aquifers with river boundary conditions, ecological monitoring, river bed sedimentation and erosion, and impact of reservoir construction on all of the above. Because the clogging processes are multifunctional, both quantitative and qualitative monitoring is needed to study these processes.

On a regional scale, the main goal is to establish methods to identify changes between surface and ground water caused by natural and artificial changes in the riverbed, including changes in clogging. These changes are identified through a series analyses of regional data for river flow, river stage (elevation), ground water elevation, and depth-dependent ground water piezometric levels. In general, changes of ground water level near the river are a function of water level and flow-rates in the river, and resulting changes in the riverbed, including the clogging processes.

The following method for evaluating clogging is outlined from the textbook by Schestakow (1979) and Mucha and Schestakow (1987).

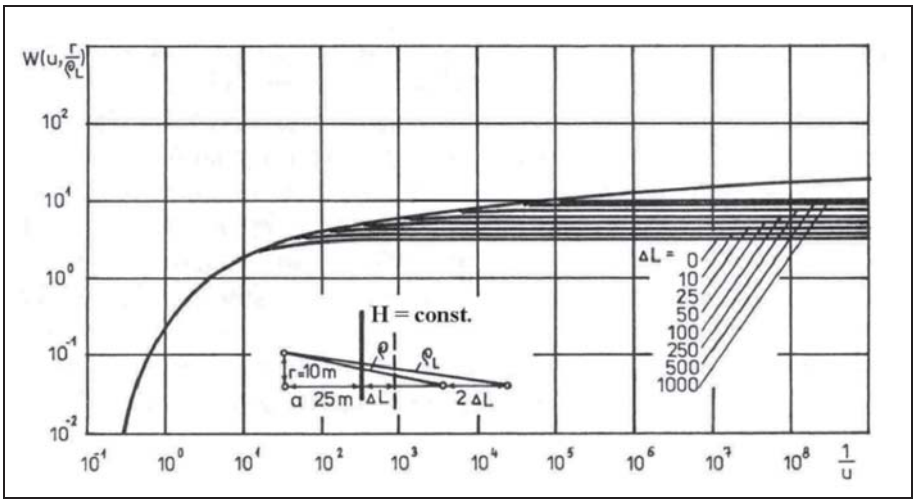

Figure 4. Pumping test curve method type

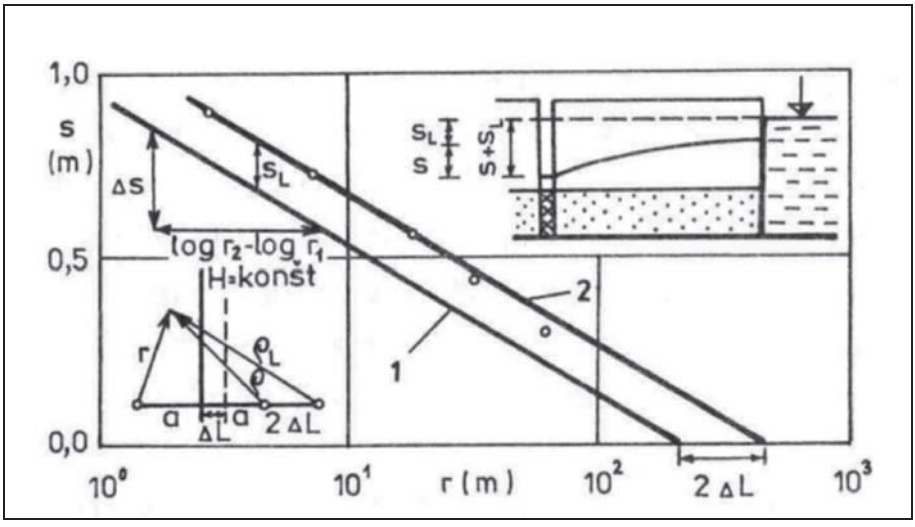

Figure 5. Pumping test semi-logarithmic (straight line) method

Because of time dependent water level fluctuation in the river, which creates boundary conditions for an aquifer, the water level fluctuation should be transformed into:

- – a gradual linear change of water level or,
- – a stepwise system of water level changes.

The general form of the equation describing changes in ground water level ΔH at a distance x from the riverbank, given a transmissibility coefficient of T and a storage coefficient of S, for the river velocity of v for linear change in the river water level (Figure 6), is:

$$\Delta H = v\ t\ R(\lambda), \quad \text{where } \lambda = x/[2(Dt)^{1/2}] \text{ and } D = T/S$$

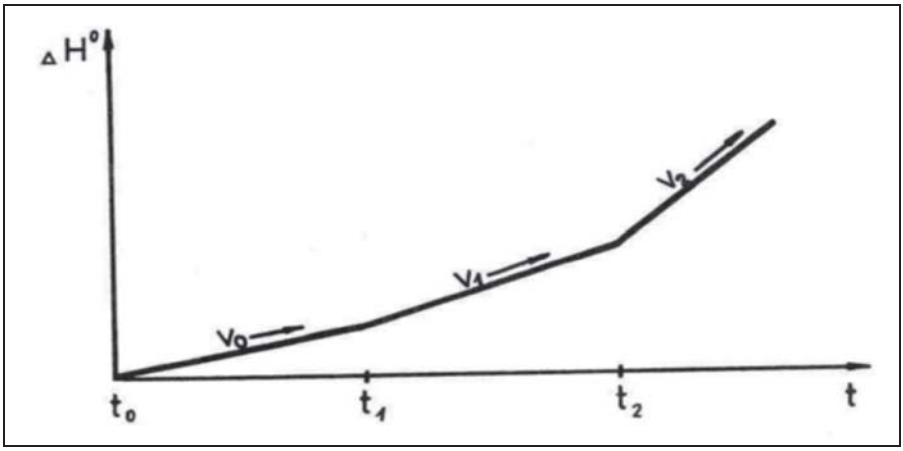

Figure 6. Linear water level changes in a river

Through computation, the real water level in the river is substituted by a broken linear line characterizing velocities of river water level changes. For the first interval it means:

$$\Delta H = v\ t\ R(\lambda), \qquad \text{where} \quad v = v_o\ .$$

For the following intervals it means:

$$\Delta H = v\ t\ R(\lambda) + \Sigma\ (v_i - v_{i-1})\ (t-t_i)\ R(\lambda_i), \text{ for } i=1 \text{ to } n$$

where

$$\lambda = x/2\,[D\,(t- t_i)]^{1/2}, \quad R(\lambda) = (1+2\,\lambda^2)\,\mathrm{erfc}\,\lambda - [2\,\lambda\,\exp(-(\lambda^2)]/[\pi^{1/2}],$$

and erfc is the complimentary error function.

Function $R(\lambda)$ is changed to $R(\lambda,\Theta)$, so that

$$\Delta H = v\,t\,R(\lambda, \Theta), \text{ where}$$

$$R(\lambda,\Theta) = R(\lambda) + [F(\lambda, \Theta) - 2\,\Theta\,\mathrm{ierfc}\,\lambda]/(\Theta^2),$$

$$F(\lambda, \Theta) = \mathrm{erfc}\,\lambda - [\exp(\Theta^2 + 2\,\lambda\,\Theta)\,\mathrm{erfc}(\lambda + \Theta)], \text{ and}$$

$$\Theta = (D\,t)^{1/2}/\Delta L.$$

Change of the ground water level just at the clogged river bottom is:

$$\Delta H = \Delta H_{River}\,F(\Theta),$$

where $F(\Theta) = 1 - \exp(\Theta^2)\,\mathrm{erfc}\,\Theta$, and

$$\mathrm{ierfc}\,\lambda = \exp(-(\lambda^2))/\pi^{1/2} - \lambda\,\mathrm{erfc}\,\lambda.$$

2.3 Stepwise River Water Level Changes

For the stepwise technique for estimating clogging, it is assumed that at boundary $x = 0$, starting from time $t = 0$, that river water level change are stepwise. The magnitude of the immediate change is ΔH^{River}.

The general form of the equation describing changes in ground water level ΔH at a distance x from the riverbank, given a transmissibility coefficient of T and a storage coefficient of S, for one step of water level change(Figure 7), is:

$\Delta H = \Delta H^{River} F(x,t,D) = \Delta H^{River} F(\lambda)$, where

$F(\lambda) = \text{erfc}(\lambda)$, $\lambda = x/ [2 (D t)^{1/2}]$, $\Delta H = \Delta H^{River} \text{erfc}(\lambda)$.

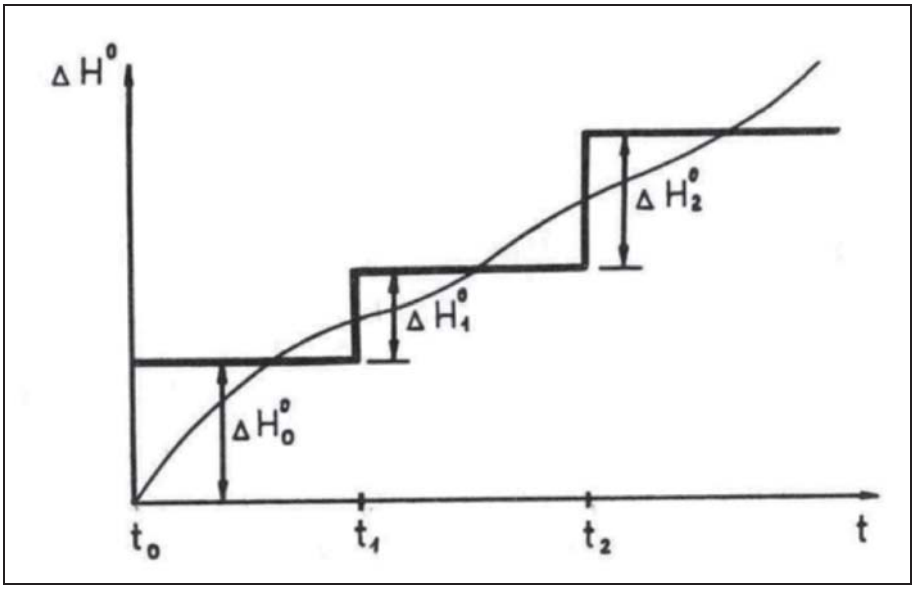

Figure 7. Stepwise water level changes in a river

The result will be valid in the time *t* in the one step of change as a result of the change in a river elevation. For the first time step change of ground water level it is:

$\Delta H = \Delta H^{River} \, erfc(\lambda)$, where $\Delta H^{River} = \Delta H_o{}^{River}$.

For the following steps:

$\Delta H = \Sigma \, \Delta H^{River} \text{erfc}(\lambda_i)$, for i=1 to n

Where

$\lambda = x/ [2 (D (t-t_i))^{1/2}]$

In the case of the boundary condition of the third order

$\Delta H = \Delta H^{River} F(\lambda, \Theta)$, where

$F(\lambda,\Theta) = erfc(\lambda) - [exp(\Theta^2 - 2\,\lambda\,\Theta)\, erfc(\lambda + \Theta)$, and

$\Theta = (D\,t)^{1/2}/\Delta L$.

ΔL is the hydraulic characteristic of the riverbed clogging.

$\Delta H = \Delta H^{River}\, F(\Theta)$, where

$F(\Theta) = 1 - \exp(\Theta^2)\, erfc\, \Theta$.

3. PRACTICAL COMPUTATIONS

Based on previous equations, simple software in MICROSOFT FORTRAN 4.0 was written (see APPENDIX). After the start of the program, the following data are requested:

- Name of file containing water level in the river; for example, **h-me.**
- Name or number of the well; for example, **1949**.
- Distance of monitoring well or distance where computation is required; for example, **120** m. In principle, the computation can be achieved for an arbitrary place in the aquifer, without respect to the existence of the observation well. The latter case is used for ground water level prediction at the place of the observation well.
- ***ΔL*** of clogging; for example, **10** m, or **0** for no clogging.
- Transmissivity of the aquifer; for example, **0.008** (m^2/s).
- Storage coefficient (water table storage – specific yield [elastic aquifer storage if the aquifer is confined]); for example, **0.2**.
- Starting date for computation; for example, 1 5 1993 (D M Y).
- Number of days for computation; for example, **20** (days).

Upon data input, the following screen is generated:

```
calculation period start 1. 1.1980 end  1. 1.2003
 (to change dates, modify file dates.ini)
Enter Filename of source water level data, without .txt extension: h-me
Enter filename of simulated well (without the .txt extension): 1949
Distance of well from river in m: 120
Colmatation distance of river (m): 0
Transmissivity in m2/s, e.g. 1.0: 0.008
Water Table Storage in (-), e.g. 0.2: 0.2
```

Starting Date of Computation as DD MM YYYY, e.g. 1 1 2000: 1 5 1993
Number of Computation Days (integer), e.g. 30: 20

Part of the output from the file 1949.dete.txt

```
1   2  3          4    5         6         7         8         9
26,  4,1993, 34085,110.2200,   .0000,   .0000,111.2800,   .0000
27,  4,1993, 34086,110.1800,   .0000,   .0000,111.1000,   .0000
28,  4,1993, 34087,110.1700,   .0000,   .0000,111.3000,   .0000
29,  4,1993, 34088,110.1800,   .0000,   .0000,111.3500,   .0000
30,  4,1993, 34089,110.1900,   .0000,   .0000,111.3200,   .0000
1,   5,1993, 34090,110.1600,110.1600,110.1600,111.2400,   .0000
 2,  5,1993, 34091,110.1500,110.1431,110.1605,111.0800,  -.1600
 3,  5,1993, 34092,110.1000,110.1025,110.1494,110.8500,  -.2300
 4,  5,1993, 34093,110.0600,110.0852,110.1400,110.9200,   .0700
5,   5,1993, 34094,110.0700,110.0586,110.1195,111.0900,   .1700
6,   5,1993, 34095,110.0900,110.0482,110.1074,111.1600,   .0700
7,   5,1993, 34096,110.0800,110.0386,110.1037,111.0100,  -.1500
8,   5,1993, 34097,110.0500,110.0333,110.1058,110.8600,  -.1500
9,   5,1993, 34098,110.0300,110.0063,110.0953,110.7700,  -.0900
10,  5,1993, 34099,110.0000,109.9629,110.0731,110.6900,  -.0800
11,  5,1993, 34100,109.9800,109.9146,110.0463,110.5900,  -.1000
12,  5,1993, 34101,109.9700,109.8952,110.0278,110.6900,   .1000
13,  5,1993, 34102,109.9700,109.8685,110.0048,110.7700,   .0800
14,  5,1993, 34103,109.9500,109.8610,109.9932,110.7900,   .0200
15,  5,1993, 34104,109.9300,109.8539,109.9868,110.7200,  -.0700
16,  5,1993, 34105,109.9100,109.8555,109.9857,110.7100,  -.0100
17,  5,1993, 34106,109.9100,109.8330,109.9741,110.6300,  -.0800
18,  5,1993, 34107,109.8900,109.8211,109.9659,110.6100,  -.0200
19,  5,1993, 34108,109.8500,109.7396,109.9308,110.1900,  -.4200
20,  5,1993, 34109,109.7900,109.7537,109.9294,110.3900,   .2000
21,  5,1993, 34110,109.8300,109.7237,109.8984,110.7100,   .3200
22,  5,1993, 4111,109.8100,    .0000,   .0000,110.7500,   .0000**
23,  5,1993, 34112,109.8300,   .0000,   .0000,110.7900,   .0000
24,  5,1993, 34113,109.8200,   .0000,   .0000,110.5700,   .0000
    *start pf computation
    **end of  computation
```

The results are written in the file, for example **1949.dete.txt**, in which 1949 refers to the name, in this case the number of the well, and

dete indicates that the deterministic model was used. Headings for the individual columns are:

1. day
2. month
3. year
4. order number in database
5. water level in observation well (for comparison with results, if inputted), (m above the sea level – m a.s.l)
6. water level computed using stepwise change of water level in river, (m a.s.l)
7. water level using linear change of water level in river
8. water level in the river, (m a.s.l)
9. difference of water levels to previous day (m).

4. DISCUSSION

4.1 Hydraulic Methods for Measuring Clogging

Hydraulic methods can be used to evaluate ground water level and river water level fluctuations. As an example, measured and computed data from the well No. 1949, are provided in Figure 8.

The following conclusions can be drawn from the examples:

- The computed values of ground water levels using ΔL are river water level dependent. ΔL is also dependent on river water level. This means that ΔL is different for different water levels.
- There is a difference in the flow rate and the water level rating curve for a gauging station in various intervals (Figure 9). This also implies differences in any development (erosion, sedimentation, meandering) of the riverbed, as well as changes in ΔL.
- Using the hydraulic method, it is possible to hypothesize what will happen if the ΔL (clogging) or other parameters are changed.
- Parameters of boundary condition of the third order, important for modeling of ground water flow, could also be evaluated from ΔL.

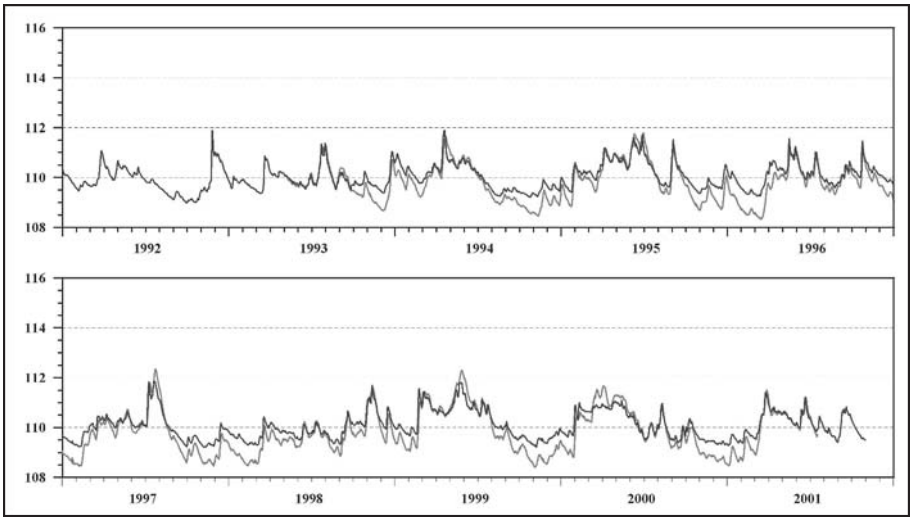

Figure 8. Measured and computed data from the well No.: 1949

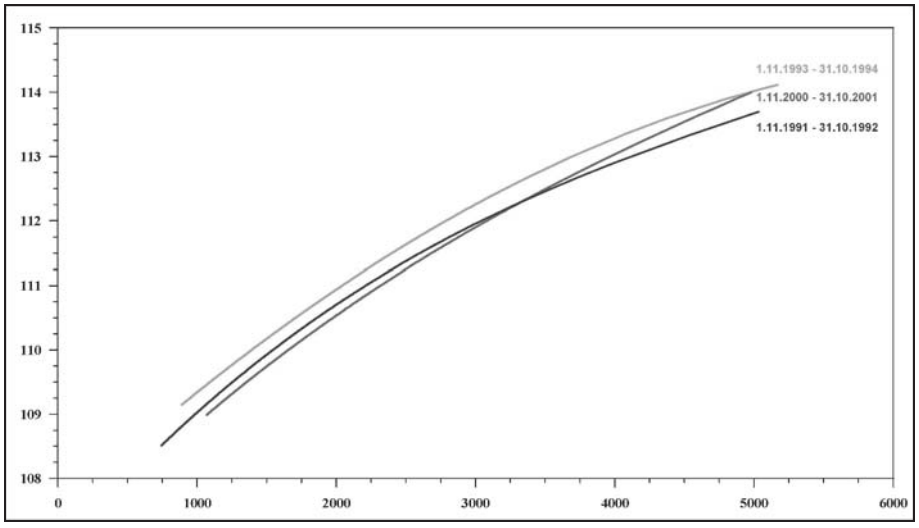

Figure 9. Changes of water level rating curve at gauging station in various time intervals

Using equation $\Delta L = A\ k_o/b_o\ T)$, and inserting assumed variables or by modeling estimated data for sedimentation variables k_o and b_o and known transmissibility T, it is possible to estimate drawdown in a well or system of wells near the river for various scenarios. The same method can be used to estimate well system

capacity for various conditions. Hydraulic conductivity can be estimated from the media size analyses (particle size distribution), for example using the Carman-Kozeny method (a computer program included in Mucha, Shestakow 1986).

4.2 Ground Water Quality and Clogging

Ground water quality processes after bank infiltration at this area have been previously described (Mucha et. al., 2002) and are therefore only summarized here. However, the river water quality is the first precondition of the ground water quality after recharge – infiltration through the clogging zone. To describe the long-term changes in the river water composition, data for the Danube River have been summarized in Figures 10-13. Figure 10 shows the fluctuation of, electrical conductance, sulfate, and chloride. Figure11 shows redox components: oxygen, total organic carbon, COD-Mn (Chemical oxygen demand) and nitrate. These data represent water quality of the Danube River at the entrance into the area of the alluvial fan at Bratislava.

To show seasonal changes of some components, graphs indicate river flow, water temperature, sulfate and chloride (Figure 12) and water temperature, oxygen, total organic carbon, and nitrate (Figure 13) for the Danube River at Bratislava.

Alluvial aquifers are the largest reservoirs and producers of ground water able to be recharged by the river or by artificial recharge canals. Rivers are usually the largest natural water sources for aquifer recharge under exploitation. Under natural conditions, without exploitation of the aquifer, rivers usually drain alluvial sediments and clogging is minimal. Following the start of exploitation some changes occur. First there is change of water flow direction from the flow of ground water toward the river to flow from the river into the aquifer. This has a general impact on ground water chemistry. This impact is further influenced by the qualitative and quantitative changes in the clogging sediments.

Clogging of the riverbed (including river branches, natural or artificial canals) essentially influences recharge abilities and the quality of the water recharging an aquifer.

Reduction and oxidation processes exert an important control on ground water quality under natural, semi natural and artificial conditions. They are responsible also for so called self-purification processes, sorption and degradation of pollution.

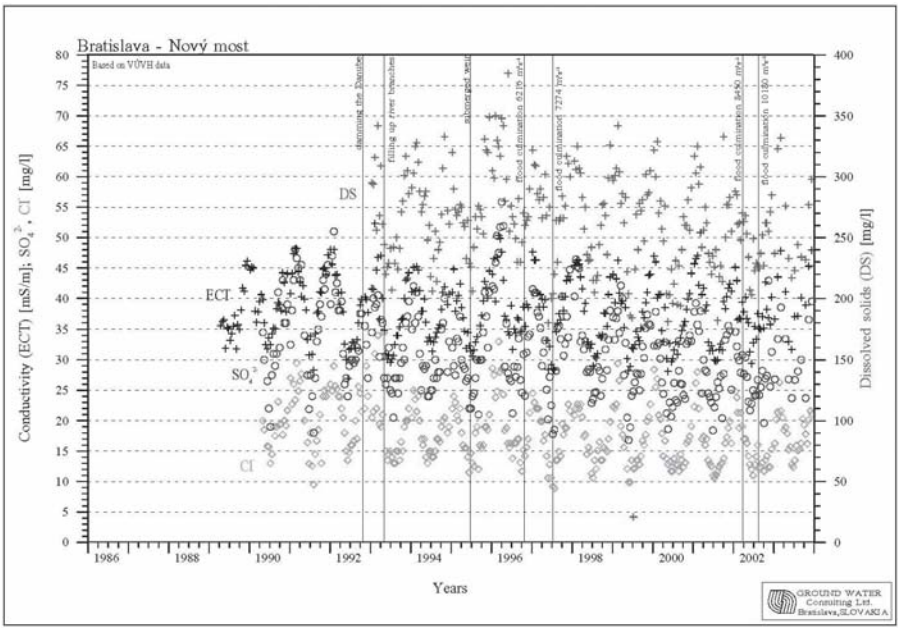

Figure 10. Fluctuation of conductivity, sulfate, and chloride in Danube River Water

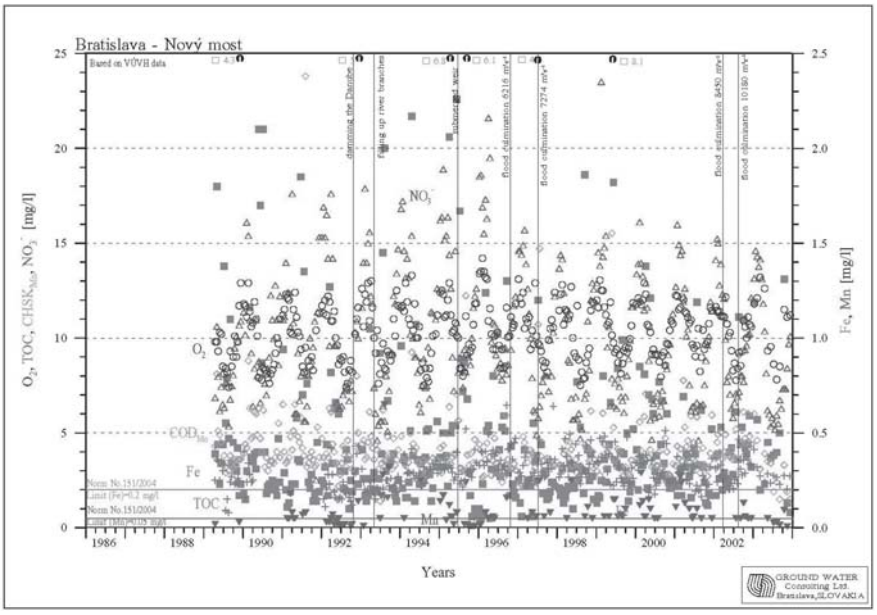

Figure 11. Fluctuation of redox components: oxygen, total organic carbon, COD_{Mn} (chemical oxygen demand) and nitrate in the Danube water

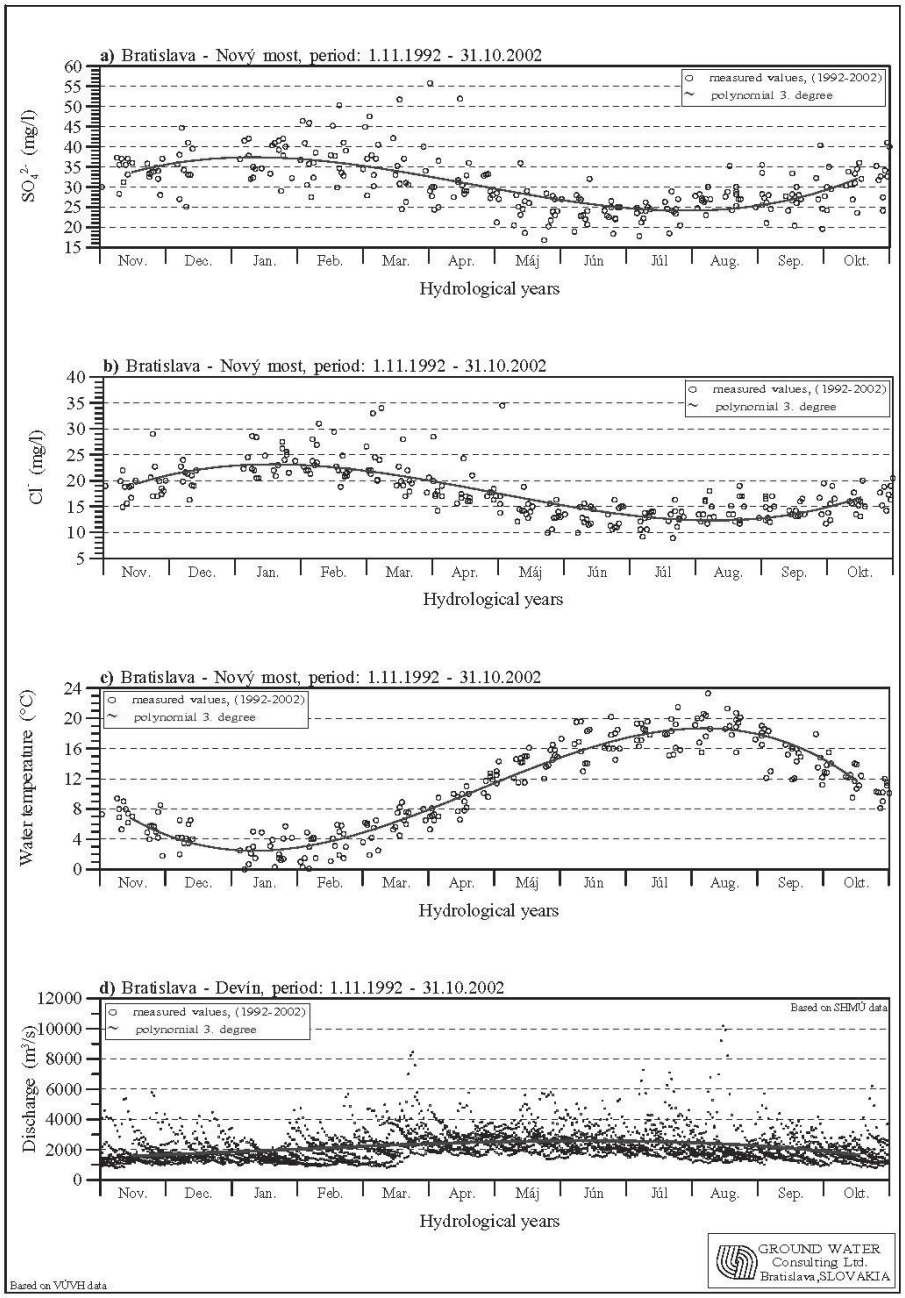

Figure 12. Seasonal changes of sulfate, chloride, temperature, and flow in the Danube

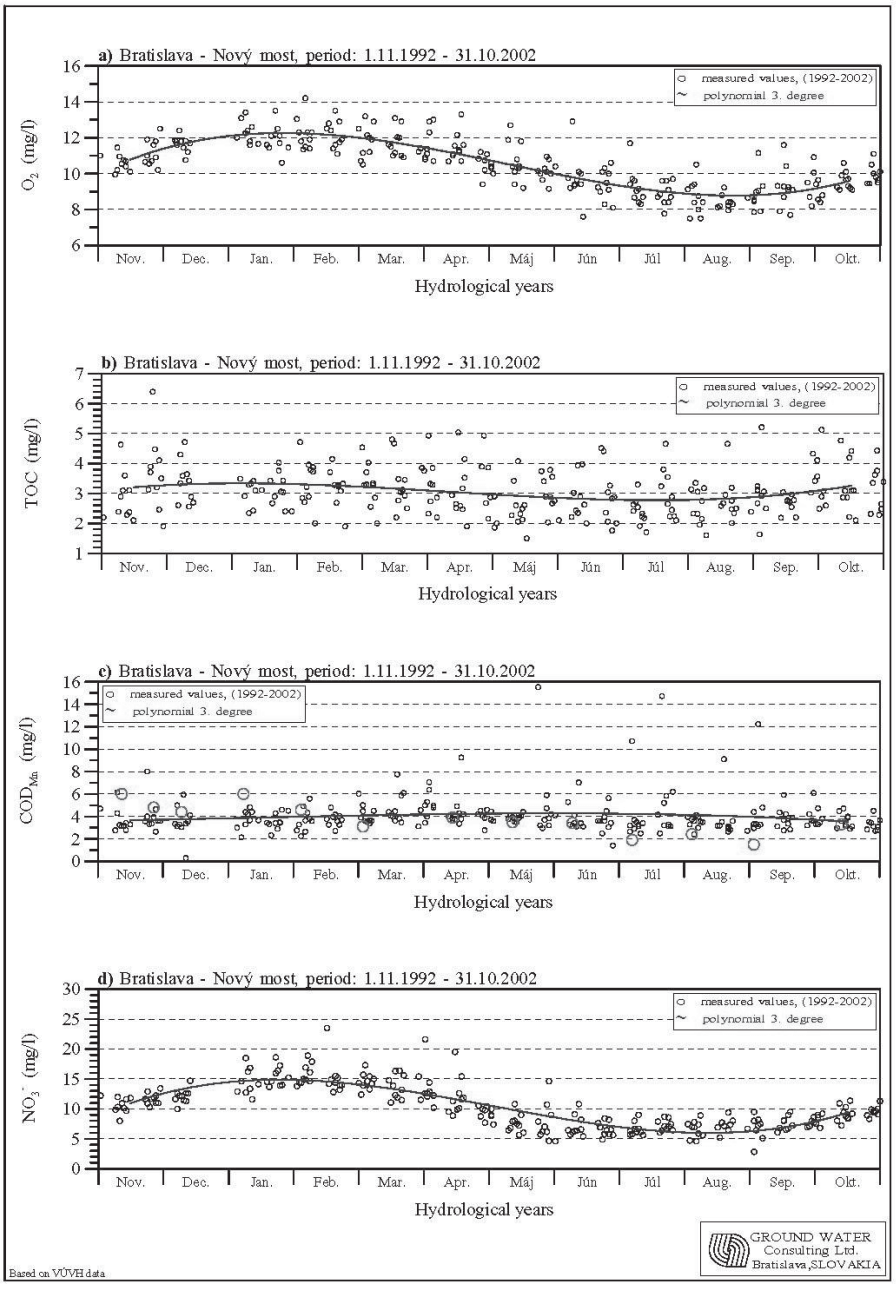

Figure 13. Seasonal changes of oxygen, total organic carbon, COD_{Mn} and nitrate in the Danube

Careful monitoring, experimental field measurements, and their evaluation and interpretation are basic research methods to better understand clogging and its role in ground water recharge and ground water quality processes.

4.3 Processes after Infiltration of River Water

The sequence of reactions along the flow path starting at the Danube for highly oxygenated water that enters aquifer is as follows (Stumm, Morgan 1981, Appelo, Postma 1993):

- **Aerobic respiration** – oxidation of organic carbon dissolved in water, oxidation of solid organic matter in riverbed sediments and the aquifer, organic matter and any reduced substances in the aquifer sediments (like pyrite, siderite, etc.).
- **Oxidation** of ammonium ions and nitrites to nitrates, precipitation of manganese in the form of oxides in aerobic conditions.
- **Denitrification,** reduction of nitrates by organic carbon in anaerobic conditions, accompanied by production of nitrites and gaseous nitrogen.
- **Dissolution of manganese** minerals, which are present in the sediments
- **Reduction of manganese** oxides by organic carbon or by re-oxidation of nitrates, followed by dissolution of manganese carbonates.
- **Precipitation of manganese** in the form of minerals (oxidation of manganese by nitrates, precipitation in form of carbonates, or catching dissolved forms by sorption and ion-exchange processes.)

If there is still enough organic carbon dissolved in the water or in sediment, and nitrates are reduced, reduction of Fe-oxyhydroxides, present in the Danube sediments occurs.

In regions where aquifer sediments and water, which recharges an aquifer, contain too many organic compounds and little or no oxygen, the aquifer becomes anaerobic. Ground water often contains Mn and Fe in soluble form. Such water, if not polluted, can easily be treated by aeration and sand filtration.

If the reducing conditions reach a deeper state of reduction, then decreases in the content of SO_4, and increases CH_4 (Fermentation) and NH_4 occur. Various other organic components undergo changes, and the water cannot be used without more sophisticated and expensive treatment.

Ground water, according to local hydrogeological situation, can have oxidizing or reducing conditions. The state of oxidizing conditions is, in fact,

the prerequisite for the utilization of ground water as a direct source for water supply, without treatment.

4.4 Typical Well Systems

Riverbank filtration wells are typical in shallow and thin aquifers. Water quality directly corresponds to river water quality and pumped ground water should usually be treated in water treatment facilities. Biochemical processes are not complete, and the water is not biologically stable.

Water wells situated a larger distance from the river are usually constructed in permeable and thick aquifers. Wellscreens are usually set deeper in the aquifer and only partially penetrate the aquifer, so that the pumped water is better protected from surface pollutants.

In general, well fields for water supply can be categorized by the following types:

- Areas where an aquifer has oxidizing or at least anoxic conditions (still some content of NO_3) and these conditions can be ensured long-term by aquifer recharge from the river using proper water management.
- Areas where there are suitable reducing conditions for simple in-situ treatment or treatment in waterworks.
- Areas where there are deep reducing conditions and expensive groundwater treatment in waterworks is necessary.

According to quality processes, two approaches are used:

- The riverbank filtration wells, situated close to the river, pumping river water filtered by riverbed sediments and a fraction of the aquifer. Natural purification processes are generally not complete and water treatment is necessary.
- The aquifer wells, situated at such a distance from the river that the so called "self-purification processes" have sufficient time and space to change the river water into ground water of satisfactory quality. The water is usually suitable for direct water supply without treatment.

As an example of changes of ground water quality, long-term data is presented in Figures 14 and 15. Comparing these figures with those representing the Danube water quality, (Figures 10, 11, 12 and 13), it is evident that damming the Danube and creating a flow-through reservoir caused changes mainly in the dilution of some ground water components such as chlorides and sulfides, and decreased nitrates by

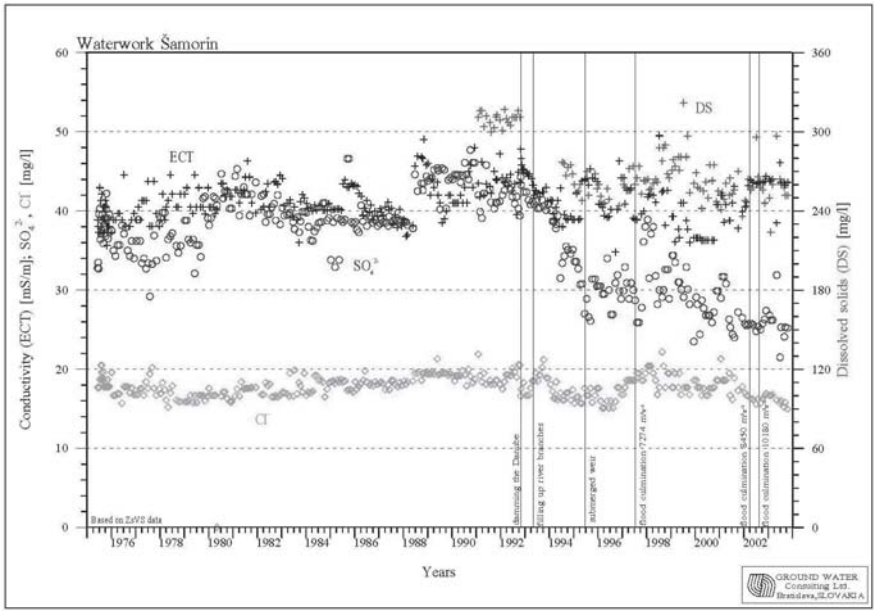

Figure 14. Long-term changes of Conductivity, SO_4, Cl, Dissolved solids in water from well at Samorin water treatment plant

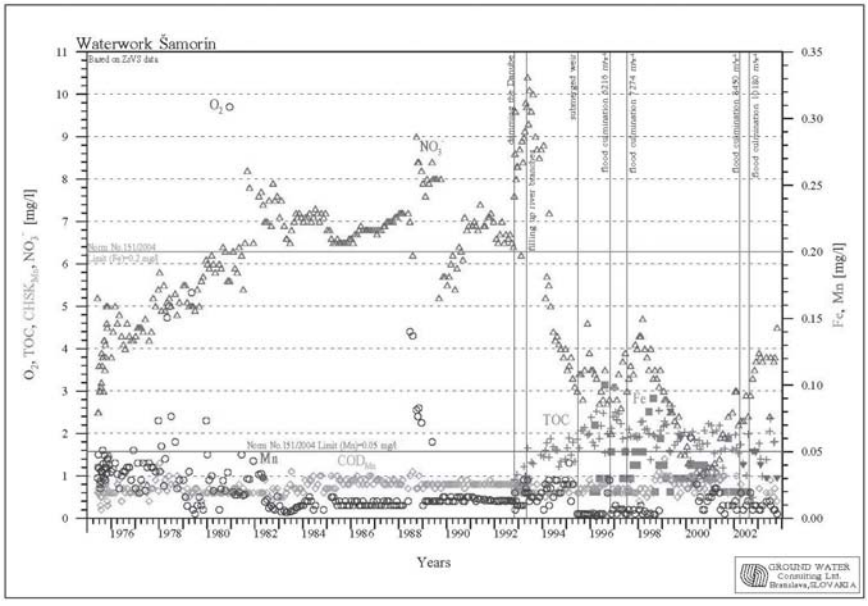

Figure 15. Long-term changes of O_2, TOC, COD_{Mn}, NO_3, Fe, Mn in water from well at Samorin water treatment plant

preserving a low content of iron and manganese. Increase of nitrates since 1975 is due to the decrease of organic carbon in the Danube water. Decrease of nitrate since 1992 is clearly due to changes in the Danube water flow through the reservoir. In general, redox sensitive components, including oxygen, nitrate, sulfate and products of reduction conditions, iron and manganese, all are excellent tracers for identification of processes in ground water, including the impact of clogging and changes in the river.

Measures for assuring good ground water quality include maintaining oxygenating conditions by minimizing the use of reducing agents in treatment. The largest impact on ground water quality results from infiltration of the surface water into aquifer via clogging riverbed zone. The largest loss of dissolved oxygen is during the process of infiltration, when the surface water crosses the riverbed.

Measures to protect ground water quality are therefore aimed at:

- avoiding placement of wells in areas of river branches and stagnant water bodies where the recharge of water containing organic carbon and other reducing agents could be expected,
- constructing sewage treatment facilities and water purification plants,
- reducing surface runoff water pollution (reducing organic carbon, suspended particles, etc.),
- reducing of content of organic carbon in riverbed sediments by supporting higher velocities at ground water recharge areas,
- supporting short flowpaths through the riverbed by higher pumping rates,
- cleaning the riverbed and riverbanks of finer sediments, which regularly contain more organic carbon using hydraulic methods, hydraulic guiding structures, etc.
- creating conditions for variable flow velocities and variable riverbed cross-section to support erosion-sedimentation processes.
- Addition of oxygen into the aquifer, directly into the ground water flow towards pumping wells. This method is well known as VIREDOX and it has been successfully applied at the Rusovce water treatment acility near Bratislava.

Riverbed clogging processes greatly influence ground water composition and ground water riverbed recharge, thus affecting well system capacity and ground water quality. Based on general knowledge and monitoring of processes on a local scale, it is possible to evaluate some technical means to influence the processes in order to improve the water quality and increase the well's discharge.

REFERENCES

Mucha, I., Rodak, D., Hlavaty, Z., Bansky, L., 2002: Groundwater Quality Processes After Bank Infiltration from the Danube at Cunovo. In C. Ray (ed.), Riverbank Filtration: Understanding Contaminant Biogeochemistry and Pathogen Removal, Kluwer Academic Publishers, The Netherlands, pp. 177-219.

Mucha, I., Schestakow V., M., 1987: Hydraulika podzemnych vod (Ground water hydraulic), ALFA, SNTL, Bratislava, Praha, 342 p.

Schestakow, V., M., 1977: Postanovka opytno-filtracionnych rabot vblizi vodotokov (Proposal of ground water hydraulic tests situated close to rivers) Journal: Razvedka i ochrana nedr, No. 9, p 38-44

Schestakow, V., M., 1979: Dinamika podzemnych vod (Ground water hydraulic), Izd. Moscow. Univ., 367 p.

APPENDIX

```
      PROGRAM GWCCLOGL
!  Program for analytical modeling of GWL fluctuation.
!  Gradual linear and stepwise river water level changes.
!  River boundary conditions of I. and III. order.
!  References: Mucha, Schestakow: Hydraulika Podzemnych Vod,
!  ALFA, Bratislava 1987.
!  Pages: 72 – 81,  Equations: 2.154, 2.158, 2.182,

!  Parameters:
!  T  - Aquifer Transmissibility coefficient (m2/s)
!  S  - Storage coefficient (specific yield) (-)
!  XL  - Distance of computation point or observation well from river (m)
!  DL  - Clogging parameter delta L (m)
!  H0  - Ground water level at the start of simulation

      INTEGER*4 I, II,III, NO, StNo, ISt, IMinus, IE
      REAL*8 Lambda,O,LambdaO,erfcLambda,erfcLambdaO,O1
      REAL*8 Lambda1, erfcLambda1,LambdaO1,erfcLambdaO1
      REAL*8 DHR,erfcO,ERFC,ERFC1, DHWell,DeltaH0
      REAL*8 DHRi,erfcO1  !
      REAL*8 vLin,FLambdaO,RLambdaO,RLambda,PISQR,vDeltaH
      REAL*8 XL,DL,T,S,D,H0,Hriver,DeltaH,Tint
      CHARACTER TCH*128,Well*24,Filename*24,ERR*80
      INTEGER*4 IDEN,IROK,IMES,DAT1,DAT2
      INTEGER*4 CDATE,CDEN,CMES,CROK
      REAL*8,ALLOCATABLE:: HR(:),HW(:),HRO(:),HWM(:),vHW(:)
      WRITE (*,*) ' DETERMINISTIC MODEL CALCULATION PROGRAM'
      WRITE (*,*) '     v 1.1  GWC Ltd.(c) 2001 '
      WRITE (*,*) ' '
!  Constants
      PISQR=1.772453851
```

```
!   Reading dates from - to computation should take place.
    ERR="Cannot open or read from file dates.ini"
     OPEN (7,FILE='dates.ini', ACTION='READ',STATUS='OLD',ERR=9998)
     READ (7,*,ERR=9998) IDEN, IMES, IROK
     DAT1=CDATE(IROK,IMES,IDEN)
     WRITE(*,'(A,I2,".",I2,".",I4)') ' calculation period start',IDEN,IMES,IROK
     READ (7,*,ERR=9998) IDEN, IMES, IROK
     DAT2=CDATE(IROK,IMES,IDEN)
     WRITE(*,'(A,I2,".",I2,".",I4)') '                end ',IDEN,IMES,IROK
     WRITE(*,'(A)') '  (to change dates, modify file dates.ini) '
    CLOSE(7)
     WRITE(*,*) ' '

     II=DAT2-DAT1
     IF (II.LE.0) THEN
      ERR='ERROR! in dates.ini end date sooner or same then start date'
        GOTO 9998
     END IF
     ERR='ERROR! cannot allocate memory'
     ALLOCATE ( HR(II),HW(II),HRO(II),HWM(II),vHW(II),STAT=I)
     IF (I.NE.0) GOTO 9998
     ERR=''

!   Default input basic parameters
    Filename = '1252.94'
     Well = '1949'
     XL = 120.
     DL = 0.
     T= .008
     S=0.2
     III=3019
     IDEN=1
     IMES=5
     IROK=1993

!   Reading input parameters
    PRINT *,'Enter Filename of Source Water Level Data, without .txt extension:'
    READ *,Filename
    PRINT *,'Enter Filename of Computed Point, Well (without the .txt extension):'
    READ *,Well
    PRINT *, 'Distance of Well from River in m:'
    READ *, XL
    PRINT *, 'Clogging Distance of River (delta L)(m):'
    READ *, DL
    PRINT *, 'Aquifer Transmissibility in m2/s, e.g. 1.0:'
    READ *, T
    PRINT *, 'Aquifer Water Table Storage in (-), e.g. 0.2:'
    READ *, S
    D=T/S
    PRINT *, 'Starting Date of Computation as DD MM YYYY, e.g. 1 1 2000'
```

```
      READ  *, IDEN,IMES,IROK
      STNO=CDATE(IROK,IMES,IDEN)
      PRINT *, 'Number of Computation Days (integer), e.g. 30'
      READ *, III

!     Reading the River Water Level Altitude Data from the database
      WRITE (TCH,'(A,A,A)') 'IN\',TRIM(Filename),'.txt'
      OPEN(7,FILE=TCH,ACTION='READ',STATUS='OLD')
      DO WHILE (.NOT.EOF(7))
      READ (7,*) IDEN,IMES,IROK,NO,Hriver
      I=CDATE(IROK,IMES,IDEN)
       IF (NO.EQ.0) THEN
         NO=I
       END IF
       IF (NO.GE.DAT1.AND.NO.LE.DAT2) THEN
         I=NO-DAT1              !Counter of database
         HR(I)=Hriver           !Water level Altitude in River
       END IF
      END DO
      CLOSE    (7)

!     Reading the Ground water level Altitude Data from the Well database
      WRITE (TCH,'(A,A,A)') 'IN\',TRIM(Well),'.txt'
     OPEN(7,FILE=TCH,ACTION='READ',STATUS='OLD')
      ISt=-1
      DO WHILE (.NOT.EOF(7))
       READ (7,*) IDEN,IMES,IROK,NO,Hriver
       I=CDATE(IROK,IMES,IDEN)
        IF (NO.EQ.0) THEN
          NO=I
        END IF
        IF (NO.GE.DAT1.AND.NO.LE.DAT2) THEN
          I=NO-DAT1
          HWM(I)=Hriver         !Water level in Well
          IF (NO .EQ. StNO) THEN
            ISt=I
            H0=Hriver
          END IF
        END IF
      END DO
      CLOSE (7)

      ERR='ERROR! start date not in well data file or date range'
      IF (Ist.EQ.-1) GOTO 9998
      ERR=''
      HW=0.0      !Field HW() substitute zero - Stepwise changes
      HRO=0.0     !Field HRO()substitute zero – Differences in water level
      vHW=0.0     !Field vHW()substitute zero – Linear changes
      HW(ISt)=H0   !Substitute initial water level before first computation
```

```
      vHW(ISt)=H0  !Substitute initial water level before first computation

      IF (DL.GT.0.01) THEN   !Computation with clogging
       DO I=ISt+1,ISt+III  !NoDays from start day +1, until end of dates
        DeltaH=0          !Substitution of zero in sum of water levels
         IMinus = I-1      !Substitution of the computed Day
         Lambda = XL/(2*SQRT(D*86400.))
         O=SQRT(D*86400.)/DL
         IF (O.GT.10.)THEN
          O = 10.
         END IF
         LambdaO=Lambda + O

         CALL ERFCC (Lambda, erfcLambda)
         CALL ERFCC (LambdaO, erfcLambdaO)
         DHR=HR(I) - HR(I-1)     !Stepwise change of water level
          vLin=DHR/86400.       !Linear water level velocity changes
            FLambdaO=(erfcLambda - (EXP((O*O)+2*Lambda*O)*erfcLambdaO))
            RLambda=(1.+2*Lambda*Lambda)*erfcLambda
            RLambda=RLambda-(2*Lambda*exp(-(Lambda*Lambda)))/PISQR
         ierfcLambda=exp(-(Lambda*Lambda))/PISQR-Lambda*erfcLambda
         RLambdaO=RLambda+(FLambdaO-2*O*ierfcLambda)/(O*O)
         DeltaH=DHR*FLambdaO    !Change of water level in aquifer
         CALL ERFCC (O, erfcO)
         DeltaH0=DHR*(1-EXP(O*O)*erfcO)  !Change directly on the river boundary
         vDeltaH=DHR*RLambdaO
         HRO(I)=DeltaH0
         IE=0
  100     IMinus = IMinus – 1   !Backward computation from the starting day with
  !                    the known water level
         IE=IE+1
         TInt=86400.*(I-IMinus)!Time interval in sec.
         Lambda = XL/(2*SQRT(D*TInt))
         Lambda1 = XL/(2*SQRT(D*(TInt-86400.)))
         IF (Lambda.GT.10.) THEN
          GOTO 100 !+++
         END IF
         O=SQRT(D*TInt)/DL
          IF (O.GT.10.)THEN
            O = 10.
          END IF
         O1=SQRT(D*(TInt-86400.))/DL
         LambdaO=Lambda + O
          IF (O.GT.10.)THEN
            O = 10.
          END IF
         LambdaO1=Lambda1 + O1
          IF (O1.GT.10.)THEN
            O1 = 10.
          END IF
```

```
        CALL ERFCC (Lambda, erfcLambda)
        CALL ERFCC (Lambda1, erfcLambda1)
        CALL ERFCC (LambdaO, erfcLambdaO)
        CALL ERFCC (LambdaO1, erfcLambdaO1)
        CALL ERFCC (O, erfcO)
        CALL ERFCC (O1, erfcO1)
        DHR=HR(Iminus-1) - HR(Iminus)
         vLin=DHR/86400.    !Velocity of linear changes on aquifer boundary
        FLambdaO=(erfcLambda - (EXP((O*O)+2*Lambda*O)*erfcLambdaO))
        FLambdaO1=(erfcLambda1 - (EXP((O1*O1)+2*Lambda1*O1)*erfcLambdaO1))
        RLambda=(1.+2*Lambda*Lambda)*erfcLambda
        RLambda=RLambda-(2*Lambda*exp(-Lambda*Lambda))/PISQR
        RLambda1=(1.+2*Lambda1*Lambda1)*erfcLambda1
        RLambda1=RLambda1-(2*Lambda1*exp(-Lambda1*Lambda1))/PISQR
        ierfcLambda=exp(-(Lambda*Lambda))/PISQR-Lambda*erfcLambda
        RLambdaO=RLambda+(FLambdaO-2*O*ierfcLambda)/(O*O)
        ierfcLambda1=exp(-(Lambda1*Lambda1))/PISQR-Lambda1*erfcLambda1
        RLambdaO1=RLambda1+(FLambdaO1-2*O1*ierfcLambda1)/(O1*O1)
        DHWell = DHR*(FLambdaO-FLambdaO1)
        vDHWell=DHR*(RLambdaO-RLambdaO1)
        DeltaH0=DeltaH0+DHR*((1-EXP(O*O)*erfcO)-(1-EXP(O1*O1)*erfcO1))
        IF (IE .LT. 50) THEN
         GOTO 100
        END IF
        IF ((FLambdaO-FLambdaO1).GT.0.001) THEN !If the impact of function
!        GOTO 100                    !is les than 1% than
        END IF                       !end of backward computation
        HW(I)=HW(I-1)+DeltaH !GWL - altitude in the well stepwise computed
        vHW(I)=vHW(I-1) + vDeltaH !GWL-altitude in the well linearly computed
        HRO(I)=DeltaH0   !Change of water level in river against previous day
      END DO

       ELSE          !Conputation without clogging of the riverbed

        DO I=ISt+1,ISt+III  !From starting day +1 up to end of data
        DeltaH=0          !Substitution of zero
         IMinus = I-1
        IE=IE+1
         Lambda = XL/(2*SQRT(D*86400.))
         CALL ERFCC (Lambda, erfcLambda)
         DHR=HR(I) - HR(I-1)
         vLin=DHR/86400.
         DHRi=DHR
         HRO(I) = DHR !Change of water level in river against previous day
         DeltaH=DHR*erfcLambda
         RLambda=(1.+2*Lambda*Lambda)*erfcLambda
         RLambda=RLambda-(2*Lambda*exp(-(Lambda*Lambda)))/PISQR
         vDeltaH=DHR*RLambda
         IE=0
200      IMinus = IMinus – 1  !Backward computation
```

```
            IE=IE+1
             TInt=86400.*(I-IMinus)   !Time interval in sec.
             Lambda = XL/(2*SQRT(D*TInt))
             Lambda1= XL/(2*SQRT(D*(TInt-86400.)))
             IF (Lambda.GT.10.) THEN
              GOTO 200 !++++
             END IF
             CALL ERFCC (Lambda, erfcLambda)
             CALL ERFCC (Lambda1, erfcLambda1)
              RLambda=(1.+2*Lambda*Lambda)*erfcLambda
              RLambda=RLambda-(2*Lambda*exp(-(Lambda*Lambda)))/PISQR
              RLambda1=(1.+2*Lambda1*Lambda1)*erfcLambda1
              RLambda1=RLambda1-(2*Lambda1*exp(-(Lambda1*Lambda1)))/PISQR
             DHR=HR(IMinus-1) - HR(Iminus)
             ERFC=(erfcLambda)
             ERFC1=(erfcLambda1)
             DHWell = DHR*(ERFC-ERFC1)
             vDHWell=DHR*(RLambda-RLambda1)
             DeltaH = DeltaH - DHWell
             vDeltaH = vDeltaH - vDHWell
             DHRi=DHR
             IF (IE.LE.50) THEN
              GOTO 200
             END IF
             IF ((ERFC - ERFC1).GT.0.001) THEN
              GOTO 200
             END IF
             HW(I)=HW(I-1)+DeltaH  !Altitude in well computed stepwise
             vHW(I)=vHW(I-1)+vDeltaH  !Altitude in well computed linearly
            END DO
          END IF

     !   Writing results on disk
         WRITE (TCH,'(A,A,A)') 'OUT\',TRIM(Well),'.dete.txt'
         OPEN(7,FILE=TCH,ACTION='WRITE',STATUS='REPLACE')
          DO I=1,II
       WRITE(7,300)                CDEN(I+DAT1),CMES(I+DAT1),CROK(I+DAT1),I+DAT1,HWM(I),
HW(I),vHW(I),HR(I),HRO(I)
     !    1. day,  2. month,  3. year,  4. database No.,
     !    5. measured water level altitude in well,
     !    6. stepwise computed altitude of water level in well,
     !    7. linearly computed altitude of water level in well,
     !    8. measured water level altitude in the river,
     !    9. water level difference in the river (at the boundary) to previous day

          END DO
     300  FORMAT (1X,I2,',',I2,',',I4,',',I6,',',F8.4,',',F8.4,',',F8.4,',',&
         &F8.4,',',F8.4)
          CLOSE (7)
         GOTO 9999
```

```
 9998 CONTINUE
      WRITE (*,*) ERR
 9999 CONTINUE

      END PROGRAM GWCCLOGL
!=======================================================================
      SUBROUTINE ERFCC (x,valerfc)
      REAL*8 valerfc,x
      REAL*8 t1,z
       IF (x.LT.10.) THEN
      z=ABS(x)
      t1=1./(1.+0.5*z)
      valerfc=t1*exp(-z*z-1.26551223+t1*(1.00002368+t1*(.37409196+t1* &
     &(.09678418+t1*(-.18628806+t1*(.27886807+t1*(-1.13520398+t1*    &
     &(1.48851587+t1*(-.82215223+t1*.17087277)))))))))
       ELSE
       valerfc=0.
       END IF
      CONTINUE
       IF (x.lt.0.) THEN
       valerfc=2.-valerfc
       END IF
       END
!=============================================================================
! FUNCTION CDATE(Year,Month,Day)
!   this function calculates date serial number staring from 1.1.1900 where
!   serial number equals 2
!   this function is compatible with MS OFFICE 2000 date/time calculation in
!   MS EXCEL and MS ACCESS

      FUNCTION CDATE(YY,MM,DD)
        INTEGER YY,MM,DD, I
        INTEGER*4 CDATE, G
!                             MS$ATTRIBUTES VALUE:: YY, MM, DD
        INTEGER ND(12)
        CDATE=0
        IF (YY.LT.1900) GOTO 999
        IF ((MM.LT.1).OR.(MM.GT.12)) GOTO 999
        ! months in the year
        ND(1)=31; ND(2)=28; ND(3)=31; ND( 4)=30; ND( 5)=31; ND( 6)=30
        ND(7)=31; ND(8)=31; ND(9)=30; ND(10)=31; ND(11)=30; ND(12)=31
        !leap year
     IF (((MOD(YY,4).EQ.0).AND.(MOD(YY,100).NE.0)).OR.(MOD(YY,400).EQ.0)) THEN
          ND(2)=29
        END IF
        IF ((DD.LT.1).OR.(DD.GT.ND(MM))) GOTO 999
        !starting year related to 1900
        YY=YY-1900
        G=YY*365+2
        G=G+INT((YY-1)/4)
        G=G-INT((YY-1)/100)
        G=G+INT((YY+299)/400)
```

```
        !months and day
        DO I=1,MM-1
          G=G+ND(I)
        END DO
        G=G+DD-1
        CDATE=G
999    END FUNCTION

      FUNCTION CDEN(SD)
            INTEGER*4 CDEN,CMES,CROK, SD, CDATE
            CDEN=SD-CDATE(CROK(SD),CMES(SD),1)+1
      END FUNCTION

      FUNCTION CMES(SD)
            INTEGER*4 CMES,CROK,CDATE,SD,I,YY
            YY=CROK(SD)
            I=2
            DO WHILE ((SD.GE.CDATE(YY,I,1)).AND.(I.LT.13))
              I=I+1
            END DO
            CMES=I-1
      END FUNCTION

      FUNCTION CROK(SD)
            INTEGER*4 CROK, SD,G, YY, I
        !starting year related to 1900
           G=0
            DO I=1,3
              YY=(SD-G-2)/365
              G=INT((YY-1)/4)
              G=G-INT((YY-1)/100)
              G=G+INT((YY+299)/400)
            END DO
            CROK=YY+1900
      END FUNCTION
```

NEW APPROACHES FOR ESTIMATING STREAMBED INFILTRATION RATES

W. Macheleidt, T. Grischek, W. Nestler
Institute for Water Sciences, University of Applied Sciences Dresden, 01069 Dresden, F.-List-Platz 1, Germany
E-mail: mach@htw-dresden.de

Abstract: Direct quantification of infiltration rates and darcy velocities at bank filtration sites by field measurements has been done only at sites that are well equipped with monitoring wells and is mostly based on the observation of changes in chloride or oxygen-18 concentrations in surface water and infiltrate. The main determinants of the interaction between surface water and groundwater are the distribution of areas with different infiltration rates, the thickness of sediment layers and the hydraulic head gradient. These conditions determine the volume and velocity of infiltrating water which, together with the direction of water flow, are required to model the interaction processes. Usually, due to difficulties with measurement, only the direction of water flow is determined and boundary conditions are estimated from simplified assumptions.

Field techniques have now been developed to help characterise surface water/groundwater interaction. Results from field experiments using a percussion probe and a large-scale laboratory column experiment set up to simulate infiltration processes are presented.

Owing to its differing concentrations in groundwater and river water, the naturally occurring isotope Radon-222 (^{222}Rn) can be used as a natural tracer to determine the residence time of infiltrated water. The principle is based on the determination of ^{222}Rn activity at defined points along the flow path. Investigations performed in a large-scale laboratory column experiment showed that different effects considerably influence infiltration measurements. Local sedimentary stratification has a substantial influence on the equilibrium concentration of ^{222}Rn. Furthermore, investigations in zones with gas formation (e.g. in biologically active zones such as river beds) must consider diffusion of ^{222}Rn into the gas phase and the reduction of permeability because of gas within the pore space. The volume of gas in the saturated, upper zone of the aquifer has an important influence on the results of ^{222}Rn measurements.

Stephen A. Hubbs (ed.), Riverbank Filtration Hydrology, 73–91.

Advantages and limitations of the use of ^{222}Rn measurements for the determination of infiltration rates are discussed based on results of laboratory experiments.

Key words: Infiltration, ^{222}Rn, gas, darcy velocity, river bank

1. INTRODUCTION

Improved knowledge of the interactions between surface water and groundwater is an important precondition for the solution of various ecological and water management problems. Estimation of infiltration rates and darcy velocities from surface waters into bed sediments is normally based on water balance calculations, mixing models or geohydraulic simulations. However, exact measurements are necessary to answer questions relating to infiltration regimes during river bank infiltration, floodplain water balances or for the impact assessment of mining areas and hydraulic constructions.

In the past, the construction of groundwater observation profiles or sophisticated measurement devices has meant that these infiltration measurements could only be made at considerable expense. Thus, the tendency has been toward an insufficient description of exchange processes.

2. THE INFLUENCE OF COLMATAGE LAYERS ON THE INFILTRATION RATE

The exchange between surface waters and groundwater is essentially determined by potential differences based upon the hydraulic resistance of colmatage layers. The colmatage process results in the reduction of permeability at the groundwater/ surface water interface (Figure 1). Preliminary studies indicate that the presence of colmatage layers when estimating surface/ groundwater interactions can lead to significant error in quantifying infiltration rates (Nestler et al. 2000).

In German literature the term ‘colmatage’ is widely used to describe the phenomena of lake and river bed siltation (Busch et al. 1993). There are two types of colmatage layers: external and internal. The internal colmatage layer is present in the bed material and consists of pores filled with fine silt and organic sediment. The external colmatage layer is built from the same fine sedimentary material, but lies external to the bed proper. Factors influencing

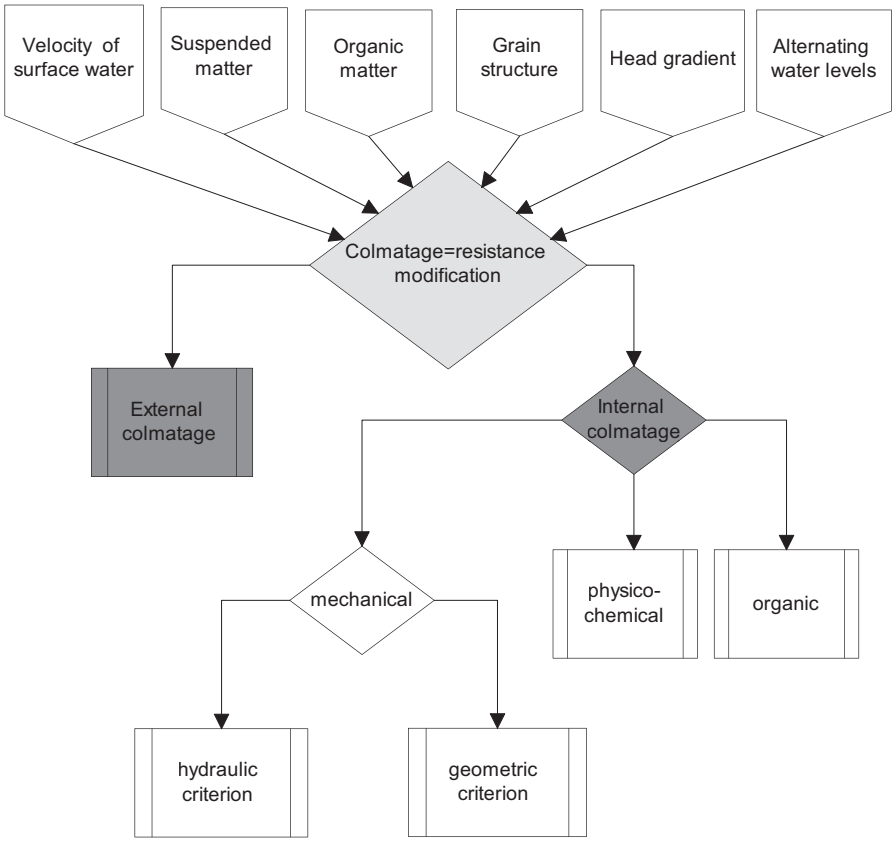

Figure 1. Influences on the colmatage process

the presence and nature of colmatage layers are illustrated in Figure 1. A colmatage layer may consist of: both internal and external colmatage, only one of either, or may not be present. For a more complete discussion of colmatage layer behaviour, refer to Busch et al. (1993).

This paper will discuss colmatage primarily in reference to rivers, as river bank filtration is a major source for water supply in Saxony, Germany.

In rivers, the flow regime (e.g. high and low water) and the flow velocity are the primary controls on colmatage layer formation. Other important factors include bed material, pore geometry and the direction of the potential gradient, because a high potential gradient from the surface water toward the groundwater results in a greater tendency for colmatage to occur.

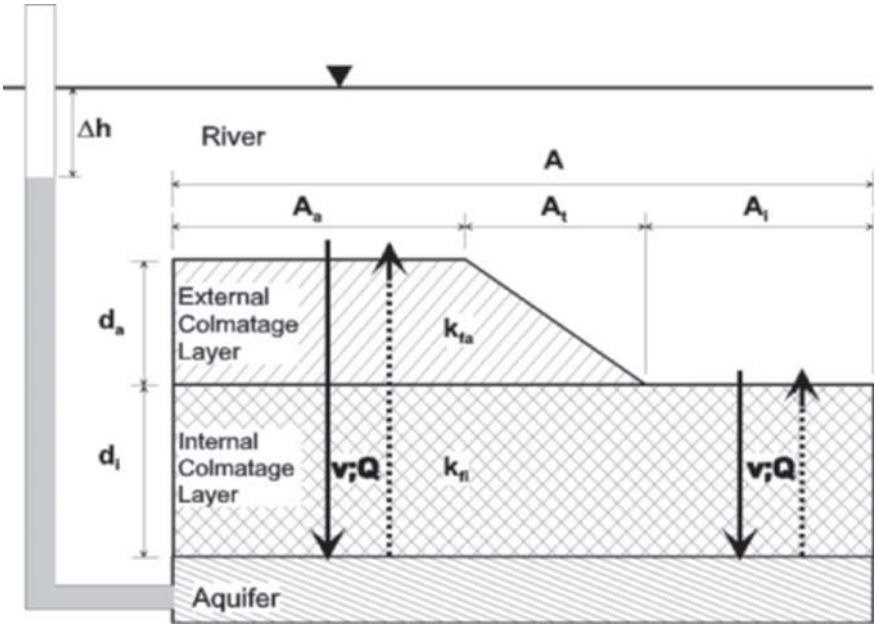

Figure 2. Conceptual model of surface water/ groundwater interaction

The influence of the colmatage layer on the exchange rate between groundwater and surface water is illustrated in Figure 2 and described by the following formula:

$$Q(t) = \int v \times dA = \int \frac{\Delta h}{d_a / k_{f_a} + d_i / k_{f_i}} dA \tag{1}$$

where:

Q	discharge	[m³ s^{-1}]
v	velocity of exchange	[m s^{-1}]
Δh	hydraulic gradient	[m]
d_a	thickness of the external colmatage layer	[m]
d_i	thickness of the internal colmatage layer	[m]
k_{fa}	average permeability of the external colmatage layer	[m s^{-1}]
k_{fi}	average permeability of the internal colmatage layer	[m s^{-1}]
A	infiltration area	[m²]
A_a	infiltration area with external colmatage	[m²]
A_i	infiltration area without external but with internal colmatage	[m²]
A_t	infiltration area between external and internal colmatage (transition area)	[m²]

To be able to determine the infiltration rate, either the darcy velocity related to the river bed or the following parameters need to be known: the area of the external colmatage layer, the thickness and the hydraulic conductivity of the external and internal colmatage layers, the gradient between the hydraulic heads of surface water and groundwater, and the temporal variation of the parameters and the direction of the exchange process. Of these, a continuous registration of dynamic changes in the exchange rate is only possible by measuring the head gradient. Otherwise, two methodological approaches may be adopted for the characterisation of exchange processes as derived from these conditions (Table 1).

Table 1. Methods of direct and indirect measurements

Direct measurement	Indirect measurement
Dating with the help of ^{222}Rn	Compilation of the geometry (d, A)
Seepage meter	Determination of hydraulic conductivity (k_f)
Tracer tests, e.g. temperature	Water head measurement

3. DEGREE OF COLMATAGE COVERAGE

The infiltration rate of a losing river depends on the degree of riverbed coverage by an external colmatage layer. However, the effects of partial coverage on infiltration are often overestimated. An external colmatage layer with low hydraulic conductivity needs more than 80% coverage to significantly limit infiltration. Modeling simulations for a river bank filtration site along the Elbe River show the following correlation between the degree of coverage and infiltration rate (Figure 3):

up to 20%	- no effect
between 20% and 60%	- only minor effect
between 60% and 80%	- low effect (67% coverage causes a reduction of 5%)
more than 80%	- considerable effect on the infiltration rate

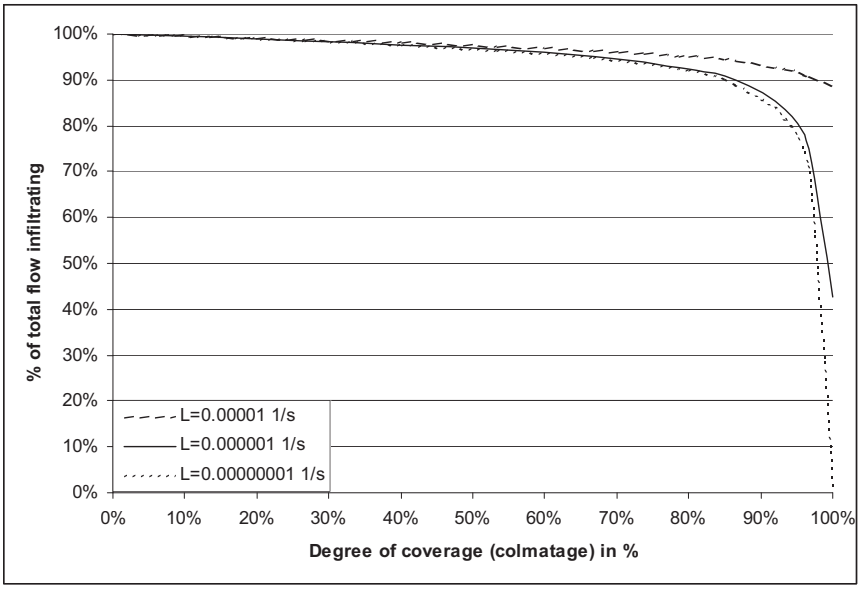

Figure 3. Effect of the degree of coverage of an external colmatage layer on the infiltration rate. L is the leakage factor

These results depend on the leakage factor, L (s^{-1}), which is given by

$$L = \frac{k_f}{d} = \frac{Hydraulic\,conductivity}{Thickness} \tag{2}$$

4. INDIRECT MEASUREMENT OF INFILTRATION RATES

4.1 Determination of Sediment Permeability

Indirect measurements of infiltration rates require the determination of the hydraulic conductivity of the colmatage layer. The very fine stratification typical of the colmatage layer results in considerable vertical heterogeneity. This effect makes it necessary to measure the hydraulic conductivity of undisturbed samples. For this reason, a special laboratory-scale experimental system has been developed (Figure 4).

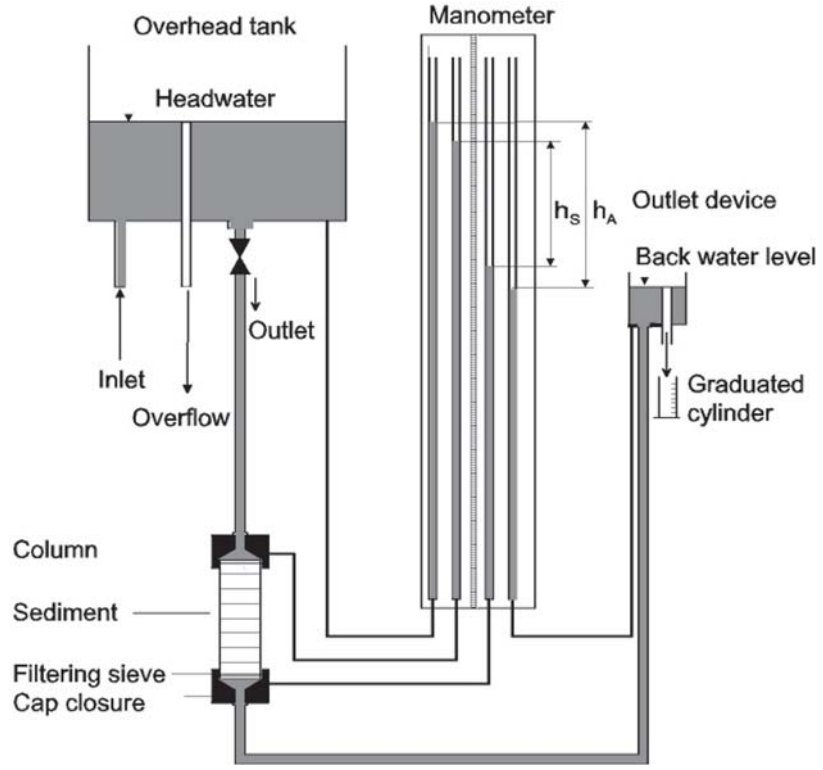

Figure 4. Operation principle for the determination of hydraulic conductivity in undisturbed sediment samples

For an overview of a riverbed, samples from every different area within the riverbed have to be taken. Sediment samples are collected in stainless steel columns (diameter, 0.1 m; length, 0.5 m) that are pressed into the upper zone (colmatage layers) of the riverbed. After filling with sediment, the liners are drawn out without loss of material and only minimal compaction (the degree and the effect of which is currently under investigation). Special adapters allowed the columns to be installed directly into the experimental system in the laboratory. The apparatus facilitates work with hydraulic head gradients up to 1.8 m. The vertical permeability of the sediment sample can be determined as a function of different head gradients. By controlling the flow direction, it is possible to examine the permeability of the sediment under either infiltrating or exfiltrating conditions. Tracer tests with transparent columns were undertaken to examine the possibility of preferential flow paths down the column sides, none of which was observed.

4.2 Determination of Darcy Velocity

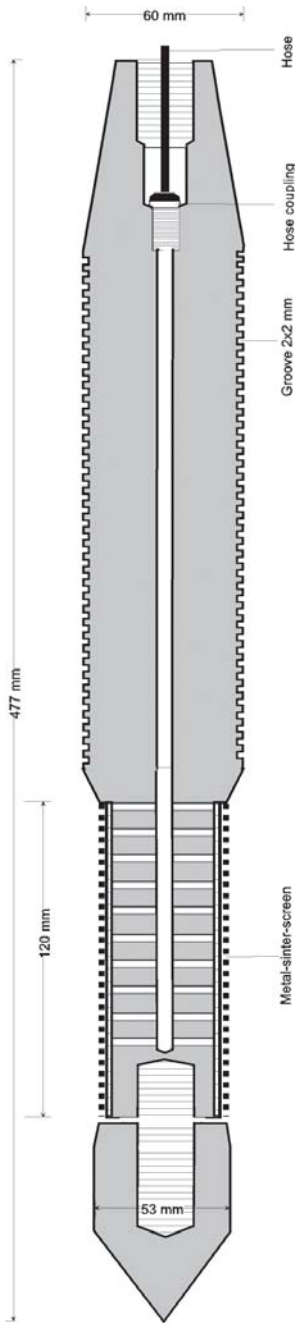

For on site investigations beneath a riverbed, a stainless steel core probe has been developed to measure the hydraulic head distribution and to obtain groundwater samples at various defined depths (Figure 5).

One advantage of the core probe is that it can be driven into sediments using ordinary percussion equipment. The probe enables hydraulic head measurements and infiltration water samples to be taken over vertical intervals of 0.3 m.

Important probe features are the exchangeable tip, the exchangeable metal-sinter-screen (which allows the adaptation of the sampling technique to different grain sizes), and the transverse notched shaft. Many tracer and head gradient experiments have been undertaken to ensure that the transverse notched shaft excludes vertical leakage along the sides of the probe (Pfützner 1997; Pätzold 1999).

Water samples are obtained using an adjustable low-pressure unit that minimizes sample disturbance. The sampling is carried out exclusively in a downward movement.

Figure 5. (Left) Stainless steel core probe

5. DIRECT MEASUREMENT OF INFILTRATION RATES USING ^{222}Rn

Darcy velocities may be measured by determining ^{222}Rn radioactivity at defined points along a flow path. ^{222}Rn is the natural decomposition product of the radioactive ^{226}Ra, which occurs in the soil. ^{222}Rn is an inert gas with a half-life of $T_{1/2}$ = 3.8 days. In stagnant groundwater there is an equilibrium between ^{222}Rn and its parent ^{226}Ra. ^{222}Rn is barely present in surface waters due to its high volatility. However, during infiltration processes, ^{222}Rn is enriched in the aquifer along the flow path until an equilibrium concentration is reached. The increase in radioactivity is described by :

$$A_t = A_e\,(1\text{-}e^{-\lambda}A_t) \qquad (3)$$

A_t	concentration of radioactivity at the time t	[Bq L^{-1}]
A_e	equilibrium (background) concentration	[Bq L^{-1}]
t	retention time	[s]
λ	decay rate (λ_{Rn} = 0.18 day^{-1})	[d^{-1}]

Taking into consideration the radioactivity A_0 of the infiltrating water, equation 3 can be solved for the retention time t.

$$t_i = \lambda^{-1}\,\ln((A_e\text{-}A_0)/(A_e\text{-}A_t)) \qquad (4)$$

Assuming a one dimensional vertical flow path, the retention time allows the derivation of darcy velocity averaged as a function of the depth z_t (Figure 6).

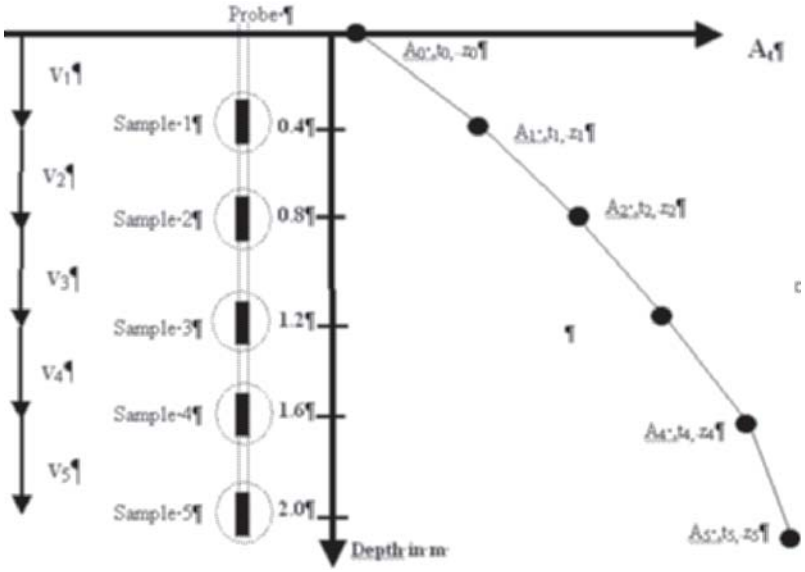

Figure 6. Theoretical increase of A_t with residence time t_i and sampling depth z_t

The velocity from the surface to the sampling point is calculated by:

$$v_i = \frac{z_i}{t_i} \tag{5}$$

The first application of this method of determining horizontal groundwater flow velocities was undertaken by Hoehn and van Gunten (1989), with further developments by Freyer et al. (1997) and Dehnert et al. (1998). The method assumes homogeneity of ^{222}Rn emanation in the soil, and determines the background equilibrium concentration A_e needed for the calculation at a remote observation borehole. However, when applying this method it was found that, due to the significantly smaller investigative scale, the assumptions regarding the homogeneity of ^{222}Rn emanation were inappropriate. This effect may be avoided, however, through the combined use of ^{222}Rn and chloride in a mixing model, as proven by Bertin & Bourg (1994). In the following study (Figure 7) performed at the Elbe River, the significant observed change in ^{222}Rn concentration at a depth of 1.5 m can be interpreted in different ways. It can be explained by a transverse water flow, by a stratigraphic change, or by alterations in the soil parameters (emanation rate). These different effects considerably influence infiltration measurements in riverbeds and thus we could not determine the vertical darcy velocity properly with this method.

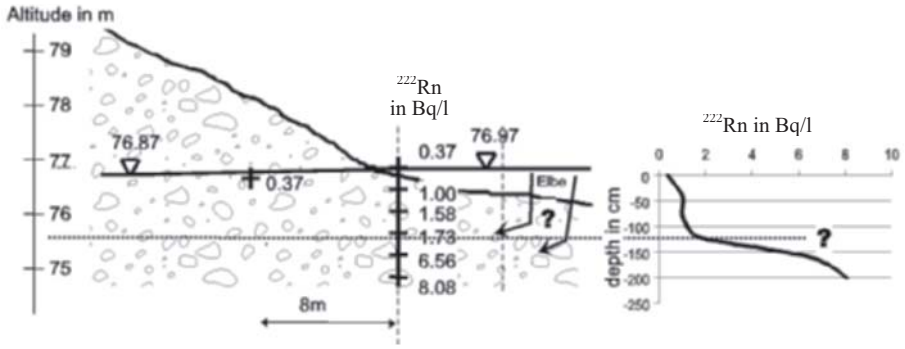

Figure 7. Example showing ^{222}Rn distribution beneath the bed of the River Elbe at Torgau, Germany

Consequently, reliable measurements can only be made if there is a well-defined, long-term stable infiltrating boundary condition between the surface water and groundwater. The calculation of darcy velocities requires knowledge of the concentration balance of ^{222}Rn for the investigated area in general (background concentration) and for individual stratigraphic layers. To get reasonable results with this method, additional information regarding the stratification of the soil, the background level of ^{222}Rn activity at the sampling point, and the density and porosity of each layer is necessary. Acquisition of this additional information represents the main challenge. At the University of Applied Sciences in Dresden, a laboratory-scale column test has been set up to try to resolve this problem. The set up of the column is shown in Figure 8.

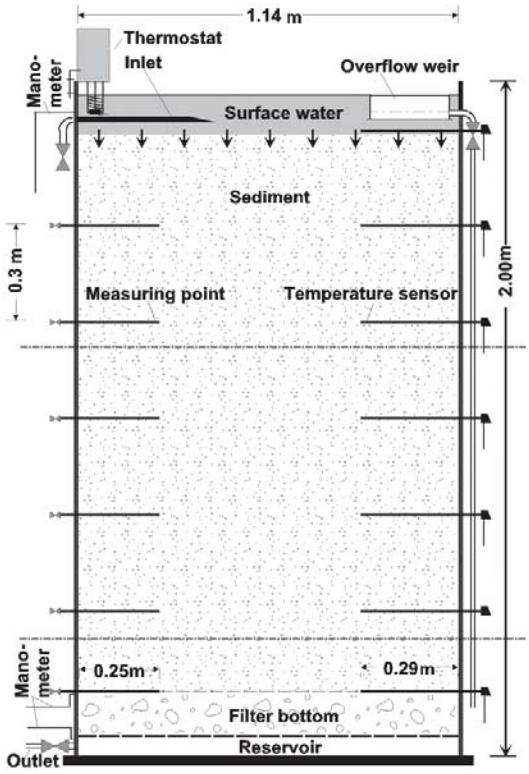

Figure 8. Schematic diagram of the column used to determine infiltration rates with the distribution of ^{222}Rn concentration

The column was filled with sediments from the Elbe River. To reproduce the field conditions at the Elbe River, the flow velocity through the column was set at 0.1 m d^{-1}. Before the test was started, the ^{222}Rn equilibrium concentration A_0 was determined at every sampling point and, having achieved a time invariant concentration profile with depth, water samples of 0.5 L each were taken at three different sampling points at each depth. The vertical distance between the sampling points was 0.30 m. As shown in Figure 9, a reasonable correlation between the theoretical and measured values was achieved, using degassed water.

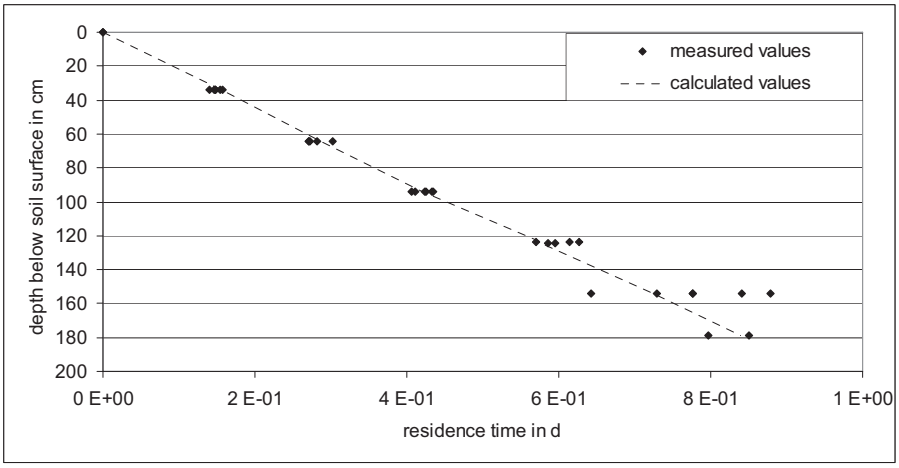

Figure 9. Depth profile of residence time of water using degassed water

If using non degassed water, there were no reasonable correlations between the theoretical and the measured values (Figure 10).

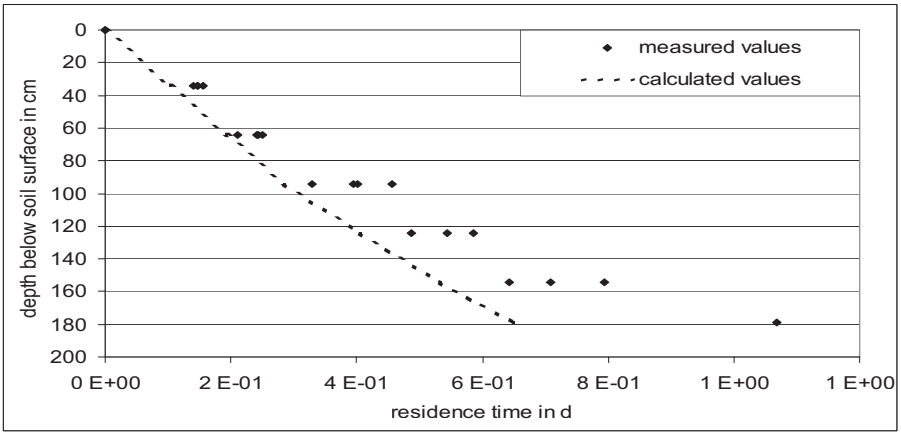

Figure 10. Depth profile of residence time of water using non degassed water

This was the reason to look for the influence of gas content on the permeability and the ^{222}Rn concentration in the sediment.

To determine the equilibrium concentration under degassed and non degassed conditions, no flow conditions were established in the column. Different values were measured using non degassed and degassed water.

Figure 11 shows the result for the equilibrium test with non degassed water, and Figure 12 the same experiment with degassed water. There the equilibrium concentration is 67% higher than with non degassed water, revealing the influence of gas content on the ^{222}Rn concentration in the aquifer. The variation in measured ^{222}Rn concentrations at each level is due to the inhomogeneity of the material and different sampling locations at each level.

The decrease in ^{222}Rn concentration with depth in the column in Figure 11 and Figure 12 is a result of increasing porosity of the sediment with depth due to the suffusion process. This is shown in Figure 13.

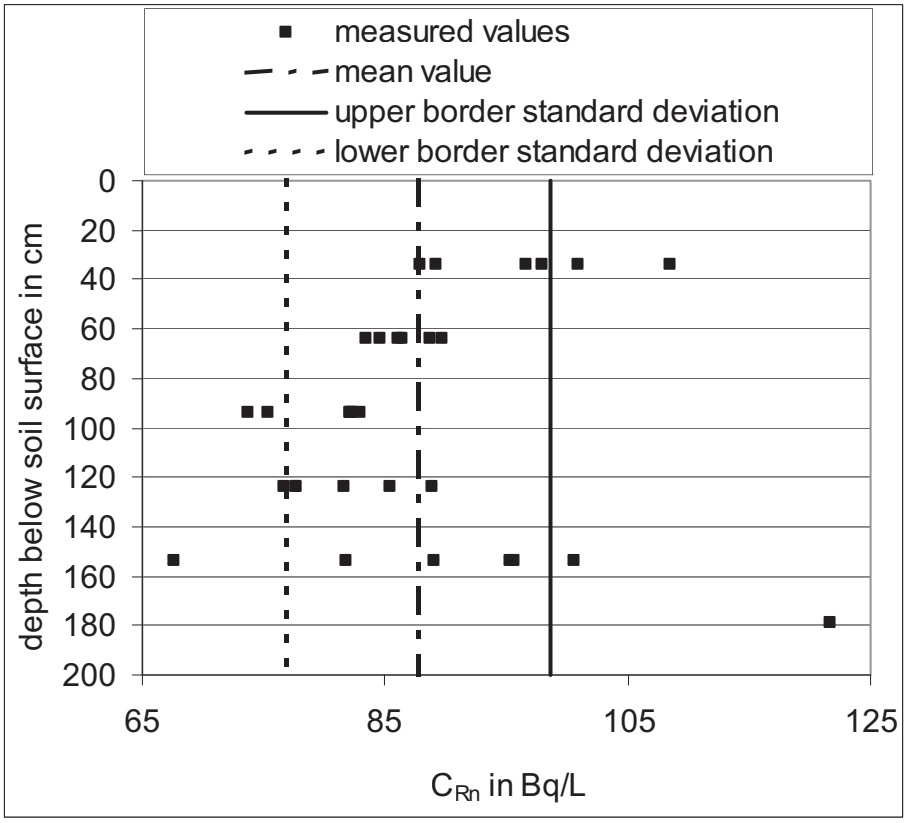

Figure 11. Results for non degassed water

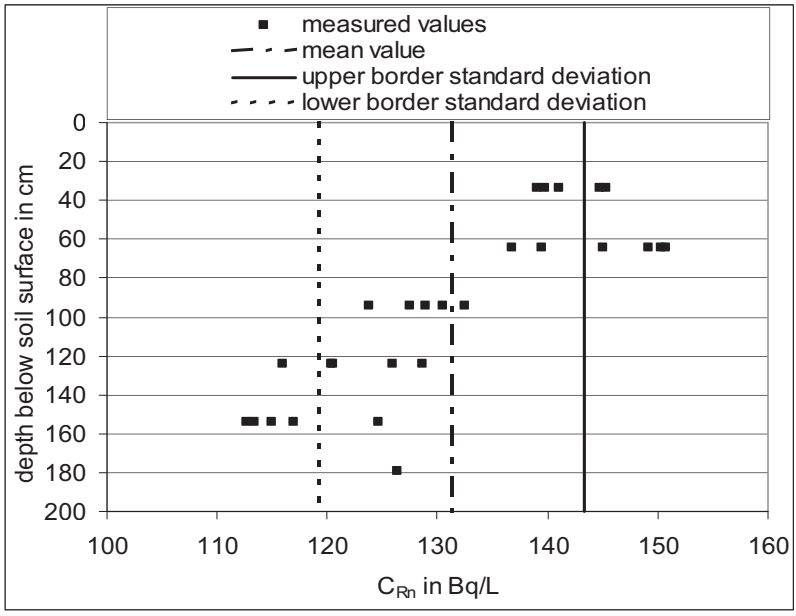

Figure 12. Results for degassed water

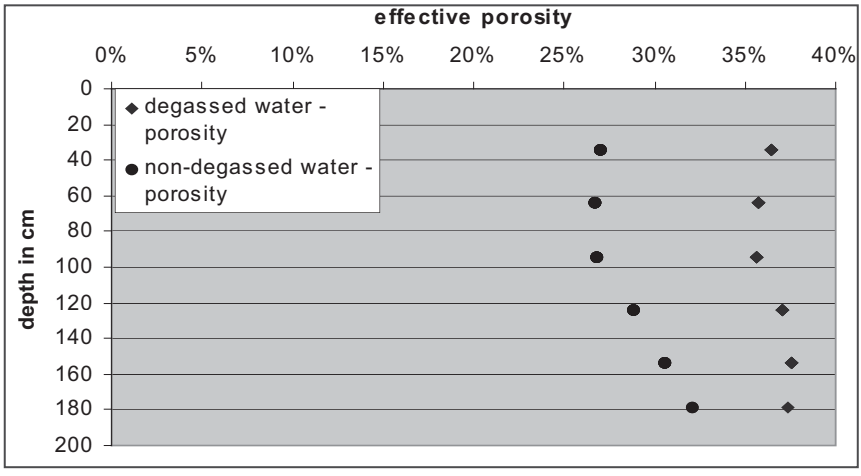

Figure 13. Dependence of effective porosity on gas content in water in a column experiment

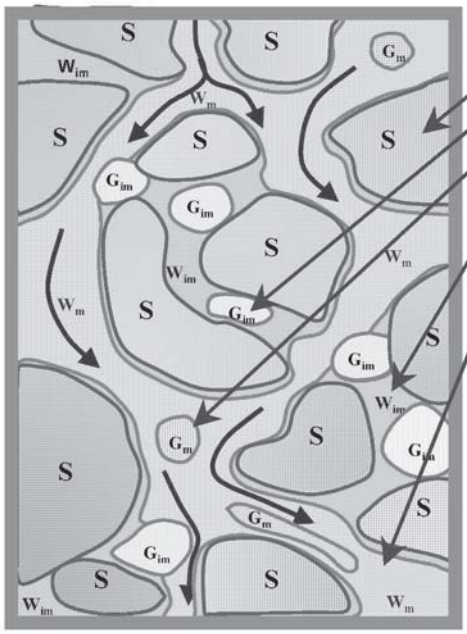

Figure 14. Conceptual model

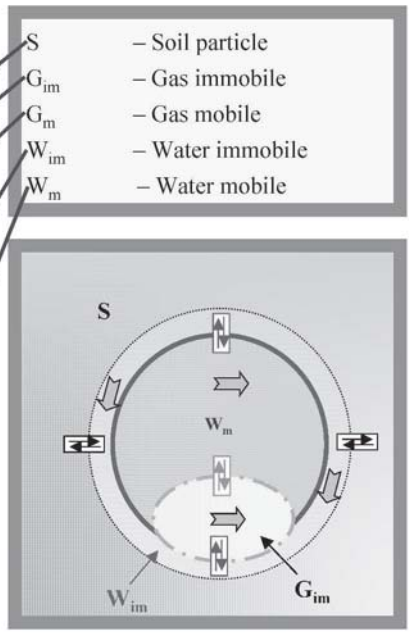

Figure 15. Model for an aquifer pore channel

The conceptual model was transferred into a mathematical model (eq. 6).

$$C_{w,i}^{t} = C_{w,i}^{t-1} + \frac{C_{w,i-1}^{t-1} - C_{i}^{t-1} + [C_{i}^{\infty} \bullet n_{0,i} / n_{f,i} - C_{w,i-1}^{t-1} - C_{w,i}^{t-1} \bullet (n_{im,i} / n_{f,i} + k_{gw} \bullet n_{g,i} / n_{f,i})] \bullet (1 - \exp(-\lambda \bullet \Delta t)}{1 + n_{im,i} / n_{f,i} + k_{gw} \bullet n_{g,i} / n_{f,i}} \quad (6)$$

where

$C^{t}_{w,i}$	^{222}Rn concentration in mobile water in layer i	[Bq/L]
C_i^{∞}	^{222}Rn equilibrium concentration	[Bq/L]
Δt	time step length	[d]
λ	decay constant of ^{222}Rn	[1/d]
k_{gw}	^{222}Rn distribution coefficient gas-water	[-]
$n_{0,i}$	total porosity of layer i	[-]
$n_{im,i}$	porosity of layer i filled with immobile water	[-]
$n_{f,i}$	porosity of layer i filled with mobile water	[-]
$n_{g,i}$	porosity of layer i filled with immobile gas	[-]

The ^{222}Rn concentration in mobile water for layer i is a function of residence time (time step length), ^{222}Rn equilibrium concentration for this specific layer i (depending on ^{222}Rn emanation from the material), the matrix porosity filled with mobile and immobile water and immobile gas. With this mathematical model, the behaviour of ^{222}Rn in the underground can be described more accurately due to the incorporation of exchange processes between mobile and immobile aqueous phases and gas phases.

Computations with this model are represented in Figure 16, whereby the influence of gas on the ^{222}Rn concentration is shown, assuming different gas and water contents in the aquifer. The curves correspond to the ratio of gas to water in the pore volume. The left most curve shows the ^{222}Rn concentration with depth for a case when 25% of the pore volume is filled with gas. The lower ^{222}Rn concentrations in water compared to a fully saturated condition (right curve) are an effect of diffusion of radon into the gas phase.

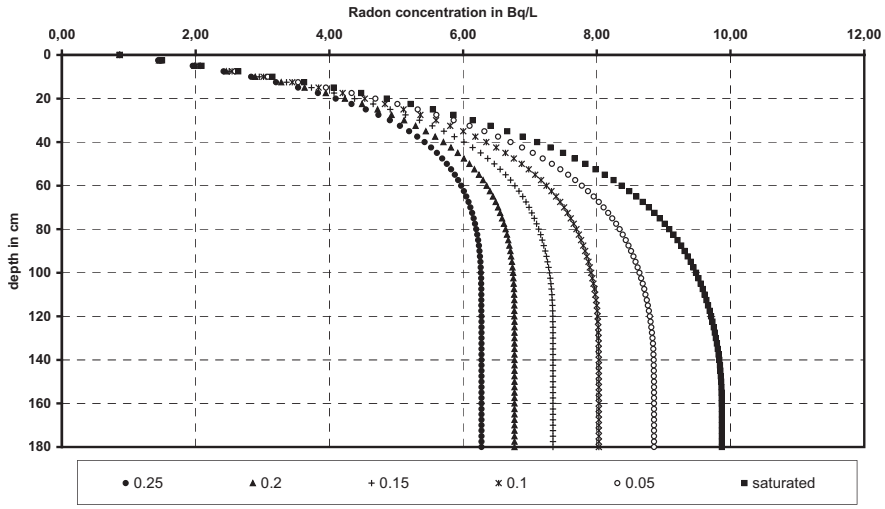

Figure 16. ^{222}Rn concentration as a function of the gas content (different ratios of gas to water in the pore volume, $v_f = 0.025$m/d)

6. SUMMARY

On riverbed filtration sites external and internal colmatage layers have to be determined to ensure accuracy in the description of exchange processes between surface and groundwater.

The effects of partial clogging of the river bed on infiltration are often overestimated. A considerable effect of clogging on the infiltration rate was only observed for more than an area of 80% of colmatage cover.

The gas formation in the colmatage layer, and thus the gas content in the aquifer can have a strong effect on its permeability.

^{222}Rn is a well defined, natural tracer that can be used for the determination of infiltration rates. Some restrictions must be considered thereby. The best results are achieved if the gas content in the infiltrating water and in the aquifer is low. Decrease in flow velocity leads to an increase in the influence of gas on measurable ^{222}Rn concentrations. The ^{222}Rn equilibrium concentration has to be determined for each measuring point.

Several field techniques have been developed and tested to characterise surface water/groundwater interaction. Despite the presented discussions, there is still a need for further enhancement of the described techniques to determine streambed infiltration rates at a field scale.

REFERENCES

Bertin, C. & Bourg, A.C.M. 1994. ^{222}Rn and chloride as natural tracers of the infiltration of river water into an alluvial aquifer in which there is significant river/groundwater mixing. *Environmental Science & Technology*, 28, 794-798.

Busch, K.-F., Luckner, L. & Tiemer, K. 1993. *Geohydraulik (Geohydraulics), Band 3, Lehrbuch der Hydrogeologie*. Verlag Gebrüder Bornträger, Stuttgart.

Dehnert, J., Freyer, K., Treutler, H.C. & Nestler, W. 1998. *Wassergewinnung in Talgrundwasserleitern im Einzugsgebiet der Elbe. (Water abstraction in the Elbe River catchment), Report 5. ^{222}Rn zur Charakterisierung geohydraulischer Prozesse (Use of ^{222}Rn to characterize geohydraulic processes)*. BMBF-Verbundforschungsvorhaben 02WT9454.

Freyer, K., Treutler, H.C., Dehnert, J. & Nestler, W. 1997. Sampling and measurement of ^{222}Rn in water. *Journal of Environmental Radioactivity*, 37, 327-337.

Hoehn, E. & Von Gunten, H. R. 1989. ^{222}Rn in groundwater: a tool to assess infiltration from surface waters to aquifers. *Water Resources Research*, 25, 1795-1803.

Nestler, W., Macheleidt, W. & Herlitzius, J. 2000. *Grundwasserströmung in der Elbaue bei Falkenberg (Groundwater flow in the Elbe River valley near Falkenberg)*. Research Report UFZ, No. 9907551.

Pätzold, J. 1999. *Untersuchungen zur messtechnischen Erfassung der Versickerung aus Flüssen und Seen* (Investigations of measurements of infiltration rates in rivers and lakes). Diploma thesis, University of Applied Sciences, Institute of Water Sciences.

Pfützner, R. 1998. *Methodische Untersuchungen zur messtechnischen Erfassung der Versickerung aus Flüssen und Seen* (Methodological investigations of measurements of infiltration rates in rivers and lakes). Diploma thesis, University of Applied Sciences, Institute of Water Sciences.

BIOCLOGGING IN POROUS MEDIA: TRACER STUDIES

Peter Engesgaard[1], Dorte Seifert[2] and Paulo Herrera[3]
[1] Geological Institute, University of Copenhagen, Denmark
[2] Environment & Resources DTU, Technical University of Denmark
[3] Department of Earth and Ocean Sciences, The University of British Columbia, Canada

Abstract: Tracer studies show that the flow regime may transform from near uniform flow at the starting conditions to non-uniform flow under conditions with severe bioclogging. The mode of observation (flux averages or point measurements) thus becomes important. It is proposed that bioclogging may lead to changes in transport patterns as well. A first phase, where the dispersivity increases approximately linearly as the hydraulic conductivity decreases is explained as the result of an increase in the number of micro-colonies located strategically in pore throats. A second phase follows, where the capacity for diffusion between the mobile water phase and the immobile biophase has increased, leading to significant tailing in solute breakthrough. A third phase may develop, where preferential flow paths results in fracture-like breakthrough. The results show that calculated changes in bulk hydraulic conductivity may be reproducible from experiment to experiment, while, in some cases, and especially those involving point injection of nutrients, the initial heterogeneous distribution of bacteria will affect the development of bioclogging patterns.

Key words: bioclogging, tracer studies, riverbank filtration

Stephen A. Hubbs (ed.), Riverbank Filtration Hydrology, 93–118.

1. INTRODUCTION

Biomass growth is a problem during artificial recharge of groundwater (Baveye et al., 1998; Pérez-Paricio and Carrera, 2001), engineered bioremediation (Baveye et al., 1998), and river bank filtration (von Gunten and Zobrist, 1993). Excessive biomass accumulation can cause bioclogging that drastically changes the flow regime. Understanding these changes and the responsible physical-microbiological processes that influence transport of nutrients and other solutes (contaminants) is essential for managing artificial recharge and river bank filtration schemes.

Visualisation of dye tracer movement and the measurement of chemical (non-reactive) tracers (Chloride) have been used to demonstrate the change in flow patterns in porous media affected by bioclogging. However, there only exist a few examples, i.e., the development of bioclogging patterns in 2D flume experiments with sand (Kildsgaard and Engesgaard, 2001) and glass beads (Thullner, 2004), and changes in longitudinal mixing in column experiments (Taylor and Jaffé, 1990; Sharp et al., 1999; Holm, 2000; Hill and Sleep, 2002; Bielefeldt et al., 2002ab, Seifert and Engesgaard, 2004). In most cases, the observed tracer distributions were used to illustrate the effect of bioclogging on flow, and not so much to quantify the effects on the hydraulic properties of the porous media, e.g., mobile/immobile porosity, dispersion, and diffusion, and rarely, to study the rapid changes from uniform flow to what may be best characterized as non-uniform flow. Non-uniform flow here describes a broad range of flow conditions, ranging from breakthrough curves with tailing effects, fracture-like breakthroughs, fingering, and by-passing.

In this work a compilation of tracer studies in bioclogging experiments in column and sand boxes are discussed with the objectives of (i) visualizing the development of non-uniform flow patterns, (ii) quantifying the temporal changes in relative mobile porosity, dispersion and diffusion, and (iii) testing two models for linking changes in porosity (due to bioclogging) to changes in hydraulic conductivity.

Two sets of experiments are discussed; (a) Column experiments, where the mode of observation was different (flux averages versus resident concentrations) and (b) Sand box experiments with a line or point source. The line source experiments in a 2D sand box are essentially the same as a (1D) column experiment, but allows visualisation using a dye tracer. The point source experiments in the sand box are included to illustrate the differences in forcing nutrients through the total zone with bioclogging and allowing the nutrients to by-pass zones with bioclogging. Parts of this work may also be found in Holm (2000), Kildsgaard and Engesgaard (2001, 2002), and Herrera (2002).

2. THEORY

The total porosity, θ, is conceived to consist of a mobile porosity, θ_m, and an immobile biomass porosity, θ_{bio}. Growth of biomass affects the biomass porosity so that at any instant the mobile porosity can be calculated as;

$$\theta_m = \theta - \theta_{bio} = \theta - \frac{\rho_b X}{\rho_X} \tag{1}$$

where X is the biomass concentration and ρ_b and ρ_X are the bulk soil and biomass density, respectively. The relative mobile porosity is then defined as;

$$\beta = \frac{\theta_m}{\theta} \tag{2}$$

Kildsgaard and Engesgaard (2001) and Thullner et al. (2004) applied bioclogging models to simulate the changes in biomass concentration, X, and, thus, biomass porosity. These models include a suite of physical and microbiological processes; advection-dispersion of nutrients and dissolved biomass, attachment-detachment of biomass, and microbial (Monod) growth and decay.

An essential feature of any bioclogging model is how to link changes in simulated relative mobile porosity (β) to that of changes in hydraulic conductivity (K). Vandevivere et al. (1995), Baveye et al. (1998), and Seifert and Engesgaard (2004) reviewed various relationsships, referred to as K-β models. As an example, two models will be discussed, the K-β model by Clement et al. (1996):,

$$\frac{K}{K_{ini}} = \beta^{19/6} \tag{3}$$

where K_{ini} is the initial (clean) hydraulic conductivity. The Clement K-β model was derived from pore-size distribution models and soil-water retention functions. Thullner et al. (2002) proposed an alternative K-β model:

$$\frac{K}{K_{ini}} = a \cdot \left(\frac{\beta - \beta_{min}}{1 - \beta_{min}} \right)^3 + (1-a) \cdot \left(\frac{\beta - \beta_{min}}{1 - \beta_{min}} \right)^2 \quad (4)$$

derived from pore network simulation results assuming a micro-colony distribution of biomass. Here β_{min} is a threshold value for the relative mobile porosity, i.e., the value of β where the hydraulic conductivity reaches zero, given the constraint $\beta \in]\beta_{min},1]$. *a* is a fitting parameter with the constraints $a \in]-2;-0.5[$. Figure 1 shows the two K-β models, where a=-1.7 and β_{min}=0.75 or β_{min}=0.50 in the Thullner K-β model. The Clement K-β model has the advantage of requiring no parameters, however, notice that, in comparison to the Thullner K-β model, significantly more biomass (low β) is needed to decrease the relative hydraulic conductivity to a low level. For example, if the relative hydraulic conductivity is 0.001, then the Clement K-β model predicts β=0.12 (88% of the total porosity is biomass) and the Thullner K-β model that β=0.75 or β=0.5. Such a significant difference in amount of biomass could have a significant effect on transport in terms of changes in effective pore water velocity and potential attenuation through diffusion between the mobile and immobile domains.

The advection-dispersion-diffusion model is used to describe transport of a conservative tracer through the mobile domain and a first-order mass-transfer model is used to represent the exchange of mass between the mobile and immobile phases as shown in the following equations,

$$\frac{\partial C_m}{\partial t} = D_m \frac{\partial^2 C_m}{\partial x^2} - v_m \frac{\partial C_m}{\partial x} - \left(\beta^{-1} - 1\right) \frac{\partial C_{im}}{\partial t} \quad (5)$$

$$\frac{\partial C_{im}}{\partial t} = \frac{\alpha}{\theta \cdot (1-\beta)} \left(C_m - C_{im}\right) = \frac{\omega \cdot v_m \cdot \beta}{L \cdot (1-\beta)} \left(C_m - C_{im}\right) \quad (6)$$

where C_m and C_{im} are the concentrations in the mobile and immobile domains, respectively. D_m is the dispersion coefficient, $v_m=q/\theta_m$ is the pore water velocity in the mobile zone, with q as the flow rate, and ω is the dimensionless mass transfer coefficient (Damkohler number) $\omega=(\alpha \cdot L)/(\theta_m \cdot v_m)$, with α as the first-order mass transfer coefficient between the mobile and immobile phase and L as the length of the considered region. If β decreases, then the pore water velocity increases and the last capacitance for mass transfer between the mobile and immobile domains increases.

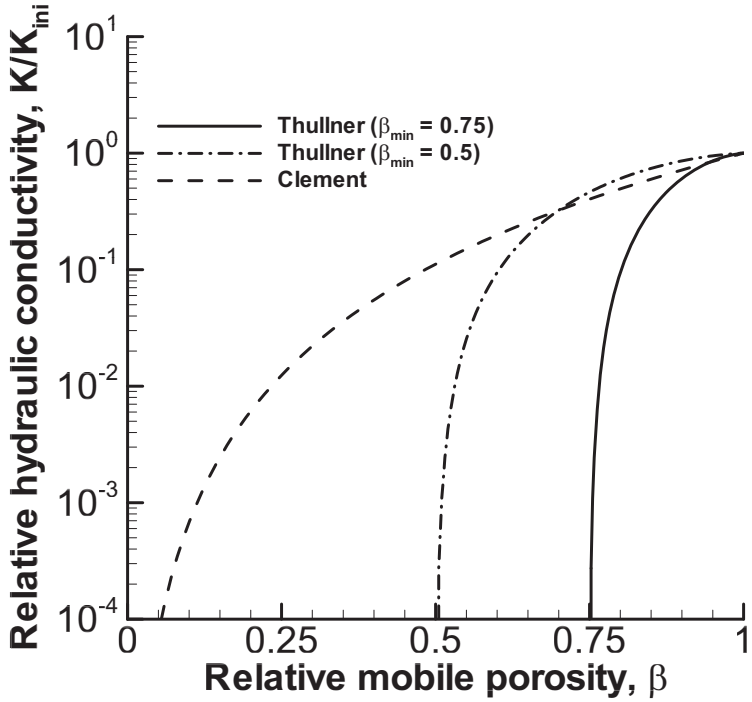

Figure 1. K-β models. The parameter set (a, β_{min})=(-1.7, 0.75) for the Thullner model

Equations (5) and (6) were solved analytically by CXTFIT (Toride et al., 1999) by automatically fitting appropriate solutions to observed tracer breakthrough curves either assuming a pure advection-dispersion model or an advection-dispersion-mass transfer model.

3. EXPERIMENTS

3.1 Column Experiments

Figure 2 shows a typical experimental column setup (taken from Holm, 2000). The length and diameter of the columns may vary. The upwards flow rate through the column is fixed. Nutrients, such as substrate (acetate) and

electron acceptors (oxygen or nitrate), are added to the inlet solution in known concentrations. The sand is mixed with pre-treated waste water and sits in a bucket for 2-3 days (with daily stirring) before the column is packed with the inoculated sand. The columns are installed with ports for measuring hydraulic head either using pressure transducers or manometers. Sampling ports are in some cases, like shown in Figure 2, placed along the column to allow for measuring the spatial distribution of nutrients and tracers. Otherwise, the concentrations only are measured at the outlet as a breakthrough curve (flux-average).

Great care is taken to pack a column as homogeneously as possible. Before the clogging experiment is started the initial hydraulic conductivity (K_{ini}) is measured. The initial porosity is known from weighing the amount of sand used for packing the column. A tracer experiment is performed to estimate the initial dispersivity and verifying the initial porosity value.

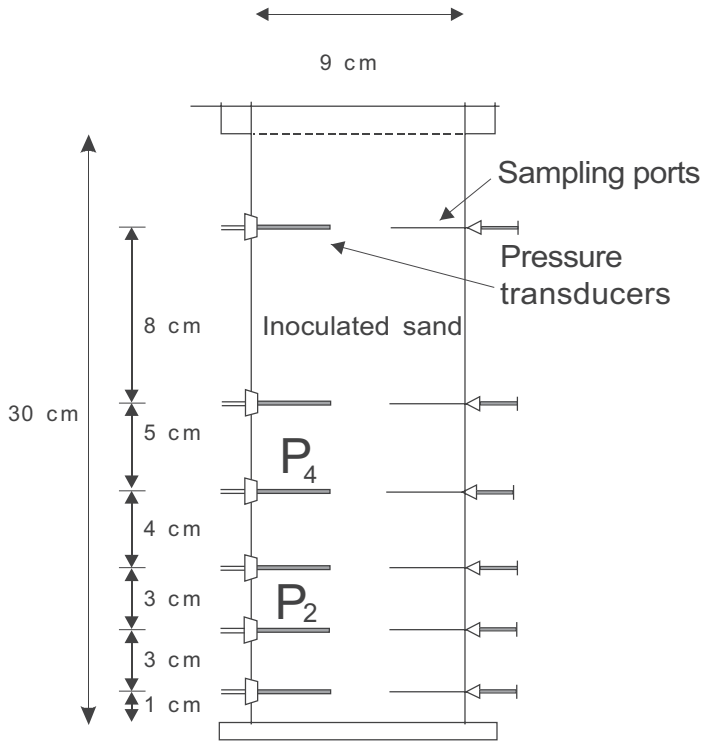

Figure 2. Experimental columns (Holm, 2000)

During the clogging experiments several tracer studies are carried out at regular intervals.

3.1.1 Example 1: Tracer studies with outlet breakthrough curves

The objectives were to investigate dispersion-diffusion characteristics and the reproducibility of bioclogging patterns. Three columns, 0.2 m long and 0.04 m ID, were packed with similar sands (0.3-0.6 mm grain size). Acetate and oxygen were injected at a constant flow rate of 2.9 L/day for the first 67 days and 5.8 L/day (double flow rate) for the remaining 83 days. Due to the prolonged experimental period changes in the flow rate were observed possibly due to growth of bacteria in the inlet tubes. The hydraulic heads were measured at the inlet and 0.04 m, 0.08 m, and 0.15 m from the inlet. 43 tracer experiments using Chloride were carried out approximately every 2-4 days. The tracer was measured at the outlet and thus represents a measure of the flux-averaged concentration (Parker and van Genuchten, 1984).

Figure 3 shows the change in the relative bulk hydraulic conductivity for the first 0.04 m from the inlet over the first 40 days. Unfortunately there are no data beyond the first 40 days, simply because the hydraulic heads were measured manually in manometers, which no longer were able to measure the high gradients. The changes in hydraulic conductivity in the remaining two sections, 0.04-0.08 m and 0.08-0.15 m, were insignificant.

The calculated hydraulic conductivities are converted to relative mobile porosity, β, using the two K-β models (3) and (4). Figure 4 shows the changes in β over the first 40 days for column 2. Notice that the Clement K-β model results in β values down to less than 20%, i.e., greater than 80% of the initial porosity is now biomass. The Thullner K-β model results in β values that are much higher (using the parameters a=-1.7 and β_{min} =0.75 or 0.5). Thus, the Clement K-β model suggests that tracer transport in the first 0.04 m would occur much faster (factor of 4 compared to the initial pore water velocity) and that there is a large capacity for diffusion into biomass. In contrast, the Thullner K-β model predicts somewhat lower pore water velocity and less capacity for diffusion. Evaluating tracer transport therefore has the possibility of investigating the limitations and capabilities of K-β models. A problem is that the breakthrough is measured at the outlet (0.20 m from the inlet), while the zone of bioclogging is only about 0.04 m from the inlet, 20% of the length of column.

The output from tracer experiments is thus a mixed signal of transport through zones of sand with bioclogging and (relative) clean sand. A simple mass balance can yield an approximation of the overall pore water velocity

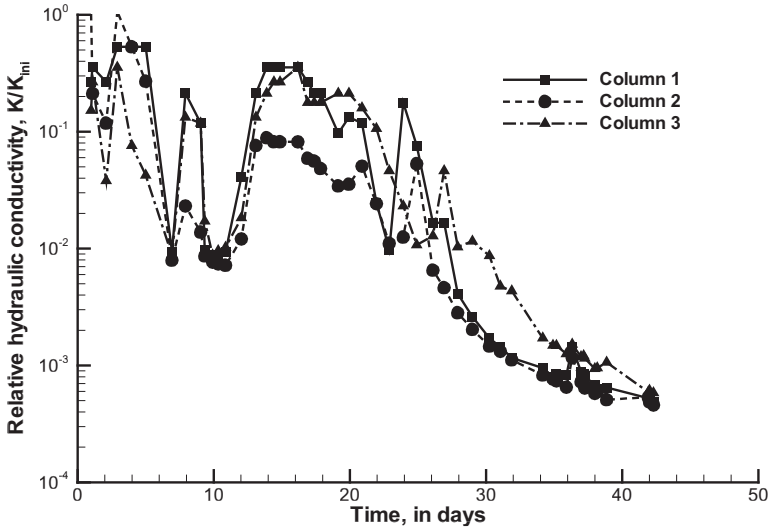

Figure 3. Calculated relative hydraulic conductivity for triplicate runs

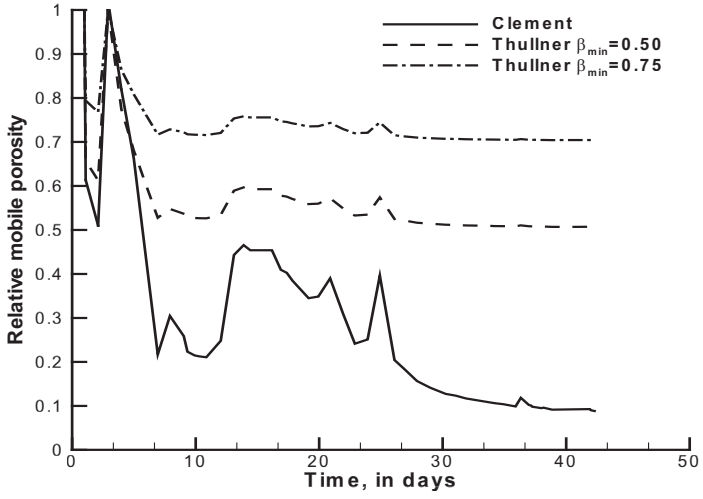

Figure 4. Calculated β values using Figure 3 and the two K-β models.

in the whole column. If it is assumed that bioclogging only affected the first L_1=0.04 m (L_2 = 0.16 m) then the mean pore water velocity (V) is;

$$V = \frac{Lv_2}{\frac{\theta_{m,1}}{\theta_{m,2}} L_1 + L_2} \tag{7}$$

where $\theta_{m,i}$ are the mobile porosities in the bioclogged and clean sections and v_2 is the pore water velocity of the unaffected zone. The Clement K-β model predicts $\theta_{m,1}$=0.1 θ, while $\theta_{m,2}$= θ, thus, V= 1.22v_2, a 22% increase above the initial velocity, which should be a noticeable increase in transport velocity through the whole column. The Thullner K-β model predicts a much smaller increase in overall transport velocity.

Figure 5 shows 33 out of the 43 tracer experiments that were carried out every 2-4 days during the 150 day long experimental period. The inlet flow velocity was increased a factor of two after day 67, so all breakthrough curves after day 67 have been shifted a factor of two in time in order to compare with the first series of breakthroughs. The arrival time of the breakthrough should thus be interpreted with some caution, also because the mobile porosities inside the column changed over the course of the clogging experiment.

However, by grouping the experiments in two periods reveal some general patterns. Figure 5a shows the first 39 days and Figure 5b show the remaining experiments from day 39 to 150. The first approximately 40 days shows the most dynamic changes in tracer transport. This coincides with the period where the hydraulic conductivity changes the most in the first 0.04 m of the column, Figure 3. From day 1 to 10 the breakthroughs occur earlier, however from day 10 to 25 there is a significant increase in the delay of breakthrough and a tailing effect. Following day 25, the breakthrough again appears earlier, but still with significant tailing. After day 39, Figure 5b, the breakthroughs occur later than at day 1 and with some tailing. If day 25 is disregarded, then days 31-39 in Figure 5a could shift to the second period showing the same degree of delay and tailing. At about day 30 the hydraulic conductivity decreases from a relative value of about 0.01 to 0.001, but with much less fluctuation compared to the period up to day 30. The breakthroughs after day 39 show an inconsistent pattern in the sense that sometimes the breakthrough arrives a little earlier sometimes a little later.

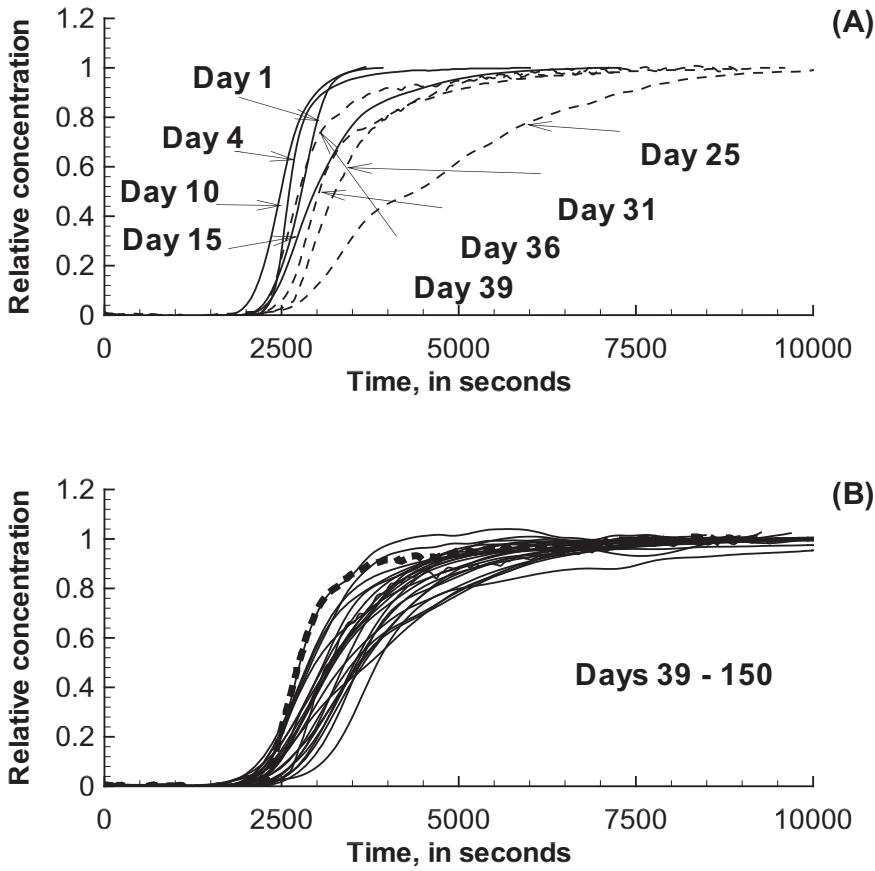

Figure 5. 33 tracer tests (Day 1 to Day 150). (A) First 39 days, (B) Day 39 (dashed line) to Days 39-150 (solid lines).

The late arrival of the breakthroughs after day 39 is not consistent with the predicted increase in velocity (see above). Thus, some other mechanism must retard tracer transport. The significant spreading and tailing indicate that growth of micro-colonies is plugging pore throats, increasing dispersion, and allowing for mass transfer. Figure 6 shows the result of fitting an advection-dispersion model (no mass transfer) to the breakthrough curves allowing the model to fit both velocity and the dispersion coefficient. The velocity was fairly constant (except that after day 67 it was increased by a factor of two due to the increase in the inlet flow rate). In all three columns an increase in dispersivity is seen (factor of 2-8). Figure 7 shows one of the results (day 99). Included is also the result of fitting and advection-

dispersion-mass transfer model. Clearly, the model, which includes mass transfer between the two domains, simulates the experiment much better.

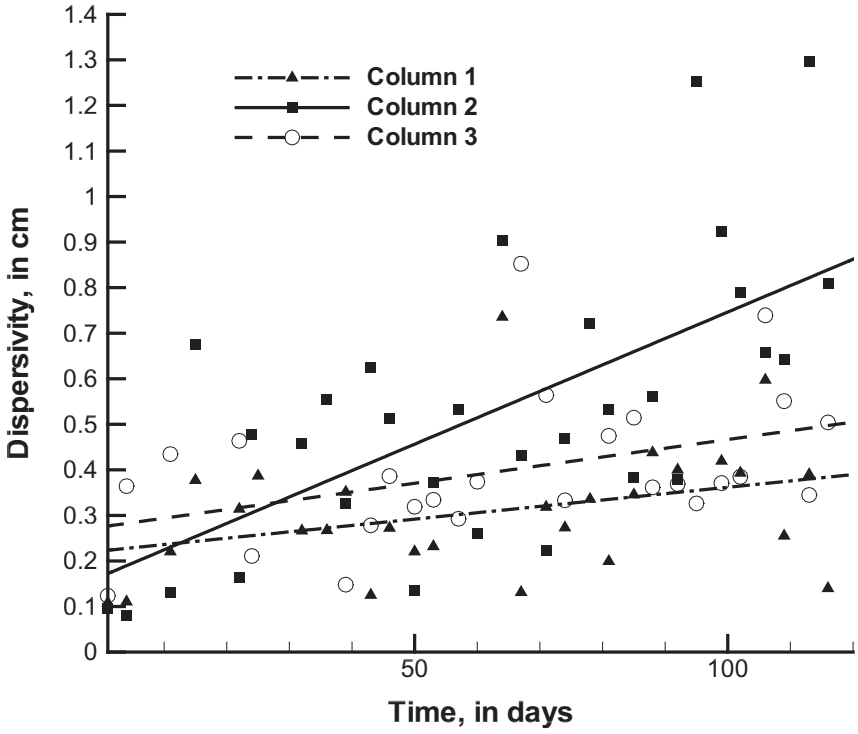

Figure 6. Fitted dispersivity values assuming pure advection-dispersion model (no mass transfer).

Figure 8 shows the results after fitting the advection-dispersion-mass transfer model to all experiments. CXTFIT was fitted to all parameters: v_m, D_m, β, and ω. The fitted dispersivity was in all cases about 0.001-0.002 m, i.e., close to the initial value. The relative mobile porosity is fairly constant around 90% for the whole column. The mass transfer coefficient (ω) showed some irregular changes, but the overall mean was fairly constant (data not shown).

A mass balance for porosity can be derived, i.e.;

$$\beta_{col} = \frac{\beta_1 L_1 + \beta_2 L_2}{L} \tag{8}$$

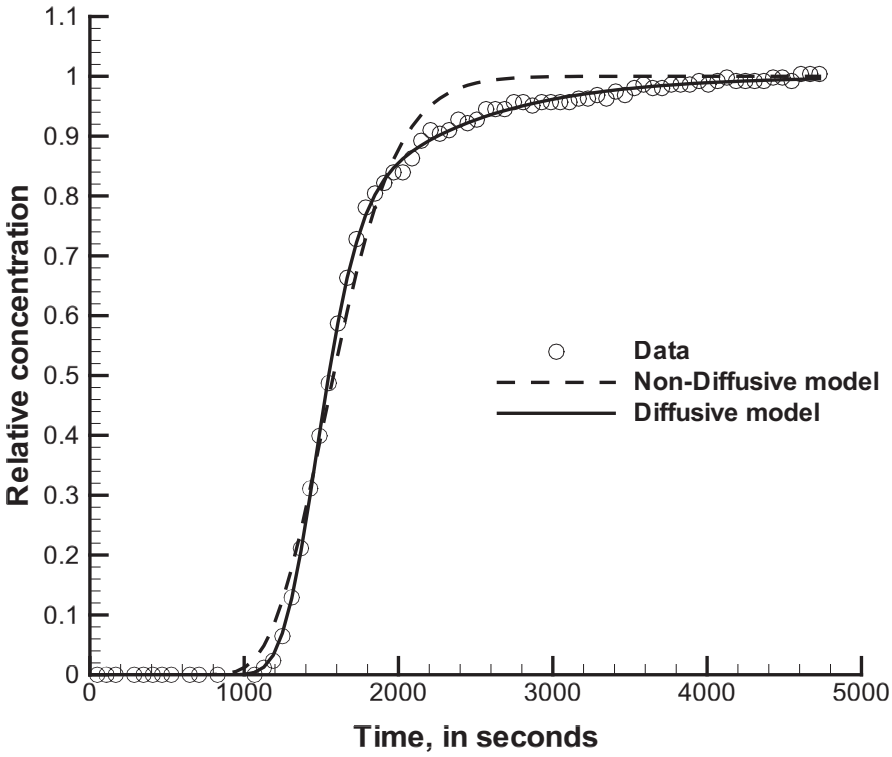

Figure 7. Breakthrough curve at Day 99. Observations and two model results with and without diffusion.

where β_i are the relative mobile porosities in the two sections of the column. With β_1=0.1 and β_2=1, the overall relative mobile porosity is approximately β_{col}=80%, a little less than the calculated mean value. To get a mean value of about β_{col}=90% requires that β_1 is about 0.5. This would give a relative hydraulic conductivity of about 0.1 with the K-β model of Clement. This is in fair agreement with the observed decrease in hydraulic conductivity for the first 20 days; however, for the remaining period a relative hydraulic conductivity of only 0.1 is close to a factor of 100 too high. In contrast, a K-β model of Thullner with β_{min}=0.50 would predict a two order change in relative hydraulic conductivity (0.1-0.001) with a β value in the range 0.5-0.6.

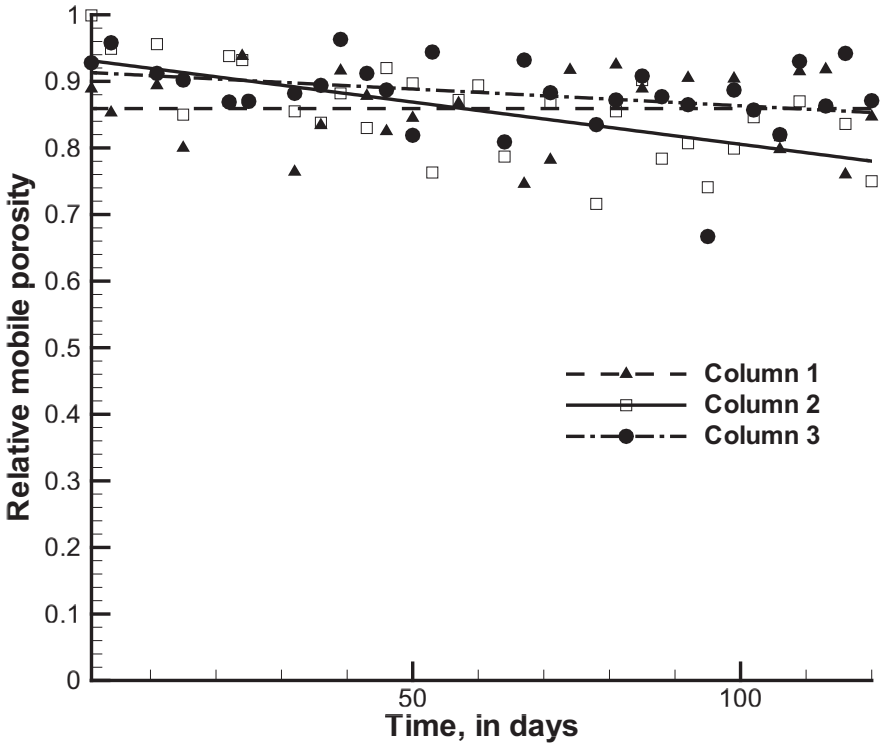

Figure 8. Fitted β values

3.1.2 Example 2: Tracer studies with in-situ breakthrough curves:

The experiment was performed in a 30 cm long and 9 cm internal diameter column packed with a medium sized sand (0.3-0.6 mm), Figure 2. Acetate was used as the substrate for microbial growth with nitrate as the electron acceptor. The initial pore water velocity was 7.2 m/day. Other details can be found in Holm (2000) and Engesgaard et al. (2002).

Figure 9 shows the development in hydraulic conductivity over the 30 day experimental period. The hydraulic conductivity in the first 1 cm of the column, K_{01}, is reduced by a factor of about 1000. A significant reduction is seen in the hydraulic conductivity even 11 cm from the inlet, where K_{34} decreases about a factor of 100. Holm (2000) found that detachment of bacteria close to the inlet and attachment further downstream could explain

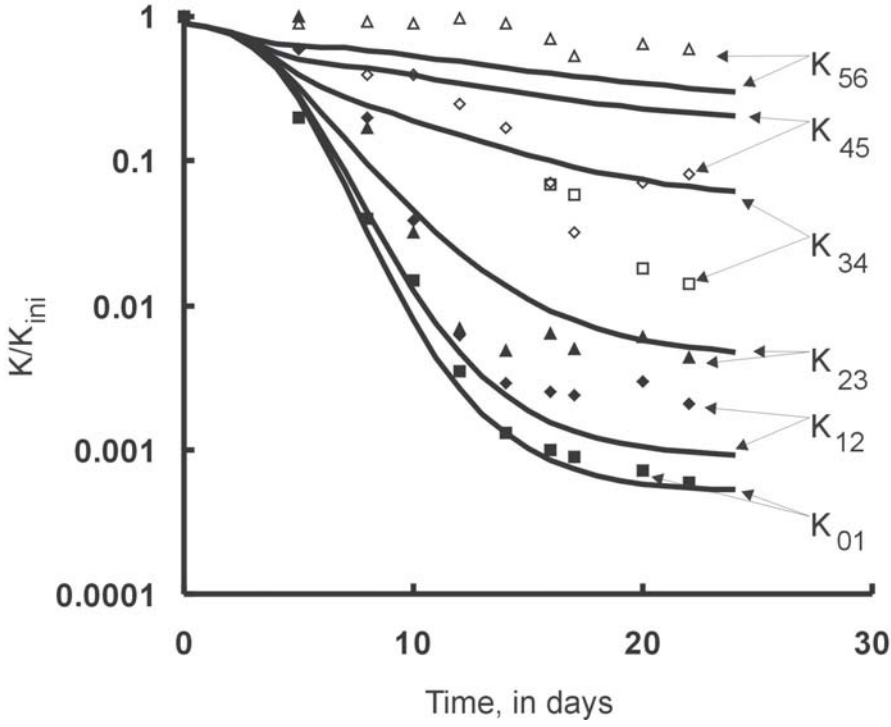

Figure 9. Reduction in relative hydraulic conductivity

the observed reductions in K. Thus, in comparison to the previous experiment, where bioclogging was restricted to the first 0.04 m, the porous medium is affected over a longer distance.

Three pulse tracer experiments were carried out; at day 7, 11, and 22. Sampling of the tracer was performed over the most bioclogged portions of the column, 4 cm from the inlet at day 7 and 11 cm from the inlet at day 11 and 22. A sampling port consist of a syringe with the needle split open so that sampling took place over the full length of the needle (0.035 m, about 1/3 of the diameter of the column). The samples do therefore not represent flux-averages, as in the previous experiment, but rather a measure of the resident concentration (Parker and van Genuchten, 1984). At day 7 the relative hydraulic conductivity was less than 0.1, while at day 11 and 22 there were much more pronounced reductions in relative hydraulic conductivity.

Figure 10 shows the three observed and modelled breakthrough curves. At day 7 the breakthrough curve is almost symmetric and the fitted pore

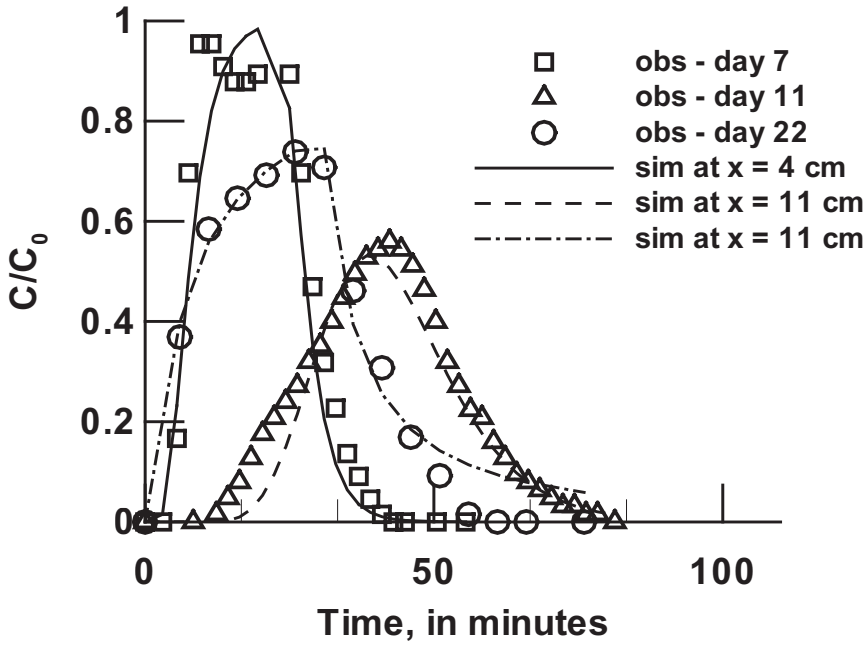

Figure 10. Three tracer breakthrough curves and model fits assuming pure advection-dispersion model.

water velocity (6.9 m/day) is close to the initial value of 7.2 m/day. Unfortunately no tracer experiment was performed before the clogging experiment started, but the fitted dispersivity is about 10 times larger than the mean grain size. Typically, one would find dispersivity values closer to the mean grain size, so the increased value indicates that the flow field at the micro-scale inside the column was already affected. The symmetry in the breakthrough suggests, however, that diffusion is not significant at this stage. At day 11 the breakthrough curve is more dispersed. The later breakthrough is primarily because sampling is now 11 cm from the inlet; however, the velocity is fitted to around 4.3 m/day, lower than the initial value by a factor of two. The dispersivity was fitted to 0.058 m, slightly larger than at day 7. As in the previous case, the effective pore water velocity is lower than the initial value.

The tracer breakthrough at day 22 resembles breakthrough curves obtained in tracer studies with preferential flow pathways, such as double-porosity media, with an early breakthrough and a long tailing due to back-diffusion of solute from low-velocity pathways (or even dead-end pores) to

high-velocity pathways. Fitting an advection-dispersion model (no diffusion) increases the dispersivity several orders of magnitude to 39 cm. The high dispersivity value is needed in the advection-dispersion model to mimic apparent non-uniform flow regimes with extremely large contrasts in the velocity field, like in a double-porosity system.

Holm (2000) developed a 1D model of transport with bioclogging and simulated the temporal evolution of the mobile (θ) and biomass porosity (θ_{bio}). Figure 11 shows the simulation results at day 22. The model is not capable of simulating the development of specific preferential flow paths, only the change in the macro-porosity values. Notice that a front with a change in the macro-porosity value occurs at about x=11 cm, where the breakthrough curve was measured at day 22. The biomass porosity is about 50% of the initial porosity. The tracer is thus advected at least twice as fast as in the rest of the column and the increased amount of biomass in the first 11 cm of the column can result in diffusion of solutes from the mobile water phase to the biophase. Figure 12 shows the result of fitting a numerical advection-dispersion-diffusion model to the observed breakthrough curves. The porosity distribution in Figure 11 was used as input. In all cases, it was possible to keep the dispersivity at a realistic value (0.22 cm), but impossible to use the same mass transfer coefficient (α).

3.2 Sand Box Experiments

One difficulty with column experiments is the inability to visually see all the changes in flow regime, for example, by carrying out dye tracer studies. However, the column experiments clearly indicate that there can be even radical changes in how a dye tracer would move through the porous medium.

Two-dimensional sand box experiments with bioclogging and dye tracer experiments were thus carried out to demonstrate how bacterial growth changes the flow field from being near-uniform to non-uniform with significant temporal changes in the pattern of flow. The sand box is shown in Figure 13 (44 by 30 by 1 cm) with flow upwards from the inlet chamber to the constant-head outlet chamber. In all experiments a strip of sand (14-26 cm from the inlet) had been inoculated with microorganisms from a wastewater treatment plant following the same procedure as with the column experiments. Great care was taken to assure that the packing was as homogeneous as possible. The change in head across the sand box was measured several times a day during the experiments. The substrate was injected either through a perforated pipe representing a line source or a "well", representing a point source. Brilliant blue was used as tracer and a digital camera was used to record the tracer distribution.

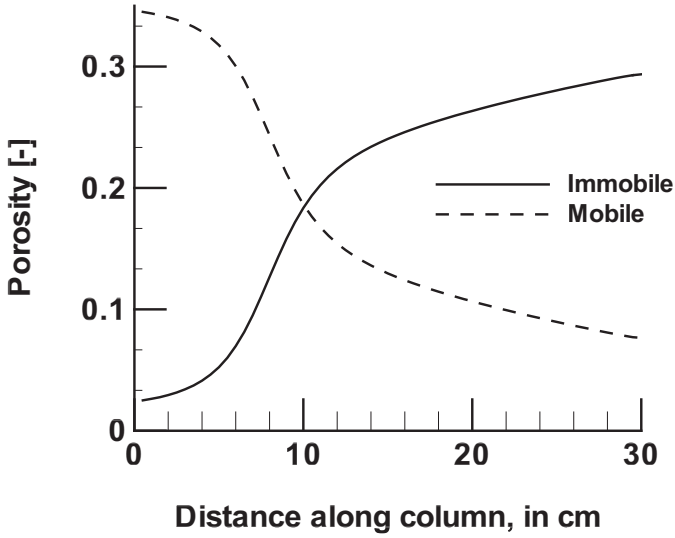

Figure 11. Numerically simulated porosity distribution at Day 22

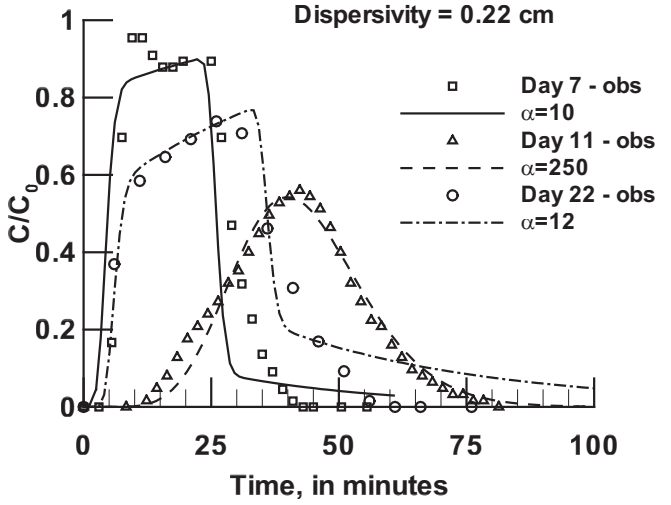

Figure 12. Results of fitting numerical tracer transport code using results of Figure 11 and assuming diffusion between mobile and biomass porosity. Units of α is day^{-1}.

3.2.1 Example 1: Tracer studies with a line source

The first set of experiments used a line source consisting of a perforated pipe extending all the way across the width of the sand box, see Figure 13. Acetate in a sterilized solution was injected through the pipe, while other nutrients and oxygen, also in a sterile solution, were added to the inlet water. The flow rate through the perforated pipe was 10% of the flow rate through the inlet chamber. The residence time was estimated to 80 minutes (pore water velocity of 8 m/day, similar to the column experiments). The experiments ran for 23-25 days with a continuous supply of substrate and nutrients. A dye tracer was introduced through the whole width of the inlet chamber at two-three day intervals.

The bulk hydraulic conductivity decreased about two orders of magnitude and, in general, all experiments showed the same pattern of change (data not shown).

Figure 14 and 15 show the distribution of the dye tracer 12 minutes after the application to the inlet source in two different experiments. The tracer distribution shows the area with less bioclogging. The tracer distribution is shown at nearly identical times for the two experiments. Both experiments show that initially the flow is relatively uniform except at the edges of the sandbox. The total flow rate was therefore not distributed uniformly across the inlet chamber. At about day 10 the tracer front is less smooth and after about 15 days finger-like structures appear. The “fingers” are different, however, in the two experiments. In the experiment shown on Figure 14, 4-5 fingers dominate, and the tracer studies at the other days showed that these fingers were permanent structures only differing in size. In Figure 15 many smaller fingers appear. So, although the starting conditions were attempted to be the same, and, although, the head drop across the sand box showed no major difference between the different experiments, the tracer studies clearly demonstrate that the flow field evolved differently in the two experiments.

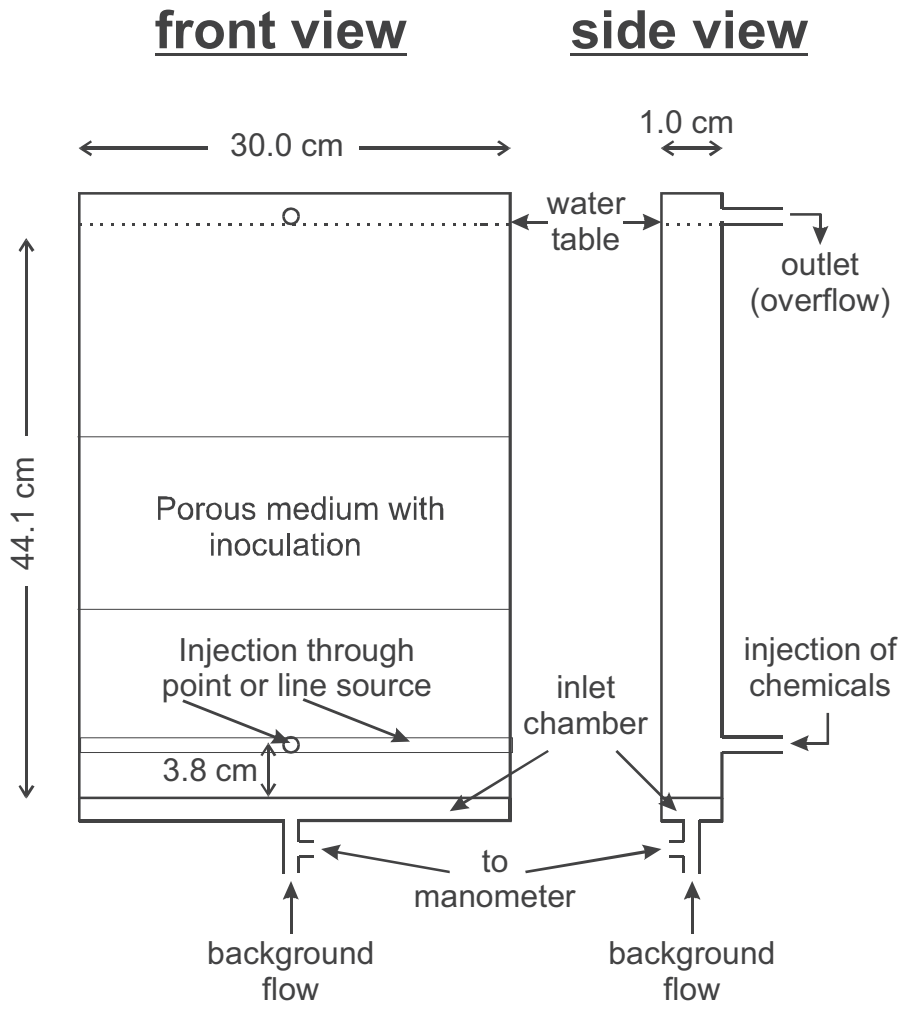

Figure 13. Experimental sand box.

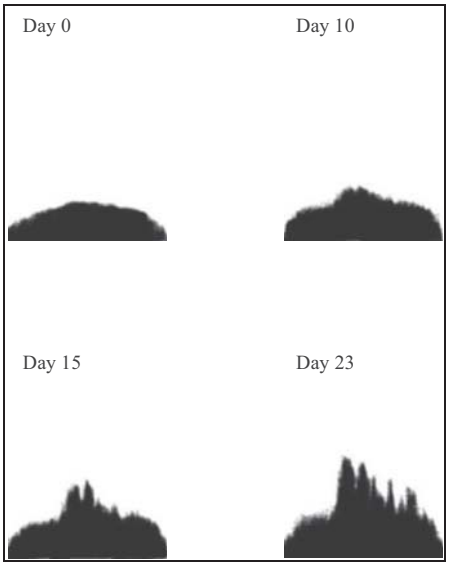

Figure 14. Black-and-White images of tracer distribution (Experiment 6).

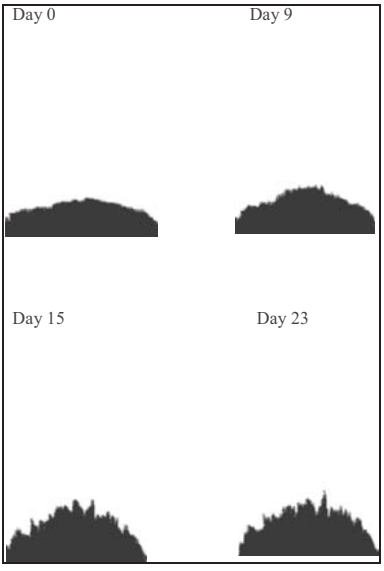

Figure 15. Black-and-White images of tracer distribution (Experiment 6).

Figures 14-15 show that the fingers move more rapid up through the sand box with later times. This is because the flow rate is kept constant and because certain areas of the box became partially blocked by biomass.

These observations may also explain the differences between the two column experiments, where the mode of observation was very different. In the long column experiments, a syringe with a perforated needle was inserted half-way into the column in order to measure (resident) concentrations inside the column. The observed breakthrough would depend very much on the position of a syringe late in the experiment, where preferential flow paths like those in Figure 14 had developed.

3.2.2 Example 2: Tracer studies with point injection

Kildsgaard and Engesgaard (2001, 2002) presented parts of these results before, but here additional pictures showing the results of the tracer studies are included in order to illustrate the differences between a line source and a point source. As before, a strip of sand with inoculated bacteria was placed in the sand box. Acetate and nitrate was injected through the point source shown in Figure 13. It is worth noting that the increase in head difference across the sand box was very small for this type of experiment.

Figure 16 shows a sequence of images after 60 minutes of dye tracer application on several days. Day 1 represents the almost undisturbed case (except for the strip of sand). At day 4 the flow rate was doubled, thus the increased travel distance. After about one week two fingers start to develop around a bioclogged zone immediately downstream to the injection point. From thereon, the two fingers are permanent structures, however differing in size and cycling between a dominant left finger, then a dominant right finger. Figure 17 shows the image after day 17, where the details of the tracer distribution are clearer. Kildsgaard and Engesgaard (2001) were able to simulate the clogging pattern so that a subsequent tracer simulation predicted the two-finger tracer distribution. However, the model was unable to explain the temporal changes in finger dominance. They explained this by not being able to include the initial heterogeneous distribution in biomass, which could trigger a cycling. Notice also that the zone of clogging moves closer and closer to the injection point.

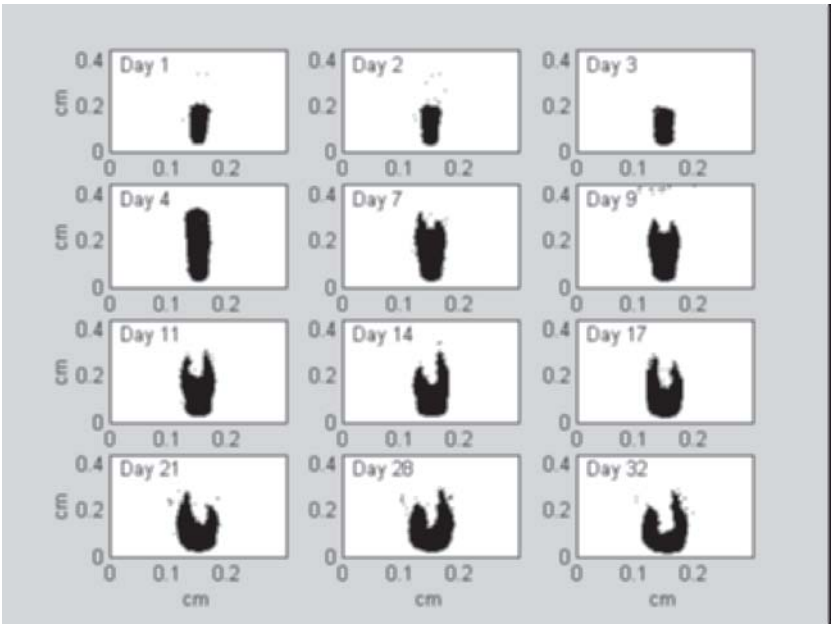

Figure 16. Images of tracer distribution after 60 minutes of injecting Brilliant Blue, from Day 1 to Day 32.

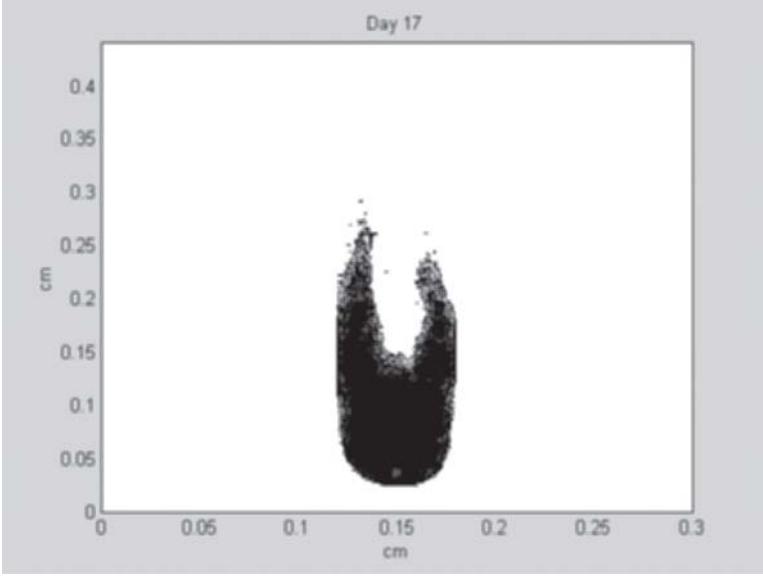

Figure 17. Image from Day 17.

4. DISCUSSION AND CONCLUSIONS

Adding a tracer to the inlet solution and measuring the breakthrough or imaging the distribution can provide information on the processes governing transport in the porous media and possibly also help to discriminate between different K-β models. We propose the following based on our observations.

Starting conditions and mode of observation

Great care was exercised in making the column and sand box experiments as homogeneous as possible. Initial dispersivity estimates in the range of the grain size confirm that it was possible to achieve a fairly hydraulically homogeneous media at the start of the clogging experiments. However, our results demonstrate that it was not always possible to achieve a microbiologically homogeneous media. Although the sand was kept well-mixed in a bucket with pre-treated waste water before packing the columns and boxes, it is very likely that scooping sand into the column produced a heterogeneous packing of the column with respect to the initial concentration of the attached bacteria. It may be that the range in concentrations differs by several orders of magnitude. This non-uniform distribution of biomass may only affect the tracer distribution in the early stages of the column experiments. Since the nutrients are forced through a small flow area, the rapid growth of bacteria near the inlet will quickly result in bacterial concentrations that are much higher than the starting conditions and the uncertainty in the distribution. In the experiments it is generally observed that changes in the hydraulic head, and therefore hydraulic conductivity, were very identical and reproducible for experiments that were run in triplicate (experiment 1, 3.1.1). The changes in hydraulic conductivity generally show overall the same development as discussed by Baveye et al. (1998) and ends at a relative decrease by a factor of 1000 near the inlet. The tracer experiments were shown for only one experiment in column experiments 1 discussed above. The same trends were observed for the other two experiments, but also with day-to-day differences. This is likely caused by the mode of observation, i.e., measuring solute breakthrough at the outlet. If more localised solute breakthrough is measured then breakthroughs are much more dynamic.

The changes in the bulk hydraulic conductivity for the sand box experiments were also reproducible. Three experiments were carried out with the line source and the decrease in hydraulic conductivity shows the same pattern (only two shown here). Two experiments with the point injection were carried out, with the same result, however, the decrease is hardly noticeably because the zone of clogging is much smaller and flow is

allowed to divert around this zone. In contrast to the column experiments, the sand box experiments reveal that the starting conditions with respect to biomass distribution may have a great influence on the resulting pattern of bioclogging, i.e., the degree of fingering and cycling.

Initial pre-clogging phase

Another noticeable feature is the increase in dispersion characteristics in the phase leading up to significant clogging, Figure 6. A moment analysis on the 2D tracer distributions with point injection in the sand box (results not shown), also indicates that dispersion increases slightly during the first 7 days before severe clogging is detected Figure 16. Increase in the number of micro-colonies and the re-arrangement of existing micro-colonies inside the porous media can explain this by leading to a perturbed flow field. The results are in agreement with other findings (Taylor and Jaffé, 1990; Sharp et al., 1999; Hill and Sleep, 2002; Bielefeldt et al., 2002ab) with an approximately linear increase in dispersivity with time.

Bioaccumulation phase with development of non-uniform flow

A phase with significant bioaccumulation accounts for much of the observed reduction in hydraulic conductivity and mobile porosity. The flow field, whether in a soil column or sand box, will depart from an almost uniform flow field to something that best can be characterized as non-uniform flow or "fingering". This has great implications for the mode of detection. Diffusion through mass transfer begins to play a significant role because of the increase in biomass porosity seen as a significant tailing in the breakthrough curves. Mass transfer will be an important process in systems where the substrates and nutrients are forced through the zones with bioclogging (column experiments, sand box experiments with line source), while of less importance in systems where the solutes can by-pass the bioclogged zone (e.g. sand box experiments with point injection). It is still a possibility that the dispersivity also changes during this phase, and to some extent is it difficult to differentiate between diffusion and dispersion effects.

Development of strong non-uniform flow

Most of the column experiments reached a quasi-stationary state with a 100-1000 times reduction in hydraulic conductivity and with tracer breakthroughs displaying some delay and significant tailing. The degree of non-uniform flow appears mild. However, at the smaller observation scale there can be strong non-uniform flow components leading to the fracture-like breakthroughs as in Figure 12 or fingering around zones with major bioclogging, Figure 17. Strong non-uniform flow likely is an inherent

feature of porous media with bioclogging caused by the random growth of bacteria due to a heterogeneous distribution at the start, locally high pore water flow velocities, and because of detachment-attachment processes.

Should bioclogging be considered after all?

The type of experiments discussed here are "hot-started" experiments meaning that the sands have been inoculated with bacteria, increasing the initial amount of attached bacteria by several orders of magnitude. However, significant increases in biomass concentrations may be seen for even unpolluted aquifers being exposed to a constant injection of pesticides in the range of 10-50 μg/L. For example, Højberg (2001) simulated an increase of 10^5 in biomass concentration near the injection corresponding to 10^5 cells/g, which was in reasonable agreement with the observation of 10^2-10^5 cells /g. This means that within 0.5 m of the injection wells, the bacterial concentration after 250 days of injecting pesticides is only about a factor of 100 less than the starting biomass concentrations in the column experiments. Thus, if such type of field/lab experiments is extrapolated to conditions of injecting nutrients in the mg/L range, then bioclogging may result. As an example, relevant for river bank filtration, the column experiments carried out by von Gunten and Zobrist (1993) used lactate as the easily degradable substrate and in concentrations of 100 mg/L. After 110 days of operation with a constant flow rate, they find greater than 10^9 cells/g in the 29 cm long column. They did not measure head drop and only did an initial tracer study to estimate the (initial) dispersivity.

REFERENCES

Baveye, Philippe, Philippe Vandevivere, Blythe L. Hoyle, Paul C. DeLeo and Diego Sanchez de Lozada, 1998. Environmental Impact and Mechanisms of the Biological Clogging of Saturated Soils and Aquifer Materials. Critical Reviews in Environmental Science and Technology, Vol. 28, No. 2, p. 123-191.

Bielefeldt, A., C. McEachern, T. Illangasekare, 2002a**.** Hydrodynamic Changes in Sand due to Biogrowth on Naphthalene and Decane. Journal of Environmental Engineering, January 2002, p. 51-59.

Bielefeldt, A., T. Illangasekare, M. Uttecht, R. LaPlante, 2002b. Biodegradation of propylene glycol and associated hydrodynamic effects in sand. Water Research 36,p. 1707-1714.

Clement T.P., B.S. Hooker, R.S. Skeen, 1996. Macroscopic Models for Predicting Changes in Saturated Porous Media Properties Caused by Microbial Growth. Ground Water, Vol. 34, No. 5, p. 934-942.

Engesgaard, P., J. Holm, K.H. Jensen, M. Henze, and H.J. Albrechtsen (2002), Development of preferential flow in bioclogging of porous media, Proceedings of the XIVth International conference on Computational Methods in Water Resources (CMWR XIV), June 23-25,

2002, Delft, The Netherlands, Developments in Water Science, Elsevier, 803-810, Eds. S.M. Hassanizadeh et al., Elsevier.

Hill, David D., Brent E. Sleep, 2002. Effect of biofilm growth on flow and transport through a glass parallel plate fracture. Journal of Contaminant Hydrologi 56, p. 227-246.

Herrera, P., 2002, Columns experiments and analytical fit of bioclogging, Techncial report, Technical University of Denmark and University of Illinois at Urbana- Champaign.

Holm, J. (2000) Effect of biomass growth on the hydrodynamic properties of groundwater aquifers, Series Papers 72, Dept. Hydrodynamics and Water Resources, Technical University of Denmark.

Højberg, A.L., (2001), Numerical analysis of pesticide migration in field injection experiments, Series Papers 77, Dept. Hydrodynamics and Water Resources, Technical University of Denmark.

Kildsgaard J. and P. Engesgaard, (2001), Numerical analysis of biological clogging in two-dimensional sand box experiments, J. Contam. Hydrol., 50, 261-285.

Kildsgaard, J. and P. Engesgaard, 2002. Tracer Tests and Image Analysis of Biological Clogging in a Two- Dimensional Sandbox Experiment. Ground Water Monitoring and Remediation, Vol. 22, Issue 2, p. 60-67.

Parker, J.C. and M.T. van Genuchten, (1984), Flux-averaged and volume-averaged concentrations in continuum approaches to solute transport, Water Resour. Res., 20, 866-872.

Pérez-Paricio A. and J. Carrera, Clogging and heterogeneity, Section 5.1 in Artificial recharge of groundwater, Final Report, EC project ENV4-CT95-0071, 51-58.

Seifert, D. and P. Engesgaard, (2004), Use of tracer tests to measure changes in flow and transport properties due to bioclogging in column experiments, in preparation for Ph.D. thesis.

Sharp, R.R, A.B. Cunningham, J. Komlos, J. Billmayer, 1999. Observation of thick biofilm accululation and structure in porous media and corresponding hydrodynamic and mass transfer effects. Water Science and Technology, 39 (7), p. 195-201.

Taylor, Steward W., Peter R. Jaffé, 1990. Biofilm Growth and the Related Changes in the Physical Properties of a Porous Medium. 3. Dispersivity and Model Verification. Water resources Research, Vol. 26, No. 9, p. 2171-2180.

Thullner, Martin, Josef Zeyer and Wolfgang Kinzelbach, 2002**.** Influence of Microbial Growth on Hydraulic Properties of Pore Networks. Transport in Porous Media. 2002, 49 (1), p. 99-122.

Thullner, Martin, Martin H. Schroth, Josef Zeyer and Wolfgang Kinzelbach, 2004. Modeling of a microbial growth experiment with bioclogging in a two-dimensional saturated porous media flow field, J. Contam. Hydrol., 70, 37-62.

Vandevivere, Philippe, Philippe Baveye, Diego Sanchez de Lozada and Paul DeLeo, 1995. Microbial clogging of saturated soils and aquifer materials: Evaluation of mathematical models. Water Resources Research, vol. 31, No. 9, p. 2173-2180.

RIVERBANK FILTRATION IN THE NETHERLANDS: WELL FIELDS, CLOGGING AND GEOCHEMICAL REACTIONS

Pieter J. Stuyfzand[1,2], Maria H.A. Juhàsz-Holterman[3] and Willem J. de Lange[4]

[1]*Free University, Dept. Hydrology & Geo-Environmental Sciences, FALW, Boelelaan 1085, 1081 HV Amsterdam, Netherlands; Tel: +31. 20.444.7968 or +31.6.10945021; Email: pieter.stuyfzand@falw.vu.nl.*

[2]*Kiwa Water Research, PO Box 1072, 3430 BB Nieuwegein, Netherlands; Tel: +31. 30.6069.552 or +31.6.10945021; Email: pieter.stuyfzand@kiwa.nl.*

[3]*Water Supply Limburg (WML), Limburglaan 25, 6229 GA Maastricht, Netherlands*

[4]*Institute for Inland Water Management and Waste Water Treatment (RIZA), PO Box 17, 8200 AA Lelystad, Netherlands*

Abstract: River Bank Filtration (RBF) contributes ca. 7% (80 Mm^3/a) to the national drinking water supply in the Netherlands, through a total of 26 well fields. These RBF well fields are classified on the basis of (1) the main driving mechanism of flow (polder or pump driven); (2) RBF periodicity (flow direction temporarily reversing or not), (3) type of riverbed (sand or gravel), and (4) type of contact of river with aquifer (with or without intercalated aquitard(s)).

Three case studies are reviewed which demonstrate the water quality, geochemical reactions and clogging phenomena in differing systems. The mass balance approach, also called 'reverse modeling', is applied to identify and quantify the extent of the most important hydrogeochemical reactions at the three case study sites.

Stephen A. Hubbs (ed.), Riverbank Filtration Hydrology, 119–153.

Clogging of the river bed seems to be a problem in the Netherlands only in RBF systems with a true gravel bed such as Roosteren along the Meuse River, and on sites where sludge is strongly accumulating due to structurally reduced river flows, as in the Hollandsch Diep estuary which was dammed in 1971 as part of the Delta Works.

Key words: river bank filtration, geoclogging, Netherlands, water supply

1. INTRODUCTION

Riverbank filtration (RBF), in a broad sense, is the process of river water infiltrating its riverbed. RBF sensu stricto is defined as the process of river water infiltrating where pumping wells (mostly for drinking water supply) create induced recharge.

Induced recharge has demonstrated in Europe, in the past 100-150 years, to be a very vital technique of collecting high quality raw water for drinking water preparation, with many advantages (Van der Kooij et al., 1986; Sontheimer, 1991; Ray et al., 2002; Jülich & Schubert, 2001).

Advantages with respect to direct surface water treatment include: elimination of suspended fines with the attached pollutants, strong reduction of quality fluctuations, and strong quality improvement by elimination of heavy metals, organic micropollutants, bacteria and viruses. Disadvantages are: (a) the impossibility of completely impeding the river to infiltrate when this would be episodically desirable because of a bad quality; (b) geochemical reactions of the infiltrate with sludge and aquifer materials that raise the concentrations of notably Fe^{2+}, Mn^{2+}, As, NH_4^+, CH_4, Ca^{2+} and HCO_3^-; and (c) risks of a cumbersome clogging of the river bed.

In this contribution, experiences from the Netherlands are presented pertaining to RBF in general, alosnd clogging and geochemical reactions (both positive and negative). Experiences with RBF along lake banks, canals and ditches are not considered here.

2. RIVER BANK FILTRATION IN THE NETHERLANDS

2.1 Historical Evolution

Various hydrological manipulations forced the water of the Rhine and Meuse Rivers to increasingly infiltrate, since about 1200 AD, along their

many water courses in the fluvial and coastal plain of the Western Netherlands, as well as in former seepage areas (Stuyfzand, 1989b). The first riverbank filtrate was pumped, for public drinking water supply in the Netherlands, probably in 1879 along the Rhine River at pumping station Nijmegen (Site 42 in Fig.1). In 1950 15 well fields pumped 11 Mm^3 and in 1995 25 pumping stations produced 79 Mm^3 of Rhine bank filtrate (including admixed autochthonous groundwater). In 1998 the first Meuse bank filtrate was pumped near Roosteren (site 80 in Fig.1). An annual total of 80 Mm^3 of riverbank filtrate in 2002 (Fig.2) constitutes nearly 7% of the total production of drinking water in the Netherlands (1200 Mm^3/a).

The deterioration of the quality of the Rhine River, especially in the period 1920-1975, had at least three impacts on the preparation of drinking water from Rhine River water: (a) a switch from the direct intake of river water to the pumping of Rhine bank filtrate in the period 1928-1962, on 10 stations (Table 1); (b) closure of well fields pumping Rhine bank filtrate in the period 1944-2000, at 17 locations (Table 1); and (c) extension of the classical treatment (aimed at removal of iron, manganese, ammonia and methane), with processes removing organic contaminants.

RBF is both a desired and undesired mechanism of groundwater recharge. It is desired where groundwater tables should not be lowered in the neighborhood of pumping wells (for instance due to risks of land subsidence by compacting clay and peat). It is undesired where recent bank filtrate with its bad quality would displace old, autochthonous groundwater of unimpeachable composition, especially in ecologically susceptible areas.

2.2 Types of Well Fields

In the Netherlands four types of well fields with RBF can be distinguished on the basis of the flow driving mechanism, RBF periodicity, type of river bed and type of contact of river with the aquifer:

1. pumping driven (and therefore receiving RBF from one side and autochthonous groundwater from the other side composed of uplands bordering the valley), periodical (flow reversing during low river stages or reduced pumping), with a fluvial gravel bed in direct contact with the aquifer;
2. as 1 but permanent (without flow reversal) and with a sandy river bed;
3. polder and pumping driven (and therefore receiving RBF from all sides), permanent, with a sandy river bed in direct contact with the aquifer; and

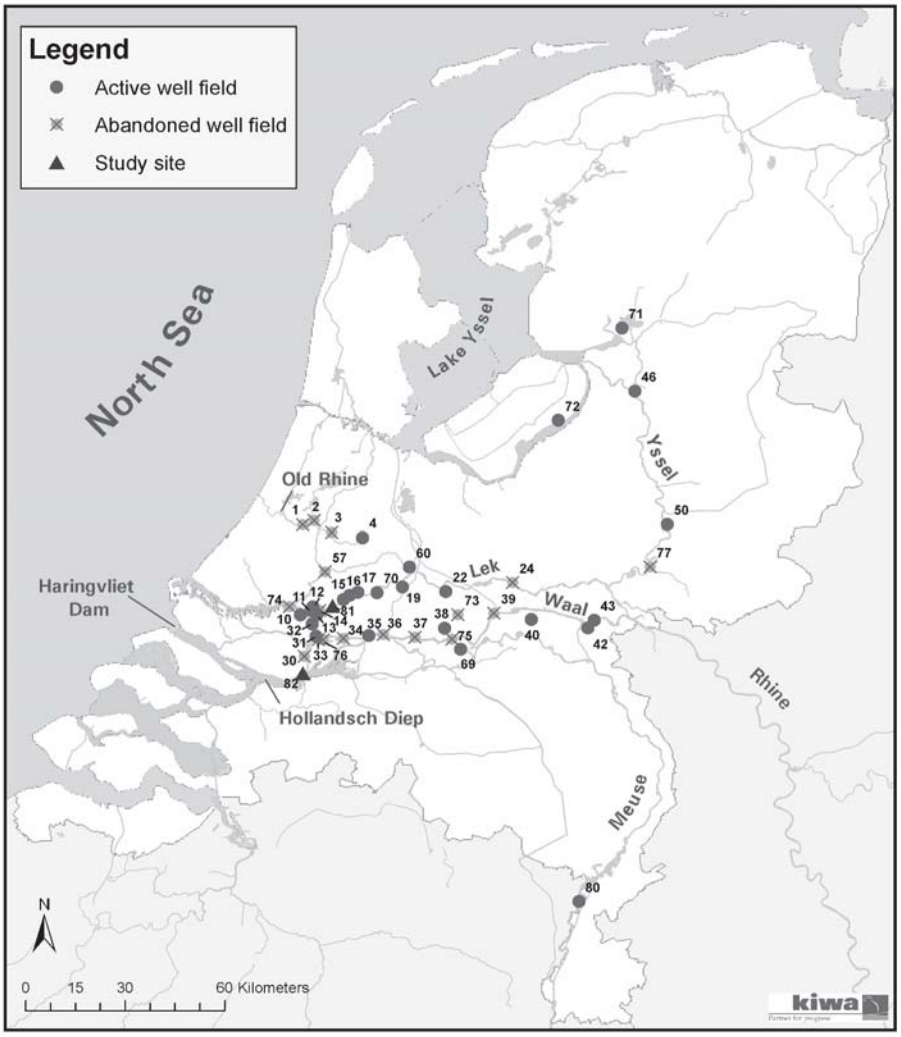

Figure 1. Location of all well fields pumping riverbank filtrate in the Netherlands, with distinction between active and abandoned sites. Numbering corresponding with Table 1.

4. as 3 but not in direct contact with the aquifer by intercalation of at least one aquitard (mostly of Holocene age).

The most frequent types in the Netherlands are 3 and 4, type 1 is unique (Table 1). Types 3 and 4 have been distinguished on the basis of the redox level of the water pumped: if anoxic (no sulphate reduction) then 3, if deep anoxic (with significant sulphate reduction and methane present) then 4.

Lake bank filtrate (type 5 in Table 1) is pumped on two sites in the Netherlands.

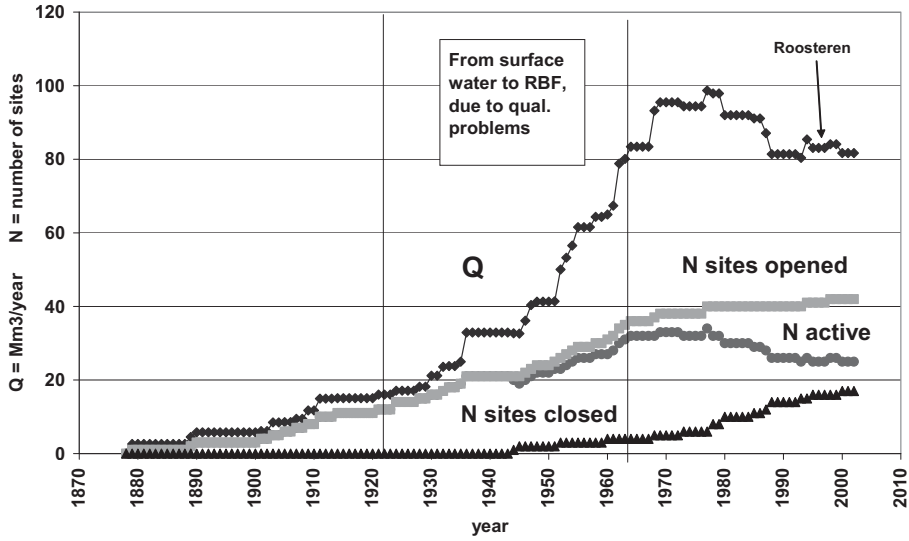

Figure 2. The total annual amount of riverbank filtrate pumped for drinking water preparation in the Netherlands (Q), and the number of well fields pumping this water (N active), from 1879 till 2002. Induced recharge along lake banks, canals and ditches excluded, admixed autochthonous groundwater included.

Table 1. Characteristics of all well fields in the Netherlands that pump(ed) river bank filtrate (type 5 = lake bank filtrate).

No.	PUMPING STATION NAME / SITE	RBF TYP	START PS	END Surf.wat	END PS	ALTITUDE m+MSL
		1	2	3	4	5
	LEK RIVER (RHINE)					
10	RIDDERKERK (KIEVIETSWEG)	4	1906	1961		-1
11	LEKKERKERK (SCHUWACHT)	3	1910	1963		1
12	LEKKERKERK (TIENDWEG)	3	1969			-1.5
13	N. LEKKERLAND	3	1964			-1.5
14	N. LEKKERLAND (LEKDIJK)	3	1922	1960	1978	0
15	BERGAMBACHT (DIJKLAAN)	3	1936			-0.5
16	BERGAMBACHT	3	1968			1.5
17	SCHOONHOVEN	3	1901			-1
19	LEXMOND (DE LAAK)	3	1936			0.5
22	CULEMBORG	3	1911			2
24	REMMERDEN	2	1977		1988	6.8
60	IJSSELSTEIN	3	1911			4.5
70	LANGERAK (DE STEEG)	3	1994			
	MEUSE RIVER					
80	ROOSTEREN (DE RUG)	1	1990			28.6
	OLD RHINE RIVER					
1	HAZERSWOUDE	3-4	1909		1995	-0.5
2	ALPHEN a/d RIJN (HOORN)	3-4	1903		2000	-1
3	BODEGRAVEN (BUITENKERK)	3-4	1907		1985	0
4	KAMERIK (HOOGE BOOM)	3	1931			-1
	OTHER WATER COURSES					
57	GOUDA	4	1883	1921	1968	-1.5
71	ST. JANSKLOOSTER	5	1936			8.5
72	BREMERBERG	5	1962			-3
	WAAL RIVER (RHINE)					
30	s-GRAVENDEEL (KIL)	4	1924		1988	-0.5
31	ZWIJNDRECHT (RINGDIJK)	4	1897	1954		-0.5
32	H-I-AMBACHT	4	1912	1948		-1
33	DORDRECHT (ORANJELAAN)	4	1893	1946	1987	-1
34	SLIEDRECHT	3	1886	1928	1973	-1
35	HARDINXVELD (`T KROMME	3	1924			-1
36	GORINCHEM (VISSERSLAAN)	3	1886	1932	1980	0
37	BRAKEL (VELP)	3	1951		1978	2
38	WAARDENBURG (KOLFF)	3	1958			1.5
39	TIEL	4	1890		1993	6.5
40	DRUTEN	3	1953			5.5
42	NIJMEGEN (NIEUWE	4	1879			14
43	LENT (ELST)	4	1935			8
69	AALST (VELDDRIEL, SELLIK)	3	1977			2.5
73	GELDERMALSEN	3	1924		1952	3
74	VEERDAM (IJSSELMONDE)	4	1903	1933	1944	-1
75	ZALTBOMMEL	3	1905		1960	3
76	DORDRECHT	3-4	1946		1980	-1
	YSSEL RIVER (RHINE)					
46	ZWOLLE (ENGELSCHE WERK)	2	1930			1
50	ZUTPHEN (VIERAKKER)	2	1889			6
77	DOESBURG	2	1914		1945	9

1 = see section 2.2 for types of well fields; 2 = start Pumping Station (well field); 3 = switch from surface water to RBF; 4 = well field abandoned; 5 = altitude of land surface in m above Mean Sea Level; 6 = depth of well screens pumping RBF (m below land surface); 7 = depth of well screens mainly pumping autochthonous groundwater (m below land surface); 8 = annual total of RBF (incl. autochthonous groundwater) pumped in 1992 or during last year prior to closure; 9 = percentage of RBF in Q as determined

Table 1(continued). Characteristics of all well fields in the Netherlands that pump(ed) river bank filtrate (type 5 = lake bank filtrate).

	PUMPING STATION	SCREEN DEPTH		Q	%	%younger	DISTANCE
No.	NAME / SITE	RBF	Autocht	m^3/a	RBF	<22 year	m
		6	7	8	9	10	11
	LEK RIVER (RHINE)						
10	RIDDERKERK (KIEVIETSWEG)	15-30	40-110	2.8	18	34	940
11	LEKKERKERK (SCHUWACHT)	15-30		1.2	100	95	205
12	LEKKERKERK (TIENDWEG)	15-30		2.2	82	92.5	1250
13	N. LEKKERLAND (MIDDELWEG)	15-28		4.3	100	64	630
14	N. LEKKERLAND (LEKDIJK)	15-45		0.7			
15	BERGAMBACHT (DIJKLAAN)	22-42		0.7	100	94	580
16	BERGAMBACHT	17-39		11.	89	50	810
17	SCHOONHOVEN	29-39		0.5	100	95	310
19	LEXMOND (DE LAAK)	18-43	70-120	9.4	47	2	1300
22	CULEMBORG	15-45	70-120	1.2	65[A]		2000
24	REMMERDEN	3-18		0.4	82	100	30
60	IJSSELSTEIN	70-110	70-110	2.5	21		2000
70	LANGERAK (DE STEEG)				??[B]		
	MEUSE RIVER						
80	ROOSTEREN (DE RUG)	6-16	16-17[H]	1.9	10[C]		145
	OLD RHINE RIVER						
1	HAZERSWOUDE	25-40		2.3	53	70	50
2	ALPHEN a/d RIJN (HOORN)	25-40		1.1	62	70	170
3	BODEGRAVEN (BUITENKERK)	15-35		0.9			
4	KAMERIK (HOOGE BOOM)	15-35	67-85	3.9	24	27	
	OTHER WATER COURSES						
57	GOUDA	13-30		0			
71	ST. JANSKLOOSTER	35	85	5.6	60[D]		
72	BREMERBERG	60	80	7.3			
	WAAL RIVER (RHINE)						
30	s-GRAVENDEEL (KIL)	12-20	50-120	5.2	18	34	175
31	ZWIJNDRECHT (RINGDIJK)	18-25	105-125	3.9	69	61	130
32	H-I-AMBACHT	15-24	80-100	0.9	65	73	300
33	DORDRECHT (ORANJELAAN)	15-25	60-130	4			
34	SLIEDRECHT	10-30		1.1			
35	HARDINXVELD (`T KROMME	12-35		1	95	89	350
36	GORINCHEM (VISSERSLAAN)	10-35		2.4			
37	BRAKEL (VELP)	40-45		0.1			
38	WAARDENBURG (KOLFF)	10-40		3.6	68	68	3110
39	TIEL	90-140	90-140	1	82	20	340
40	DRUTEN	10-30	30	1.7	29	35	2980
42	NIJMEGEN (NIEUWE	55	75	2.8	40[E]	58	370
43	LENT (ELST)	60	100	1.3	66	40	350
69	AALST (VELDDRIEL, SELLIK)	22-72	22-72	3.6	49	2	3500
73	GELDERMALSEN	20-27		0.2			
74	VEERDAM (IJSSELMONDE)	19-24		0.2			
75	ZALTBOMMEL	29-39		0.0			
76	DORDRECHT (W.PARK/JEUGD)	13	70	3.5			
	YSSEL RIVER (RHINE)						
46	ZWOLLE (ENGELSCHE WERK)	30-95	130-170	12.	85	47	815
50	ZUTPHEN (VIERAKKER)	25-40	25-40	2	30	17	1500
77	DOESBURG	32-39		0.1			

by natural tracers; 10 = percentage of young water (age < 22 years) in total mix, as determined by tritium analysis; 11 = horizontal distance between central part of well field and river bank during summer.

A = after 199? <5%; B = ; C = since 1998; D = around 2000; E = in the 1980s ;

H = Horizontal well

3. CASE 1: MEUSE RBF NEAR ROOSTEREN (SITE 80)

3.1 Situation

Well field No 80 (in Fig.1 and Table 1) near Roosteren along the Meuse River, belongs to type 1 (section 2). It is situated in an area of Pleistocene fluvial terraces, 130 km upstream of tidal influences (28 m+Mean Sea Level). Originally this well field pumped groundwater exclusively recharged by rainwater on the hilly uplands and on the Meuse fluvial plain. In 1998 pumping wells X and XI were installed at 147 m distance from the steep river bank (Fig.3). Since 12 January 1998 they contribute to the supply of raw water for drinking water supply, and since then the river at that site changed from a predominantly effluent into a predominantly influent river.

Intensive hydrological and hydrochemical research was carried out in the period January 1998 – October 1999 (Stuyfzand & Juhàsz-Holterman, 2000; Juhàsz-Holterman, 2001).

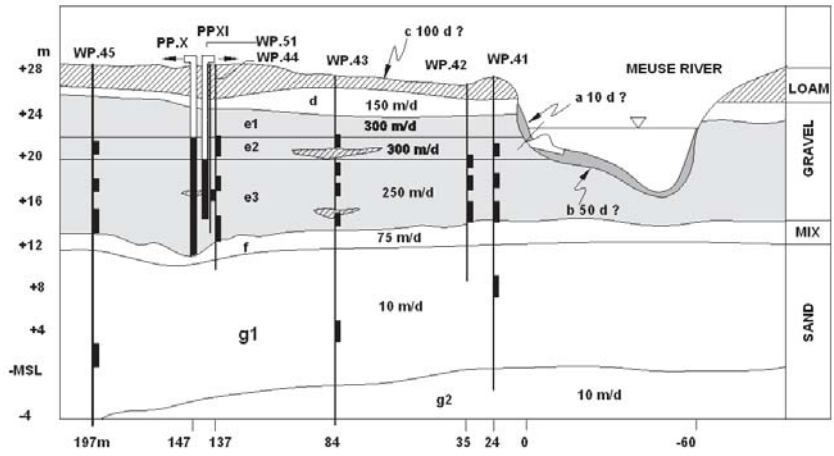

Figure 3. [Please provide a caption for this figure]

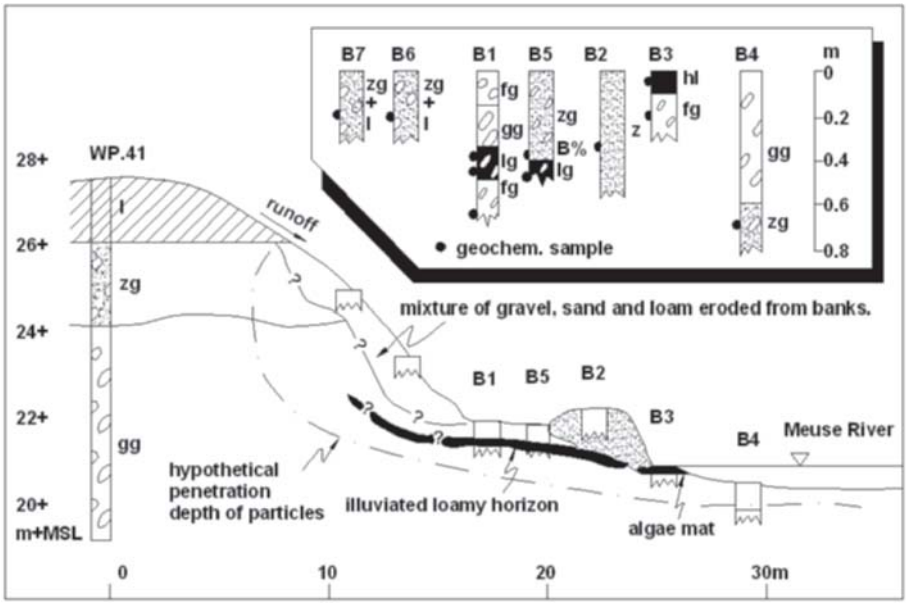

Figure 4. Detailed lithology of the southern bank and bed of the Meuse River as observed in autumn 1999 (after Stuyfzand & Juhàsz-Holterman, 2000). fg = fine grained gravel; gg = coarse grained gravel; hl = loam with algae; l = loam; zg = sandy gravel; lg = loamy gravel.

3.2 Hydrological Aspects (incl. Clogging)

Groundwater flow is directed towards the Meuse River during periods when the wells PP.X and PP.XI do not pump or pump at reduced capacity, and when there is no rapidly rising water level in the Meuse River. The median travel time of infiltrating Meuse River water to the pumping wells at ca. 147 m distance, as determined by natural tracer analysis, strongly depended on the river's water level (pumping rate constant at 140 m^3/h): 18 days during the rising leg of a high flood wave reaching 25.5 m+MSL, 43 days during mean high water of 23.4 m+MSL and >>54 days during low flows (21.2 m+MSL).

The river bed is composed of gravel (incl. boulders up to 25 cm) with a high tendency to clog. This is due to deep bed filtration of clogging particles (lack of cake filtration) and a small chance of resuspension of the upper boulders that pave the clogging zone.

Piezometric data did not reveal, however, any significant clogging of the river banks and river bed during the 640 days of monitoring. There was indeed no clear increase in hydraulic resistance between the river and the piezometers in the first observation well (WP.41). This does not mean,

however, that clogging did not occur. On the one hand it was calculated that a partial clogging of the river bed would create only 2 cm of hydraulic resistance due to the very high permeability of the upper aquifer. And on the other hand, such small hydraulic changes could be easily caused by variations in pumping rate of the wells upgradient.

3.3 Geochemistry

Geochemical reactions of the infiltrate are strong with the recent clogging layer (a + b in Fig.3) and weak with the coarse grained aquifer (e + f + g in Fig.3).

The sedimentological/geochemical characteristics of the four most important aquifer layers are given in Table 2. The gravel aquifer is very inert indeed with extremely low organic carbon and cation exchange capacity (CEC), no calcite, no pyrite and no reduction capacity.

The aquifer sands underlying the gravels, are a bit more reactive especially regarding their reduction and exchange capacity.

The river's bank and bed, in its upper 0.5 m, are quite reactive in all respects, due to significant amounts of clay sized particles, calcite, pyrite, organic matter and a high CEC.

These highly reactive materials derive from suspended matter in the river, and chemical precipitation (calcite and pyrite).

Table 2. Composition of the 4 most important aquifer layers at RBF site Roosteren

	unit	River bank	River bed	Gravel aquifer	Sand aquifer
Layer in Fig.3		a	b	e1-e3	g1
No of samples		2	9	9	2
Grains < 2 µm	% d.w.	10.3	7.6	0.4	0.9
Grains > 2 mm	% d.w.	26	44	85	0
$CaCO_3$	% d.w.	2.5	1.3	<0.007	<0.002
C-organic	% d.w.	1.7	2.0	0.02	0.1
CEC	meq/kg d.w.	107	103	2.8	7.5
S-FeS_2	% d.w.	0.017	0.004	<0.0009	0.018
Fe-oxalate	% d.w.	0.47	0.28	0.055	0.027
Mn-oxalate	% d.w.	0.0148	0.0111	0.0044	0.0060

3.4 Hydrochemistry

Some data on water quality changes during aquifer passage are given in Table 3, for a period with a high river stage (23.7 m+MSL), normal for the winter period, and thus relatively high infiltration rates. Water quality changes depended mainly on the number of pore flushes with Meuse River water, infiltration intensity (water stage in river; Fig.5) and temperature. Passage of the anoxic clogging layers a (river bank) and b (river bed) clearly resulted in redox reactions and the dissolution of calcite (increase of Ca^{2+} by 10 mg/L and of HCO_3^- by 15 mg/L). These reactions were insignificant in the aquifer beyond the clogging layers. The redox reactions consisted of oxidation of organic matter and pyrite (or FeS). This was evidenced by a decrease of O_2 (5 mg O_2/L) and NO_3^- (1-4 mg NO_3^-/L), a pH-decrease (from 7.9 to 6.7) and an increase of total inorganic carbon and SO_4^{2-} (with 10 mg/L). Iron and Mn hardly dissolved, NH_4^+ was nearly completely nitrified.

Organic matter (DOC) was lowered by about 50%, probably by breakdown. Phosphate was nearly completely removed by adsorption while SiO_2 increased by either desorption or dissolution of feldspars. Fluoride break-through was delayed (retardation factor ca. 4), Barium was clearly mobilized (30-50 µg/L). The concentrations of all other trace elements (incl. heavy metals) remained quite low, lower than in the Meuse River, probably by filtration and sorption. Concentrations of Organic Micropollutants (OMPs) were very low (<0.01-<0.1 µg/L) in wintertime (November – April), when the Meuse River is relatively clean and infiltrating well during normal high river flows. The only OMP detected during aquifer passage in winter was 1,2-dichloroethane, with most removal occurring close to the river (in the clogging layers). Although OMP concentrations were clearly much higher during summer (May-October), they could not be detected in Meuse RBF. The most important causes are: (1) the Meuse River hardly infiltrates in that season during the usual low river discharges; (2) the OMPs are delayed by sorption, and did not reach the observation wells during the research period due to a lack of sufficient pore flushes; and (3) decomposition.

3.5 Microbiology

Bacteria and viruses were effectively removed in the gravel aquifer by >4 log10 units during the research period. During extreme flood peaks in winter, however, very low numbers of coliforms, SSRC and coliphage

Table 3. Mean composition (18 Nov. 1998 – 26 March 1999; days 300-479) of Meuse River water and its bank infiltrate along the row of monitoring wells near Roosteren.

		MEUSE	SHALLOW		MIDDLE DEEP	
	Unit	RIVER	WP.41-f1	WP.42-f1	WP41-f2	Wp.43-F2
Distance	m	0	24	35	24	84
Travel time	d	0	4.5	7.5	7	18
Pore flushes		0	27	20	20	6
Temp	°C	5.9	(6)	(7)	(7)	(8)
EC (20°C)	µS/cm	367	404	400	404	481
pH	-	7.91	7.01	6.83	6.93	6.75
O2	mg/L	12.1	8.3	8.3	5.3	4.2
DOC	mg/L	2.7	1.6	-	1.3	0.8
UV-Ext	E/m	8.7	3.6	2.3	3.0	1.4
SiO2	mg/L	6.7	9.5	-	9.0	8.5
TIC ##	mmol/L	2.57	3.49	3.78	3.62	4.87
SI-calcite	-	0.12	-0.66	-0.83	-0.73	-0.74
Cl	mg/L	26	25	23	26	31
SO4	mg/L	33	40	41	41	62
HCO3	mg/L	151	166	163	166	200
NO3	mg/L	15	16.2	16.8	13.9	10.8
F	mg/L	0.20	0.23	0.11	0.19	0.07
Na	mg/L	15.6	16	-	17	20
K	mg/L	2.8	1.9	-	2.4	2.5
Ca	mg/L	58.6	68.5	68.5	68.1	84.1
Mg	mg/L	6.2	4.9	-	5.6	6.3
Fe	mg/L	0.08	0.02	0.02	0.02	0.02
Mn	mg/L	0.04	0.01	0.01	0.01	0.01
NH4	mg/L	0.25	0.03	0.03	0.03	0.03
SiO2	mg/L	6.7	9.5	-	9.0	8.5
Al	µg/L	36	6	-	6	<5
As	µg/L	1.5	0.6		0.6	0.7
Ba	µg/L	20	61		61	56
Cd	µg/L	0.14	0.10		0.10	<0.1
Ni	µg/L	1.5	1.7		3	0.8
Zn	µg/L	40	20		<10	<10
AOX	µg/L	9.5			5	4
1,2-Dclea	µg/L	0.23	0.07		0.07	<0.05
Trichloroethylene	µg/L	0.25	<0.1		<0.1	<0.1
AMPA	µg/L	0.12			<0.05	<0.05
Atrazin	µg/L	0.02	<0.02		<0.02	<0.02
Diuron	µg/L	0.05			<0.05	<0.05

##: TIC = Total Inorganic Carbon = $H_2CO_3 + HCO_3^- + CO_3^{2-}$

reached the pumping well (Medema et al., 2001). This is explained by low temperatures (depressing inactivation), and short travel times in the gravel aquifer, being 10-14 instead of 45-65 days. The latter is caused by a >20% shortening of the travel distance and a >400% steepening of the hydraulic

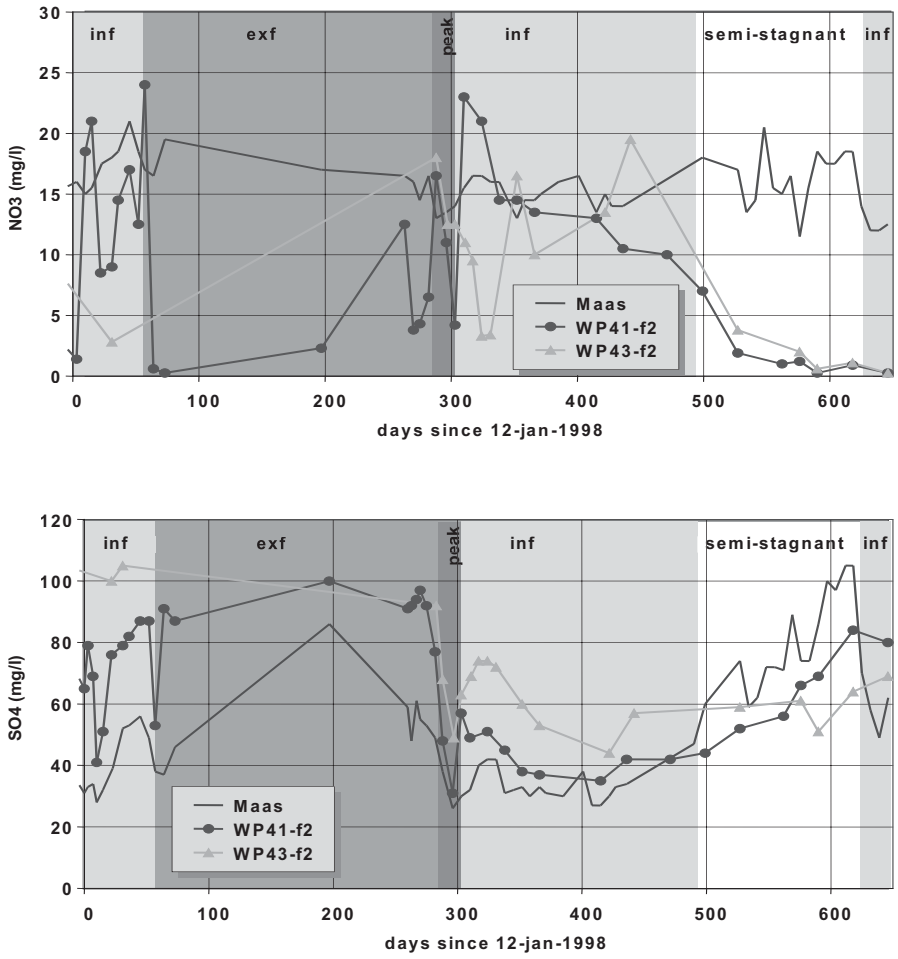

Figure 5. Changes in nitrate and sulphate concentrations in Meuse River water and its RBF at 24 and 84 m distance from the riverbank, in the period January 1998 – October 1999. inf = Meuse infiltrating; exf = Meuse draining; peak = high peak flow; semi-stagnant = hardly any or slight infiltration.

gradient. As elsewhere, the removal rates were highest during the first 7 meters of the aquifer.

4. CASE 2: RHINE RBF NEAR OPPERDUIT (SITE 81)

4.1 General Description of Site

The study site Opperduit is situated 3 km to the west of well field Dijklaan (No 15 in Fig.1 and Table 1), along the northern bank of the Lek River (a tributary of the Rhine River), in the Holocene flood plain, with minor tidal influences (land surface at 0 m+MSL). The river bed is composed of sand (deep fairway) and a complex of Holocene clays and peat (in between the groins and in the winter bed). The site is more or less representative for well fields of type 3 (section 2). Intensive hydrological and hydrochemical research was carried out in the period 1981 – 1994 (Stuyfzand & Lüers, 1996).

4.2 Hydrological Aspects (incl. Clogging)

Groundwater flow is permanently directed towards the central parts of the deep polder (land surface at 1.6 m-MSL) bordering the northern river bank. The pumping of RBF at well fields in the neighborhood has a negligible impact on the local flow pattern. A cross section over the study site is given in Fig.6, showing the position of the sandy aquifer of Middle Pleistocene age (10-35 m-MSL), and the upper Holocene aquitard (clays and peat). The travel time towards the most distant observation well (294, 675 m from river bank) was about 8 years.

There is a moderate tendency to clog in between the groins, and no clogging at all in the fairway (deep summer bed). It seems likely that the winter bed (dry land in summer) is clogging to some extent, but data on this aspect have not yet been studied in detail.

Periodic flood waves appear capable of completely removing the superficial clogging layer (by cake filtration) on the sandy floor of the fairway, where the bulk of aquifer recharge is occurring. RBF sites along sandy river beds thus seem to be protected from the nuisance of river bed clogging.

4.3 Geochemistry

The main aquifer (10-35 m-MSL) is composed of anoxic, calcareous (5%), coarse sands, with 0.1-0.2 % organic carbon, a CEC of 20-60 meq/kg and <0.1% ironsulfides. The top layer (2 m thick) of the winter bed in

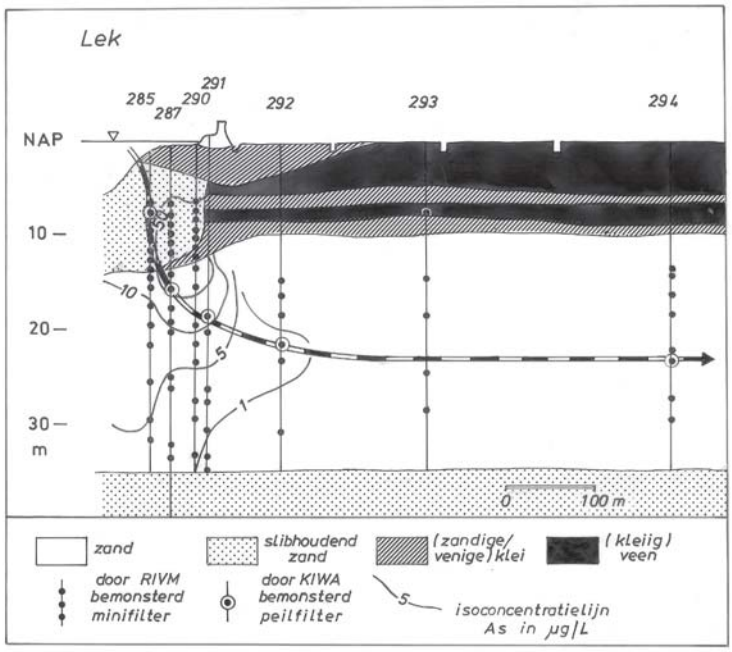

Figure 6. Hydrogeological cross section over the 'polder driven' Rhine bank filtration site Opperduit (site 81 in Fig.1), with isoconcentration lines for arsenic. Stuyfzand (1992).

between the groins is composed of anoxic calcareous (13%) sludge, with on average 8% organic carbon and a CEC of 200 meq/kg

4.4 Hydrochemistry

Some data on mean water quality changes during aquifer passage are given in Table 4. The analyses refer to measurements in 1994-1995. The results indicate that the system is largely anoxic (oxygen and nitrate being completely reduced), and partly deep anoxic (monitoring wells 293-a and 294-a exhibiting sulphate reduction). The system is calcite saturated as expected.

The data reveal clear variations downgradient. Many are connected with trends in the pollution record of the Rhine River. Examples of this are Cl, K, Ca, Mg, NH4, B, Ba, F, and bentazone. The concentrations of many pollutants were lower in 1994-1995 lower than in surveys at the same site in the 1980s (Stuyfzand, 1998). These positive developments are due to strong quality improvements in the Rhine River since 1975. They are composed of strong concentration decreases for Na, Cl, Ca, SO4, DOC, NH4, PO4 and

Table 4. Mean water quality of Rhine River water (Lek tributary) and its RBF near Opperduit (site 81) in 1994-1995 (based on Stuyfzand & Lüers, 1996). Lek = average 1994.

	Unit	Rhine (Lek)	291-b	292-b	293-a	294-a	Well field 15
Distance	m	0	10	100	220	675	581
Travel time	days	0	450	900	1800	2900	2000
Temp	°C	12.9	12.6	12.9	12.1	11.4	
EC (20°C)	µS/cm	690	797	863	871	837	828
pH	-	7.95	7.58	7.55	7.33	7.54	7.38
O2	mg/L	9.1	<1	<1	<1	<1	<1
DOC	mg/L	3.8	1.6	1.5	2.1	2.0	1.4
TIC	mmol/L	2.76	3.15	3.47	5.82	4.16	3.52
SI-calcite	-	0.33	0.04	0.11	0.11	0.03	*0.11
Cl	mg/L	111	145	166	144	154	145
SO4	mg/L	60	74	69	18	46	77
HCO3	mg/L	163	180	198	318	233	194
NO3	mg/L	15.5	<0.4	<0.4	<0.4	<0.4	<0.2
PO4-ortho	mg/L	0.32	0.35	0.37	0.34	0.73	
F	mg/L	0.15	0.28	0.30	0.14	0.08	0.18
Na	mg/L	61	86	82.9	81.1	84.8	80.5
K	mg/L	5.1	6.2	5.5	9.0	4.6	5.2
Ca	mg/L	72	77	89	92	82	84
Mg	mg/L	10.8	10.8	12.3	12.5	12.5	11.5
Fe	mg/L	0.98##	1.7	1.8	2.65	1.6	2.1
Mn	mg/L	0.13##	1.57	0.84	1.04	0.21	0.65
NH4	mg/L	0.18	0.34	1.21	5.04	2.9	1.19
SiO2	mg/L	4.6	7.3	7.7	9.2	11.1	10.7
Al	µg/L	225##	35	7	8	9	2
As	µg/L	2##	2	<1	<1	1.5	0.5
B	µg/L	100	96	113	158	110	120
Ba	µg/L	118	96	113	158	110	96
Cd	µg/L	0.03	0.04	0.02	<0.01	0.01	<0.05
Cr	µg/L	4##	<0.5	<0.5	<0.5	<0.5	<0.5
Cu	µg/L	5	<0.5	<0.5	<0.5	<0.5	4
Hg	µg/L	<0.01	<0.1	<0.1	<0.1	<0.1	<0.02
Ni	µg/L	3.3	0.5	0.4	0.6	<0.5	<1
Pb	µg/L	0.3	1.3	1.3	0.4	0.8	<1
Se	µg/L	0.2	0.02	0.01	0.01	0.02	<1
Zn	µg/L	26##	<5	<5	<5	<5	5
Tetrachloroethene	µg/L	0.13	<0.01	<0.01	<0.01	<0.01	
Trichloroethylene	µg/L	<0.1	0.21	0.17	<0.01	<0.01	-
AMPA	µg/L	0.54	<0.03	0.05	0.06	0.08	-
Atrazin	µg/L	0.07	<0.01	<0.01	<0.01	<0.02	-
Diuron	µg/L	-	<0.01	<0.01	<0.01	<0.01	-
Bentazone	µg/L	<0.1	<0.07	<0.07	0.33	1.96	0.45
Mecoprop (MCPP)	µg/L	0.03	<0.03	<0.03	0.04	0.13	-
Trichloroethylphosphate	µg/L	0.13	0.05	0.05	0.06	0.02	

= in unfiltrated samples, thus including suspended species

the more hydrophylic organics like bentazone, mecoprop (MCPP), 1,3,3-trimethyloxindole and chlorobenzenes (see Fig.7 and Table 5).

Table 5. Comparison of the concentration levels of 16 organic pollutants from 1995 with those from 1983 (Stuyfzand & Lüers, 1996).

Compound	log KOW	1983	1995	1995/ 1983
		µg/L	µg/L	
N-acetyl-N-ethylaniline	?	0.03-0.04	<0.01-0.05	<0.3-1.3
p,p'-bis(dimethylamino) benzofenone	?	0.1-0.3	<0.03	0.1
bis-(2-methoxyethyl)ether	?	1	<0.03	<0.03
o-chloroaniline	1.85	0.1-0.5	<0.02-0.27	<0.2-0.5
Sum chloroalkylethers	ca. 2	0.1-3.1	0.07-0.24	0.1-0.7
chlorotoluidine	2.25	0.02-0.04	<0.02-0.06	<1-1.5
diacetonglucose	-0.6	1-1.4	<0.01-0.05	0.02
dichloroaniline	2.7	0.1	<0.01-0.03	0.2
Sum dichlorobenzenes	3.38	0.4-1.4	<0.01-0.02	0.02
difenylsulfone	2.4	0.1-0.3	<0.02-0.07	0.2
dimethylaniline	1.8	0.1-0.4	0.01-0.03	0.1
N-ethyl-N-fenyl-acetamide	?	0.5	<0.03	<0.06
lactones	?	0.02-0.7	0.02-0.19	0.3-1
tributhylphosphate	2.5-4	0.04-0.06	0.01-0.14	0.25-1.5
triisobuthylphosphate	?	0.03-0.3	0.01-0.09	0.3
1,3,3-trimethyloxindole	?	0.1-0.35	0.02-0.06	0.2

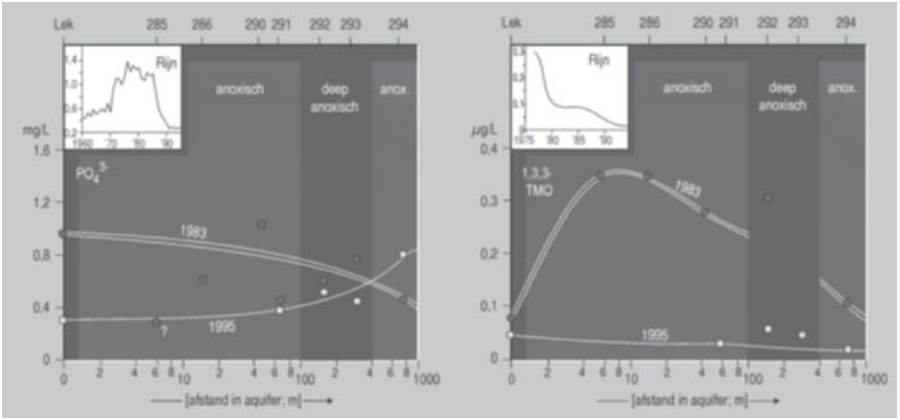

Figure 7. Quality evolution down gradient in the aquifer recharged by the Rhine River at site 81 (Opperduit), in 1983 and 1995 (Stuyfzand & Lüers, 1996). The inset shows concentration trends in the Rhine. 1,3,3-TMO = 1,3,3-trimethyloxindole (a constituent of paint).

A detailed study in the 1980s revealed the behavior of the trace elements As, Co, Cu, Ni and Pb (Fig.8). These showed breakthrough fronts in 1983 at relatively close distance to the supposed infiltration point (<40 m), with Ni advancing most rapidly. Arsenic showed an anomalous peak at 10 m, suggesting that it is mobilized from the aquifer (or rather the river bed; Fig.6) and retarded by sorption downgradient from the source area.

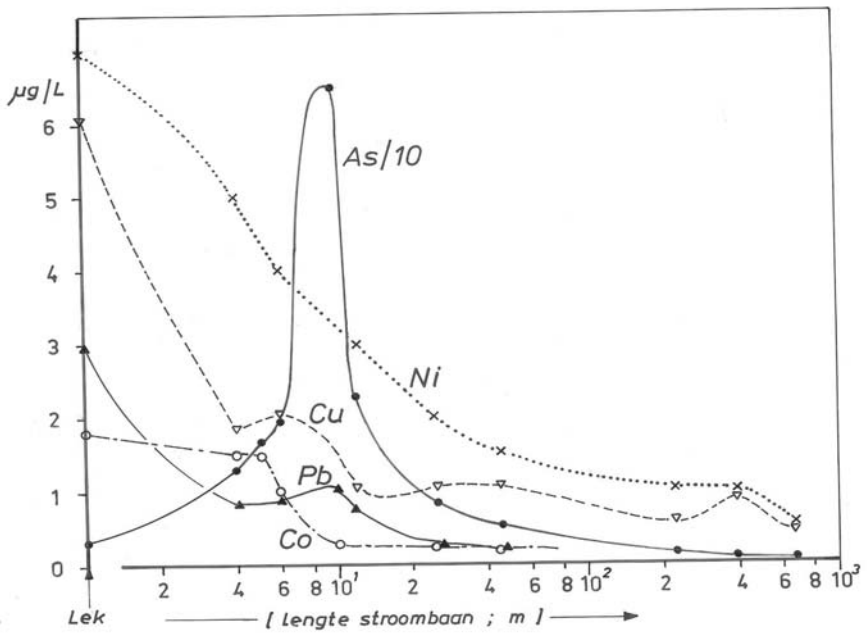

Figure 8. Survey of trace element concentrations in RBF along the Lek at site Opperduit (site 81 in Fig.1). Stuyfzand (1992)

5. CASE 3: ESTUARINE RBF (HOLLANDSCH DIEP, SITE 82)

5.1 Situation

The last case study presented here, involves a polder area 4 km to the south of well field No 30 (in Fig.1 and Table 1), near Gravendeel, where estuarine water from the Hollandsch Diep (composed of a mix of mainly

Rhine and Meuse River water) is infiltrating. The site is situated in the compound Rhine-Meuse delta, where tidal influences were operating before closure in 1971 of the Haringvliet outlet by a dam with sluices, as part of the famous 'Delta Works'.

The sandy river bed seriously clogged on this site due to reduced river flows. This clogging layer therefore was not primarily the result of RBF. However, its presence has a tremendous impact on water quality, and serves therefore as an interesting example. The site is somehow representative for well fields of type 4 (section 2), although it exhibits exceptional characteristics. Intensive hydrological and hydrochemical research was carried out in the period 1997 – 1999 (Stuyfzand & Zindler, 1998; Stuyfzand et al., 1999, 2004).

5.2 Hydrological Aspects (including Clogging)

Groundwater flow is permanently directed towards the central parts of the deep polder (land surface at 1.6 m-MSL) bordering the northern estuary bank. The pumping of RBF at well field 30 had no impact on the local flow pattern, because it was abandoned in 1988.

A cross section over the study site is given in Fig.9, showing the position of the recent sludge layer at the bottom of the Hollandsch Diep estuary in 1990-2000, an upper sandy aquifer of Holocene age (0-15 m-MSL) with an intercalated, discontinuous peat aquitard (5-8 m-MSL), a continuous aquitard of Middle Pleistocene age (15-20 m-MSL) and a sandy aquifer of Middle to Lower Pleistocene age (20->35 m-MSL).

It follows from diagnostic concentrations of Cl and ^{18}O (Stuyfzand et al., 2004) that water which infiltrated the Hollandsch Diep in the study area during the period 1972-1996 consisted of a mixture of Rhine River water (72%), Meuse River water (28%) and North Sea water (0.1%). The clogging sludge layer of 0.2-4 m thickness in 1997 thus formed in 26 years. Along the estuary banks the deposition is limited by wave action, and in the fairway it is curtailed by shipping and frequent dredging.

5.3 Geochemistry

Only the upper aquifer system and the sludge layer have been studied in detail. Analyses of cores of the upper, recent sludge layer (formed after 1971), the underlying old sandy sludge layer (formed before 1971) and Holocene sands are presented in Table 6. All sediment samples are deep anoxic and calcareous. The recent sludge layer contains most fine particles,

calcium carbonate, bulk organic material and iron sulphides, the sand the least.

5.4 Hydrochemistry

Water quality data are presented in Table 8, for four generic groundwater types whose spatial distribution is shown in Fig.9: anoxic water type A (along the estuary banks) with little sludge contact; water type C (in the deeper parts of the sludge layer and just beneath thick sludge) with the most intense sludge contact; water type B (downgradient of type C), with strong sludge contact; and water type F (in the deeper aquifer), without sludge contact but with strong imprints of the aquitard at 15-20 m-MSL.

All watertypes are fresh (Cl < 300 mg/l; E and F excluded which are slightly brackish), (deep) anoxic mainly by reaction with abundant labile organic material in sludge and aquitards, and calcite saturated.

Contact with the recent sludge at the bottom of the estuary yields extremely high concentrations of Ca, HCO3, DOC, Br, NH4, Mg, K, Fe, CH4, As and B. The high Br concentrations, which probably derive from organic material, result in anomalously low Cl/Br ratios in watertype C. Pore water samples taken from and under the recent sludge layer also reveal extreme concentration levels, even higher than groundwater type C (Table 7). Calculations show that the extreme NH4 and Mg concentrations approximate equilibrium with the mineral struvite ($MgNH_4PO_4.6H_2O$) which is known to form in sewage treatment plants (Schellekens, 2004). This could imply that parts of the sludge layer are composed of sewage treatment waste.

Passage of the thick aquitard of Middle Pleistocene age at 15-20 m depth does not result in the extreme concentration increases as the passage of the recent sludge layer does. This is due to a prolonged leaching of this old fluviatile layer and a far better water quality during its deposition. The raised concentrations of Na, K and Mg in water type F are mainly due to cation exchange as a result of an earlier fresh water intrusion in this formerly brackish aquifer.

For a further discussion of the hydrochemistry, including all watertypes, geochemical reactions and a discussion of the potential effects of pressure filtration in compacting sludge layers, refer to Stuyfzand & Zindler (1998) and Stuyfzand et al. (1999).

Table 6. Composition of recent sludge (formed after 1971), old sandy sludge (formed before 1971) and Holocene sands (upper aquifer) on site 82 in the Hollandsch Diep.

Description	Unit	Recent sludge			Old sandy sludge		Holocene sand	
depth top	m-LS	0.1	1.25	1.4	2	2.75	2.95	4.7
depth bottom	m-LS	0.25	1.4	1.55	2.15	2.9	3.45	4.9
Fraction<2 um	%	11	29.1	23.2	5.6	10.3	0.6	2
Fraction<16 um	% dw	19.7	48.8	39.7	11.2	18.3	2.4	2.6
C-organic	%	2.1	6.8	7.0	2.3	3.4	1.2	0.1
Bulk Org Matter	%	8.7	13.9	14.9	7.6	9.2	2.9	0.1
CaCO3	%	10.0	10.8	12.5	10.0	7.5	4.2	4.2
CEC	meq/kg	121	362	335	103	164	43	13
TOTAL ELEMENT CONTENT (ANALYSIS BY XRF)								
Al	%	4.07	5.95	4.89	2.65	3.11	2.39	1.94
As	mg/kg	10.2	42.2	72.9	58.0	115.0	18.1	1.0
Ca	%	4.36	4.86	5.02	3.96	3.92	1.67	2.12
Fe	%	2.09	4.18	3.56	1.64	2.15	0.73	0.53
K	%	1.64	1.97	1.69	1.31	1.31	1.16	1.11
Mg	%	0.70	1.14	0.91	0.44	0.50	0.17	0.08
Mn	%	0.070	0.108	0.083	.040	0.054	0.017	.015
Na	%	0.56	0.42	0.47	0.56	0.52	0.58	0.53
P	%	0.17	0.51	0.51	0.12	0.16	0.04	0.02
S	mg/kg	1100	4700	4900	2000	3100	1000	-
Sorg (calc)	mg/kg	168	544	560	184	272	96	7
Si	%	32.4	24.6	26.0	35.3	33.2	40.2	42.1
Ti	%	0.25	0.44	0.43	0.20	0.26	0.08	0.05

5.5 Hydrochemical Evolution

The hydrochemical situation in the area is complicated by pollution related changes in river water quality, variations in the contribution of intruding sea water, an intricate hydrogeological structure with many discontinuous aquitards, changes in the mixing ratio of Rhine and Meuse River water and man-made changes by the construction of weirs, dams, storm surge barriers and fairways.

Nevertheless, a clear picture of the hydrochemistry, origin and ages of the groundwaters in the Hollandsch Diep estuary could be made (Fig.9). The

Table 7. Chemical composition of pore water and groundwater from recent sludge (formed after 1971), old sandy sludge (formed before 1971) and Holocene sands (upper aquifer) on site 82 in the Hollandsch Diep.

Water sample type		Pore water						Groundwater	
Sediment type		Recent sludge			Old sandy sludge		Sand	sludge	sand
Depth	cm-LS	10-25	125-140	140-155	200-215	275-290	295-345	250	350
pH		7.49	7.6	7.46	7.77	7.9	7.92	7.00	7.22
EGV	uS/cm	630	690	640	920	1140	960	3060	1710
^{3}H	TU	66.4	139	81.5	65.2	79.6	73.6	68.1	55.5
Cl^-	mg/l	93	141	149	148	179	161	200	160
HCO_3^-	mg/l	1066	2821	2598	1340	1326	601	2180	970
SO_4^{2-}	mg/l	2.2	3.4	5.9	10	14	114	<1	<1
NO_3^-	mg/l	<2.2	<2.2	<2.2	<2.7	3.5	-	<0.1	<0.1
PO_4^{3-}	mg/l	<1.5	<1.5	<1.5	<1.8	<1.8	<1.5	0.28	0.28
Na^+	mg/l	64	109	118	134	138	114	130	110
K^+	mg/l	15	44	47	34	40	38	29	22
Ca^{2+}	mg/l	151	212	203	54?	130	120	310	83
Mg^{2+}	mg/l	29	78	85	19	39	35	84	42
Fe^{2+}	mg/l	11	2.3	1.5	<0.2	<0.3	<0.2	48	24
Mn^{2+}	mg/l	6	0.6	0.4	0.1	0.2	0.2	0.8	0.6
NH_4^+	mg/l	36.1	857	868	415	384	255	168	112
DOC	mg/l	27	67	62	30	56	50	48	24
Σ anions	meq/l	20.14	50.3	46.9	26.34	27.1	16.76	41.37	20.4
Σ cations	meq/l	15.70	70.4	71.6	33.96	38.0	28.94	39.84	20.0

Table 8. Quality survey of 5 water types: the estuarine water in the Hollandsch Diep, and river bank filtrates A, B, C and F. Spatial distribution of RBF water types in Fig.9.

Water type		Holl Diep	A	C	B	F
Sludge contact		none	weak	very strong	strong	weak
Depth #	m-LS	0	6	9	14	22
Recharge	period	1996	1960-1998	1972-1998	1972-1992	1920-1952
Watertype @			F3Ca HCO3	f6NH4 HCO3+	F5Ca HCO3+	B4Na HCO3+
Temp	oC	10.5	10.5	10.5	10.5	10.5
EC (20oC)	uS/cm	820	720	3490	1690	1780
pH	-	8.2	7.45	6.8	6.99	6.99
O2	mg/l	9.1	<0.1	<0.1	<0.1	<0.1
CH4	mg/l	0	0.1	19	16	20
3H	TU	49	56	144	54	<0.2
δ18O	‰V-SMOW	-9.2	-8.8	-9.4	-9.1	-9.3
DOC	mg/l	2.9	6	33	23	9
TIC	mmol/l	2.72	4.74	54.1	23.0	13.4
SI-calcite	-	0.55	0.13	0.65	0.53	*0.05
Cl/Br	(mg/l)	-	423	93	141	254
Cl	mg/l	146	110	260	130	330
SO4	mg/l	65	18	<1	<1	<1
HCO3	mg/l	162	265	2400	1120	650
NO3	mg/l	16.1	<0.1	<0.1	<0.1	<0.1
PO4-ortho	mg/l	0.31	5.51	0.46	0.49	0.21
F	ug/l	210	270	320	120	230
Na	mg/l	80.5	59	200	94	220
K	mg/l	6.4	6.3	36	19	10
Ca	mg/l	75	88	230	190	87
Mg	mg/l	12.9	11	110	40	59
NH4	mg/l	0.19	3	230	53	15
Fe	mg/l		2	36	39	4
Mn	mg/l		0.6	0.5	3	0.2
SiO2	mg/l	4.7	27	16	18	24
As	ug/l	<2	6	81	413	0.6
B	ug/l	120	110	580	190	130
Br	ug/l		260	2800	920	1300
Cu	ug/l	<5	3	<1	<1	<1
Ni	ug/l	3.4	2	3	<1	<1
Pb	ug/l	<2	15	<0.5	<0.5	<0.5
Zn	ug/l		56	7	<5	7
phenanthrene	ug/l	0.011	5.2	0.15	0.02	<0.02

below the bottom of the estuary; @ = using classification of Stuyfzand (1989).

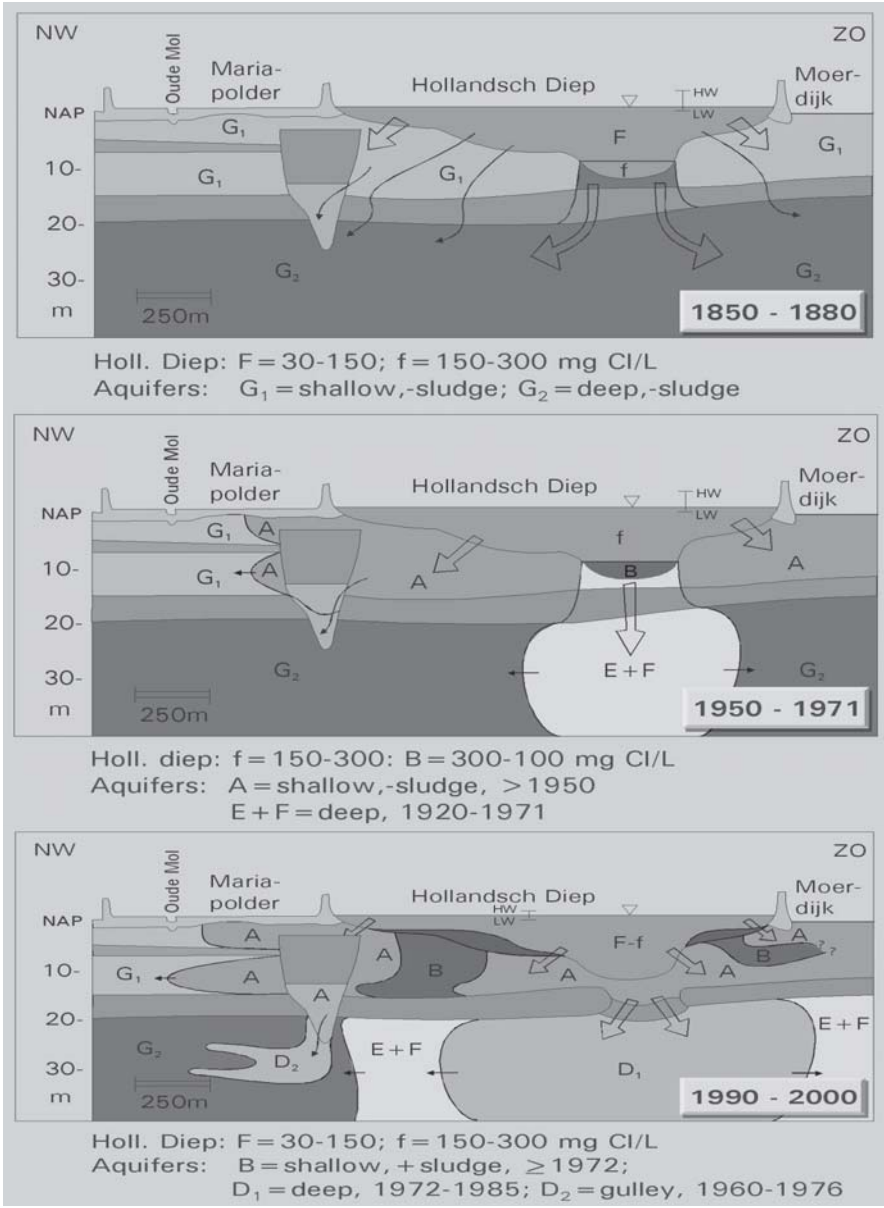

Figure 9. Changes in the spatial distribution of generic groundwater types (some explained in Table 8) along section AA' in the study area, in the period 1850-2000 (after Stuyfzand et al., 2004). Codes for surface water in Hollandsch Diep: F = 30-150 mg Cl^-/l; f = 150-300 mg Cl^-/l; B = 300-1000 mg Cl^-/l; HW = mean High Water level; LW = mean Low Water level.

study area shows a largescale fresh water intrusion of a mix of mainly Rhine and Meuse river waters into an aquifer system that salinized probably during the Holocene transgression and during and after the socalled St. Elisabeth's storm surge in 1421 AD. The fresh water intrusion probably started after 1600 when many dikes were completed in the area, and drainage of the diked land intensified. Remnants of the old saline groundwaters were not observed, because maximum age of the groundwaters studied is about 200 years.

Prior to the construction of the dam in the Haringvliet outlet, there was a period of about 50 years (1920-1970) with reduced river flows and a somewhat increased seawater intrusion. This is evidenced by the limited occurrence of brackish groundwater (water types E+F), dated 30-80 years old by various tracers, in the deep aquifer.

The dam in the Haringvliet outlet, completed in 1971, strongly reduced the seawater intrusion in the study area. The resulting deposition of a 0.1-4 metres thick sludge layer generated, however, a strongly polluted groundwater plume (watertypes B and C in Fig.9). Urgent problems with exfiltrating water from this plume are not expected. The first reason is that this plume does not flow, in the study area, in an upward direction but in a subhorizontal direction towards a remote deep polder 4-5 km to the northwest. The second reason is that accretion and compaction of this layer over time results in an ever increasing hydraulic resistance and thus in a shrinking recharge of the plume.

6. CLOGGING

Experiences with RBF in the Netherlands indicate that there are serious risks of clogging in case of a river bed in gravel, and hardly any such risks where the river bed is sandy and periodically cleaned by flood waves. This means there is an interesting paradox (Fig.10): sand is less permeable than gravel, but can sustain a higher recharge rate (on average) for a longer time in (semi)natural systems. The reason is that cake filtrated material on sand can be more easily removed by river flows than deep bed filtrated material in gravel.

When surface water flow reduces to low velocities, sedimentation of suspended material may become a serious enemy of RBF, as experienced in the Hollandsch Diep.

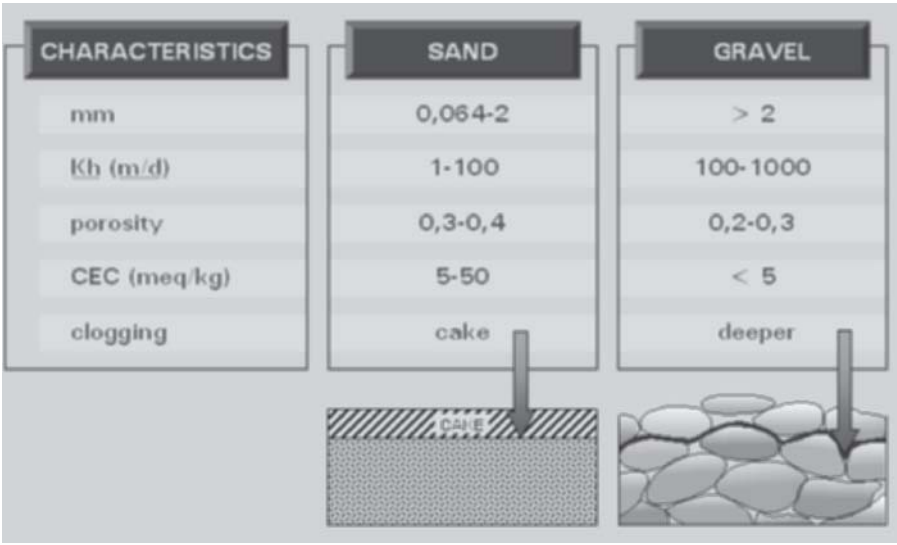

Figure 10. The clogging paradox: less permeable sand sustains, in (semi)natural systems, higher recharge rates for a longer time than gravel, because of another clogging mechanism.

7. GEOCHEMICAL INTERACTIONS

7.1 Overview of Compartments and Processes

RBF systems are subject to the following processes in the four compartments depicted in Fig.11:

1. The surface water compartment: the admixing of rain water (+ dry deposition), evaporation, nutrient uptake, biogenic hardness reduction, volatilisation, photolysis and (bio)degradation;
2. The water sediment interface: filtration, additional O_2 and CO_2 inputs (unsaturated zone or root respiration), mineralisation of organic matter, dissolution of $CaCO_3$ and iron(hydr)oxides, precipitation of sulphides, nitrification and DOC oxidation;
3. During aquifer passage: displacement of native groundwater, cation exchange, oxidation of pyrite and organic matter, dissolution of various mineral phases (like $CaCO_3$, FeCO3, MnO_2, opal, silicate minerals), sorption of trace elements, Organic MicroPollutants (OMPs) and micro-organisms,

radioactive decay, (bio)degradation of OMPs and inactivation of micro-organisms;

4. The recovery system: the mixing of various RBF water qualities, and the admixing with native groundwater.

In this section the focus is on the geochemical reactions in compartments 2-3. The most important reactions demonstrated by river bank filtrate in the Netherlands are listed in Table 9.

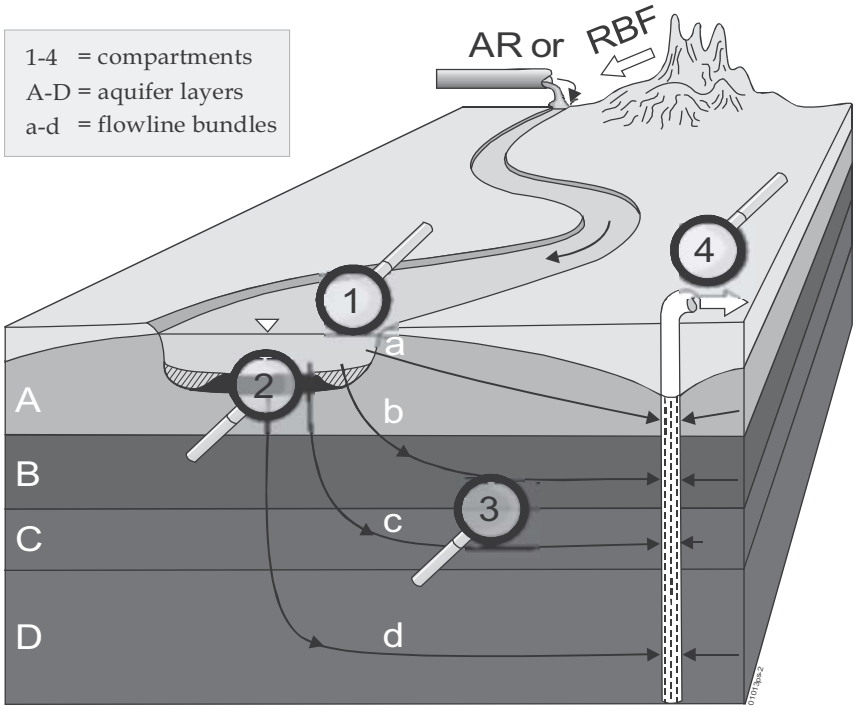

Figure 11. The 4 compartments in RBF systems, with schematisation of the aquifer system, flow, sludge interaction and recovery. Numbering of compartments same as in text above.

7.2 Quantifying Geochemical Reactions by the Mass Balance Approach

The extent of all reactions at the water sediment interface and in the aquifer can be quantified by applying the mass balance approach, a technique also referred to as 'inverse modelling'. Chemical mass balances are drawn up by using a set of reaction equations in appropriate order and

Table 9. Listing of the most important hydrogeomical reactions during RBF in the Netherlands, excluding organic micropollutants and micro-organisms.

REACTION EQUATION	Occurrence @	Comments
IN UNSATURATED ZONE		
2.25O2 + FeS + CaCO3 + 1.5H2O → Fe(OH)3 + SO4 + Ca + CO2	RRR (80)	Oxidation of deep bed filtrated matter especially during winter
Atmospheric O2-addition	R (80)	Especially during quickly rising river levels
OX of BOM + RESPIRATION: O2+CH2O → CO2 + H2O	R (80)	Additional CO2-inputs along strongly vegetated river banks
IN SATURATED ZONE		
FILTRATION	CCC	Relevant for all silt-bound compounds
Normal redox sequence due to oxidizing NOM #		
O2+CH2O → CO2+H2O	CCC	Oxidation NOM in aquifer and/or sludge
0.5O2+0.4NO3+CH2O-DOC→ 0.6CO2+0.4HCO3+0.2N2+0.8H2O	CC	Oxidation DOC-input, by assumed mix of O2 and NO3
4NO3+5CH2O → 2N2+CO2+4HCO3+3H2O	CC	Normal denitrification
NO3+0,5CH2O → NO2+0,5CO2+0,5H2O	R	Partial denitrification
4NO2+3CH2O+CO2 → 2N2 + 4HCO3 + H2O	CC	Nitrite removal by reduction
MnO2+0,5CH2O+1,5CO2+0,5H2O → Mn+2HCO3	CCC	Typical reaction for RBF, raising Mn/Fe-ratio above nornal
Fe(OH)3+0,25CH2O+1,75CO2 → Fe+2HCO3+0,75H2O	CCC	Iron dissolution from iron(hydr)oxide (often coatings)
SO4+2CH2O+Fe → FeS+2CO2+2H20	CC	S-reduction with FeS formation (lack of SO4)
2SO4+3.5CH2O+Fe → FeS2+2HCO3+1.5CO2+2.5H2O	CC	S-reduction with pyrite formation (enough SO4)
CO2+2CH2O → CH4+2CO2	CC	Methanogenesis
Redox reactions with pyrite and siderite		
3.75O2+FeS2+4HCO3 →Fe(OH)3+2SO4+4CO2+0,5H2O	R	Pyrite oxidation with maximum O2 availability
3,5O2+FeS2+2HCO3 → Fe+2SO4+2CO2+H2O	R	Pyrite oxidation with limited O2 availability
O2+4FeCO3+6H2O → 4Fe(OH)3+4CO2	RR	Siderite oxidation by O2 with maximum O2 availability
NO3+5FeCO3+8H2O → 5Fe(OH)3+0,5N2+4CO2 + HCO3	RRR?	Siderite oxidation by NO3 with maximum NO3 availability
3NO3+FeS2+HCO3+H2O → Fe(OH)3+2SO4+CO2+1,5N2	RRR	Pyrite oxidation with maximum NO3 availability
2,8NO3+FeS2+0,8CO2+0,4H2O → Fe+2SO4+1,4N2+0,8HCO3	RR	Pyrite oxidation with limited NO3 availability

Table 9 (continued). Listing of the most important hydrogeomical reactions during RBF in the Netherlands, excluding organic micropollutants and micro-organisms.

REACTION EQUATION	Occurrence @	Comments
Exchange reactions		
[Cations-X]-EXCH+Cations-Y ←→ [Cations-Y]-EXCH+Cations-X	CCC	Especially Na+, K+, Ca2+, Mg2+, NH4+, Fe2+ and Mn2+ (any combination)
[Anions-X]-EXCH+Anions-Y ←→ [Anions-Y]-EXCH+Anions-X	CCC	Especially F, H4SiO4, PO4, DOC and HCO3 (any combination)
Dissolution/precipitation and pH-buffering		
CaCO3+CO2+H2O ←→ Ca+2HCO3	CCC	Calcite/aragonite dissolution, more rarely also precipitation
2CH2O + CaCO3 → H2O + CO2 +Ca(Hum)2	C	Calcite/aragonite dissolution, relevant in high DOC-waters
$Fe_{1-X}Mn_XCO3$ + CO2 + H2O ←→ 1-X Fe + XMn + 2HCO3	R	Manganous siderite dissolution/precipitation
Fe3(PO4)2.8H2O + 4CO2 ←→ 3Fe+2H2PO4+4HCO3+4H2O	R	Vivianite dissolution/precipitation
Ca5(PO4)3OH+7CO2+6H2O ←→ 5Ca+3H2PO4+7HCO3	R	Apatite dissolution/precipitation (strong supersaturation)
beta-Ca3(PO4)2 ←→ 3Ca+2PO4	R	Metastable phase, forming often in surface water
MgNH4PO4.6H2O ←→ Mg + NH4 + PO4	RRR? (82)	Struvite dissolution/precipitation
SiO2(.nH2O)+2H2O → H4SiO4 (+nH2O)	CC	Quartz and Opal dissolution; opal (diatoms etc.) more soluble
Fe(OH)3+xH4SiO4+H2O → SixFe(OH)[3+4x].H2O	C/R	Binding of Si in freshly precipitating iron(hydr)oxides
CaAl2Si2O8+2CO2+8H2O ←→ Ca+2HCO3+2H4SiO4+2Al(OH)3	R	Dissolution of anorthite
CaSO4.2H2O ←→ Ca + SO4	RRR?	Not relevant in the Netherlands
REACTIONS UPON MIXING (IN WELL)		
O2+4Fe+8HCO3+2H2O → 4Fe(OH)3+8CO2	CC	Most important clogging reaction for pumping wells
2O2+NH4+2HCO3 → NO3+2CO2+3H2O	CC	Nitrification, also during first meters of aquifer passage
0.5 O2 + Mn2+ + 2HCO3- → MnO2 + 2CO2	C	Black staining
NO3+5Fe+9HCO3+3H2O → 5Fe(OH)3+0,5N2+9CO2	R	Requires enough time and microbiological mediation
NO2+3Fe+5HCO3+2H2O → 3Fe(OH)3+0.5N2+5CO2	R	Requires enough time and microbiological mediation

@: RRR, RR, R = resp.extremely, very and rather rare in the Netherlands; CCC, CC, C = resp. extremely, very and rather common in the Netherlands. (80) = observed on site 80 (see Table 1);

NOM simplified as CH_2O, to be replaced by $CH_2O(NH_3)_Y(H_3PO_4)_Z$ with Y = 0.075-0.151, and Z = 0.0045-0.0094

summing up all resulting mass transfers between an arbitrary starting and ending point in a flow system. In the present case the observed composition of the river bank filtrate (during aquifer passage, in an observation well) is simulated by adding to its initial composition (prior to infiltration) the losses and gains by all relevant reactions with the aquifer matrix (Fig.11). If such a simulated transformation of water prior to infiltration into the observed groundwater succeeds well, we may have confidence in the mass balance and we have quantified the relative contribution of each reaction.

Such a simulation approach is, however, never unequivocal and requires further independent evidence from geochemical inspection and laboratory experiments

Mass balances were drawn up with the spread-sheet model REACTIONS+ (Fig.11; for further details see Stuyfzand & Timmer, 1999). Each reaction requires the input of either the reactant or one reaction product, after which the total mass balance is directly recalculated. The distribution of a reactant or reaction product over various reactions may need various trials. The best distribution and the best mass balance are obtained when the result, the simulated water quality after interaction with the aquifer, closely approximates, in this case, the observed water quality as sampled from a monitoring well. The most important calibration terms in the balance are CO_2 and HCO_3^-, because they are not balanced them selves but result from balancing the other parameters.

7.3 Results

Mass balances were drawn up for five observation wells in different hydrochemical RBF environments. As an example part of the results are presented for Meuse River water near Roosteren in Fig.11, with omission of the reactions that did not contribute. A very concise form of presenting the results for all five observation wells is to (1) add up all reactions pertaining to each mineral phase, Natural Organic Matter (NOM), cation and anion exchange, and oxidation of NH_4 + DOC dissolved in the river water prior to infiltration, and (2) separately express all dissolved/precipitated minerals, all oxidized NOM, all exchanged cations and anions, and the sum of NH_4 and DOC oxidized, in µmol/L.

REACTIONS+ : version 4.5 by Pieter J. Stuyfzand, Kiwa NV		O2	CO2	SO4	NO3	HCO3	Cl
	03-sep-04	03:05 PM	= date print		Figures in bold = autobalanced (rest term)		YELLOW = FILL
CHARACTERISTICS OBSERVATION POINT of OUTPUT -->		t50 (d) = 7		X (m) = 13			
MEAN INPUT = Meuse Water, sampling point grindschip, WINTER PERIOD 1998-1999		O2	CO2	SO4	NO3	HCO3	Cl
MG/L: MEASURED		12.1	3.9	33	15	151	26
UMOL/L: CALCULATED		378	89	344	242	2475	733
UMOL/L: CORRECTED FOR IONIC INBALANCE		378	89	346	244	2491	738
CONVECTIVE TRANSPORT		0	0	0	25	0	5
REACTIONS UNSATURATED ZONE	REAC.No						
2.25O2 + FeS + CaCO3 + 1.5H2O --> Fe(OH)3 + SO4 + Ca + CO2	3C		50	50			
atmospheric O2-addition		100					
OX of BOM + RESPIRATION: O2+CH2O --> CO2 + H2O	5C		603.60				
REACTIONS SATURATED ZONE	REAC.No	O2	CO2	SO4	NO3	HCO3	Cl
FILTRATION	-						
2O2+NH4+2HCO3 --> NO3+2CO2+3H2O	2	-8.00	8.00		4.00	-8.00	
OXIDATION BOM-aquifer/sludge: O2+CH2O --> CO2+H2O	5A	-177.38	156.81		20.57	-20.57	
OXYDATION DOC input: 0.5O2+0.4NO3+CH2O --> 0.6CO2+0.4HCO3+0.2N	5B	-58.33	70.00		-46.67	46.67	
3.75O2+FeS2+4HCO3 --> Fe(OH)3+2SO4+4CO2+0,5H2O	3A	-68.79	73.37	36.69		-73.37	
4NO3+5CH2O --> 2N2+CO2+4HCO3+3H2O	9A		2.37		-19.27	19.27	
4NO2+3CH2O+CO2 --> 2N2 + 4HCO3 + H2O	9C		-0.77			3.06	
[Fe,Mn,NH4,Mg]-EXCH+Ca+Na+K <--> [Ca,Na,K]-EXCH+Fe+Mn+NH4+Mg	14						
[OH]-EXCH+F+CO2 <--> [F]-EXCH+HCO3	15		-0.46			0.46	
[HCO3]-EXCH+H2PO4 <--> [H2PO4]-EXCH+HCO3	17					4.35	
SiO2+2H2O --> H4SiO4	21						
Fe(OH)3+xH4SiO4+H2O <--> SixFe(OH)[3+4x].H2O	22						
CaCO3+CO2+H2O --> Ca+2HCO3	18		-164.46			328.91	
SUM BALANCE TERMS + INPUT		166	887	433	227	2792	743
MEASURED OUTPUT = wp41-f2 (period F)		O2	CO2	SO4	NO3	HCO3	Cl
UMOL/L: CORRECTED FOR IONIC INBALANCE		166	887	433	227	2757	743
MG/L: MEASURED		5.3	39.1	41	13.9	166	26
UMOL/L: CALCULATED		166	887	427	224	2720	733
ALL ZONES INCLUDED:							
SUMMATION of CHANGE in MINERAL CONTENT (phases in red)	SiO2-minerals	CH2O	FeS(2)	CaCO3	Fe(OH)3	EXCH.Cat	MnO2
TOTAL CHANGE IN SOIL CONTENT (UMOL/L water)	-30	-117	-68	-214	68	53	0

Figure 12. Fragment of the spread sheet model REACTIONS+ (in EXCEL), showing Meuse River water as input, the RBF water in monitoring well WP41-f2 (fromTable 3) as output, and the required reactions to transform the first into the latter.Yellow cells = fill in; Blue cells = use default or change; Roze = check that value >=0; Green = compare results.

The results of this (shown in Table 10), allow a comparison of the extent of the principal reactions diagnosed. It can be concluded from Table 10, that the principal hydrogeochemical reactions are, in general decreasing order: (a) oxidation of NOM from the aquifer (by successively O_2, NO_3, MnO_2, $Fe(OH)_3$, SO_4 and CO_2); (b) calcite dissolution; (c) cation exchange; (d) reductive dissolution of ironhydroxides (by NOM and methane); (e) pyrite formation; (f) dissolution of SiO_2 containing phases; (g) anion exchange, (h) the oxidation of imported NH_4 + DOC, and (i) the reductive dissolution of Mn-phases.

The dissolution or precipitation of other phases like siderite and the various phosphate minerals listed in Table 9 could not be identified with the mass balance approach, although their presence is not contradicted by mineral equilibrium calculations.

Table 10. Comparison of the total hydrogeochemical reaction scheme for riverbank filtrate on 5 locations: reactions with water sediment interface plus aquifer in µmol/L (+ = formation; - = loss of phase).

Location	Well/ water type	CH2O	FeS(2)	CaCO3	Fe(OH)3	C-exc	A-exc	SiO2-minerals	NH_4 + DOC oxid	MnO2
Roosteren	WP. 41-f2	-117	-68	-214	68	53	5	-30	-121	0
Opperduit	292-b	-185	67	-1	-100	313	11	-52	-196	-13
Holl Diep	Type A	-1238	478	-184	-512	225	43	-371	0	-8
Holl Diep	Type B	-27163	737	-4254	-1439	2361	249	-221	0	-53
Holl Diep	Type C	-72691	1171	-10550	-1833	8591	323	-188	0	-7

CH_2O = oxidation of bulk organic matter from aquifer;
FeS(2) = hydrotroillite (FeS.nH2O) or pyrite (FeS2) formation (if +, otherwise oxidation)$^-$;
$CaCO_3$ = calcite/aragonite dissolution;
$Fe(OH)_3$ = reduction of iron(hydr)oxides (if -, otherwise weathering product of pyrite);
C-EXC = cation exchange (µmol/L sum of all cations involved divided by 2);
A-EXC = anion exchange (µmol/L sum of all anions involved divided by 2);
SiO2 minerals = dissolution mainly of opal (biogenic SiO2.nH2O), also of various silicate minerals;
NH4 + DOC oxidation = oxidation of species dissolved in river water during infiltration (external load)
MnO2 = dissolution of MnO_2-like phases

Deviations of the above-mentioned sequence are mainly due to differences in redox environment:

- (sub)oxic near Roosteren, where O_2 and NO_3 are still present in the aquifer (Table 3)
- anoxic to slightly deep anoxic near Opperduit, where O_2 and NO_3 are absent and some sulfate reduction occurs without much methane forming (Table 4); and
- (very) deep anoxic at the Hollandsch Diep study site, where – especially in watertypes B and C) -- sulfate totally disappeared and high methane concentrations evolved (Table 8).

The mass balance approach also reveals where specific processes have to be taken into account, which are otherwise easily overlooked. At the Roosteren site this was the additional input of O_2 and CO_2 in the unsaturated

zone, because there was otherwise a strong deficit in O_2 to sustain NOM and pyrite oxidation, and in CO_2 to yield the increased TIC levels observed. At the Hollandsch Diep site, for watertypes B and C, additional CO_2 inputs by methanogenesis were needed to explain the very high Ca and HCO_3 concentrations. In fact the measured CH_4 and CO_2 concentrations were probably far too low due to the escape of pressurized gas. In addition, the permanent upward escape of gas bubbles through the calcareous sludge layer probably resulted in a progressive reaction with $CaCO_3$ (CH_4 escaping to the atmosphere, CO_2 being partly consumed by reaction).

7.4 Physico-Chemical Indications of River Bed Clogging

For adequate monitoring, prevention and curative measures it is important to recognize any clogging of the river bed at an early stage. One way is to use hydraulic head measurements with due attention to effects of temperature and, only on specific sites, salinity changes or differences.

The other way is to use hydrochemistry as an indicator. Experiences with artificial recharge in the coastal dunes of the Western Netherlands indicate that the clogging of recharge basins is hydrochemically manifested by a.o. concentration decreases for oxidants (O_2 and NO_3 or even SO_4), and concentration increases for TIC (=CO_2 + HCO_3 + CO_3^{2-}, largely as HCO_3), NH_4, Fe and Mn and sometimes also SiO_2 (Stuyfzand, 1985). However, seasonal fluctuations in river water quality and in interaction of the water with the aquifer need to be subtracted from trends in the hydrochemical monitoring network when aiming at an early detection of river bed clogging.

On-line measurements by electrical conductivity (EC) probes buried or drilled into the river bed at selected points could help as well, because clogging will lead to increased concentrations of dissolved solids, evidenced by EC increases. Even more potential is offered by comparing the frequent EC fluctuations in the river with those in the sensors. Changes in lag time between identical peaks reveal changes in travel time, which may be related to clogging (temperature changes need to be taken into account).

In a similar way, temperature fluctuations as measured by thermistor probes can be used, as is currently under investigation in the artificial recharge area in the Amsterdam dune water catchment area (T.N. Olsthoorn, pers. comm.).

8. CONCLUDING REMARKS

River bed clogging on RBF sites in the Netherlands is not a frequent problem. This does not exclude, however, its existence and importance in the long term!

An exception is observed near Roosteren, where the river bed is made up of coarse gravel, and clogging seems to occur. In the Hollandsch Diep estuary, where RBF was abandoned in 1988, clogging was caused by reduced river flows in consequence of damming the Haringvliet outlet as part of the Delta Works. Passage of this clogging layer led to an extreme water quality, with unusually high concentrations of a.o. Ca, HCO_3, DOC, Br, NH_4, Mg, K, Fe, CH_4, As and B.

Use of the mass balance approach is strongly recommended for quickly identifying and quantifying the most probable hydrogeochemical reactions, including those which are easily overlooked otherwise. Examples of the latter are additional O_2 and CO_2 inputs in systems with periodically unsaturated zones and dense vegetation in or along the river banks, and additional CH_4 and CO_2 inputs in systems with thick compacting sludge layers on the river bed.

It is a challenge to further develop and apply physico-chemical methods to detect clogging at an early stage. On-line measurements with thermistor and electrical conductivity probes seem most promising. An important question to be answered is: When or where is riverbed clogging to be prevented and restored? There are situations where clogging is easily circumvented by the system itself, and where clogging thus is beneficial to the RBF process by incrementing both travel times and (too) short flow distances in the aquifer.

9. ACKNOWLEDGEMENTS

This survey was conducted as part of the research theme ‘Interaction between groundwater and surface water’ at the Faculty of Earth and Life Sciences of the Free University of Amsterdam. It is based on the results of various previous investigations conducted by Kiwa Water Research together with water supply companies, Water Supply Limburg (WML) in particular, and with the Institute for Inland Water Management and Waste Water Treatment (RIZA).

REFERENCES

Hiemstra, P. & too many others 2001. Natural recharge of groundwater: bank infiltration in the Netherlands. In: W. Jülich & J. Schubert [eds], Proc. International Riverbank Filtration Conference, Nov 2-4, 2000 Düsseldorf Germany, IAWR-Rhein Themen 4, 67-79.

Juhàsz-Holterman, M.H.A. 2001. Reliable drinking water by bank filtration along the River Maas (Meuse), by knowledge of the system combined with simple resources. In: W. Jülich & J. Schubert [eds], Proc. International Riverbank Filtration Conference, Nov 2-4, 2000 Düsseldorf Germany, IAWR-Rhein Themen 4, 225-234.

Jülich, W. & J. Schubert 2001. Proceedings of the international Riverbank Filtration Conference. Nov 2-4, 2000 Düsseldorf Germany, IAWR-Rhein Themen 4, 309p.

Medema, G.J., M.H.A. Juhàsz-Holterman & J.A. Luijten 2001. Removal of micro-organisms by bank filtration in a gravel-sand soil. In: W. Jülich & J. Schubert [eds], Proc. International Riverbank Filtration Conference, Nov 2-4, 2000 Düsseldorf Germany, IAWR-Rhein Themen 4, 161-168.

Ray, C. [ed] 2002. Riverbank filtration: Understanding contaminant biogeochemistry and pathogen removal. Proc. NATO Workshop Tihany, Hungary 5-8 Sept 2001, NATO Science Series IV Earth and Env Sciences 14, Kluwer Acad Publ.

Schellekens, M. 2004. Measures against the deposition of struvite on water mains. H_2O 2004-17 (in dutch), 36-37.

Sontheimer, H. 1991. Trinkwasser aus dem Rhein? Academia Verlag, Sankt Augustin.

Stuyfzand, P.J. 1985. Quality changes during artificial recharge in the coastal dunes of the Netherlands: Macroparameters. Kiwa Meded. 82 (in dutch), 336p.

Stuyfzand, P.J. 1989a. A new hydrochemical classification of watertypes. IAHS Publ. 182, 89-98.

Stuyfzand, P.J. 1989b. Hydrology and water quality aspects of Rhine bank ground water in The Netherlands. J. Hydrol. 106, 341-363.

Stuyfzand, P.J. 1998. Fate of pollutants during artificial recharge and bank filtration in the Netherlands. In: Peters J.H. (ed), Artificial recharge of groundwater, Proc. 3rd Intern. Symp. on Artificial Recharge, Amsterdam the Netherlands, Balkema, 119-125.

Stuyfzand, P.J., W.J. de Lange & A. Zindler 2004. Recognition, dating and genesis of fresh and brackish groundwaters in the Hollandsch Diep estuary in the compound Rhine-Meuse delta. Proc. SWIM-18 Cartagena, 31 May-3 June 2004, in press.

Stuyfzand, P.J. & M.H.A. Juhàsz-Holterman 2000. Effects of aquifer passage on Meuse River water during river bank filtration near Roosteren: final report on the monitoring from January 1998 till November 1999. Kiwa-rapport KOA 00-049 (in dutch).

Stuyfzand, P.J. & F. Lüers 1996. Behaviour of environmental pollutants during river bank filtration and artificial recharge; effects of aquifer passage as measured along flow lines. Kiwa-Meded. 125 (in dutch), 272p.

Stuyfzand, P.J., F. Lüers & G.K. Reijnen 1994. Geohydrochemical aspects of methane in groundwater in the Netherlands. H_2O 27 (in dutch), 500-510.

Stuyfzand, P.J. & A. Zindler 1998. Origin, age and geochemical reactions of estuarine surface water infiltrated in the Hollandsch Diep. Kiwa-report KOA 98.161 (in dutch), 72p.

Stuyfzand, P.J., A. Zindler & W.J. de Lange 1999. Age and flow of water infiltrated in the Hollandsch Diep, as determined by hydrochemical patterns. Kiwa-report KOA 99.206 (in dutch), 59p.

Stuyfzand, P.J. & H. Timmer 1999. Deep well injection at the Langerak and Nieuwegein sites in the Netherlands: chemical reactions and their modeling. Kiwa-report SWE 99.006, 44p.

Van der Kooij [ed] 1986. Drinking water from Rhine riverbank filtrate. Kiwa Meded.89 (in dutch).

CLOGGING-INDUCED FLOW AND CHEMICAL TRANSPORT SIMULATION IN RIVERBANK FILTRATION SYSTEMS

CHITTARANJAN RAY[1] AND HENNING PROMMER[2]
[1]University of Hawaii at Manoa, Honolulu, Hawaii, USA [2]Utrecht University, The Netherlands

Abstract: Riverbank filtration is a low cost treatment technology which is effective in removing various chemical, and biological contaminants from the surface water. In the United States, utilities that employ horizontal collector wells, have reported clogging of the riverbed in vicinity of the wells, particularly around the laterals that go toward the river. In this paper, we show the impact of clogging and associated reduction in leakage on flow and transport simulations.

Key words: clogging, riverbank filtration, transport, contaminant, atrazine, nitrate

1. INTRODUCTION

Riverbank filtration (RBF) systems have been operating in Germany for more than a century (Schubert, 2002). In the United States, RBF systems have been operating for more than half a century providing water to industries and municipalities located on riverbanks. There is a current surge of interest in the use of RBF for public water supply due to the availability up to 1.0 log filtration credit for *Cryptosporidium* in the Long-Term 2 (LT2) Enhanced Surface Water Rule of the U.S. Environmental Protection Agency (USEPA, 2003). Since many old filtration plants may not achieve 4-log removals (99.99%) of *Cryptosporidium* oocysts, receiving a credit of up to

Stephen A. Hubbs (ed.), Riverbank Filtration Hydrology, 155–177.

1-log unit at the front end of the treatment plant may enable many existing rapid sand filtration systems to achieve additional 99.9% (3 log units) removal to meet the LT2 regulations. In addition to pathogen removal, the RBF systems have been found to be effective in removing turbidity, dissolved organic carbon (DOC), pesticides, nutrients, and some of the emerging contaminants that might be present in surface waters (see Ray et al., 2002).

Primarily, two types of wells are used for RBF systems. In Europe, the preference is for vertical wells where these wells are placed some distance away from the river. Distances of these wells from rivers are typically 100+ meters. A small number of European utilities, for example at Düsseldorf, Germany, Budapest, Hungary) use horizontal collector wells. In Düsseldorf, the collector wells are built some distance away from the River Rhine and none of the laterals go under the riverbed. The City of Budapest uses Ranney type collector wells, similar to those used in the United States. Several laterals of each of these wells lie directly beneath the riverbed. As a result, the collector well water quality is more susceptible to that of river water. In Asia, especially in Korea and India, utilities prefer to use riverbed filtration as opposed to riverbank filtration. This is done to avoid drawing ground water to wells since the background ground water at many of these countries are polluted with anthropogenic or naturally occurring contaminants. Under those circumstances, collector wells may be more appropriate.

The effectiveness of RBF systems must be examined from two perspectives: (a) the ability to produce the required amounts of water, and (b) the ability to produce water of desired quality. It is well known that the degree of hydraulic connection between the river and the aquifer affects the amounts of water abstracted to the aquifer and finally to the water-supply wells (Ray et al., 2002). This is particularly important for collector wells, where one or more laterals lie underneath the riverbed or extend towards the river. Riverbed scouring and clogging can significantly affect this process. A clogged bed would obviously reduce the amount of induced infiltration to a pumping well on the riverbank compared to normal conditions. Similarly, a bed that is scoured and has lost the finer particles may have a “better” hydraulic connection with the aquifer. However, could such a change of (hydraulic) conditions lead to an increased turbidity and/or the breakthrough of pathogens or other chemicals in the well(s)? Similarly, for a severely clogged riverbed, the amount of leakage from the river becomes small and the time of travel from the riverbed to the well increases accordingly. This affects the zonation of the redox environment along the flow path, which, in most cases, is driven by the kinetically controlled, microbially mediated transformation/mineralization of either sediment-bound or dissolved organic carbon. Ultimately both the retention time and the biogeochemical

environment also determine the fate of pathogens and pharmaceuticals as well as other micropollutants.

Thus, the clogging process has implications for both the flux of water flow and the quality of the pumped water. We have used combinations of realistic and hypothetical scenarios to illustrate how conservative and reactive chemicals move from river water to pumping wells under conditions of clogging and scouring and how the riverbed hydraulic properties might affect the attenuation of concentration peaks that occur in rivers in the events of chemical spills.

Exchange of water between the river and the alluvial aquifer is a natural phenomenon that is present everywhere along the riverbank and not confined to situations where water is abstracted. Conceptually, this is presented in Figure 1. The exchange can be slower or faster depending on the hydraulic parameters of the layer at the river-aquifer interface. It is some times referred to as "bank storage". The alluvial aquifer stores the river water during periods of high flow in the river and gradually drains back the stored water to the river when the river stage recedes. In mid-continental United States, for example, many streams have high concentrations of herbicides in spring seasons. The herbicides from river water infiltrate into the bank storage area and subsequently drain back slowly to the river at periods when the concentrations in the rivers are lower, thus increasing the persistence of herbicides in river water (Squillace et al., 1993). The volume of bank storage depends on the hydraulic property of the interface, the hydraulic conductivity of the adjoining aquifer, and the extent of the alluvial fan/aquifer.

The concentrations of pre-emergent herbicides such as atrazine can be quite high in Midwestern U.S. Rivers. Concentrations exceeding 12 µg/L have been observed in the Illinois River (Ray et al., 1998). Similarly, concentrations as high as 26 µg/L have been found in the Platte River near the collector wells for the City of Lincoln, Nebraska (Verstraeten et al., 1999). Transient simulations have shown that these chemicals can find their way to the pumping wells. However, the degree of scouring or clogging of the bed and bank and the sorption and degradation parameters for atrazine affect the concentration in the pumping wells. At the same token, spills of chemicals in navigable rivers are of concern to utilities. It is important for water utilities to know the fate and transport of contaminants during flood or spill events so that the filtrate quality can be predicted from these events.

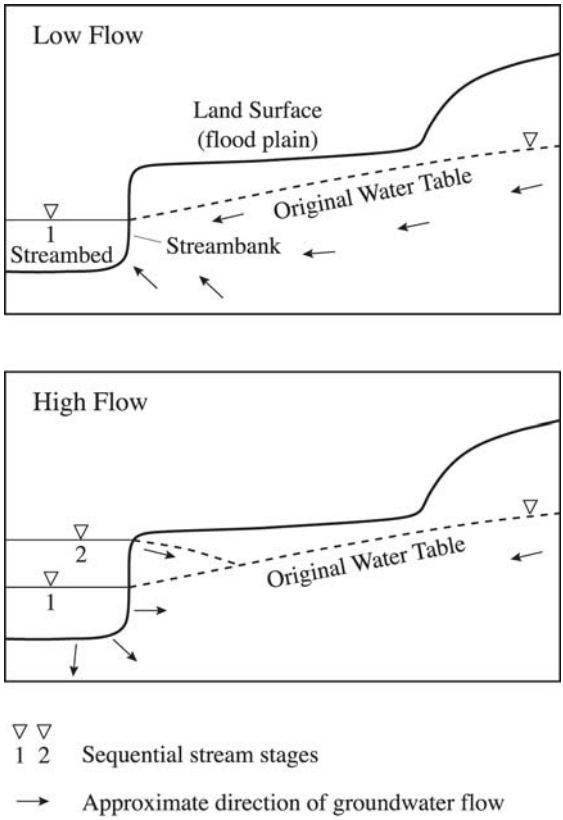

Figure 1. Natural exchange of water between a river and its bank during high and low flow events (modified from Winter et al., 1998).

Our objective here is to present and discuss the effects of riverbed/bank hydraulic properties for three scenarios: (a) herbicide transport during a flooding event in the river, (b) chemical transport from the river water to pumping wells during an emergency spill event, and (c) coupled transport and multispecies biochemical reactions such as DOC mineralization and microbially mediated atrazine degradation during a flooding event.

2. METHODS AND MATERIALS

2.1 Site Description

The study site is at the town of Henry, Illinois (USA), located on the west bank of the Illinois River. The location of the site is presented in Figure 2. Details about the site hydrogeology have been presented in Ray et al. (2002) and Ray (2004). Below the surface alluvium (1 to 2 meter thick), sand belonging to the Henry formation (Willman et al., 1975) extends to an elevation of 130 m above mean sea level (AMSL). Below this, deposits of coarse sand and gravel belonging to the Sankoty sand of the Banner formation extend to (about 118 m AMSL) the Pennsylvanian shale bedrock of the Carbondale formation (see Mehnert et al., 1996). The site has two pumping wells, each with a pump capacity of 31.2 L/s.

Figure 2. Location map of the Henry bank filtration site.

The Illinois River originates from the Chicago area, with part of the flow originating from Lake Michigan. However, a major part of the watershed is agricultural. As a result, spring runoff from farm fields contributes large quantities of agricultural chemicals in the river water. Being navigable, there is significant barge traffic between Chicago and downstream cities through a series of 9 locks and dams in the Illinois River. The river joins the Mississippi River near the town of Grafton, Illinois. The minimum water level in the navigable pool of the river is 134.7 m above mean sea level near the study site.

2.2 Model Setup

A three-dimensional flow model for river-well-aquifer interaction was setup using the well-known US Geological Survey model MODFLOW-96 (Harbaugh and McDonald, 1996). MODFLOW uses a block-centered approach to solve flow equations for unconfined/confined aquifers and it determines the hydraulic heads at each of the cellblocks. An area that is 396 m (along the river) by 427 m (Figure 3) was used for modeling. The aquifer was discretized into 8 layers, each with saturated thickness ranging from 0.6 to 3.9 m. The Henry sand was discretized into three layers and the Sankoty sand was discretized into five layers. The 3rd layer from the bottom (6th layer from top, Figure 3) was used to represent the lateral locations of the collector well. This layer had a minimum thickness of 0.6 m beneath the riverbed and it increased to about 1.0 m towards the edge of the model domain. The horizontal discretization for the model was approximately 3 m. In total, the model domain consisted of 140 rows and 130 columns.

We used a collector well for the RBF simulation because such wells are more impacted by the river compared to vertical wells. It was a hypothetical well at the site with a pumping rate of 87.5 to 175 L/s. The caisson of the collector was assumed to be located at the site of the existing production well 3 at the site (Figure 3). The collector well was emplaced in the 6th model layer (details not shown here) and had five laterals, each 0.6 to 0.9 m thick and 3 m wide. The lengths of individual laterals ranged from 77 to 85.7 m and they were connected to the caisson in the 6th layer at this location. In this configuration the lengths of the laterals that were located beneath the riverbed exceeded 30 m.

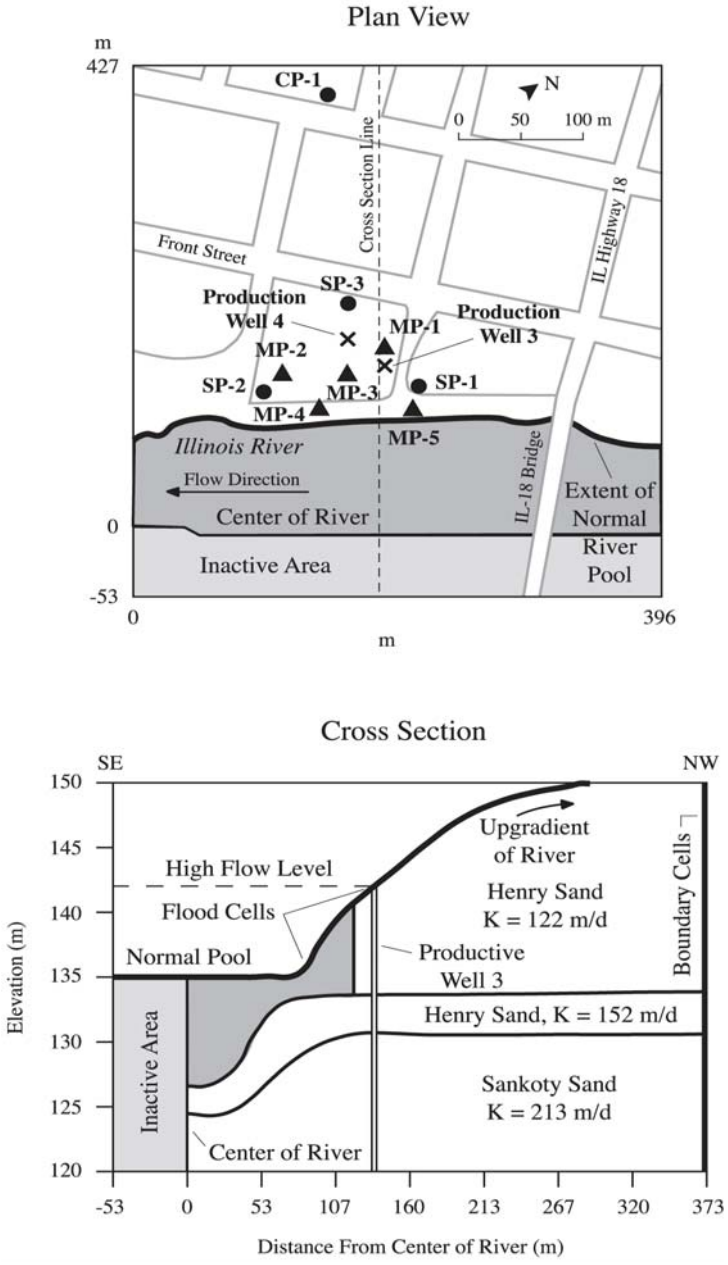

Figure 3. Model area of the Henry bank filtration site. Here SP and MP are single-port and multiport monitoring wells (from Ray, 2004).

For scenarios (a) and (b), MT3D (Zheng, 1992), a mass transport model that is fully compatible with MODFLOW, was used. MT3D simulations are based on the same model grid, i.e., the same spatial discretization and use the three-dimensional velocity field determined by MODFLOW to compute the advection term in the advection-dispersion equation. Simple cases of sorption and degradation reactions were considered in the single-species simulations for (a) and (b).

2.3 Model Parameters

The flow simulation requires information on the hydraulic parameters of the formation, estimates of initial heads, and the selection of suitable boundary condition. For the purpose of the simulation, some site specific data were available. Other information and data used in the simulation were those from literature or estimates. The horizontal hydraulic conductivity of the Henry sand ranged from 122 m/d at the surface to 152 m/d towards the bottom. Horizontal hydraulic conductivity of the Sankoty sand was 213 m/d. The vertical hydraulic conductivity values in the two formations were assumed to be one-half of the corresponding horizontal values because the drilled samples were relatively homogeneous. A porosity value of 0.28 was used based on a separate study conducted in a nearby area. The specific yield of the alluvial aquifer material was 0.11 from an earlier pump test (see Ray et al. 2002).

Hydraulic conductivity of the riverbed and riverbank sediments controls the entry of water into the aquifer near RBF site. Ray et al. (2002) took several sediment core samples to determine particle sizes. Direct measurement of the hydraulic conductivity of the sediment was not attempted. From the particle size data, estimates of hydraulic conductivities were made using the procedure of Vukovic et al. (1992). The riverbed materials (up to 0.9 m) that lie below the mean pool level had an estimated hydraulic conductivity of 5.3×10^{-8} m/s. The bank area above the mean pool level appeared to be sandy at the surface. Based on the grain size data, the estimated hydraulic conductivity was 1.27×10^{-3} m/s. However, it was unclear if the surficial sand contacted the aquifer material or whether low permeability material was beneath the surficial sand. During normal flow conditions the hydraulic properties of the bank material do not play any role on water transmission since these areas lie above the river water level. However, it plays an important role during the period of flooding. The topsoil was found to have a mean hydraulic conductivity of 1.4×10^{-5} m/s (see Ray et al., 2002). When the area surrounding the well caisson gets submerged during floods, some floodwater could enter the pumping zone from the submerged area.

The top boundary of the model area was a specified-head boundary with a head of 135.1 m. The left and right boundaries were no flow boundaries since the flow from the land was directly towards the river during low flow conditions and vice versa. Source and sink terms for the model include the pumping well and the river cells. The mid point of the river was assumed as the no-flow boundary. The model domain, to the south of the river was considered inactive. The Illinois River is over 250 meters wide at the study site. Therefore it was assumed that the drawdown cone of the collector well would not reach the boundary (mid point of the river).

For the transport simulations, the longitudinal dispersivity was set to a rather low value (0.3 m). In the absence of measured values, the organic carbon content of the bed sediments was estimated to be 0.25%, which is a comparably low value. For the subsequent layers, the organic carbon content was assumed to be 50% of the top layer (typical for aquifer sand). The bulk density of the aquifer material was assumed to be 1700 kg/m^3. Two different chemicals were considered in these transport simulations: the fate of atrazine was investigated in the flood event modeling while ethylene dibromide (EDB) served as model compound during a spill event (details explained in the next section). The half-life for atrazine (7.5 weeks) was taken from the literature (Oshiro et al., 1993) and the organic carbon partition coefficient (K_{oc}) used for the modeling was 52 mL/g. For EDB, mostly non-reactive transport was simulated in order to address worst-case scenarios.

2.4 Simulation Events

2.4.1 Flood Simulation

The first flood simulation scenario involved the transport of atrazine from the river to the pumping well. The total simulation time was 70 days, which consisted of initially two weeks of normal flow at a water level of 134.7 m prior to the flood and two weeks of normal flow at the same water levels under post-flood conditions. The flood event itself lasted for six weeks. We discretized this event into three steps: for the first two weeks of flood, the mean level was 136.9 m, the subsequent two weeks reached an average level of 138.4 m, and then, for the next two weeks it dropped to 136.9 m. The atrazine concentration in the river water prior to the flood event was 0.2 µg/L. During the six weeks of flood, the mean concentrations in the three stages were 3, 4, and 3 µg/L. After the flood, the residual concentration in the river dropped to 1 µg/L during the last two weeks of simulation.

Flood events are typically accompanied by heavy or at least above-average rainfall in Midwestern US. As a result, recharge rates and subsequently the ground water levels do also increase. Accordingly the hydraulic heads along the top boundary for the five stress periods (2 weeks of pre-flood, 3 weeks of flood, and two weeks of post-flood period) was set to values of 135.1, 136.0, 136.9, 138.8, and 135.1 m, respectively. These values were based on water levels observed in a monitoring well located close to the top boundary. The simulated recharge rates during the flood period were assumed to vary. For the five simulation periods (of each 2 week duration), the recharge rates were 2.54×10^{-2}, 0.635, 1.27, 0.635, and 2.54×10^{-2} m/yr respectively. We assumed that there was neither atrazine in the rainwater nor in the aquifer. Thus, the sole source of atrazine for the aquifer was the infiltrating river water.

Simulations were considered for (i) bed and bank hydraulic conductivity values of 0.0046 and 110 m/d, respectively, (ii) bed and bank hydraulic conductivity each 0.0046 m/d without any chemical reaction, and (iii) for case (b) with sorption and degradation.

2.4.2 Simulation of a Chemical Spill

The migration of dissolved compounds from the surface water body to the pumping wells was studied for the case of a hypothetical spill event and, as for the flood simulation; particular attention was given to the effect of the magnitude of the riverbed hydraulic conductivity. For this modeling scenario, the flow in the river was assumed to be at the normal pool level. The spilled chemical investigated was ethylene dibromide (EDB). Its assumed peak concentration in the river water was about 3.8 µg/L. The chemical plume was assumed to pass through the site of the collector well for a period of about 10 days with the peak appearing two days after initial detection. The river stage was 134.7 m and the top boundary had a value of 135.1 m. The pumping rate of the collector during the spill simulation was 87.5 L/s. Since the river was at the normal flow level, the bank areas above the normal pool had no effect on the transport. We considered four cases with incrementally increasing hydraulic conductivity of the bed material, i.e., 0.0046, 0.046, 0.46, and 0.61 m/d, respectively. The thickness of the riverbed material, as before, was assumed to be 0.6 m. An average annual recharge of 250 mm/year was assumed for this simulation.

In the transport simulations, no sorption and degradation of the chemicals were considered, corresponding to a worst-case scenario with respect to arrival times and peak concentrations at the collector wells. The total simulation period was 30 days during which the pumping rates of the wells were assumed to be constant.

2.4.3 Multi-Species Transport – Atrazine mobility under variable redox conditions

In the previously discussed model scenarios the rates of chemical reactions have, for simplicity, been assumed to be independent of the presence and concentrations of other chemicals. However, in reality the mobility of herbicides such as atrazine is in various ways affected by the local hydrogeochemistry of the aquifer and thus varies both in time and space during a flood event. Some of the complicating factors arising from those dependencies are discussed for the simulations of scenario (c). In particular we examine the effect of the riverbed hydraulic conductivity on the aquifer's redox zonation during a flood event and its potential impact on the attenuation reactions of atrazine, which we use as a model compound in these simulations. Environmental factors that are known to influence the mobility of atrazine in saturated porous media are, for example, redox conditions, pH and soil-type. Putters et al. (2002) and others noted a great variability of reported atrazine half-lives and found statistical evidence that atrazine mineralization rates vary with redox conditions, and are, for example, significantly lower under denitrifying conditions compared to aerobic conditions. Moreover Clausen et al. (2004) reported considerable differences in the sorption behavior of herbicides (dichlobenil and its metabolite 2,6 dichlorobenzamide) between aerobic and anaerobic soils. The prevailing redox conditions within the aquifer before the start of a flooding event might depend on many different factors. However, during the flood event it is thought that the redox conditions within the infiltrating water are to a large extend controlled by the concentrations of degradable dissolved organic carbon within the infiltrating river water. Depending on the concentrations and the reactivity of the DOC the redox conditions become successively more reducing along the flow path between the river and extraction wells as DOC degrades and thereby consumes dissolved (such as oxygen, nitrate or sulfate) or mineral-form (such as iron- or manganese-oxides) electron acceptors. Besides the dependency on the prevailing redox and other environmental conditions, an additional complicating factor that affects the risk of atrazine breakthrough under flood-related transient conditions, is the fact that degradation rates reported in the literature are typically provided for situations where microbial communities of specific atrazine degraders are already well-established. In contrast, such degraders might not be present in sufficient numbers at the beginning of a flood-event, causing a lag-period during which the degraders multiply and no or minimal atrazine degradation occurs. As the time-scale of this microbial lag period may be similar to the time-scale of a flood-event, microbial growth dynamics

will have, together with the redox-dependency of degradation rates, a significant influence on the contaminant breakthrough at the abstraction well.

The influence of the microbial lag effect is schematically demonstrated for a typical flood scenario that is again loosely based on the previously presented study by Ray et al. (2002). The key processes considered in the model were the kinetically controlled mineralization of DOC, the growth and decay of atrazine degraders and microbially mediated atrazine degradation. To simulate more complex chemical interactions, the reactive multi-component transport model PHT3D (Prommer et al., 2003) was used. It incorporates the geochemical model PHREEQC-2 (Parkhurst and Appelo, 1999) into the MT3D/MT3DMS simulator and can therefore account for a wide range of homogeneous and heterogeneous chemical reactions. Like for the transport simulations with MT3D for scenarios (a) and (b), the groundwater flow field used by PHT3D was computed beforehand with MODFLOW. The mineralization of DOC was modeled by an additive Monod term expression (Parkhurst and Appelo, 1999):

$$r_{DOC} = -\sum k_{Ea,i} \frac{C_{Ea,i}}{k_{hs,Ea,i} + C_{Ea,i}} \tag{1}$$

where $C_{Ea,i}$ is the concentration of the ith electron acceptor (such as oxygen, nitrate or sulphate), $k_{Ea,i}$ is the rate constant corresponding to the ith electron acceptor, and $k_{hs,Ea,i}$ is the appropriate half-saturation constant for the ith electron acceptor.

Atrazine degradation was modelled in a more complex manner by explicitly incorporating microbial growth and decay of atrazine degraders. For simplicity only degradation under aerobic conditions was considered, assuming that anaerobic degradation was negligible in the context of the (short-term) flood simulations. The mass balance equation used for the atrazine degraders describes the change of microbial concentration as a function of time (Prommer et al., 2002, Prommer and Barry, 2005):

$$\frac{\partial X}{\partial t} = \frac{\partial X_{growth}}{\partial t} + \frac{\partial X_{decay}}{\partial t} \tag{2}$$

with

$$\frac{\partial X_{growth}}{\partial t} = v_{\max} Y_x \frac{C_{Atraz}}{k_{Atraz} + C_{Atraz}} \frac{C_{Ox}}{k_{Ox} + C_{Ox}} X \tag{3}$$

and

$$\frac{\partial X_{decay}}{\partial t} = -v_{dec} X \tag{4}$$

where C_{Atraz}, C_{ox} and X are the concentrations of atrazine, oxygen and of atrazine degraders, respectively, k_{Atraz} and k_{Ox} are half-saturation constants, v_{max} is the maximum growth rate of the atrazine degraders, v_{dec} is a decay rate constant for the atrazine degraders and Y_x is a stoichiometric factor. During growth ($v_m > 0$), both atrazine and oxygen are consumed at rates that are proportional to the growth rate of the bacteria.

Compared to the earlier discussed scenarios (a) and (b) the geometric model setup was slightly modified. In particular the model discretisation in the vertical direction was changed and refined such that numerical errors by artificial mixing of reactants were minimized. The hydraulics (boundary conditions such as time-variant heads, etc.) of the modeled flood event resembled essentially those of scenario (a).

Three different cases of bed hydraulic conductivities (A: 122 m/d = no increased bed resistance, B: 0.122 m/d and C: 0.0122 m/d, respectively) were investigated in combination with two different DOC concentrations in the river water. The "low DOC" case is thought to represent a situation where the availability of easily degradable DOC is limited. Therefore in this scenario oxygen will not become depleted during the time span of the flood event and denitrification will not occur. Conversely, in the "high DOC" case oxygen might become depleted during DOC mineralization and denitrifying conditions perhaps take over. The initial groundwater and the river water compositions used in the simulations are listed in Table 1.

Table 1. Initial ground water and river water parameters used for simulations.

Component	Initial concentrations (Ambient water) mol l^{-1}	River water mol l^{-1}
DOC (low/high DOC case)	1.67×10^{-4} / 1.67×10^{-4}	3.75×10^{-4} / 1×10^{-3} mol
Atrazine	0	4.0×10^{-8}
Oxygen	$2.5e \times 10^{-4}$	5.0×10^{-4}
Nitrate	2.14×10^{-4}	3.57×10^{-4}
DIC	0	0
Atrazine degraders	1.0×10^{-8}	n.a.

3. RESULTS AND DISCUSSION

3.1 Flood Simulation Results

Figure 4 shows the impact of a higher conductivity bank on the concentration of atrazine in the caisson of a simulated collector well that was pumping 175 L/s. The peak shift between the surface water and filtrate was

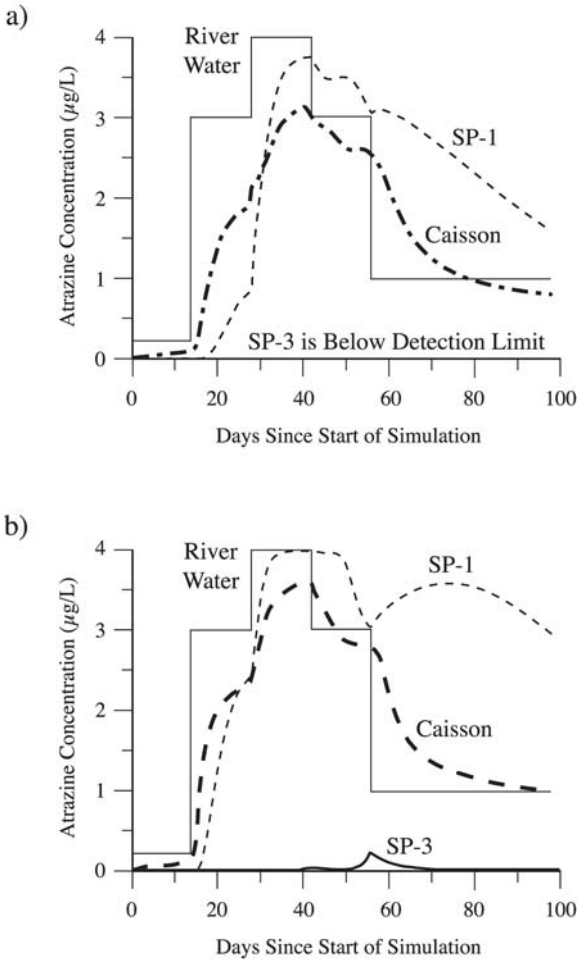

Figure 4. Concentration of atrazine at the hypothetical RBF well caisson and a monitoring well caisson at Henry, Illinois with highly conductive bank: a) case with sorption and decay and b) case without sorption and decay (from Ray et al., 2002).

about 10 days. The distance of the collector wells from the river's bank during the peak flow were less than 25 m and the laterals of the collector well were about 15 m below the bottom of the river. As shown in the figure, if one assumes the chemical to undergo sorption and degradation (using literature values), the peak concentrations in the caisson and at a monitoring well on the riverbank will be slightly reduced.

Figure 5 illustrates a case in which the bank and the beds assumed the same low conductivity values of 0.0046 m/d. However, they both were allowed to increase by two log orders (one log order for each step rise in river stage (please note that the flood hydrograph had a two step rise followed by a two step recession). This combination of conductivity is marked as set B-B in Figure 6. As can be observed there was some rise in atrazine concentrations with rising hydraulic conductivity of the bed and bank. For the case with varying K values during the flood, the peak concentration reached 1.5 µg/L for the nonreactive case and about 1 µg/L with sorption and degradation occurring. Set A-A in this figure is for the case when both the bed and bank remained at low conductivity (0.0046 m/d) during the entire simulation period.

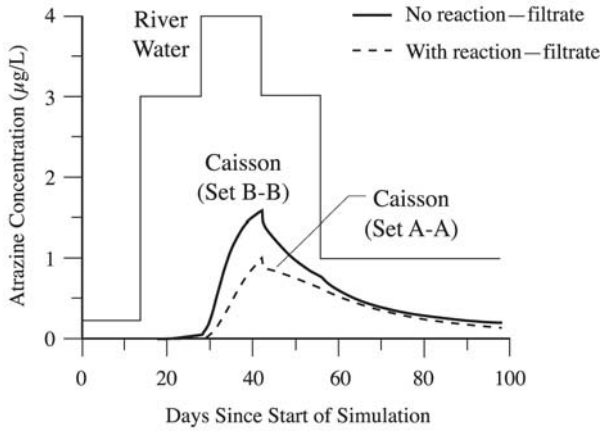

Figure 5. Atrazine concentration in the caisson when the bed and bank same low conductivities, but they increased by two log order with flood and then came down to the original values (from Ray et al., 2002).

Figure 6 shows an expanded view of set A-A from Figure 5 with or without sorption/reaction. With no changes in hydraulic conductivity from the base value, the concentrations in the caisson with or without reaction were almost below detection.

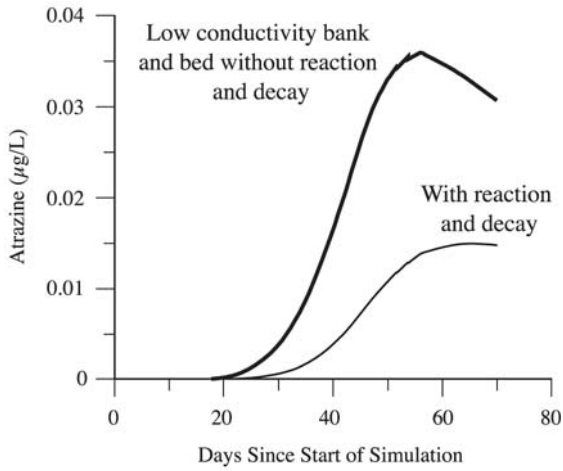

Figure 6. Concentration of atrazine at the Henry RBF site for a low conductivity bank with and without reaction (from Ray, 2004).

3.2 Results of Spill Simulation

Concentrations in the caisson of the collector well (averaging effect of all laterals) and the lateral that is perpendicular to the river (river lateral) are presented in Figure 7. We show the peak concentrations in the caisson and river without considering the effects of sorption and biological degradation (worst-case effect). The case with lower hydraulic conductivity (e.g., case a) shows a lower peak concentration than the case with higher conductivity (e.g., case d), possibly due to large amounts of ground water (rather than river water) in the filtrate. Also, the shift in peak concentration in the filtrate gets smaller with higher conductivity values of the riverbed.

3.3 Multi-Species Transport Simulations

The result of the model simulations clearly illustrates the influence of both the load of degradable DOC and of the bed hydraulic conductivity on the redox zonation as well as its indirect effect on the atrazine concentrations.

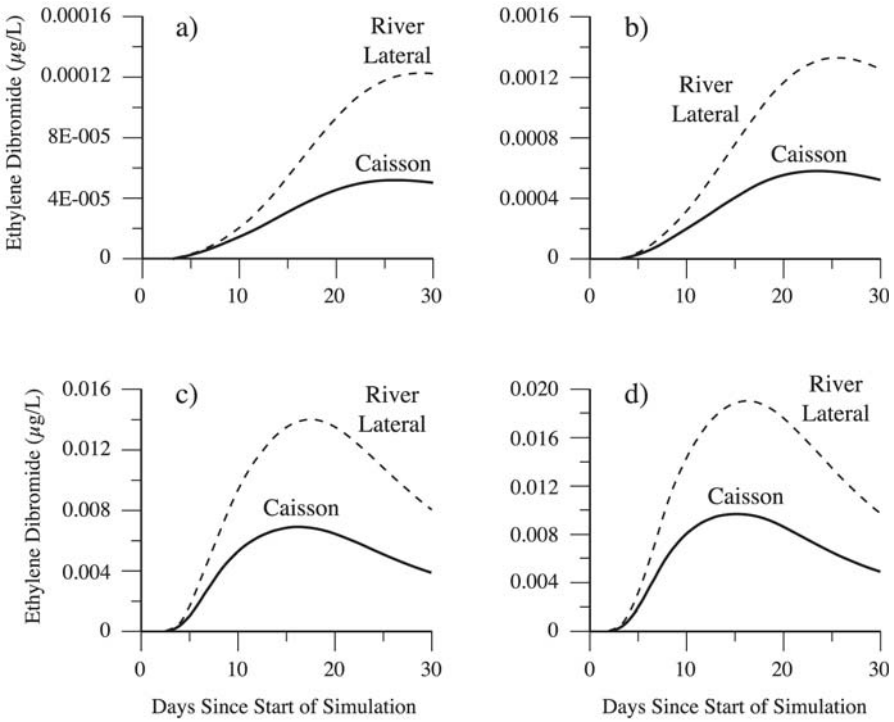

Figure 7. Simulated concentrations of EDB for a hypothetical collector well at the Henry RBF site pumping at 87.5 L/s, 5 laterals for hydraulic conductivity values of a) 0.0046, b) 0.046, c) 0.46, and d) 0.61 m/d (from Ray, 2004).

3.3.1 Influence of bed conductivity on redox zonation

As can be seen in Figures 8 and 9 for the "high DOC case", the simulated oxygen and nitrate concentrations vary as a function of the bed conductivity. The two figures show the simulated concentrations after a 50-day simulation time for a vertical cross-section between river and extraction well. With decreasing bed conductivity the DOC from the river water penetrates less rapidly into the aquifer during the flood event, which is reflected by the smaller zones with oxygen depletion. It can also be seen that in the absence of a clogged riverbed some oxygen might penetrate from the (aerated) river into the aquifer while in the case with the highest bed resistance essentially all oxygen is consumed during the slower passage through the river bed. Furthermore it can be seen that the increased nitrate concentrations from within the river (compared to ambient concentrations in the groundwater) penetrate further with decreasing bed resistance.

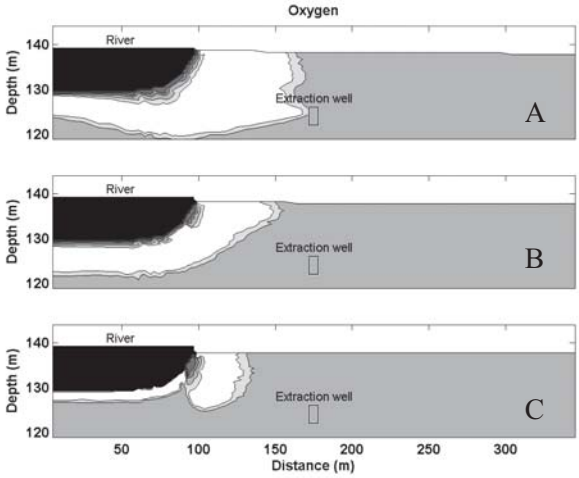

Figure 8. Simulated oxygen concentrations in the "high DOC" scenario 50 days after the start of the flood event for three different bed conductivities (A, B, and C). The darkest color corresponds to a DOC concentration of 1×10^{-3} mol/l. (e.g., river water), the ambient DOC concentration is 1.67×10^{-4} mol/l (gray), white corresponds to 0 (DOC depleted).

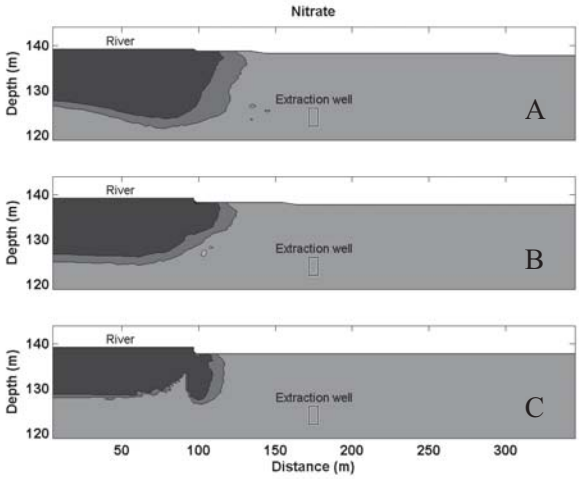

Figure 9. Simulated nitrate concentrations in the "high DOC" scenario 50 days after the start of the flood event for three different bed conductivities (A, B, and C). The darkest color corresponds to a DOC concentration of 1×10^{-3} mol/l. (e.g., river water), the ambient DOC concentration is 1.67×10^{-4} mol/l (gray).

3.3.2 Simulated fate of atrazine

The simulation results show how during the flood event atrazine penetrates into the groundwater system. To illustrate the influence of the bed conductivity, Figure 10 shows concentration snapshots after 50 days simulation time for the three investigated bed conductivities. At that time (50 days) a hydraulic gradient has already been established from the river towards the extraction well. Microbial concentrations are still very low at this point in time and thus atrazine concentrations are unaffected by degradation reactions. Figure 11 shows atrazine concentrations another 30 days later, i.e., at 80 days simulation time. It can be seen that while atrazine has spread further into the aquifer, concentrations, in particular near the river bed, have decreased somewhat as a result of microbial activity. However, due to the assumption that atrazine is only degraded under aerobic conditions, atrazine is not degraded further where oxygen becomes depleted during DOC mineralization. In all cases, independent of the bed conductivity, breakthrough of elevated atrazine concentration occurs, as overall not enough atrazine degradation occurs.

3.3.3 Influence of DOC load on redox zonation and atrazine fate

The influence of the load of degradable DOC in the river water is demonstrated by a variation of the above simulations. The DOC load within the river flood was reduced from 1×10^{-3} mol l^{-1} to 3.75×10^{-4} mol l^{-1}. As a result of the lower DOC concentrations anaerobic (for example denitrifying) conditions did not develop. Therefore the oxygen that infiltrates from the river does not get fully depleted and conditions for atrazine degradation remain more favorable. After an initial lag period of very little atrazine degradation the concentrations of atrazine degraders become then sufficiently high to allow for significant removal rates, preventing the breakthrough of elevated atrazine concentrations at the extraction well. The effect of a lower DOC load is illustrated in Figure 12, which shows the concentration of oxygen, nitrate and atrazine after 50 days simulation time.

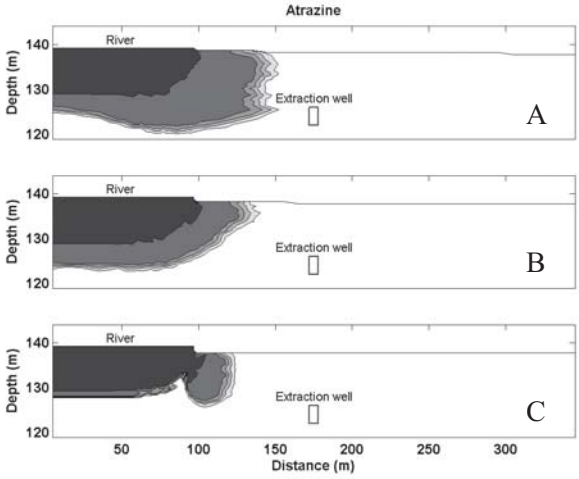

Figure 10. Simulated atrazine concentrations in the "high DOC" scenario 50 days after the start of the flood event for three different bed conductivities (A, B, and C). The darkest color corresponds to the maximum atrazine concentration of 4.0×10^{-8} (e.g., river water), white corresponds to 0 (no atrazine).

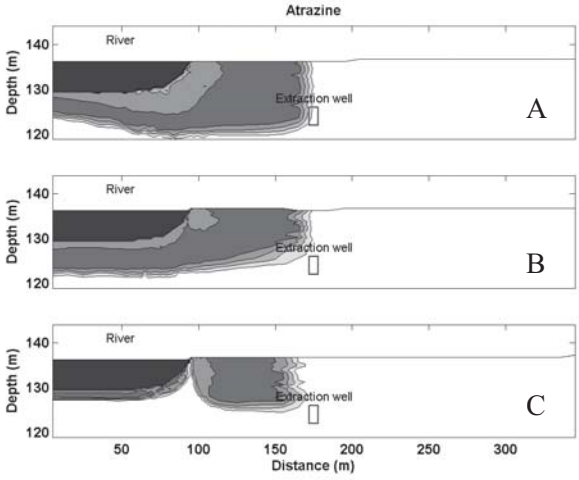

Figure 11. Simulated atrazine concentrations in the "high DOC" scenario 80 days after the start of the flood event for three different bed conductivities (A, B, and C). The darkest color corresponds to the maximum atrazine concentration of 4.0×10^{-8} (e.g., river water), white corresponds to 0 (no atrazine).

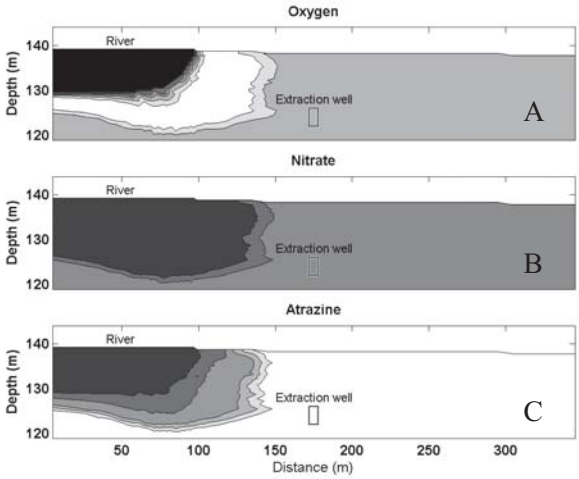

Figure 12. Simulated a) oxygen, b) nitrate, and c) atrazine concentrations in the "low DOC" scenario 50 days after the start of the flood event for one single river bed conductivity (case A). Gray shading scheme as shown in Figures 8 through 10.

4. SUMMARY AND CONCLUSIONS

Clogging of riverbed materials can affect the amount of river water that reaches a pumping well. A clogged riverbed reduces the amount of leakage, hence the rate of transport of contaminants from the river to the aquifer/well. If the concentration of the respective contaminant is low in the ground water compared to the surface water, there will be some dilution effects. Sorption of the contaminant to riverbed sediments and aquifer materials and the degradation of the contaminant in subsurface can reduce or eliminate their presence in the filtrate.

If the riverbed and bank materials have high conductivity values, there is a chance for some of the river water contaminants to reach the well screen, especially during floods when the rivers traversing in agricultural watersheds contain high concentrations of pesticides. However, many different factors such as the travel time of the river water to the well, background concentrations, and the sorption and degradation properties of the contaminant determine the final concentration in the filtrate. As found from our simulations, based on the well setup and the pumping rate, banks with high conductivity materials can easily propagate the contaminants to the bank areas, ultimately leading to their appearance in well water. Further, it

was shown that if the bank and bed hydraulic conductivity increase because of increased flow velocity in the river, there could be a rise in concentration of a chemical in the filtrate.

For spill simulations in navigable rivers, bank area hydraulic conductivity may not have a major role in contaminant transport since most spills occur in normal flow regimes in navigable pools of the river. The hydraulic conductivity of the riverbed material and the sorption and degradation properties of the spilled chemical determine the ultimate concentration in the filtrate.

Simulations of single-species transport in the river-aquifer system with pumping wells are straightforward. In reality, most RBF systems have to deal with multiple river water contaminants that undergo sorption, kinetically-controlled biodegradation, and other geochemical reactions. As a result, multi-component reactions must be considered. Biogeochemical reactions, most notably microbially-mediated redox reactions, will impact the mobility and fate of many contaminants in a complex manner. The reactive processes that take place and the interactions that occur in combination with the transient, typically fully three-dimensional flow-field can be quantified through reactive multi-component transport modeling. For the present paper we have used this technique to illustrate the impact of varying riverbed conductivities on the redox environment and the resulting effect on the fate of atrazine.

REFERENCES

Clausen,L., Larsen, F., and Albrechtsen, H.-J., 2004. Sorption of the herbicide dichlorbenil and the metabolite 2,6-dichlorobenzamide on soils and aquifer sediments. *Environmental Science and Technology*, 38, 4510-4518.

Harbaugh, A.W., and McDonald, M.G., 1996. User's Documentation for MODFLOW-96, an update to the U.S. Geological Survey Modular Finite-Difference Ground-Water Flow Model, Open File Report 96-485, U.S. Geological Survey, Reston, VA.

Parkhurst, D.L., and Appelo, C.A.J., 1999. *User's Guide to PHREEQC – A Computer Program for Speciation, Reaction-Path, 1D-transport, and Inverse Geochemical Calculations*. Technical Report 99-4259, US Geol. Survey Water-Resources Investigations Report.

Prommer, H., Barry, D.A., and Davis, G.B., 2002. Modelling of physical and reactive processes during biodegradation of a hydrocarbon plume under transient groundwater flow conditions**,** *J. Cont. Hydrol.* 59, 113-131.

Prommer, H., Barry, D.A., and Zheng, C., 2003. PHT3D – A MODFLOW/MT3DMS based reactive multi-component transport model. *Ground Water*, 42(2), 247-257.

Prommer, H., and Barry, D.A., 2005. Modeling Bioremediation of Contaminated Groundwater. In: Bioremediation (edited by R.M. Atlas and J. Philp). American Society for Microbiology, in press.

Putters, B., Borovkova, S.A., and Prommer, H., 2002. Quantification of the influence of soil conditions on atrazine degradation rates, *In*: Proc. of the Third Intern. Conf. on Remediation of Chlorinated and Recalcitrant Compounds, Monterey, California, May 20-23, 2002.

Oshiro, W.C., Miles, C.J., and Green, R.E., 1993. Physical–Chemical Properties of Selected Pesticides for Environmental Fate Modeling. Research Series 069, College of Tropical Agriculture and Human Resources, University of Hawaii.

Ray, C., 2004. Modeling RBF efficacy for mitigating chemical shock loads, *Journal AWWA*, 96(5): 114-128.

Ray, C., Soong, D., Roadcap, G.S., and Borah, D.K., 1998. Agricultural chemicals: Impacts on riparian municipal wells during floods, *Journal AWWA*, 90(7): 90-100.

Squillace, P.J., Thurman, E.M., and Furlong, E.T., 1993. Groundwater as a non-point source of atrazine and deethylatrazine in a river during base flow conditions, *Water Resour. Res.*, 29(6): 1719-1729.

USEPA. 2003. *National Primary Drinking Water Regulations: Long Term 2 Enhanced Surface Water Treatment Rule*, Proposed Rule (June 30, 2003), 40 CFR Parts 141 and 142, Washington, D.C.

Verstraeten, I.M., Carr, J.D., Steele, G.V., Thurman, E.M., and Dormedy, D.F., 1999. Surface-Water/Ground-Water Interaction: Herbicide transport into municipal collector wells, *J. Environ. Qual.*, 28(5):1396-1405.

Vukovic, M., Soro, A., and Miladinov, D., 1992. Determining Hydraulic Conductivity of Porous Media from Grain-Size Composition, Water Resources Publications, Littleton, CO, 83 p.

Willman, H.B., Atherton, E., Buschbach, T.C., Collinson, C., Frye, J.C., Hopkins, M.E., Lineback, J.A., and Simon, J.A., 1975. Handbook of Illinois Stratigraphy, Bulletin 95, Illinois State Geological Survey, Champaign, IL.

Winter, T.C., Harvey, J.W., Franke, O.L., and Alley, W.M., 1998. *Ground Water and Surface Water a Single Source*, U.S. Geological Survey Circular 1139, Denver, Colorado.

Zheng, C., 1992. MT3D version 1.8 Documentation and User's Guide, S.S. Papadopulos & Associates, Inc., Bethesda, MD, USA.

Zheng, C., and Bennett, G.D., 1995. Applied Contaminant Transport Modeling: Theory and Practice, Van Nostrand Reinhold, New York, NY.

USE OF AQUIFER TESTING AND GROUNDWATER MODELING TO EVALUATE AQUIFER/RIVER HYDRAULICS AT LOUISVILLE WATER COMPANY, LOUISVILLE, KENTUCKY, USA

Dave C. Schafer
David Schafer & Associates1 White Pine Road North Oaks, Minnesota 55127, USA

Abstract: In 1999, the Louisville Water Company completed construction of a radial collector well adjacent to the Ohio River in Louisville, Kentucky at their B. E. Payne Water Treatment Plant. The well was completed in a sand and gravel aquifer to a depth of 105 feet as part of a pilot study to evaluate the feasibility of converting their surface water supply to riverbank infiltration. One of the objectives of the study was to estimate the total yield capacity available along the shoreline on the Payne Plant property. It was hoped that the supply developed at this location could supply 25 percent or more of the water company's requirement of 240 million gallons per day.

Beginning in August 1999, a 70-day constant-rate pumping test was conducted on the well to evaluate aquifer properties. The parameters of interest included aquifer transmissivity, leakance between the Ohio River and the aquifer, and vertical anisotropy ratio of the aquifer sediments. The aquifer coefficients determined from the pumping test were applied in a groundwater flow model to predict yields of various extraction facilities designs for the site.

Three design options were considered for the Payne Plant site. One design incorporated two or more new collector wells in addition to the pilot well, connected by a subterranean tunnel drilled in the shale and limestone bedrock beneath the sand and gravel aquifer. The second option was to install a large diameter tunnel within the sand and gravel aquifer and extend well screen laterals from the tunnel to produce water. The third option was to drill conventional vertical wells, but connect them to a subterranean tunnel drilled in the bedrock.

Stephen A. Hubbs (ed.), Riverbank Filtration Hydrology, 179–198.

Modeling showed that all three of the design options could produce the desired yield. This meant that the design and construction decision could be driven by the economics of the project. Modeling was used further to track the decline in yield of the pilot collector well over time caused by clogging and compaction of the riverbed sediments. Modeling showed average riverbed leakance reductions of approximately an order of magnitude.

Key words: Riverbank filtration, modeling, leakance, hydraulic conductivity

1. INTRODUCTION

Louisville Water Company in Louisville, Kentucky is investigating converting their surface water supply of 240 million gallons per day (mgd) [more than 10,000 liters per second] to riverbank filtration to improve the quality, consistency and reliability of the supply. To that end, a 20 mgd radial collector well, shown on Figures 1 and 2, was constructed at their B. E. Payne Water Treatment Plant where they hope to develop a capacity of 60 million gallons per day (mgd), or about 25 percent of their supply needs. The collector well was used to test the aquifer and also will serve as one component of the extraction facilities installed at the Payne location. Results of testing this pilot well provided the basis for making yield projections for the site.

The B. E. Payne Water Treatment Plant is located along the Ohio River between the river and River Road in northeastern Louisville as shown on Figure 3. Louisville Water Company's new collector well is located in the northern-most corner of the property, about 120 feet from the river's edge.

The collector well is completed in a glacial sand and gravel aquifer approximately 70 feet thick, extending from slightly above elevation 400 feet above mean sea level (amsl) to just below 330 feet amsl. The aquifer is confined by a clay unit from 400 feet amsl to land surface which is about 435 feet amsl across much of the site, including the well location. Because of the high permeability of the aquifer, its piezometric surface matches the pool level of the adjacent Ohio River, averaging about 420 feet amsl under most conditions. The aquifer is underlain by relatively tight shale and limestone bedrock. About 2300 feet east the river, the bedrock rises, essentially truncating the sand and gravel aquifer at that location. Thus, for all practical purposes, the aquifer is a finite-width strip, paralleling the Ohio River.

The collector well was installed by excavating a caisson to a depth of about 105 feet below land surface to the top of the bedrock at the base of the sand and gravel aquifer. After pouring a 12-foot high concrete plug in the

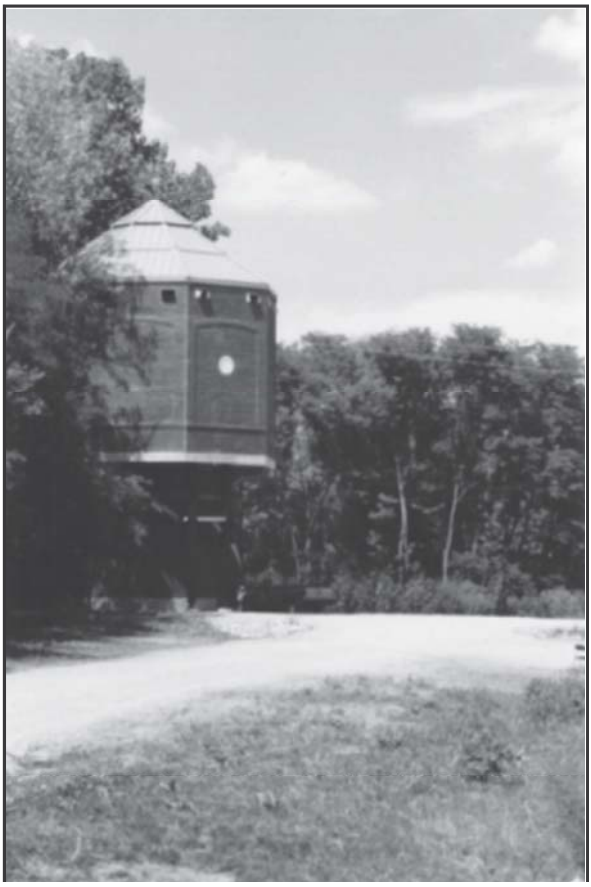

Figure 1. Louisville Water Company's Existing Collector Well

Figure 2. Located 100 feet from the Ohio River in Louisville, Kentucky

bottom of the caisson, seven 12-inch diameter screen laterals were installed at an elevation of 346 feet amsl in the radial pattern shown on Figure 4. Laterals 1, 2 and 7 extended to a length of 200 feet while 3, 4, 5 and 6 were 240 feet in length.

During test drilling, prior to constructing the collector well, several piezometers were installed at the locations shown on Figure 4 to be used in a subsequent pumping test. In addition, Louisville Water Company had divers install three shallow piezometers under the river near Lateral 4. These piezometers were installed in about 20 feet of water to depths of two feet, five feet and ten feet below the riverbed.

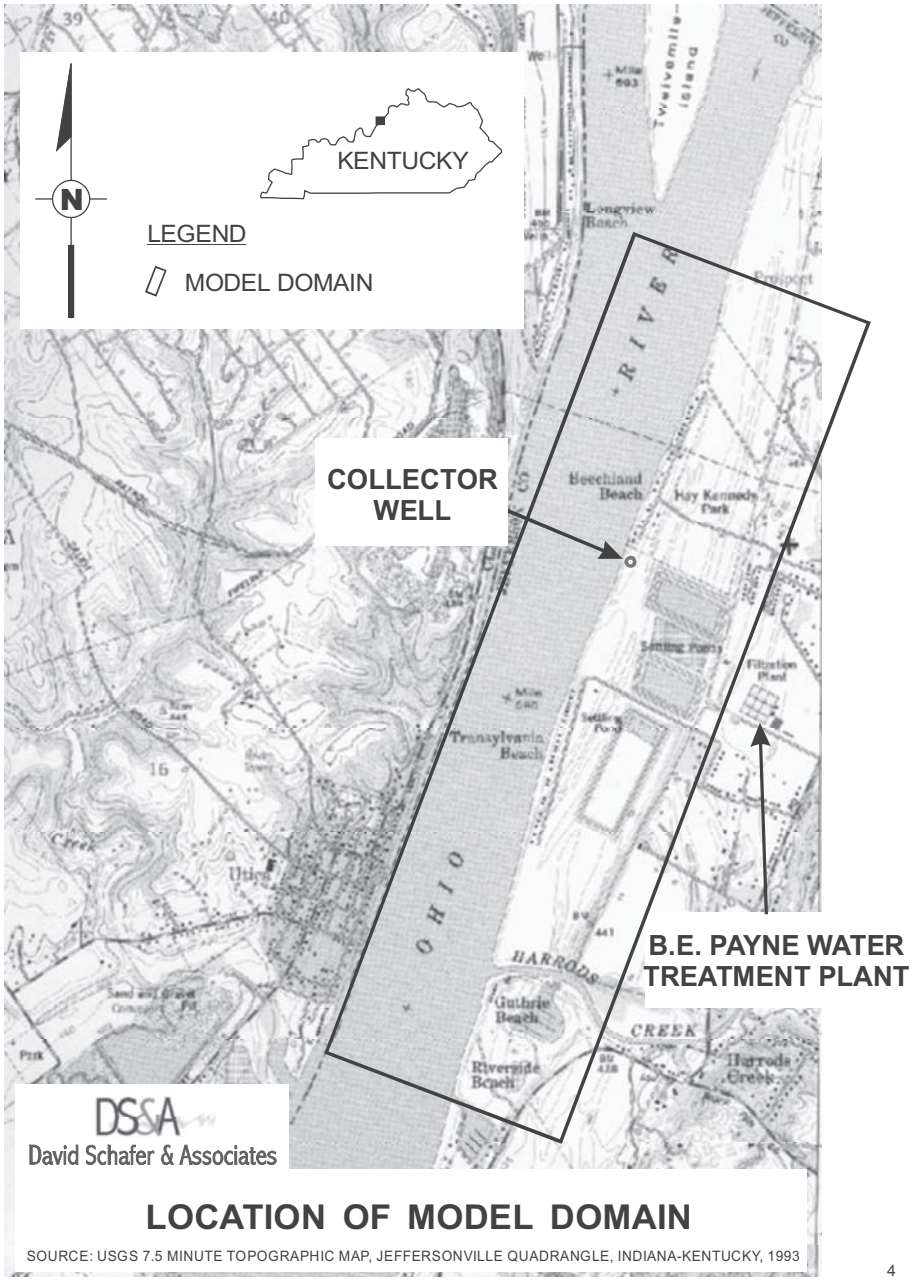

Figure 3. Location of Model Domain

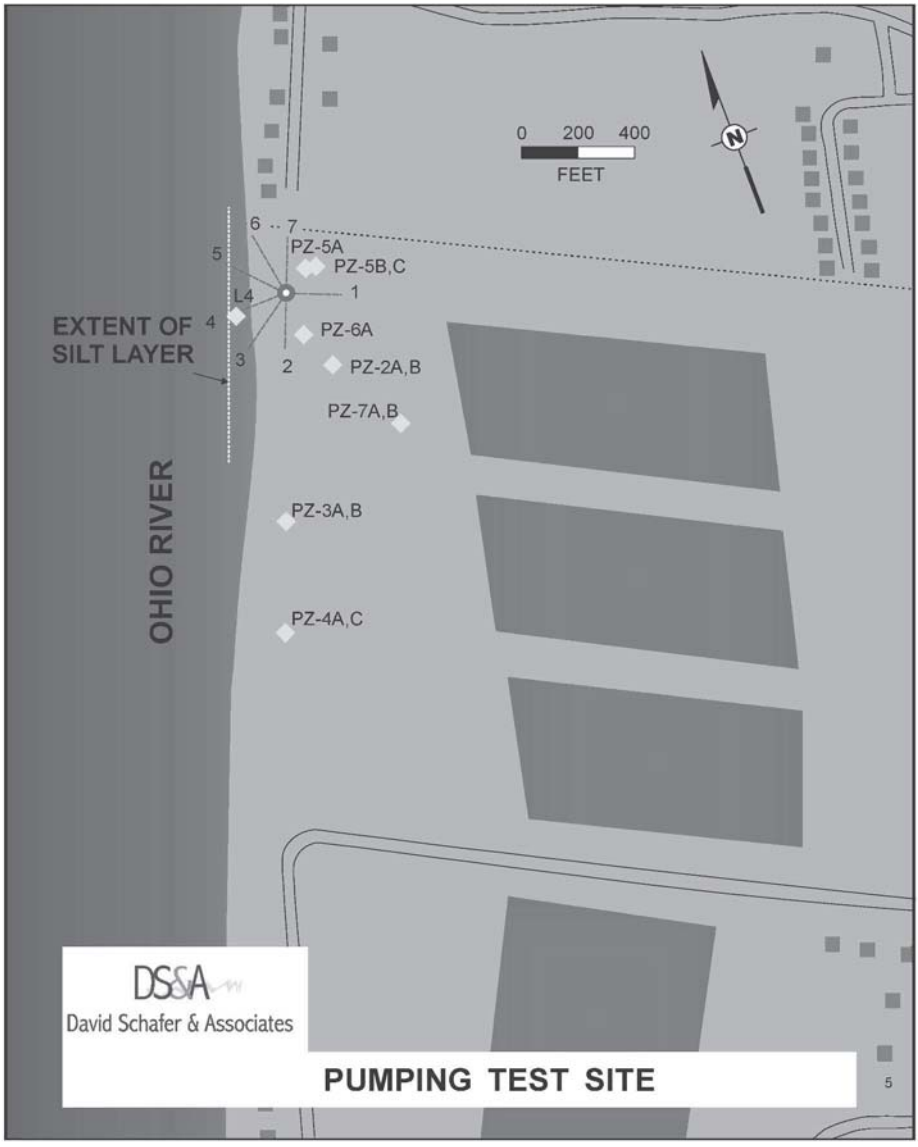

Figure 4. Pumping Test Site

2. PUMP TEST

A long-term, constant-rate pumping test was conducted to provide data from which to compute aquifer properties. Pumping began at noon on August 9, 1999 and continued for 70 days until mid-afternoon on October 18, 1999. Water level measurements were made in the collector well and piezometers during the pumping period and for a week following shut down. In addition, periodic measurements were made of the discharge rate from the collector well and the surface water elevation of the Ohio River.

Figure 5 shows water levels recorded in the collector well during the test. The pumping rate was maintained near 19.4 mgd throughout most of the test. One exception to this can be seen by the increase in drawdown on the hydrograph when the rate was increased to 21.4 mgd for several days during early September. Subsequently, the rate was returned to 19.4 mgd and was maintained at that rate for the remainder of the test. Similar hydrographs (not included here) were developed for each of the piezometers monitored during the test.

Examination of the hydrograph shows that water levels stabilized during the first half of September (except for the temporary pumping rate increase) and then drifted downward somewhat for the remainder of the pumping test. During this time period, the temperature of the water in the river and aquifer was dropping because of the onset of colder weather. The reduction in water temperature had the effect of reducing the hydraulic conductivity of the aquifer, thereby causing an increase in drawdown. A detailed analysis of the changes in water temperature and drawdown showed that all of the observed increase in drawdown was temperature induced. Thus, for all practical purposes, the pumping had reached steady-state conditions during the aquifer test. This conclusion allowed the well and aquifer system to be simulated with a steady-state model rather than a transient one.

3. GROUNDWATER FLOW MODEL

Computer modeling was used to “interpret” the pumping test. Pumping test analysis was accomplished by building a computer model of the site and adjusting key aquifer properties so that a match was achieved between observed and simulated water levels in the piezometers at the site. Adjustable parameters included aquifer conductivity, vertical anisotropy

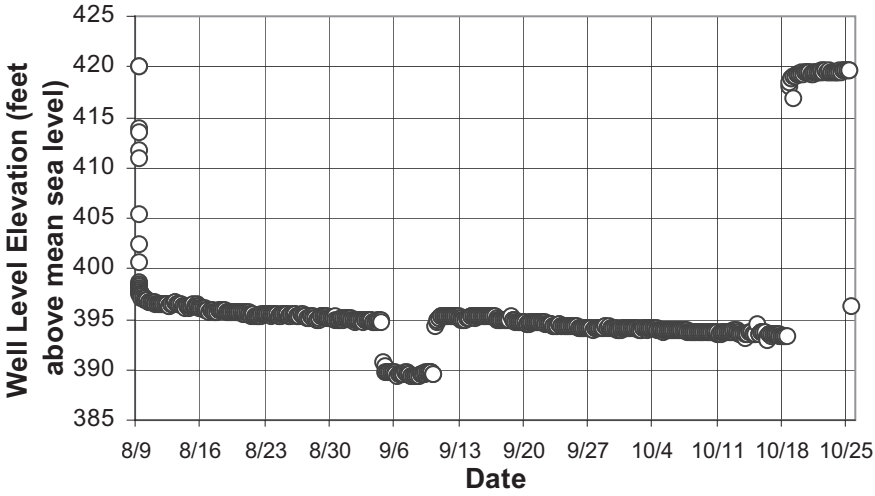

Figure 5. Water Levels in Collector Well in 1999

ratio, leakance between the aquifer and the Ohio River and the conductance value of the drain cells used to represent the collector well laterals.

The computer code selected for modeling the pumping test was the US Geological Survey Groundwater Flow Code MODFLOW (McDonald and Harbaugh, 1988). MODFLOW was implemented using Waterloo Hydrogeologic Software's Visual MODFLOW.

The model constructed to represent the site covered an area of 4000 feet by 14,000 feet and consisted of 119 rows and 53 columns. As shown on Figure 3, the rectangular model domain was oriented parallel to the Ohio River. Model grid cells ranged in size from a minimum of 20 feet by 20 feet to a maximum of 200 feet by 200 feet, as diagrammed on the model grid shown on Figure 6. The model domain was divided into eight vertically stacked layers as shown on Figure 7.

Constant-head cells were used to represent the Ohio River and the conductivity of these cells was varied to adjust the leakance parameter in the model. This was mathematically equivalent to implementing the MODFLOW River Package. However, this approach was more efficient because adjusting river cell attributes in Visual MODFLOW is not as well automated as adjusting conductivity values. Drain cells were used to simulate the pumping well's screen laterals as shown on Figure 8. In MODFLOW, a drain removes water from the aquifer based on a specified

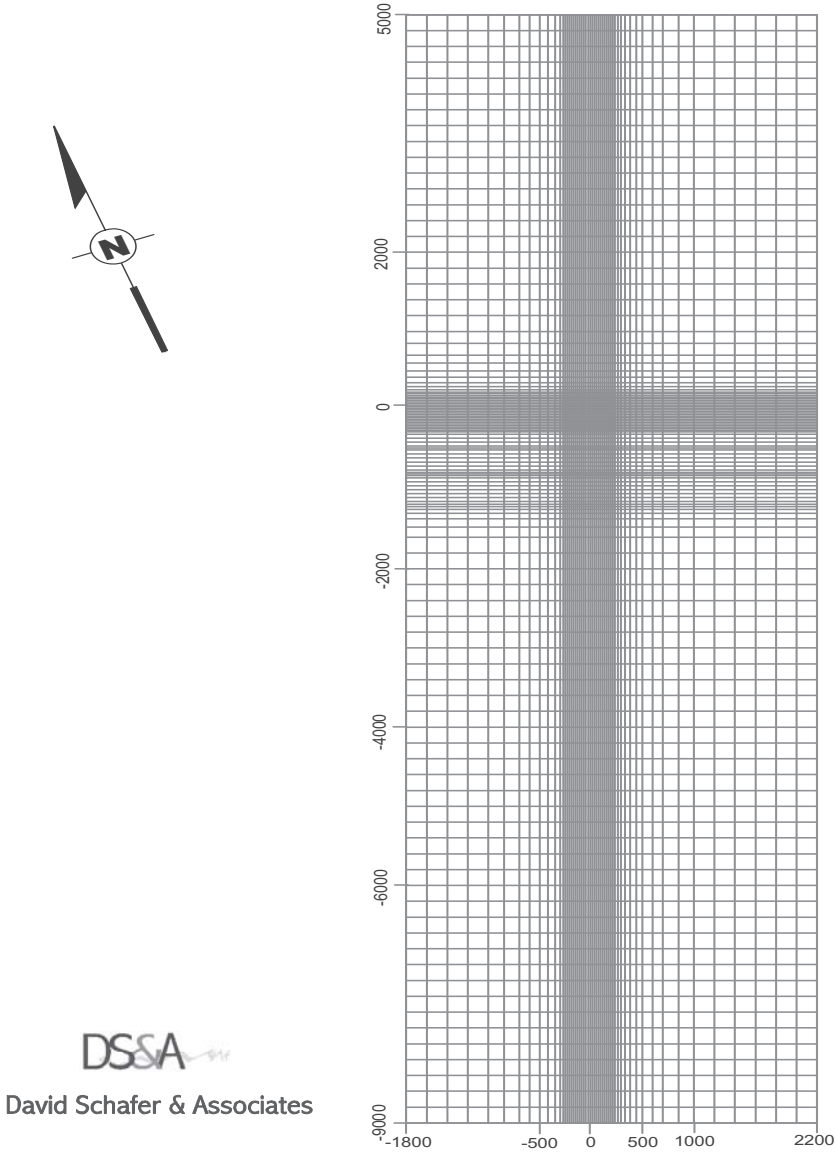

Figure 6. Grid Layout Used in Finite Difference Model

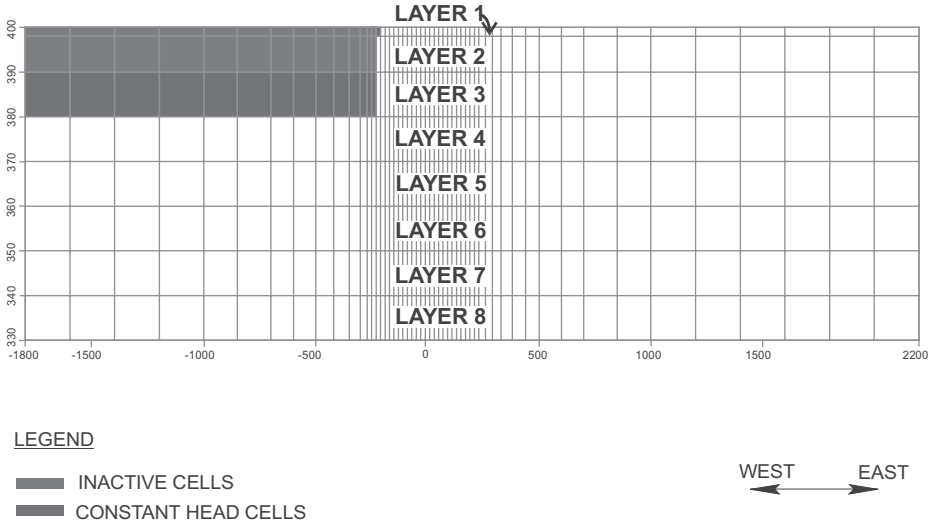

Figure 7. Layers Used in Finite Difference Model

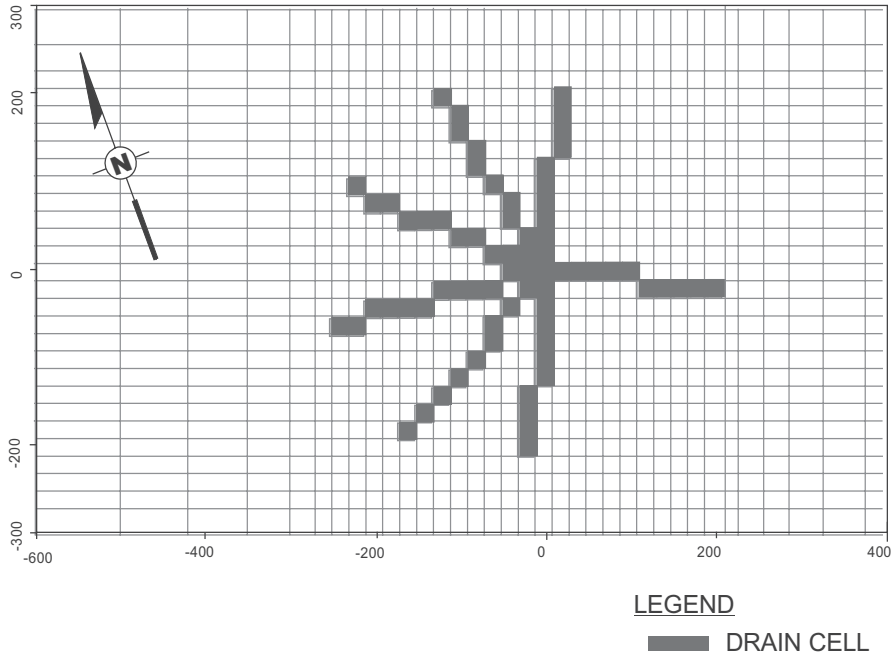

Figure 8. Drain Cells Used to Simulate Collector Well Laterals

head value and an assigned conductance term (expressed as area per unit of time), which represents the ease with which water passes from outside the drain cell to inside the drain.

Figure 9 shows an artistic rendering of what the cone of depression around the collector well looked like at the end of the pumping test. Drawdown occurred not only in the aquifer onshore, but also in the sediments beneath the Ohio River.

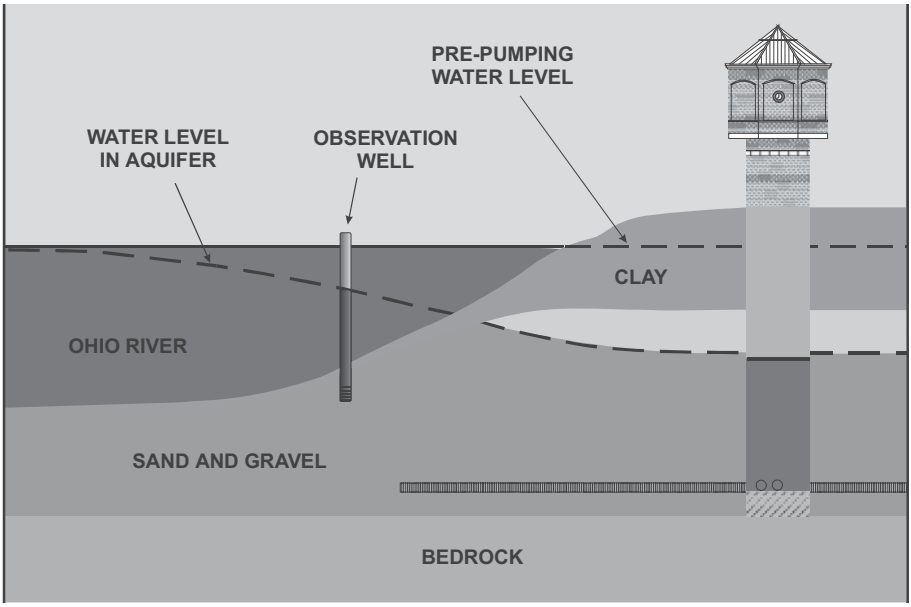

Figure 9. Initial Well Operation

The model was calibrated to the pumping test data by adjusting the variable parameters mentioned above. In this process, homogeneous aquifer conditions were assumed, i.e., a single conductivity value, because there was insufficient spatial data to justify multiple conductivity values (hydraulic conductivity zonation).By varying these parameters, it was possible to achieve an accurate calibration as shown on Figure 10. This figure shows a bivariate plot of observed versus simulated drawdown. In a perfect match, all of the plotted data points would fall directly on the straight line shown on the graph. As indicated, the simulated drawdown values matched the actual values nearly perfectly, with an error of only 1 percent of the range in water levels spanned by the data points. Calibration parameters for October 1999 water temperatures included a hydraulic conductivity of 390 feet per day, a leakance of 2.35 inverse days and a vertical anisotropy ratio of 3:1. The

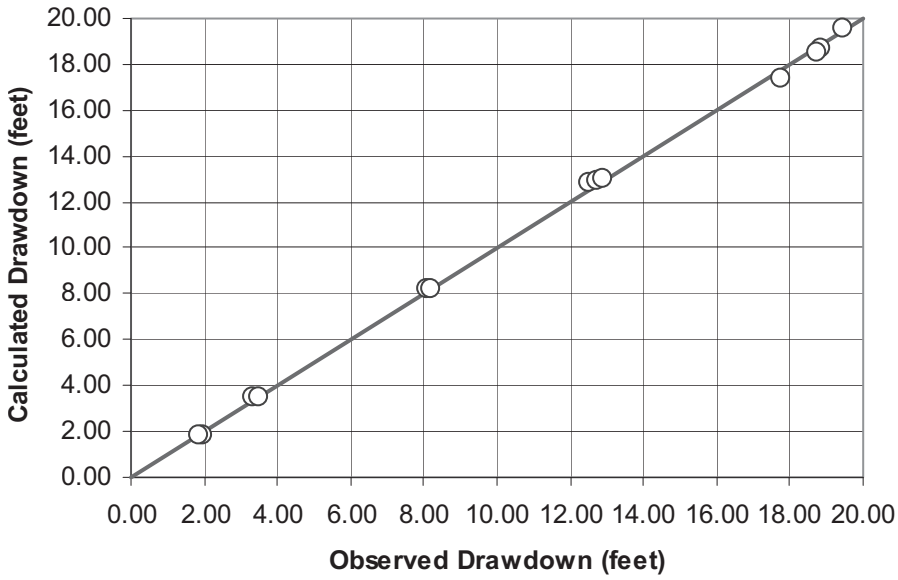

Figure 10. Observed and Calculated Drawdown

calibrated model was used to project yields of various proposed extraction facilities for the site.

4. YIELD PROJECTIONS

The calibrated model was run for various extraction facility designs and water temperatures to predict yields that could be obtained from the Payne Plant site via riverbank filtration. Figure 11 shows one such design in which the existing well would be retrofitted with additional laterals and two additional wells would be constructed on 800-foot centers adjacent to the existing well. Simulations also were run for a four-well system spanning a greater length of shoreline. It was possible to simulate various combinations of river water and groundwater temperatures by applying temperature correction factors to the model inputs, such as hydraulic conductivity, leakance, and drain conductance.

Figure 12 shows another extraction design that was under consideration at the time in which a large diameter tunnel would be excavated through the base of the sand and gravel aquifer and screen laterals would be installed beneath the river from within the tunnel.

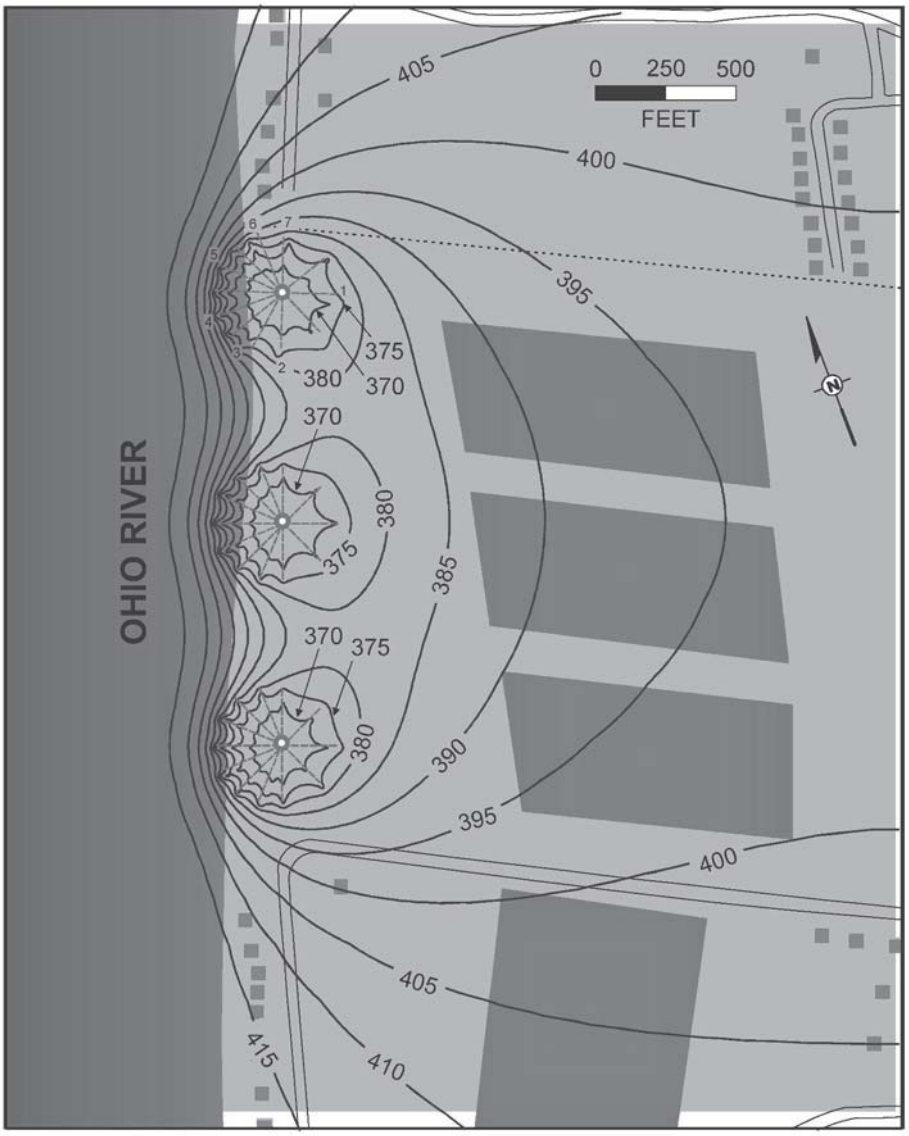

Figure 11. Model Predictions for Multiple Collector Wells

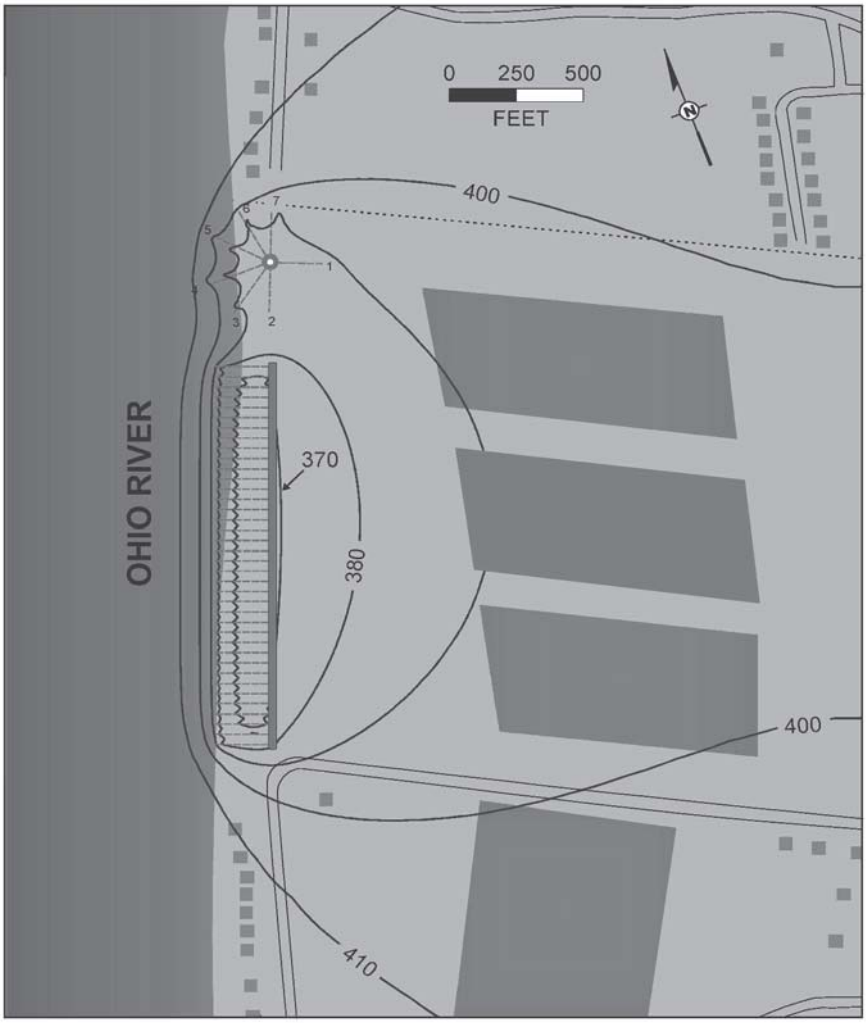

Figure 12. Model Predictions for Tunnel and Lateral System

Figure 13 shows the extraction system design that was ultimately chosen for the project. It incorporated 31 conventional vertical wells spanning about 6000 feet of shoreline. To minimize aesthetic impacts to the beautiful landscape along river, the design called for capping the wells flush with the ground surface and connecting them to a pumping plant via a subterranean tunnel constructed in the shale/limestone bedrock beneath the aquifer. Figure 14 shows a section view, looking toward the river, of the bedrock

tunnel and vertical well system. Figure 15 also shows a section view, but looking upriver, in the direction of the tunnel alignment

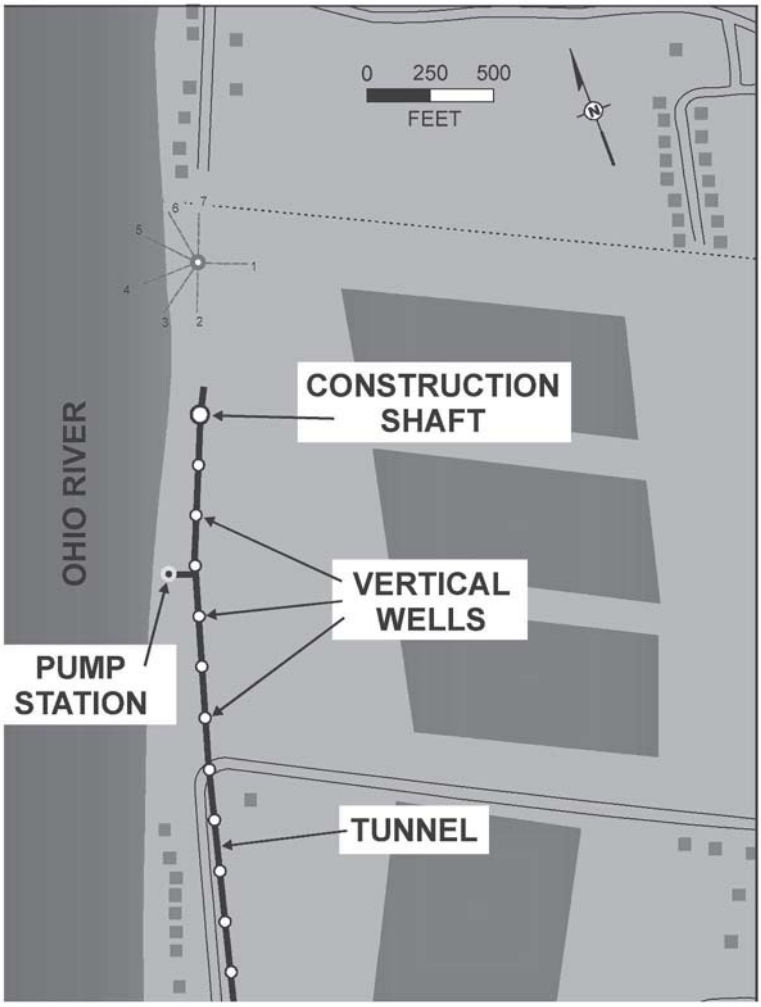

Figure 13. Vertical Wells Connected by Hard Rock Tunnel

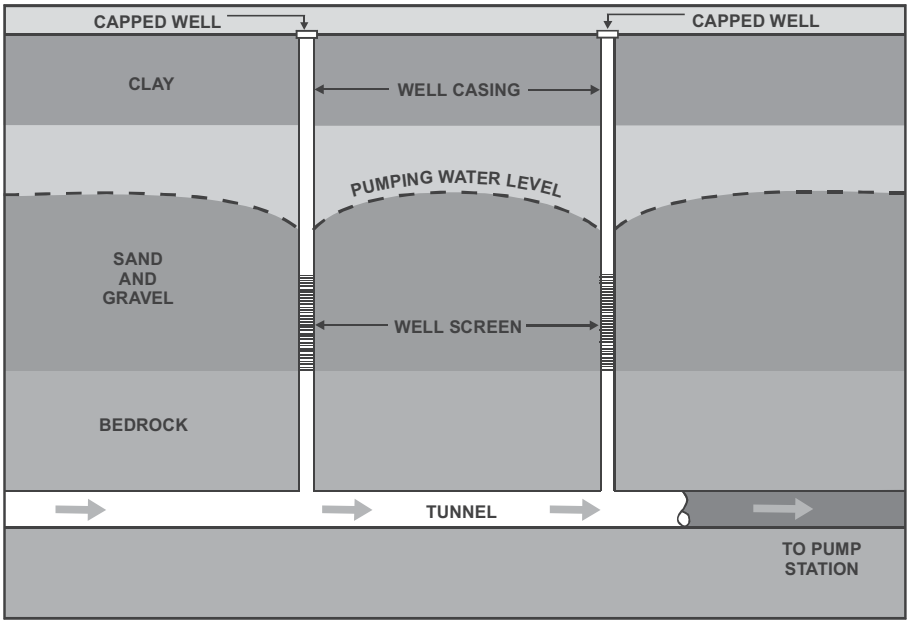

Figure 14. Vertical Wells Connected by Hard Rock Tunnel (Looking Toward the River)

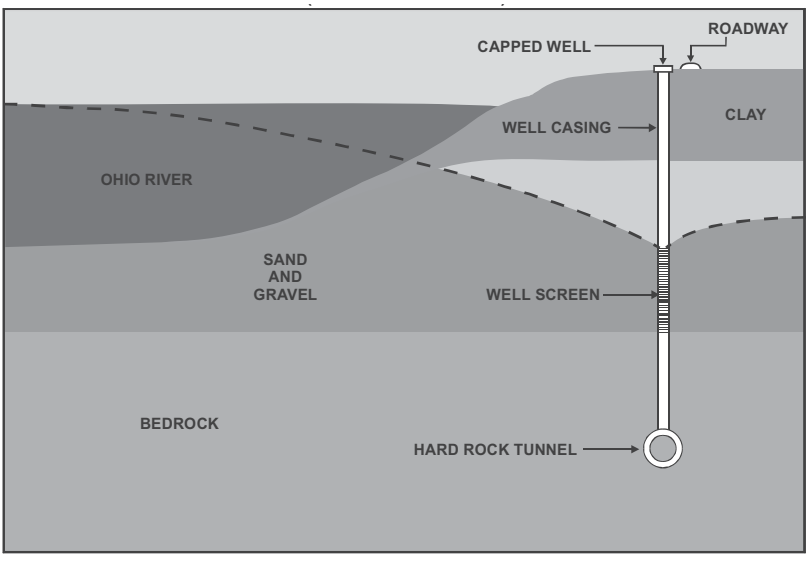

Figure 15. Vertical Wells Connected by Hard Rock Tunnel (Looking Upstream)

5. CHANGING HYDRAULIC CONDITIONS IN THE RIVERBED

Following the conclusion of the pumping test, the collector well was operated steadily, providing a portion of the water demand for the Payne Plant. After several months, a decline in well production was detected based on a reduction in specific capacity beyond what could be explained based on water temperature reduction alone.

Preliminary analysis suggested that the cause of the reduction was probably related to reduced leakance between the Ohio River and the aquifer rather than clogging of the screen laterals. To confirm this, another pumping test was conducted for three days in late March 2000. Data from this test were used to re-calibrate the computer model to determine the cause of the reduced yield. Calibration confirmed that there had been a significant reduction in leakance from the river to the aquifer. It was assumed that infiltrating river water had caused clogging of the riverbed sediments, as well as compaction of the aquifer, resulting in a reduction in hydraulic conductivity of the uppermost portion of the aquifer beneath the river.

Figure 16 shows how operation of the well induces flow of river water into the aquifer, carrying with it the solids normally suspended in the water. Buildup of these solids on the riverbed could reduce the hydraulic conductivity of the upper layer of riverbed materials, thus reducing the leakance.

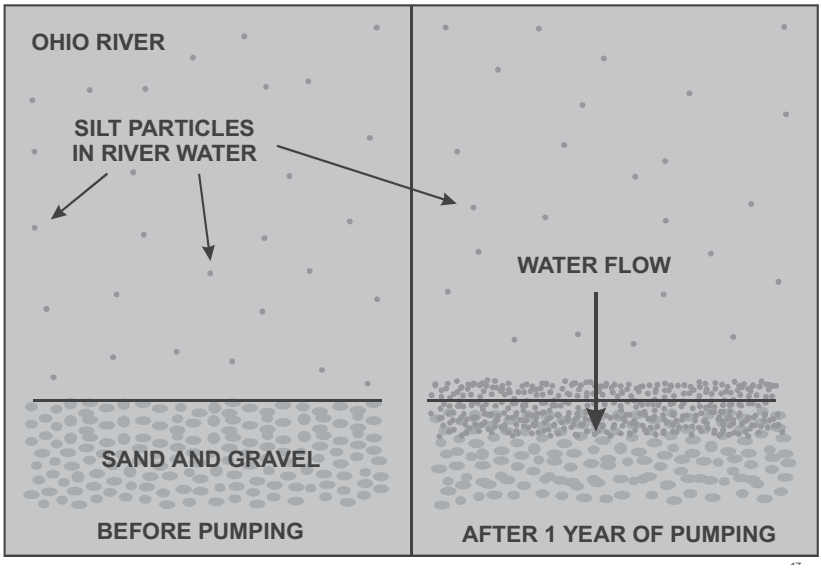

Figure 16. Build-up of Silt on the River Bottom

It is expected that the greatest reduction in riverbed conductivity would be near the well initially, as shown on Figure 17. Clogging of the sediment near the well would then force more water to enter the aquifer at a greater distance from the well, exacerbating clogging at greater and greater distances. It is expected that the clogged zone would grow over time.

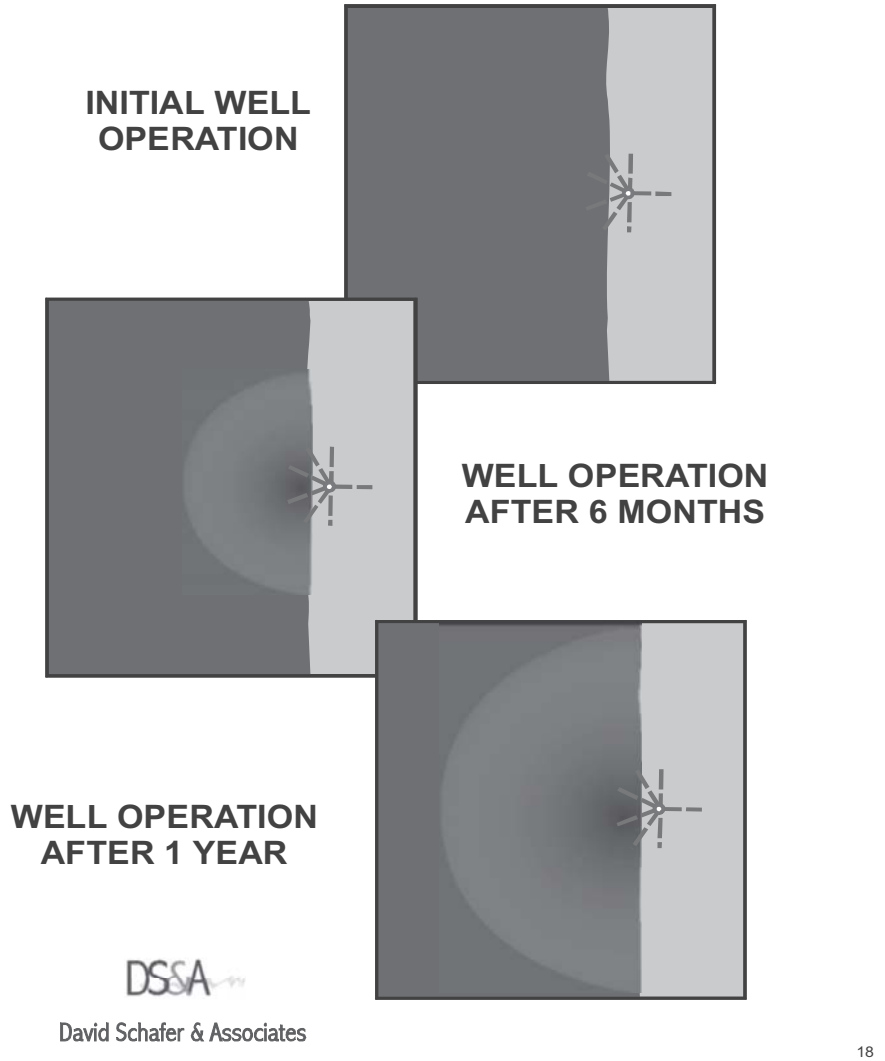

Figure 17. Aerial View of Silt Build-up

The effect of reduced river leakance is increased drawdown. Figure 18 compares the original cone of depression around the collector well to a new,

deeper cone of depression that has resulted from reduced hydraulic conductivity of the riverbed sediments. Note that as the cone of depression expands, the area of dewatered sediments beneath the river increases, further restricting water entry into the aquifer because of the degradation in permeability of partially saturated sediments compared to fully saturated sediments. The ultimate effect of the increased drawdown is increased interference among multiple wells, eventually limiting the quantity of groundwater that can be pumped.

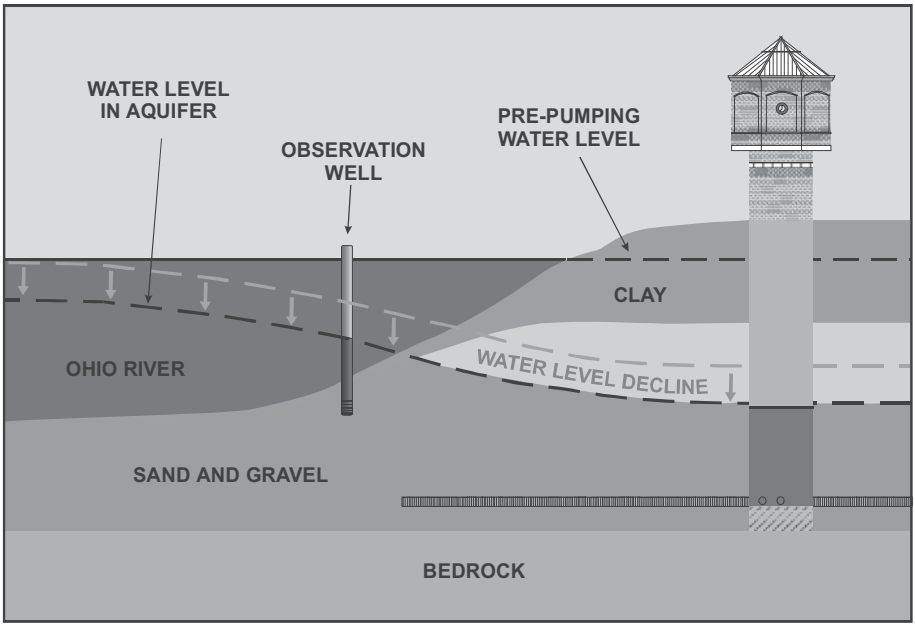

Figure 18. Well Operation after 1-Year

As the Louisville Water Company pilot collector well has continued operation, there has been regular monitoring of the pumping rate, drawdown and water temperature to track the pumping performance and riverbed conditions. The river leakance has been evaluated by computer modeling of the pumping performance at regular intervals. Figure 19 shows the results of the leakance evaluations. As shown on the graph, the greatest leakance reductions occurred during the first year of operation. Over the next two years of operation, the rate of leakance reduction was substantially less.

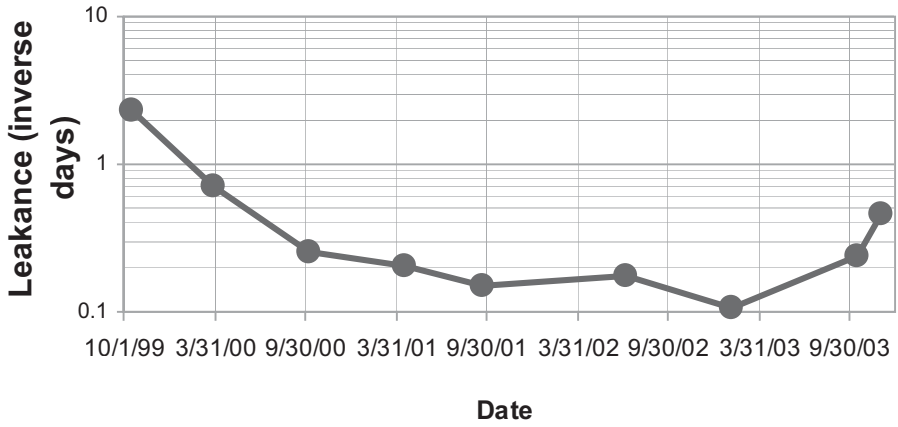

Figure 19. Measured Leakance Values Corrected to 68 Degrees Fahrenheit (October 1999 River Temperature)

Finally, the last couple of measurements showed an increase in leakance, presumably in response to episodes of river scour that may have repaired some of the damage caused by clogging. Note that the last data point on the graph, determined from December 2003 pumping data, corresponds to a time when the Ohio River was four feet above the normal pool level. It is possible that riverbed scour associated with this higher than normal flow in the river may have allowed a transient improvement in performance, greater than what is generally observed at normal pool level.

As time goes on, operation of the pilot well will continue with regular monitoring of the pumping rate, drawdown and water temperature to see if pumping performance stabilizes or continues to change over time. The data collected will help identify the range of river leakance values that may be expected during long term operation of the extraction facilities.

CHANGES IN RIVERBED HYDRAULIC CONDUCTIVITY AND SPECIFIC CAPACITY AT LOUISVILLE

Stephen A. Hubbs
WaterAdvice Associates, 3715 Hughes Road, Louisville, KY USA stevehubbs@bellsouth.net

Abstract: The Louisville Water Company constructed a 76,000 m^3/day capacity radial collector well and started pumping from the alluvial aquifer in July, 1999. After start-up, the specific capacity of the wellfield was measured to be much greater than was predicted during the design phase, and after one year of pumping additional riverbank filtration (RBF) capacity was planned using these higher estimates of specific capacity. Subsequent years of pumping indicated a steady decrease in specific capacity, and designs for additional RBF capacity was adjusted based on more reliable estimates of long-term sustainable yield. This paper reviews the data collected from this site, provides calculations of specific conductance over a 5 year period, and interprets data into values for riverbed conductivity at start-up and after 5 years of operation.

Key words: Riverbank Filtration, RBF, scouring, clogging, hydraulic conductivity

1. INTRODUCTION

The Ohio River Valley was formed as glaciers retreated during the Ice Age, leaving rich deposits of well-sorted sands and gravels in a limestone bedrock channel. The RBF facility at Louisville is constructed on the Ohio River 450 kilometers upstream of its confluence with the Mississippi river. The river channel at this site is 600 meters wide and averages 10 meters deep. The aquifer is approximately 25 meters thick and 2 kilometers wide, and is overlain with approximately 6 meters of fine material. The river channel itself penetrates the top 6 meters of the sand and gravel aquifer, and

Stephen A. Hubbs (ed.), Riverbank Filtration Hydrology, 199–220.

the entire riverbed is exposed to the aquifer. (This site is also described in Chapters 8 and 14)

The flow in the Ohio River is managed through a series of dams along its entire length, and except during periods of high flow the pool at Louisville is maintained at an elevation 128 meters above mean sea level (amsl). Bank-full flows of approximately 6 meters above normal pool occur at a frequency of about once every four years. The 100 year flood is estimated at 138 meters amsl, and the flood of record occurred in 1937, cresting at 140 meters amsl, 12 meters above normal pool. The daily stage hydrograph is shown in Figure 1 for the water year 1999 through 2004.

The average daily flows for the Ohio River at Louisville are provided in Figure 2 for the period 1991-2001. Figures 1 and 2 show that the Ohio River is characterized as a large, stage controlled river with occasional stage increases above pool. The flow hydrograph compared to the stage hydrograph illustrate the independence between flow and stage, except during conditions of high flow. Because of the artificial impact of the dams on river stage, the flow hydrograph better depicts the characteristic of the river with relation to RBF systems, particularly when considering sediment transport and riverbed scour.

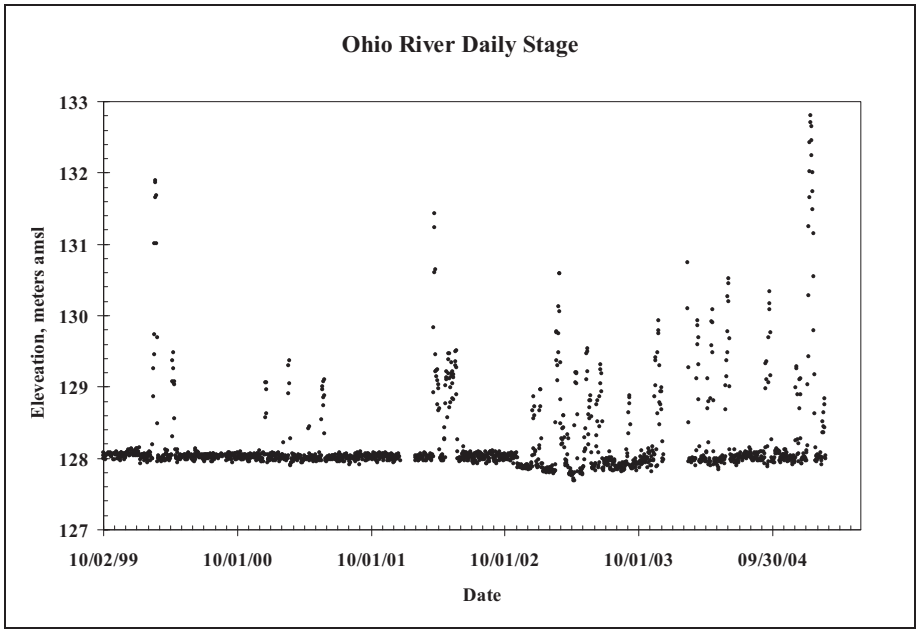

Figure 1: Stage Hydrograph-Ohio River at Louisville: 1999-2004

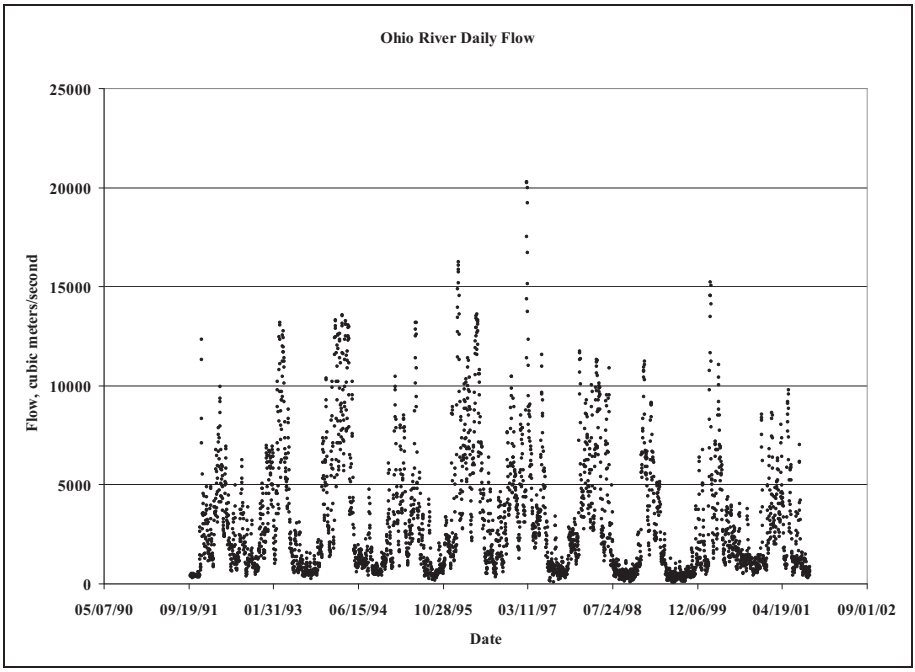

Figure2. Flow Hydrograph-Ohio River at Louisville, 1991-2001

Characteristics of the sediments in the stream and streambed are provided in Figure 3. Data for the sediment load in suspension and in the riverbed are provided for typical flow conditions. These data characterize the Ohio River as highly turbid stream with a fairly consistent riverbed media of medium to fine sand. Very little cobble is found on the riverbed at the site of this riverbank filtration system. Those areas of the stream characterized by lower streambed scouring velocities (backwaters and shallow areas) are typically associated with smaller sediment sizes.

Aquifer characteristics for this site are described in Chapter 14 (Caldwell). The site is characterized as having high hydraulic conductivity (125 m/day) with a highly transmissive layer towards the bottom of the aquifer. This formation is typical of many of the glacial outwash aquifers in the Midwest United States. A plan and profile view of this system is provided by Schafer in Chapter 8 and by Wang (2002).

Water quality characteristics of the river at this RBF site are also provided in Chapter 14 (Caldwell). The Ohio River is characterized as a stream impacted by industrial, agricultural, and human populations, with over 25 million people living in the watershed. Water quality in the Ohio River, however, is fairly good as a result of the efforts over the past 50 years of the Ohio River Sanitation Commission (ORSANCO). Most municipal

wastewater receives secondary biological treatment before discharge (storm flow bypass does not always receive biological treatment). The TOC is in the range of 2.5 to 3.5 mg/l, and there has been no indication of biological clogging at this site.

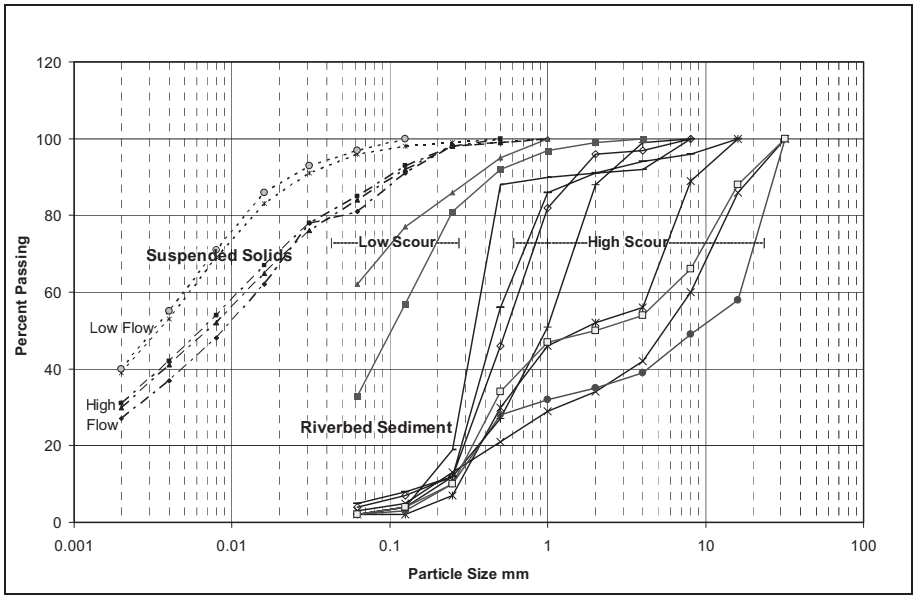

Figure 3. Stream sediment characteristics for the Ohio River at Louisville

A unique feature of the RBF site at Louisville is that it is immediately downstream of a small stream entering the Ohio River. Sediment from this stream has apparently accumulated in the riverbed approximately 60 meters upstream of the well, which causes a flow separation in the river during moderate flow conditions. This flow separation occurs approximately 30 meters from the bank, and dissipates approximately 300 meters downstream. It is characterized by a standing wave approximately 60 meters from the bank, and a reversed flow direction (upstream) at the bank. Sediment deposition and in the slack water of this flow separation has resulted a shallow riverbed (0.6 meter or less) extending as far as 15 meters from the bank. The riverbed in this area is subject to change depending on the stream flow regime. Between 1999 and 2004, portions of the riverbed have varied as much as 2 meters in depth, indicating significant erosion and deposition in the riverbed adjacent to the well. (Unthank, 2005) The bulk of the riverbed adjacent to this site, however, experiences only modest changes in streambed elevation with time.

2. CHANGES IN SPECIFIC CAPACITY WITH TIME

Specific capacity is defined as the discharge flow of a well divided by the drawdown (cubic meters/day/meter of drawdown). Factors that impact the drawdown and discharge of the well include riverbed infiltration characteristics, aquifer transmissivity, wellscreen dynamics, and temperature. The seasonal and annual variation in specific capacity at this site has been described for the period 1999-2003 by Hubbs (2004). This work showed a significant seasonal variation in specific capacity coinciding with temperature cycles, and an annual decreasing trend of riverbed conductivity over time.

Figure 4 provides the calculated values for specific capacity from the beginning of pumping through 2004 for the well at Louisville. Data were unavailable for the period of February 2002-October 2002 due to a loss of computer-generated data. From November 16, 2003 through April 9, 2004 flow from the well was reduced from 64,000 m^3/day to 38,000 m^3/day as the result of a pump failure, coinciding with an apparent increase in specific capacity. The well was out of service for repair from April 15 through July 28, 2004. On April 15 2004 the river experienced a sharp flood wave, cresting 2.5 meters above pool on April 19 and returning to normal pool on April 23 Upon re-start of the well July 28, 2004 at full capacity of 64,000 m^3/day another increase in specific capacity was observed. (See Figure 4).

The higher values of specific capacity observed from August 2004-December 2004 are likely the result of riverbed surface renewal during the flood event when the well pumps were off. The aquifer was charged with colder water prior to well shut-down in April 2004, which would have been expected to have a negative impact on specific capacity values upon start up. Specific capacity for this system appears to have stabilized between 5000 and 7000 cubic meters/meter/day at a typical flow of 64,000 m^3/day.

The annual decrease in specific capacity observed during the first 4 years of operation was assumed to be a function of riverbed clogging with sediment from infiltrated water. This annual decrease was well represented statistically as function of the natural log of time from initiation of pumping, with the magnitude of the decrease in specific capacity diminishing with time (Hubbs, 2004). The impact of streambed scour as a restorative agent was observed, and the impacts of decreased riverbed hydraulic conductivity with time and restorative impacts of scour appeared to balance after about 4 years.

Scour velocities at this site have been discussed in Chapter 2 (Hubbs), and compared to other RBF sites in Chapter 14 (Caldwell). Scour shear stresses of 5 Newtons/square meter can be expected to occur several times in a typical year at this site. Such scour stresses are capable of transporting fine

to medium gravel (Julien, 1998). This is consistent with the composition of the riverbed, which includes coarse sand and fine gravel (USGS 2004).

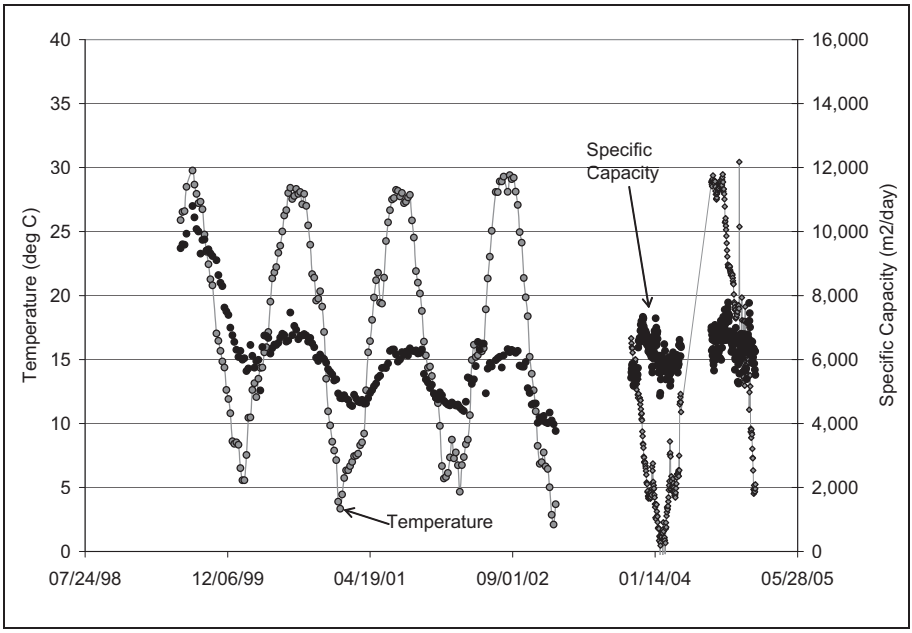

Figure 4. Variation of Specific Capacity with Time and Temperature

3. CHANGES IN PIEZOMETRIC SURFACE: WINTER AND SUMMER

Since the initiation of pumping in the summer of 1999 and through 2004 data were collected from piezometers placed in the riverbed immediately over the end of lateral collector L4 (Figure 5). The original installation included three Geokom model 4500 vibrating wire piezometers placed approximately 0.6 meter (P39), 1.5 meters (P38), and 2.7 meters (P37) below the riverbed. These probes provided data on the pressure and temperature in the aquifer. The probe 1.5 meters below the riverbed failed in the winter of 2001, but the remaining two piezometers continued to operate through the duration of this study.

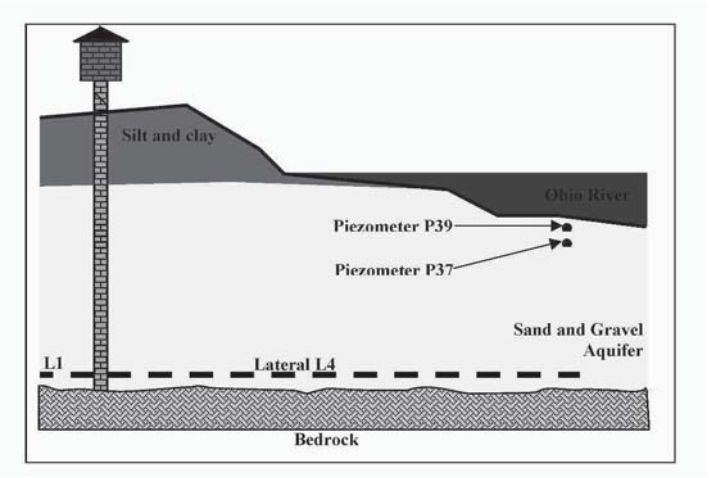

Figure5. Location of Piezometers in relation to lateral L4

In the summer of 2002 additional pressure and temperature transducers were set in the riverbed perpendicular to the bank at distances approximately 120, 200, and 275 meters from the well (Figure 6). The probes were set approximately 1.5 meters below the riverbed, and were functional for only a short period of time, becoming disabled with the flood event in the spring of 2003. These probes allowed the shape of the piezometric surface under the river to be measured under various river conditions.

Data from these probes are presented in the Figure 6. Of particular interest is the location of the piezometric surface in conjunction with the shape of the riverbed. During warm weather conditions, the piezometric surface intersects the riverbed surface approximately 67 meters from the well. During cold weather conditions, however, these two surfaces intersect as far as 90 meters from the well. If the piezometric surface drops slightly lower than shown in Figure 6, the intersection of these two surfaces could extend out as far as 120 meters from the well.

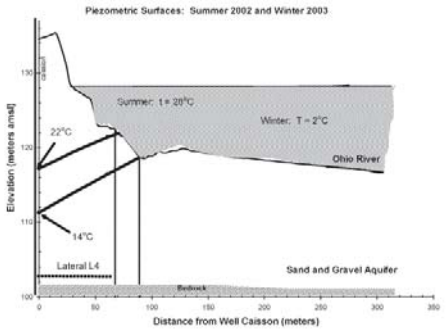

Figure 6. Piezometric Surface: Summer and winter

4. 1999 AND 2004 PUMP TESTS

Pump tests were conducted in June 1999 during the initial start-up of the RBF system, and July 2004 after the system had been idle for a period 4 months. High-frequency data collection extended for several weeks during these tests. Data were used to evaluate piezometric surfaces and estimate hydraulic conductivity of the riverbed.

4.1 Start-up Pump Test, June 1999

Data from the initial start-up was used to estimate initial travel velocities across the riverbed and through the aquifer as a part of an investigation into water quality changes occurring in the RBF process (Wang, 2002). These data were re-analyzed to provide estimates of riverbed hydraulic conductivity in the riverbed prior to the influence of clogging. Data used in this evaluation are presented in Figure 7. These data for pressure and temperature were used to estimate the vertical velocity component and headloss across the distance traveled to yield a unit headloss. The velocity was estimated as the time required to reach the midpoint of the temperature breakthrough curve.

4.2 Start-up Pump Test, July 2004

The collector well was shut down from April through July 28, 2004 for maintenance. This four month period of idle allowed a temperature difference between the aquifer and river to re-establish, and the pump test of June 1999 was repeated. The results, however, were strikingly different, as is illustrated in Figure 8. The temperature breakthrough curve at 2.7 meters below the riverbed indicated that the conditions controlling the velocity of water in 1999 had changed significantly in 2004. Similar to the pump test in 1999, the majority of the head loss occurred in the first 0.6 meter of the riverbed. The head loss after 48 hours of pumping was approximately 3 meters greater in 2004 that in 1999.

5. DIRECT FLUX MEASUREMENTS IN THE RIVERBED

Direct measurements of the flux rate in the riverbed were taken with a seepage meter designed for use in deep rivers. The device included a weighted round steel hood with an area of 0.093 m^2, with an attached hose allowing a bladder to be connected at the river's surface.

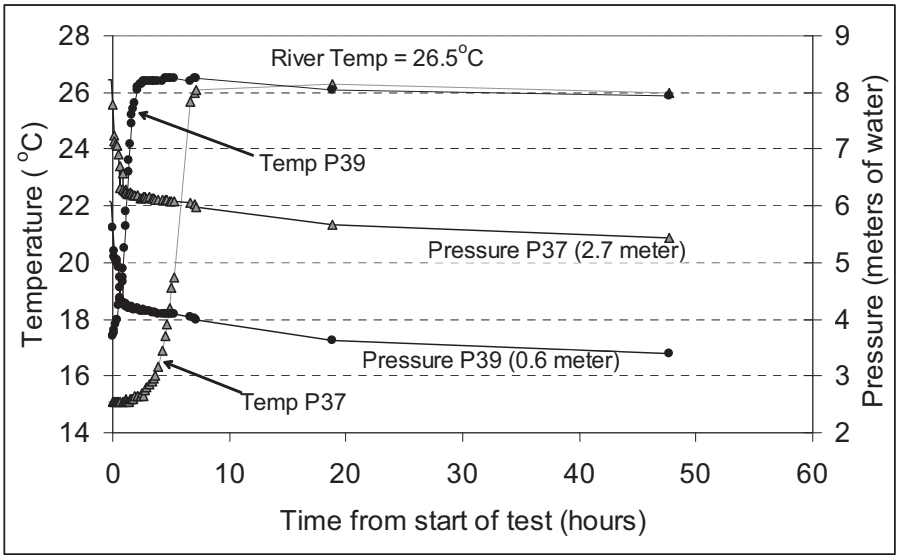

Figure 7. Pressure and Temperature versus time, initial pump start-up June 1999

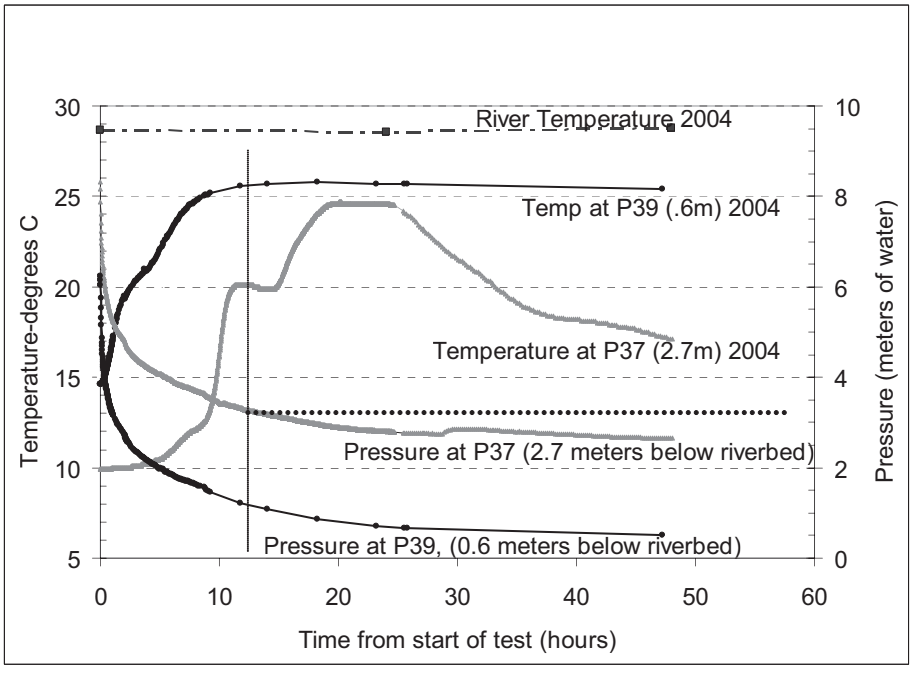

Figure 8. Pressure and Temperature versus time, July 2004 pump test.

This device worked adequately in depths up to 10 meters. The accuracy of the measurement was significantly impacted by river velocities, wind action, and waves. Under ideal conditions (river velocity under 0.3 meter/hour, low wind, and no waves), reproducible data were obtained. As conditions deteriorated, so did the quality of the data obtained. A camera attached to the device allowed observation of the integrity of the seal between the device and the riverbed during the monitoring process.

Initial data taken in the summer of 2003 with a prototype device indicated that discharge velocities as high as 0.3 meters/hour might be expected in zones of high infiltration. These values were considerably higher than those measured in 1999 using the temperature profile technique. Assuming an aquifer porosity of 0.2, the maximum discharge velocity measured at the location of the probes in 1999 was 0.1 meter/hour. It is noted that the direct flux measurements were taken at a point where infiltration was believed to be high based on information on the riverbed hardpan from a diver and piezometric data.

Data taken during August, 2004 are presented in Table 1. The monitoring locations are presented as distance from the well perpendicular to flow, with the exception of the location at 127 meters, which was 75 meters downstream of the well. Pumping rates were held constant at about 17 MGD throughout the monitoring period. River conditions were acceptable on some of the days of monitoring and marginal on others. The data presented represent those data felt to be the most reliable, based on multiple measures at the same point, and are believed to best represent the riverbed flux rates for the given monitoring point. A limiting condition for the riverbed flux measurement was the erosion of the seal between the monitoring device and the riverbed. Under higher river velocities, the sand around the upstream face of the monitoring device would gradually erode away, exposing the inside of the hood directly to the stream. This resulted in a gradual decrease in measured flux rate with time, to a point of no measured flux. Thus the data were scrutinized, and data that were believed to have been influenced by the erosion of the seal were not included in the averages presented below.

Data from several other monitoring locations were either very low, or no seal could be obtained between the riverbed and the device. These data are not presented in Table 1.

A deliberate attempt was made to locate the point of highest flux in the riverbed, and the data indicate that under the conditions existing in August 2004, this point was between 146 and 175 meters from the well, perpendicular to the riverbed at the location of the well. This location was beyond the area where the hardpan was observed by the diver and beyond the point where unsaturated conditions under the riverbed were indicated.

Table 1. Direct riverbed flux measurements, August 2004. (1)-This point is 75 meters downstream of lateral L4.

Radial distance from well, meters	Discharge velocity, meters/hour
127 (1)	0.0
146	0.23
150	0.82
175	0.55
183	0.23

In conjunction with the flux measurements taken above in late August, 2004, an attempt was made to characterize the hardness of the riverbed. In August 2002 a diver had probed the riverbed with a knife and identified the hardpan as extending as far as 150 meters from the well. This hardpan was assumed to be the response of the riverbed to unsaturated conditions below. This hardpan was also indicated by "blow counts" from the setting of temporary piezometers in the river.

6. EVALUATING UNSATURATED CONDITIONS UNDER THE RIVERBED

A review of data from probes P37 and P39 indicated that the pressure in probe P39 (0.6 meters below the riverbed) very closely followed the pressure in P37 when adjusted for the 2.1 meter difference in elevation between the two probes, except when the pressure in P37 dropped below 2 meters of water. The vibrating wire piezometers used in this study were capable of measuring negative pressures, and thus if the water column between P39 and P37 remained saturated, a negative pressure would be expected whenever the pressure in P37 dropped below 2.1 meters of water. Conversely, unsaturated conditions would be indicated if the pressure in P39 was near atmospheric pressure whenever P37 dropped below 2.1 meters of water.

Data from July 2004 through December 2004 were analyzed to examine the difference in pressures between P37 and P39 (Figure 9). The x axis in this figure represents the pressure at the lower probe (P37), and the y axis represents the difference in pressure between the two probes. The difference in pressure between these probes would be expected to be nearly constant (approximately 2.1 meters of water) when the aquifer was saturated, and would be expected to be a function of the piezometric surface at P37 if the aquifer in the area of the upper probe (P39) became unsaturated. The change in correlation of the pressure differential between P39 and P37 at the point where the potentiometric surface dropped below the elevation of P39 (pressure at P37 less than 2.1 meters of water) indicated that the aquifer at probe P39 had become unsaturated.

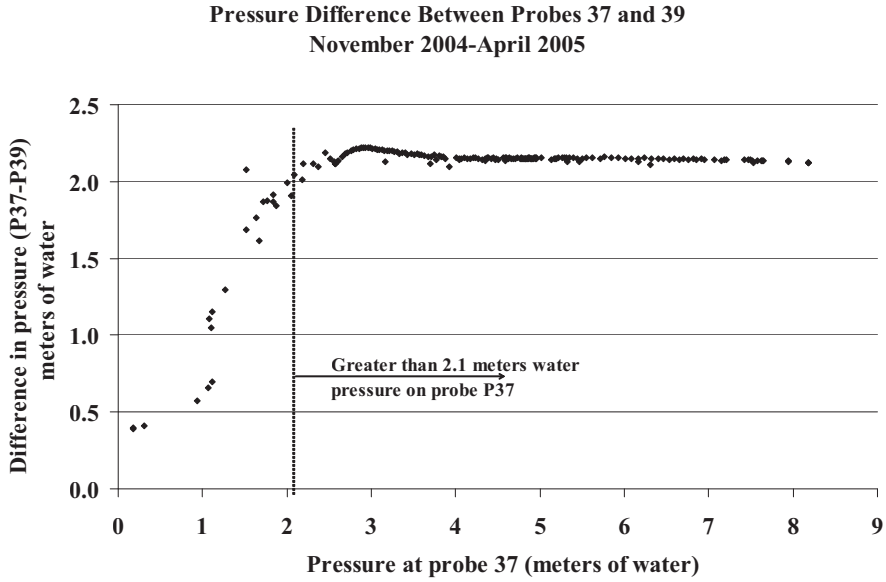

Figure 9. Pressure difference between piezometers P37 and P39 as a function of pressure at piezemeter P37.

Pumping conditions were controlled in May 2005 to further investigate the transition that occurs when the pressure at probe P37 approaches 2.1 meters of water and the pressure at P39 approaches atmospheric pressure. Pumping was adjusted initially to establish a slowly declining pressure at P37 between 2.2 and 2.0 meters of water, followed by an increase in pumping adequate to drop the pressure in P37 to approximately 1 meter of water. Pressures in both probes were closely monitored during a period of 4 days. These data are presented in a time series in Figure 10.

It is noted that probe P39 shows a negative pressure as the water level drops below 2.1 meter in probe P37. Over a span of two days, however, this negative pressure tends to increase towards atmospheric pressure despite the continued decrease in pressure at P37. At mid-day May 15 the pumping rate was increased approximately 7000 m^3/day to drive the potentiometric surface even lower. The initial response was that the pressure at both P37 and P39 dropped; however, after approximately 4 hours the pressure drop in P39 stopped, and reversed with a trend towards atmospheric pressure despite the continued drop in pressure at P37.

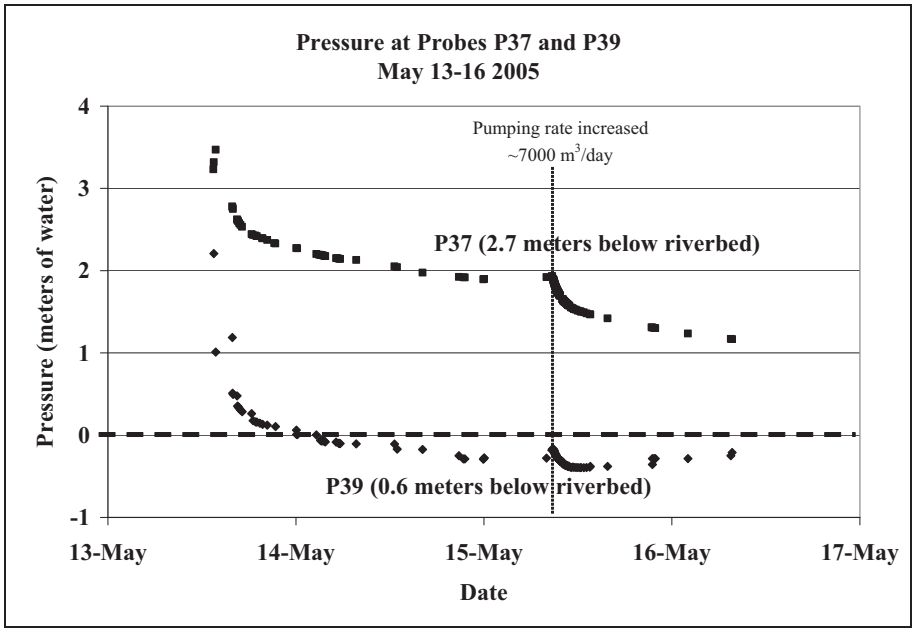

Figure 10. Transition between saturated and unsaturated conditions.

These data are considered supportive of the hypothesis that under conditions when the total head measured in the aquifer drops below 122 meters amsl (approximately 2 meters of water pressure head at P37), the aquifer at probe P39 becomes unsaturated, and the total head at P37 represents the piezometric surface in the aquifer under the riverbed.

7. INDIRECT MEASURE OF RIVERBED HYDRAULIC CONDUCTIVITY

Data from the initial start-up of the well in 1999 and the repeat of this test in July 2004 were used to estimate riverbed hydraulic conductivity by estimating velocity into the riverbed using temperature as an indicator. This technique provided a measure of the vertical velocity component in the aquifer, which was then adjusted by porosity to provide an estimate of the discharge velocity (or Darcy velocity). This technique can provide an accurate in-aquifer measure of vertical velocity, but can only be used when there is a significant temperature difference between the river water and the aquifer water at the point of measurement. These conditions typically exist at the beginning of system pumping, or after a several month period of no pumping.

This technique also requires the water velocity in the aquifer be primarily vertical in order to determine the length of the flowpath for determining velocity. If the flow velocity has a significant horizontal component, the result will be an underestimation of the flow path, and thus an underestimation of the fluid velocity. Thus, assuming that all flow is in the vertical direction will result in the computation of a minimum value for riverbed hydraulic conductivity; any deviation from this assumption would result in the calculation of a higher value of hydraulic conductivity.

Hydraulic conductivity was calculated according to Darcy's equation as follows:

$$K_{rb} = (\text{flowpath distance/time})(\text{flowpath distance/headloss})$$

where time was measured at the mid-point of the temperature breakthrough curve, flowpath distance was the distance between the riverbed and the probe, and the headloss was measured as the difference between total head at the riverbed (river surface elevation) and the total head measured at the probes.

Given the above assumptions and limitations, data from June 1999 and July 2004 were used to estimate riverbed hydraulic conductivity. Prior to the 2004 test, the pressure of each probe and the difference in pressure between the two probes were compared to readings for similar non-pumping conditions and river level in 1999, and were found to be remarkably consistent over the 5 year period of in-situ use (within 0.03 meter of water head over the 5-year period).

The well discharge flow rate during the June 1999 study was 76,000 m^3/day compared to 64,000 m^3/day in 2004. River and aquifer temperatures were also different in the two periods: in 1999, river temperature was 26.5^{o}C, while the aquifer temperature at 3 meters below the riverbed was 15.1^{o}C. The temperatures at these same sample locations were 28.6^{o}C and 9.9^{o}C, respectively before the start of the 2004 test. The colder aquifer temperature in 2004 was likely the result of the aquifer being charged with cold river water prior to the cessation of pumping in April 2004.

A significant scouring event occurred shortly after the well was taken out of service in April 2004, and it is likely that the riverbed over the probes was deeply scoured and fresh sediment was deposited over the area between April and July. This erosion/deposition pattern is consistent with bathemetry data from 2004 and observations from previous years.

Data used to estimate hydraulic conductivity for 1999 and 2004 are presented in Figures 7 and 8. It is noted that in 1999, the temperature at 0.6 meter and 2.7 meters below the surface reached the same temperature as the river water (26.5 ^{o}C) within 7 hours. For the 2004 data, these temperatures reached equilibrium only after 13 days.

Riverbed hydraulic conductivity values were estimated from these data. It was necessary to assume that for the very early period of initial pumping the velocity was predominantly vertical. Otherwise, the distance required to compute velocity would be unknown. This assumption was likely more valid in 1999 than in 2004.

The data from 1999 were easily interpreted, as the shapes of the temperature breakthrough profiles at 0.6 meter and 2.7 meters below the riverbed were as would be expected for a conservative tracer under non-varying conditions of hydraulic conductivity. The 1999 data indicated a mean vertical velocity of 0.46 and 0.53 meters/hour at the 0.6 and 2.7 meter depths, respectively, indicating good agreement between the two datasets.

The data from 2004, however, were distinctly different from those of 1999, with indications that the velocity through the riverbed was neither constant nor vertical during the 13 days required for temperature levels to stabilize. The data from the first 20 hours of the 2004 test were used to estimate vertical velocity, however, as these data indicated periods during which the temperature breakthrough curves were consistent and somewhat interpretable, with the flow velocity vector assumedly in a primarily vertical direction. Beyond 20 hours, the temperature breakthrough displayed trends indicative of significant changes in riverbed conductivity. The data and calculations are provided in Table 2 for riverbed hydraulic conductivity between the riverbed and the first 0.6 meter and 2.7 meters below the riverbed, for data from 1999 and 2004.

Table 2. Field data and calculations for Riverbed Hydraulic Conductivity. (1)-headloss and velocity from the first 2 hours of the pump test; (2)-headloss and velocity from hours 2 through 8 of the pump test; (3)-headloss and velocity from hours 12 through 18 of the pump test; (4)-headloss and velocity from the first 10 hours of the pump test; (5)-discharge velocity was calculated assuming aquifer porosity of 0.2. Riverbed aquifer temperature at start of test 1999 was approximately 5^{o}C warmer than in 2004. River temperature was approximately 2^{o}C colder in 1999 than in 2004.

Year	Distance (m)	Headloss (m)	Time (hours)	Headloss (m/m)	Velocity (m/h) (5)	Riverbed K (m/hr)
1999	0.6	1.87	1.30	3.07	0.094	0.031
2004 (1)	0.6	3.64	2.5	5.97	0.05	0.008
2004 (2)	0.6	4.17	5.2	6.84	0.02	0.003
2004 (3)	0.6	5.53	70	9.08	0.002	0.0002
1999	2.7	2.15	5.7	0.79	0.09	0.12
2004 (4)	2.7	4.72	10.4	1.75	0.05	0.03

The velocity data for the earlier part of the 2004 dataset are approximately half that observed in 1999. However, at approximately 11 hours after the start of pumping, temperature data indicate dramatic changes in velocity at 2.7 meters below the riverbed for the 2004 dataset. Given only

gradual changes in head, it is inferred that these dramatic velocity changes were the result of a dramatic change in riverbed hydraulic conductivity in the vertical flow path.

For comparison of changes in riverbed hydraulic conductivity between 1999 and 2004 it is felt that the earliest portions of the datasets for the 2004 data are most comparable to the 1999 data, in that they show the least indications of transient changes in riverbed conductivity. These are the data from the first 2.5 hours for the 0.6 meter depth, and the first 10.4 hours for the 2.7 meter depth for the 2004 test.

Using data for head loss between the probes P37 and P39, and the velocity estimates in Table 2, **vertical** aquifer conductivity was calculated between 0.6 and 2.7 feet in the aquifer, exclusive of the head loss in the first 0.6 meters of the riverbed. These values were 1 m/hr for the 1999 dataset and 1.5 m/hr for the 2004 dataset. These data compare favorably with the **horizontal** conductivity value of 5 meters/hour for the entire aquifer derived by Schafer (2000) using traditional pumping tests in at the site.

8. COMMENTS

8.1 Interpreting the 2004 Pump Test: the Influence of Unsaturated Conditions in the Aquifer

Figure 11 shows the temperature and head data for the 2004 test over a 3 week period, to the point where the temperature data stabilized with the river temperature. Note that the riverbed elevation at the point where the probes are located was approximately 122.5 meter amsl when the probes were set in 1999. The streambed has been modified significantly by sediment erosion and deposition over the 5 year period. The general pattern is erosion in the spring, and deposition through the remainder of the year. In June, 2004, the approximate elevation near the location of the probes was 122 meters amsl.

Interpreting the pressure head data for 2004 in relation to the depth of the riverbed at the point of measurement, the dramatic change in velocity occurs near to the time when the pressure head measured at the probes approached the elevation of the riverbed over the probes. The pressure head measured at the probes was at elevation 123 meters amsl approximately 10 hours after the start of the 2004 pump test at which time dramatic changes in the temperature breakthrough curves were observed. (See Figure 7 for greater detail). If the change in riverbed conductance was tied directly to the passage of the piezometric surface under the riverbed, then this velocity

change might have been expected to occur when the probes indicated a pressure head of approximately 122.5 meters amsl.

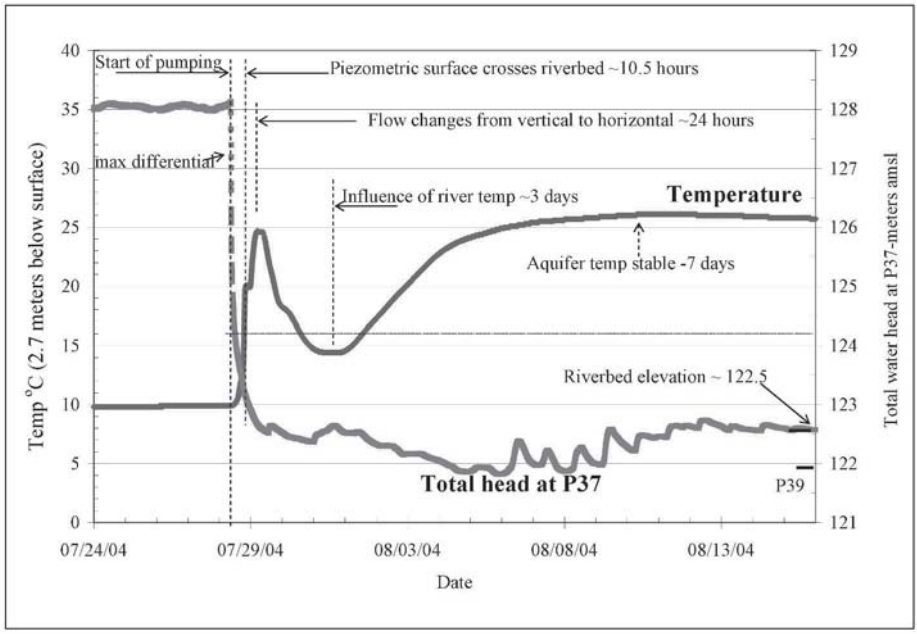

Figure 11. Pressure and head measurements during the first 4 weeks of pumping of the July 2004 pump test.

If it is assumed that changes in the temperature breakthrough curve in Figure 11 are the result of changes in riverbed hydraulic conductivity, then the shape of the curve might be explained as follows:

- From the start of the test through hour 10, the flow through the riverbed was primarily vertical, with the temperature reflecting water velocity as the river water penetrated the aquifer.
- The colder aquifer water temperature and riverbed clogging resulted in greater drawdown in the well and lower pressures in piezometers P37 and P39 compared to 1999 data.
- Between hours 10 and 11, the piezometric surface as measured at P37 and P39 dropped below the elevation of the riverbed, resulting in increased pressure on the riverbed as unsaturated conditions began to develop. The resulting decrease in hydraulic conductivity greatly decreased the vertical flow into the riverbed above the probes.

- Between hours 10 and 15, flow continued past the lower probe P37 in a vertical direction, as the aquifer above the probes drained. Very little flow was entering the aquifer above the probes.
- Between hours 15 and 24 the probe 2.7 meters below the riverbed was influenced by flow with an increasing horizontal component, as the riverbed impacted by decreased hydraulic conductivity (clogged zone) expanded.
- Between hours 24 and 72, the flow past the probe was primarily horizontal, with colder aquifer water from further away from the well passing under the clogged zone, dropping the temperature at probe P37.
- Between days 3 and 7, the temperature at probe P37 reflected the impact of river recharge from a point distant from P37. Flow was primarily horizontal, with water temperature increasing with time reflecting the impact of river temperature at the point of recharge. The temperature at P37 reflected river temperature with a lag time of approximately 7 days.

The above described scenario is possible and reasonable, given the observations from this pumping test and indications of changes in riverbed flux rates observed as a function of distance from the well.

The dramatic change in velocity during the 2004 test resulted in a calculated riverbed hydraulic conductivity of 0.001 meter/hour after 11 hours from the start of pumping, compared to 0.24 meter/hour for data from the first two hours of this test. If the correlation between the piezometric surface dropping below the riverbed surface and the change in velocity is accepted, and if it is further assumed that this change in velocity is the result of a change in the hydraulic conductivity of the riverbed, then at least two hypotheses can be presented to explain this change:

- The change in hydraulic conductivity is the result of the difference in the conductivity of the formation under saturated versus unsaturated conditions.
- The transfer from saturated to unsaturated conditions, with the accompanying increase in pressure on the riverbed, compresses the silt laden riverbed, resulting in a decrease in riverbed conductivity. This acts in tandem with the decreased conductivity resulting from the unsaturated conditions existing in the first few feet of the riverbed.

To test these hypotheses, it is necessary to know the conductivity of the formation prior to clogging with particles (the 1999 dataset), the hydraulic conductivity of the riverbed as it exists under saturated and unsaturated conditions (the 2004 dataset), and to be able to predict the impact of increased compressive forces and unsaturated flow on the conductivity of the riverbed as it existed during the 2004 test. (These forces have been discussed in Chapter 2). Testing these hypotheses against conductivity data from known media will be the subject of future research.

8.2 Measures of Riverbed Hydraulic Conductivity

The accuracy of measures of riverbed hydraulic conductivity using temperature as an indicator are subject to assumptions made regarding flow direction, accurate depth measurement between the probes and riverbed, and accurate measures of pressure and temperature. The assumption of vertical flow is acknowledged as being violated shortly after the start of pumping as the cone of depression is developed and the piezometric surface dips towards the well. As flow varies from vertical to having a horizontal component, the affect would be to underestimate the length of the flow path between the riverbed and the point of measure, thus underestimating the velocity. Noting the relatively flatness of the piezometric surface under typical operating conditions (measured at a slope of approximately 1/20 horizontal/vertical at the location of the probes), the magnitude of the vertical head loss (up to 6 meters loss per meter of vertical travel), and the similarity between the steepest slopes of the temperature breakthrough curves in 1999 and 2004, the early data from these pump tests provide reasonable estimates of riverbed hydraulic conductivity.

The distance between the probes can be inferred by the pressure measured from them during non-pumping conditions. This distance has been measured within 2 cm, or within 1% of the approximate 2.14 meter distance between them. Calculations under non-pumping conditions using probe pressure also identify the depth of the probe below the river surface with similar accuracy.

The distance between the riverbed and the probes, however, is both poorly measured and highly variable. The probes were initially set at distances assumed to be 0.6 meter and 2.7 meters below the riverbed. The riverbed near the location where the probes were set has been measured to vary in depth by more than 2 meters from spring to fall. This variation could have had a significant impact on the calculation of riverbed hydraulic conductivity in both 1999 and 2004.

Data from 2004 indicate that a significant change occurred when the probes were reading a water head of approximately 123 meters amsl. This is approximately the elevation of the riverbed at that point and time. The riverbed elevation has been observed to vary between 120.8 and 123.3 meters amsl near the location of the probes, with the higher elevations typical of later summer/early fall. This assumption is consistent with the bathemetry indicating that the riverbed at this location aggrades from spring to fall.

8.3 Changes in Riverbed Hydraulic Conductivity: 1999 and 2004

The comparison of data from the 1999 and 2004 datasets leads to the conclusion that the riverbed hydraulic conductivity at the point of observation decreased significantly over the 5 year period. This conclusion is consistent with the observations for the entire riverbed system made by Schafer for this site (Schafer, 200xx). The cause of this decrease, however, remains undetermined. It is known that the riverbed in the vicinity of the well experiences significant erosion and deposition. It is also suspected that the aquifer under the riverbed is at times unsaturated, and likely cycles annually between saturated and unsaturated in the area where the riverbank meets the riverbed, approximately 70 meters from the well.

The impact of the change in specific capacity as a function of distance to point of recharge has been modeled by Schafer. This work indicates that an increase in distance of 60 meters to the point of recharge would be expected to decrease well capacity by approximately 10%. Thus, the progression of zone of decreased conductivity from 60 meters to 120 meters into the riverbed could account for approximately one third of the total reduction in specific capacity observed at this site.

The highly variable condition of the riverbank/riverbed interface at this site further complicates the interpretation of data. That portion of the riverbed experiencing the greatest changes with regards to saturation also experiences the greatest annual changes in bathemetry, erosion, and sediment deposition. Thus, it is difficult to determine how the several factors impacting riverbed hydraulic conductivity (temperature, clogging, scouring, and saturation) interacted to impact riverbed hydraulic conductivity as observed in 1999 and 2004.

8.4 Implications on Modeling RBF Systems

At the Louisville site it is reasonable for future modeling activity to consider the point of recharge to be that point where relatively clean sand is consistently observed in the riverbed. For this site, this point lies approximately 120 meters from the well, and is beyond the observed area of riverbed hardpan thought to be induced by unsaturated conditions below the riverbed. The riverbed at and beyond this point is characterized as flat, and composed of clean medium to fine sand.

Riverbed hydraulic conductivity values across a 0.6 meter depth of riverbed in the area of recharge at Louisville were estimated to vary between 0.03 meter/hour initially to values of 0.008 meters/hour after four years of

operation. Flux rates (discharge velocities) at the riverbed as high as 0.8 meters per hour might be expected at points of maximum infiltration.

An iterative approach may be appropriate for locating the effective point of riverbed recharge beyond the point where unsaturated conditions are indicated by the piezometric surface. Selecting the greater of the two distances for recharge indicated by the presence of clean riverbed media and expected unsaturated conditions would yield a conservative value for modeling the point of recharge.

The impact of water temperature in modeling includes the effect on the point of recharge in unsaturated conditions develop as well as the effect on viscosity. Thus, temperature effects may need to be separated into viscosity impacts and impacts to the distance to recharge.

The conceptual model for a site can be greatly enhanced by collecting riverbed media samples in the vicinity of a proposed facility. Better estimates of effective point of recharge, riverbed hydraulic conductivity, and general sediment transport can be made if the riverbed media is well characterized.

8.5 River Flow Characteristics at the Site

The significance of site-specific river dynamics on the infiltration characteristics of a riverbed warrants evaluation. Bathemetry, bends, and obstructions can have impacts on sediment transport and bed conductivity. Proposed sites for RBF installations should be visually evaluated under various flow conditions for flow separations, standing waves, and other indications of flow anomalies that would affect bed shear.

At the Louisville site, bed shear stresses at the point of flow separation (flow reversal resulting from an obstruction in the riverbed) warrant further consideration, as it is highly likely that eddy currents dominate stress forces at this point in the river. This is supported by the presence of larger media at this point in the riverbed. The fact that this flow separation also sits very close to the divide between high and low riverbed flux rates indicates that this particular site on the Ohio River may be an anomaly with regards to riverbed conductance. The trough and predominance of larger particles in the trough also indicate higher riverbed shear stresses, perhaps from the x-z shear plane and resulting eddy currents established by the flow separation.

8.6 Predicting Sustainable Capacity

Initial specific capacity calculations can be expected to be influenced by the temperature dynamics between the river and the aquifer, with warm-river water start-ups providing the conditions for highest initial specific capacity.

Temperature variations in the aquifer tend to stabilize after one annual cycle, providing site-specific data on the range of specific capacity to expect across the annual temperature variation. At Louisville, the range of impact on specific capacity was from 4,000 to 6000 m^3/m/day across a temperature swing of 25^0C in the river and 15^0C in the well discharge after 3 years of operation.

A gradual decrease in specific capacity can be expected as the piezometric surface in the aquifer balances between well discharge and aquifer recharge. Specific capacity decreases as the piezometric surface extends into the river, and if unsaturated conditions exist under the river, the specific capacity can be expected to decrease as the effective point of recharge extends further into the riverbed and/or upstream and downstream.

The balance between riverbed scour and clogging is critical in predicting changes in riverbed hydraulic conductivity with time. Frequent bed scour capable of moving the bulk of the bed material will result in less reduction in riverbed hydraulic conductivity with time. A review of flow hydrographs, scour shear stresses, and riverbed material size provides insight to the suitability of a site for riverbank filtration.

REFERENCES

Hubbs S. High Yield Riverbank Filtration Systems for Public Water Supply: Measuring the Impact of Riverbed Plugging. Proceedings of the World Water Congress 2004, Critical Transitions in Water and Environmental Resources Management, World Water and Environmental Resources Congress, Gerald Sehlke, Donald F. Hayes, David K. Stevens - Editors, June 27 – July 1, 2004, Salt Lake City, Utah, USA

Julien P. *Erosion and Sedimentation.* Cambridge University Press, 1998

Schafer, D. Hydraulics Analysis of Groundwater Extraction at the B.E.Payne Water Treatment Plant, Louisville Water Company Report, Louisville KY, July 2000.

Schafer D., Use of Aquifer Testing and Groundwater Modeling to Evaluate Aquifer/River Hydraulics at Louisville Water Company, Louisville, Kentucky, USA. Presented at NATO Advanced Research Workshop, Samorin, Slovakia. September 7-10, 2004

Unthank M. Riverbed Sediment Samples, August 2004, Personal Communication. USGS, Louisville, KY. October 2004

Unthank M. Riverbed Bathemetry, Personal Communication. USGS, Louisville, KY. March 2005

Wang, J., S. Hubbs, R. Song, "Evaluation of Riverbank Filtration as a Drinking Water Treatment Process", AwwaRF Report 90922, 2002.

EXPERIENCE WITH RIVERBED CLOGGING ALONG THE RHINE RIVER

There is no such thing as a free lunch

Jürgen Schubert
Dürener Str. 38, Düsseldorf, Germany

Abstract: Clogging of the riverbed caused by the operation of riverbank filtration wells is a highly dynamic process, governed not only by varying pumping rates, but by the runoff dynamics of the river and by the quality of the river water. Investigations of the riverbed and the river–aquifer interactions at two RBF sites in the Lower Rhine region will be presented. The different behavior of both RBF plants confirms the importance of stream processes and the adaptation of pumping rate for sustainable yield.

Key words: Riverbank filtration**,** clogging of the riverbed, operational experience, field studies, river-aquifer interactions.

1. INTRODUCTION

In the Lower Rhine region, riverbank filtration for water supply has been employed for more than 130 years. During the first 80 years (1870 - 1950) the quality of the river water permitted the production of drinking water without further treatment; the well water had only to be disinfected.

After 1950 the quality of the river water began to deteriorate gradually. Increasing quantities and insufficient treatment of effluents from industry and communities caused a noticeable drop in the oxygen concentration of the river water. The consequence of this and the increasing organic load in the river water changed the redox situation in the adjacent aquifer: it switched from former aerobic to anoxic conditions. At this time the well water had to be treated to remove iron, manganese and ammonium and furthermore organic micro-pollutants. But more important for the sustainability of riverbank filtration was the effect of particulate organic matter, which

Stephen A. Hubbs (ed.), Riverbank Filtration Hydrology, 221–242.

intensified clogging of the riverbed and thus reduced the yield of the wells significantly. This was the reason for a first field study of the riverbed in front of the Flehe waterworks (Düsseldorf) with a diving cabin in 1953 and 1954

The trend of decreasing river water quality was reviewed between 1970 and 1975 chiefly under the fourth amendment of Water Ecology Act and the Waste Water Charging Act (Friege, 2001). After 15 years the difficulties concerning the river water quality appeared to be overcome. But on 1st November 1986, a fire broke out in an agrochemicals store of a Basel chemical plant. Insecticides, herbicides and fungicides were carried into the Rhine with the fire-fighting water. The effects of this accident on the Rhine River were serious. On the stretch of the Rhine up to the Middle Rhine region, the entire stock of eel was destroyed. In addition, other species of fish were also affected and damaging effects were detected on fish food organisms up to the mouth of the River Mosel. The question then arose that if this wave of poison could prevent any life in the Rhine for years to come, then it could simultaneously destroy the basis for water procurement in the adjacent aquifer.

This accident has given fresh impetus to the improvement of pollution control on the Rhine and was the reason for different research projects to understand and to manage the effects of accidental shock loads on riverbank filtration plants (Schubert, 1993). In 1987 a second study of the riverbed in front of the Flehe waterworks was carried out. Based on the knowledge of the properties of the infiltration areas and the data of the alluvial deposits beneath the riverbed, a research project on river - aquifer interactions was designed and started in 1988. One result of this project is a three-dimensional, dynamic flow and transport simulation model, which describes the effect of shock-loads, resulting from accidental pollution of the river, on the raw water in the wells (Gotthardt, 2001). Another result is a tailor-made monitoring system (Schubert, 1996), which has proven invaluable in determining and reporting any pollution of the Rhine due to accidents.

The objective of this paper is to present the experience on the long-term behaviour of clogged areas and the results of field studies on riverbank filtration, with emphasis on the clogging process.

2. GENERAL REMARKS

2.1 Riverbank Filtration – a Dynamic Process

River - aquifer interactions are governed by the fluctuating water level of the river (Fig. 1).

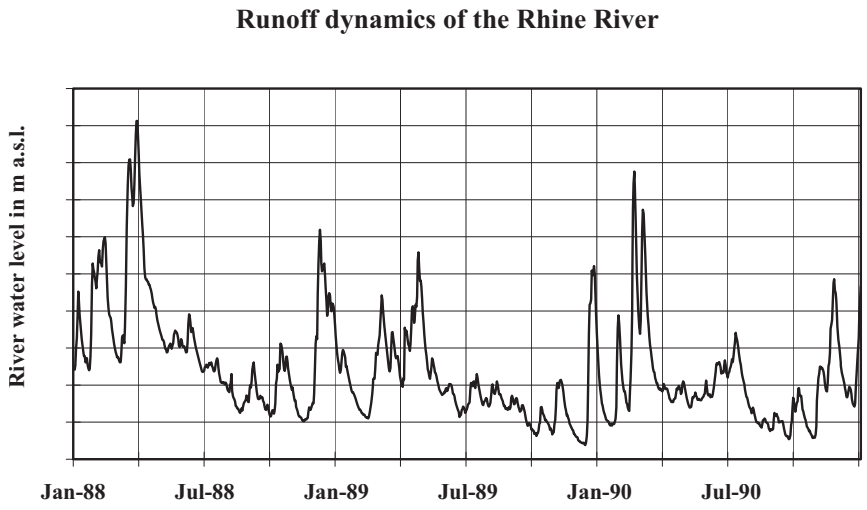

Figure 1. Stage hydrograph of the Rhine River (1988 –1990) at river-km 744.2 (Düsseldorf)

The resulting gradients between the quickly changing river level and the gradual adaptation of the groundwater table in the adjacent aquifer control flow and transport in riverbank filtration. The dynamic behaviour of the river level does not only influence clogging of the riverbed and flow and transport phenomena but also water quality, both in the river water and raw water in the production wells. To understand river-aquifer interactions in riverbank filtration, monitoring concepts have to be accounted for the dynamic hydrology of the whole system. This means that monitoring data have to be collected over long periods of time and monitoring wells have to be fit for depth-orientated samples even during flooding. Infiltration of river water to an aquifer is a natural phenomenon at the upstream side of river bends and during rising river levels, without any wells near the riverbank.

2.2 Properties of the River Concerning Riverbank Filtration

Different regions can be distinguished along a natural river: the upper part with erosion, the middle part with transport of bed load and the lower part with deposition. The assumption of this simple model does not really match most natural rivers, which normally do not have only one erosion basis (the mouth of the river) along their flow path but many more due to the prevailing geological conditions. If sites for bank filtration have to be selected, erosion regions and also regions with deposition of fine sand and silt (e.g. upstream of dams, river mouth regions) should be avoided. Besides the geological data, the hydraulic gradient of the river level gives a first rough estimate of the mean flow velocity in the river, the mean grain size diameter in the riverbed and the capability of bed load transport, which is the most important part of the self-cleaning mechanism for clogged areas.

Therefore, in addition to the hydro-geological data of the aquifer, the runoff regime and the runoff dynamics of the river have to be considered. An important parameter is the shear force that is responsible for erosion and bed load transport.

Natural rivers flow in bends in their middle and lower parts. A cross section through a bend shows a stabilised and sometimes “paved” bed at the outer section of a bend and movable ground at the inner side. Clogging is more strongly marked by bank filtration wells along the outer section of a bend. The yield of bank filtration wells along the inner bend is normally higher, not only due to the movable ground of the riverbed but also by a natural cross flow of bank-filtered water due to the gradient of the river level.

2.3 Clogging of the Riverbed

Clogging of parts of the riverbed during the operation of riverbank filtration wells is unavoidable (Riesen, 1975). The flow in the infiltration area is permanently directed from the river to the aquifer. Suspended solids cannot infiltrate the aquifer and are removed and deposited in the upper layer of the aquifer (mechanical clogging). Clogged areas tend to expand from the well side bank to the middle of the riverbed. Clogging is limited by bed load transport in the river, which whirls up and removes the deposits in regions with sufficient shear force.

High loads of biodegradable substances in the river water can lead to chemical clogging beneath the infiltration areas due to strong changes in redox-potential and pH values which may cause precipitation of substances (e.g. $FeCO_3$) in the pores of the aquifer. Therefore the river water quality

must be considered. Also the quantity, size and type (e. g. suspended residuals from waste water treatment plants) of suspended solids will influence the clogging process. Several attempts have been made to forecast and to simulate clogging of the riverbed. But until now, the recommended "tools" do not surpass operational experience.

3. THE STUDY SITES

3.1 Short History of the Düsseldorf Waterworks

Not a lack of water, but doubts on the hygienic quality of the used water from rainwater storage tanks and private wells were the deciding factor for the foundation of Düsseldorf waterworks. The English engineer William Lindley was called in to provide expert advice on the choice of the location and planning of the technical equipment. An area in Düsseldorf-Flehe (river km 731) at the banks of the Rhine River was recommended for the construction of the first shaft wells (Fig. 2). On May 1, 1870, the waterworks, with a capacity of 8,800 m^3/d, was put into operation for the first time.

In the following years, the race began between the increasing water demand, due to the increasing population, and the extension of the waterworks. This continued, almost non-stop, up to the Seventies of the last century. With the start-up of a well gallery with 80 vertical filter wells in 1910 the total capacity of the Flehe well field has been exhausted. But the demand for water continued to increase and additional sites for water procurement had to be explored and determined. Construction of the Lörick waterworks on the left bank of the Rhine River began in 1914, but due to the war was completed only in 1926. Construction of the Staad waterworks on the right side bank between km 748 and km 752 began in 1926 and operation started on June 30, 1930. However, the additional capacity of 65,000 m^3/d was quickly soaked up by increasing demand and the incorporation of further settlements.

A critical situation arose after world war two. In eight years between 1948 and 1956 the water demand doubled, from 26 million m^3/year to 52 million m^3/year in 1956. But more important was the deterioration of the quality of the river water, which was observed since 1950. Increase in water demand and, thus, increase in wastewater, combined with inadequate wastewater treatment, caused severe problems for the waterworks along the Rhine River. Heavy clogging occurred and several RBF facilities north of

Düsseldorf, particularly those, which were located too close to the bank of the river, had to be shutoff. After more than 80 years of RBF operation the clogging process got into focus for the first time. Investigations were started to understand this process and to study the influence of the quality of the river water, location of the wells, and pumping rate on clogging.

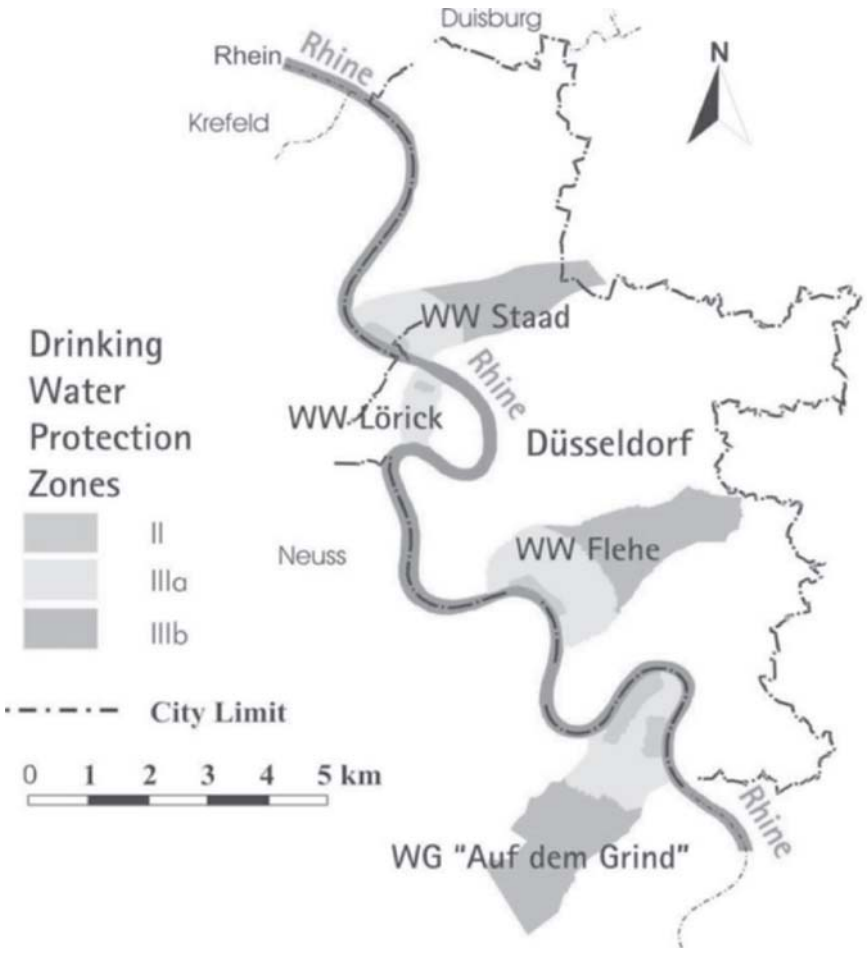

Figure 2. Floor plan of Düsseldorf waterworks

The first two of the current seven horizontal collector wells at the Grind well field went into operation in 1954. Due to the problem of clogging, the distance between the riverbank and the wells was more than 220 m, to limit the driving head between the river water level and the table of the draw down curve beneath the riverbed. In the existing waterworks Flehe and Staad this could be realized by reduction of pumping rate.

3.2 Study site at Flehe Waterworks

The production wells of the Flehe waterworks are situated on the outer bend of the river Rhine between km 730.7 and km 732.5 (Fig. 3). In the flow direction of the river are following:

One horizontal collector well situated approximately 80 m from the waterline at mean discharge, and 70 vertical filter wells connected by siphon pipes, forming a well gallery parallel to the riverbank, situated approximately 50 m from the waterline at mean discharge. The total length of the well gallery is 1400 m in full, with the pumping rate during the field studies roughly constant between 1250 and 1400 m^3/h. In addition there are 9 vertical filter wells with separate pumps, although these were not operated during the field studies.

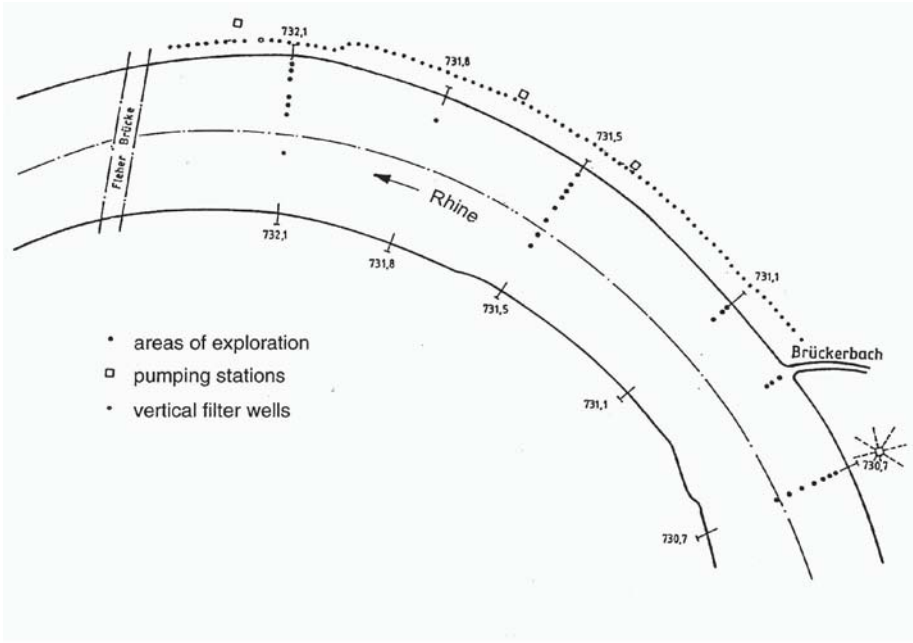

Figure 3. Map of investigation area: Flehe waterworks, Düsseldorf.

The aquifer consists of sandy, gravely Pleistocene sediments. The hydraulic conductivity, determined by means of pumping tests and additional flow-meter exploration, ranges between $4*10^{-3}$ and $2*10^{-2}$ m/s. This layer, which is overlain by a 0.5 - 2 m thick meadow loam, is

approximately 20 m deep. Below the Pleistocene sediments there is a nearly impermeable Tertiary layer with fine sands. The bank slope is coated with a 0.5 m thick clay layer in the upper region, and protected by basalt blocks below the mean river water level. The thickness of the aquifer beneath the riverbed varies between 5 and 10 m.

3.3 Study Site at Grind Well Field

The well field "Auf dem Grind" is situated inside the loop of a meander at the left side of the River Rhine between km 719 and km 726. This peninsula, created in former times by the meandering river, is 1.5 km wide and approximately 3 km long. The aquifer consists of sandy, gravely Pleistocene sediments. The hydraulic conductivity, determined by means of pumping tests ranges between $1*10^{-3}$ and $1*10^{-4}$ m/s. This layer, which is overlain by a 1 m up to more than 5 m thick meadow loam, is significantly profiled by former shifting of the riverbed and is 6 to 25 m deep. Below the Pleistocene sediments there is a Tertiary layer with fine sands. The surface of the peninsula is between 32 and 38 meter above sea level and may be flooded during high river water level. The areas around the caissons of the production wells are elevated and can be reached by boat during flood events.

Along the downstream side of the bend follow five horizontal collector wells with a capacity of 2800 m^3/h each:

- PW IV at km 723.0; 250 m distant from the bank,
- PW III at km 723.55; 250 m distant from the bank,
- PW I at km 724.2; 235 m distant from the bank,
- PW II at km 724.75; 220 m distant from the bank and
- PW V at km 725.2; 360 m distant from the bank.

At the upstream side of the bank follow two horizontal collector wells:

- PW VII at km 719.5; 220 m distant from the bank and
- PW VI at km 719.9; 280 m distant from the bank.

Due to the shape of the river loop and the natural cross flow of bank-filtered water the well water consists of more than 90 % of bank filtrate.

Investigations have been carried out in the region of PW III. Figure 4 shows a cross section of the peninsula with the production well and some of the monitoring wells. The monitoring wells C, B, A, and F consist of three wells each for depth-orientated sampling; most of the other monitoring wells are classical wells for groundwater observation.

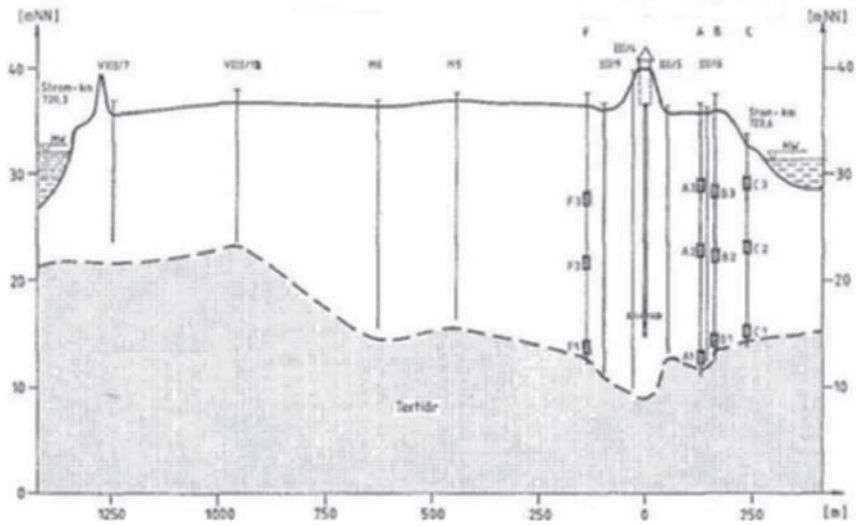

Figure 4. Cross section of the study area at Grind well field, PW III

4. INVESTIGATIONS OF THE RIVERBED IN FRONT OF FLEHE WATERWORKS

First field studies of the riverbed in front of Flehe waterworks were carried out with a diving cabin in 1953/54 to investigate riverbed clogging during high loads of organic contaminants and suspended solids in the river water. Two clogged layers could be detected, one on the surface of the infiltration area (mechanical clogging) and the other stretching about one decimetre below (chemical clogging) (Gölz et al., 1991). Parallel to the well gallery the clogged area stretched from the well side bank approximately 120 m to the middle of the river. After the investigation of the riverbed, a remarkable experiment followed. To find out the influence of the clogged area on the water yield of the wells, a "window" was dredged into the riverbed in front of the well gallery, with a length of 300 m and 70 m wide. As expected, the water yield increased significantly. But the effect was only temporary; a few months later, the dredged window was clogged as before.

In 1987 a second investigation of the riverbed followed in the same area, where in the meantime the water quality of the river had improved. The diving cabin of the Carl Straat ship is well equipped with tools to take

samples from the riverbed. The diving cabin of the ship can be positioned accurately at any point of exploration. The working area of the diving cabin is approximately 20 m^2. Areas of exploration were especially selected at three cross sections of the Rhine River at km 730.7, 731.5 and 732.1 (Fig. 3). At the points of exploration the bed material was inspected (sedimentary structure, grain size, silt layers, organic coatings) and samples were taken for further investigation. At selected areas, the aquifer beneath the riverbed was explored by slot probes, and also in-liner borehole cores (diameter 200 mm, depth 1.35 m) were taken for further investigation. With a special probe, water samples were taken approximately 0.6 m below the infiltration areas.

As a result of this investigation, three different zones on the riverbed are distinguished (Fig.5):

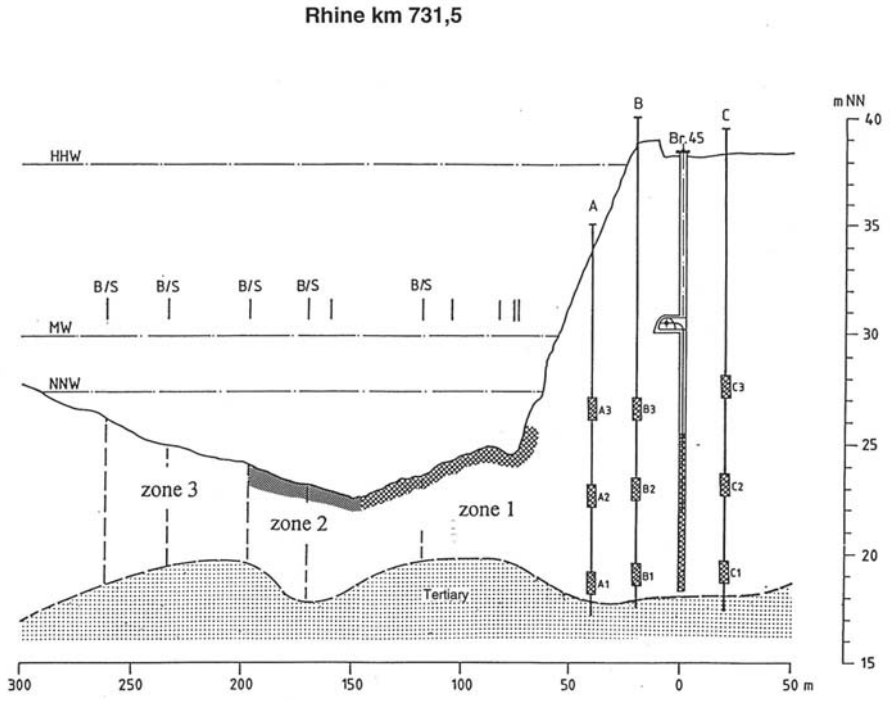

Figure 5. Zones of classification of the riverbed in front of Flehe waterworks, Rhine Km 731.5.

B = borehole cores, S = slot probes.

Zone 1: Nearest to the wells there is a region (about 80 metres wide), which has a fixed ground (pavement) and is fully clogged by suspended solids. This region is almost impermeable (permeability of the silt layer k_f = $1*10^{-8}$ m/s).

Zone 2: The attached region also has a fixed ground but is only partly clogged with good permeability for infiltrating river water. This region covers another 80 to 100 meters (permeability of the upper layer $k_f = 3*10^{-3}$ m/s).

Zone 3: The region between the middle of the river and the opposite bank has a movable ground, which is shaped by normal flow and mainly by flood events. The permeability is higher than in the other regions (permeability of the upper layer $k_f = 4*10^{-3}$ to $2*10^{-2}$ m/s).

Only an upper thin layer caused by deposits of suspended matter (mechanical clogging) was be detected in 1987; chemical clogging did not appear under the aerobic conditions, now present in the aquifer. A schematic image of the clogged area with silt layers between and beneath the stones is shown in Fig. 6.

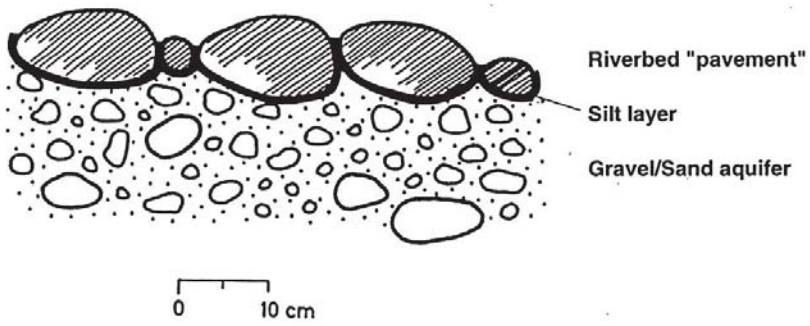

Figure 6. Pattern of clogged areas of the riverbed.

The grain-size distribution curves of aquifer material under the riverbed (gravel and sand) and silt in the clogged area are shown in Fig. 7.

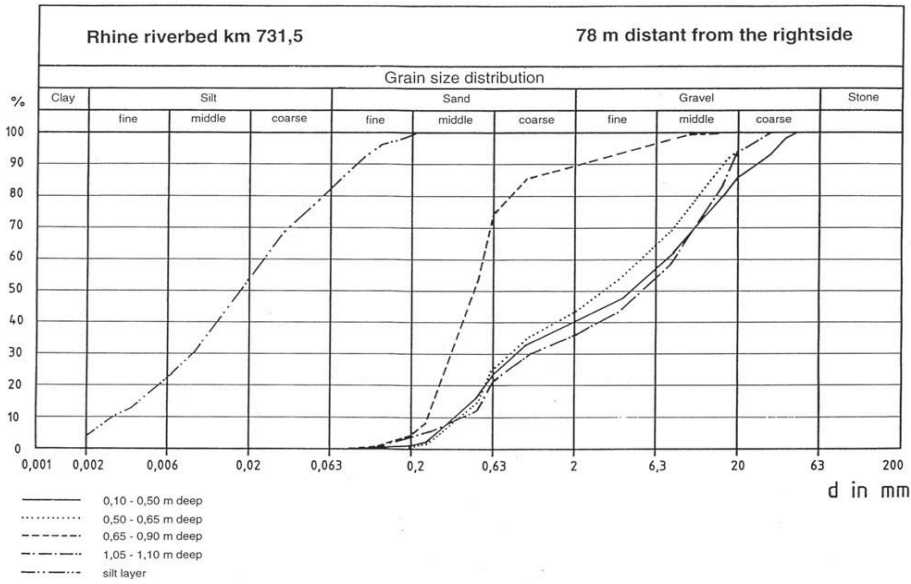

Figure 7. Grain-size distribution of the aquifer beneath the riverbed and the silt layer in clogged areas.

5. RIVER – AQUIFER INTERACTIONS

5.1 Investigations at Flehe Waterworks – Outside Bend of the River

To prepare the monitoring devices for related field studies and the basic assumptions for a three dimensional dynamic flow and transport model a simple hypothesis was used (Fig. 8):

Flow path length: $s_1 < s_2 < s_3$

Flow velocity: $v = k\,(h/s)$ (h/s is average hydraulic gradient) $v_1 > v_2 > v_3$

Flow time: $t = s/v$ $t_1 << t_2 << t_3$

The variation in flow time between different infiltration points in the riverbed and the production well must be much greater than the variations in flow path length. To verify these rough conclusions by field studies, a monitoring concept was chosen with three rows of sampling and observation wells (at two selected cross sections), two between the well gallery and the river and one on the opposite side of the well gallery. Each row consists of three wells, set 1.5 m apart from each other, with 1 m long filter screens at

different depths to allow depth-orientated sampling (also during flooding, e. g. for row A). Fig. 5 shows the arrangement of the wells at cross section km 731.5. The wells along sampling rows A, B and C are equipped with pumps (type Comet, 24 V D.C., pumping rate approximately 2 l/min) and automatic gauges to measure the pressure head. The same arrangement was chosen at km 732.1 with rows D, E and F to check the results of the central cross section at km 731.5.

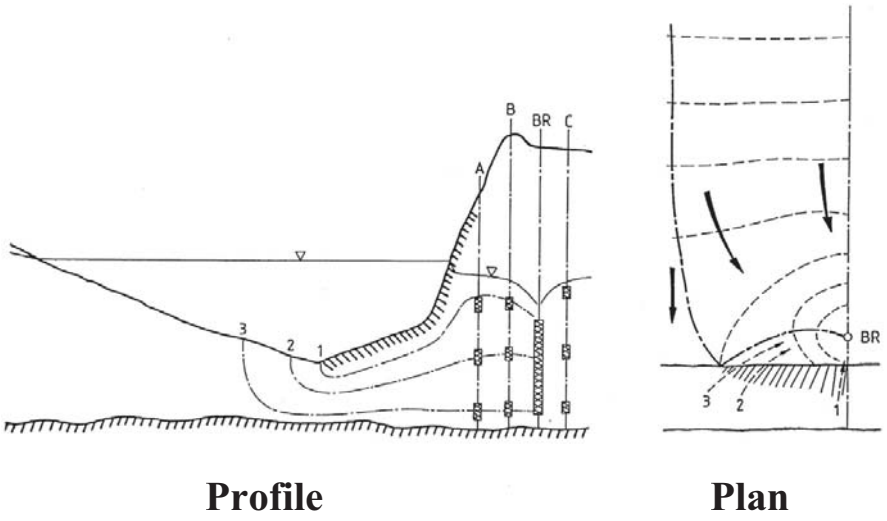

Figure 8. Hypothesis of groundwater flow in riverbank filtration.

Between the production wells and the river, the cross section at km 731.5 is at right angles to the river axis. On the groundwater side the cross section follows the axis of the well field catchment area. The distances of the sampling and observation wells along the cross section at km 731.5 and related to the production well BR45, are shown in Table 1. Samples from each row were taken simultaneously after 12 minutes of pumping from the sampling wells. Pumping tests showed that after 10 min of pumping from the sample wells the temperature variations in these wells were less than 0.1 ^{0}C and the variations of a chloride tracer less than 2 %.

Table 1. Distances of monitoring wells along the cross section at km 731.5 (Flehe)

River side		Groundwater side	
Row A	- 40.2 m	P16	+ 1.6 m
Row B	- 20.4 m	Row C	+ 18.1 m
P07	- 12.0 m	P08	+ 35.3 m
BR45	0 m	P09	+ 108.7 m
		P10	+ 195.0 m

Daily monitoring was conducted for hydraulic data (river water level at 3 points, groundwater table at about 40 points, pumping rate), and quality data (water temperature, electrical conductivity, chloride concentration (tracer), UV-extinction (254 nm), DOC (dissolved organic carbon), AOX (adsorbable organic halogens), oxygen concentration, nitrate and sulphate concentrations). In the field, measurements included temperature, electrical conductivity and dissolved oxygen in the well water. In the laboratory, the analyses of the other quality parameters were carried out according to German guidelines and DIN methods.

From previous investigations (Schubert, 1984) it was known that "snapshots" are not able to guarantee insight into the flow and transport phenomena of riverbank filtration. Therefore, the monitoring period for each series of field studies was scheduled at not less than 6 months.

The first series of field studies was carried out between 1 October 1988 and 30 April 1989. The water level of the river Rhine (RH) and the water table at sampling wells A1, B1 and observation well P07 along the cross section at km 731.5 are shown in Fig. 9.

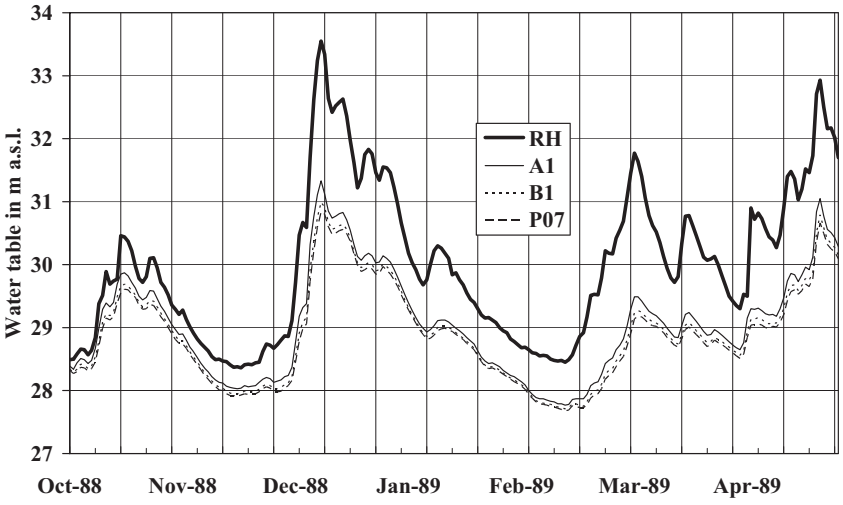

Figure 9. Water level of the Rhine River (RH) and water tables at the sampling wells A1, B1, P07 at km 731.5.

Sharp rises in the river level lead to infiltration of previously unsaturated soil layers with high velocities and short residence times. This may cause insufficient removal of micro-organisms, which require acclimated soil layers for adequate removal (Medema et al., 2001).

Based on these data and the data of the landside observation wells P10, P09, P08 and C the filtration rates on both sides of the well gallery at cross section km 731.5 can be evaluated. The filtration rate on the river side (v_f (A-B)) varies between + 0.3 and + 3.2 m/d (Fig. 10); the filtration rate of the land side (v_f(P10-P08)) varies between + 0.3 and - 0.8 m/d! The magnitude and the direction of the groundwater flow on the landside of the well gallery depends significantly on the fluctuating river water level; the "+ sign" means flow direction to the production well BR45, the "- sign" means opposite flow direction. During flood events, bank storage occurs and bank-filtered water will pass the well gallery. This was also demonstrated by tracer data of the sampling wells at row C.

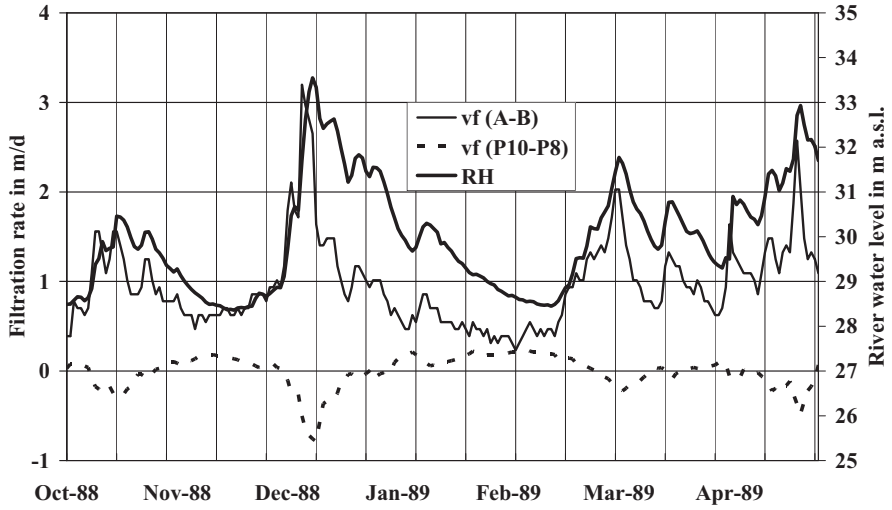

Figure 10. Filtration rate between rows A and B (riverside) and between P10 and P08 (landside) at km 731.5.

The permeability of clogged areas varies with the flow dynamics of the river. There are not only variations in the driving head between the river and the aquifer but also remarkable variations in the concentration of suspended solids in the river water. The concentration of suspended solids in the Rhine River varies from 10 to more than 400 g/m^3 with an average concentration of less than 40 g/m^3. High values appear in the phase of rising water level (Breitung, 1999).

Variations of water temperature in the subsoil depend not only on the changing river water temperature but also significantly on the runoff

dynamics of the river (Fig. 11). The water temperature at observation well A2 follows the average gradient of the river water temperature with a lag time of about 4 weeks and drops significantly during the sharp rise of the river water level in December 1988. The sudden increases of water temperature in October and in December at observation well C2 (land side) confirm the transport of bank-filtered water to the landside of the well gallery.

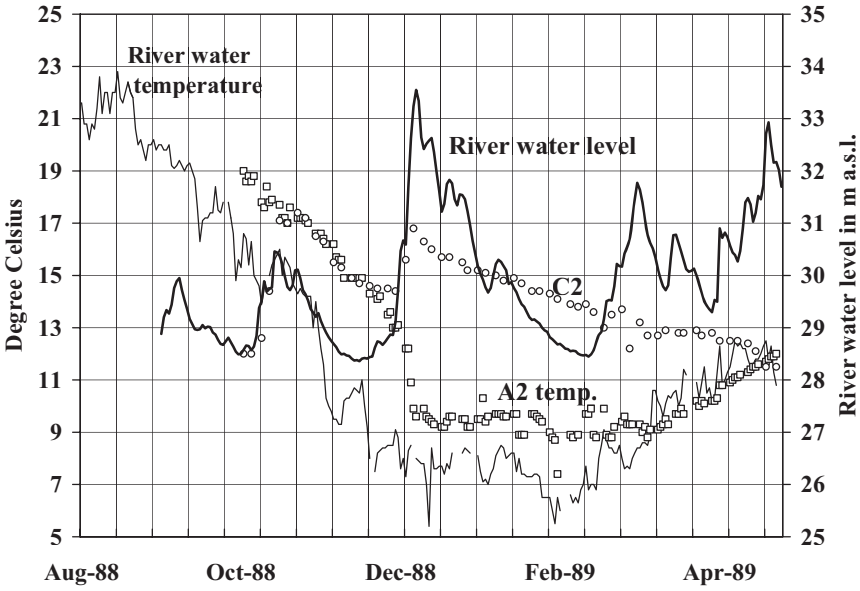

Figure 11. Variations of water temperature in the subsoil (A2, C2).

The driving head between the river level and the first row A of sampling wells reflects the variations in the permeability of the clogged area. For a first assessment of the dynamic characteristics of clogged areas the specific driving head were adjusted to the measured values in November 1988 (Fig. 12). With these data and the assumption of constant permeability the resulting pressure head R-A* is shown (dotted line) together with the measured values R-A.

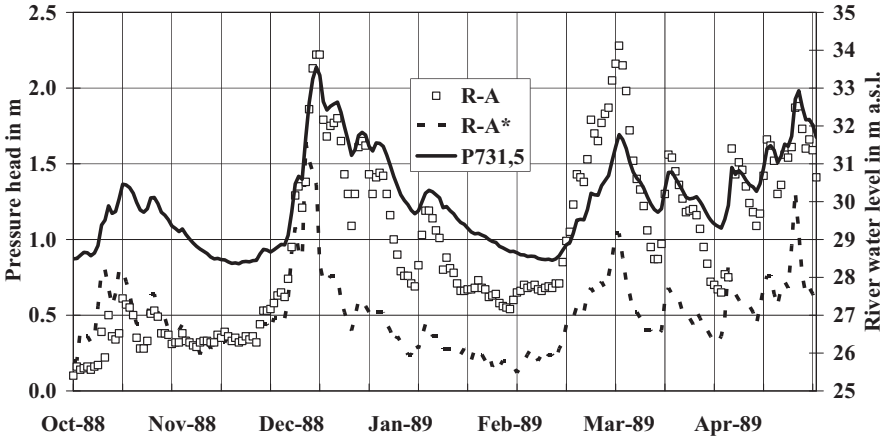

Figure 12. Variations in driving head on clogged areas.

As demonstrated by this example, the permeability of clogged areas can vary significantly in short time. In the investigated areas in front of the Flehe waterworks, the clogged areas spread out during flood events due to the high concentration of suspended solids and the increasing driving head between the river water level and the water table of the adjacent aquifer. An illustration of the variations in permeability between the riverbed and row A is presented in Figure 13 by the relative permeability. Contrary to traditional expectations of scouring clogged areas by flood waves, the permeability dropped significantly with the first smaller flood wave in October 88 and drops again a second time in December 88.

Regarding the pattern of clogged areas along the outside bend of a river (Fig. 6) only silt and stones characterize the surface of the riverbed. As known from the conditions for erosion (Schubert, 2004, Hjulström-Diagram) those grain sizes are able to resist even higher flow velocities. After the flood wave end of April 89 a period of decreasing and slightly fluctuating river water level followed up to December 89 (Fig. 14) and restored the former permeability.

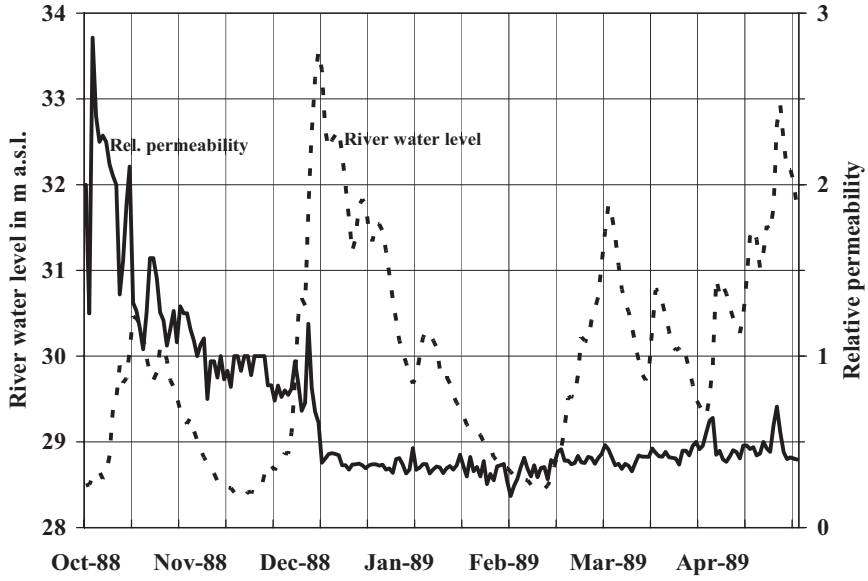

Figure 13. Variations in permeability of the riverbed

These interactions, concerning the variations of permeability, are mainly governed by variations of the concentration of suspended solids in the river water, the driving head between the river and the aquifer and self-cleaning mechanisms. Most important for self-cleaning of the riverbed is erosion and bed load transport. But during the investigations of the riverbed with the diving cabin at low water level, benthos organisms could be observed, grazing the silt deposits in the clogged area for nourishment. This grazing, and possibly additional (micro-) biological activity will principally influence the permeability of clogged areas during times with low hydraulic gradients between the river and the aquifer. Biological activity is apparently an important cleaning mechanism in lakes, able to restore the permeability of lake bank filtration schemes where operated.

5.2 Investigations at Grind Well Field - Inside Bend of the River

The monitoring concept was chosen with three rows of sampling wells C, B, A between the river at km 723.6 and the production well PW III (horizontal collector well with 12 laterals, screen length 804 m in total) and one row (F) on the opposite side of the production well. Two additional rows of sampling wells (D, E) are located parallel to the bank at right angle on both sides of the production well. Each row consists of three wells, set 1.5 m

apart, with 1 m long filter screens at different depths to allow depth-orientated sampling. Fig. 4 shows a cross section with the arrangement of the sampling wells C, B, A, and F and additional observation wells between km 723.6 and km 720.3 (upstream side of peninsula). The distances of the sampling wells along the cross section related to the production well PW III, are shown in Table 2.

Table 2. Distances of monitoring wells along the cross section km 723.6 (Grind)

River side		Groundwater side	
Row C	- 240 m	Row F	+ 135 m
Row B	- 170 m		
Row A	- 135 m		
PW III	0 m		

Due to the distance between the well and the riverbank, the residence time of bank-filtered water is two to three times longer than in Flehe waterworks. Therefore the monitoring period had to be extended to more than 40 weeks (01.06.89 to 23.03.90). The runoff dynamics are characterized by slightly decreasing river level with minor fluctuations over the first 28 weeks (Fig. 14), followed by four flood waves in only 14 weeks.

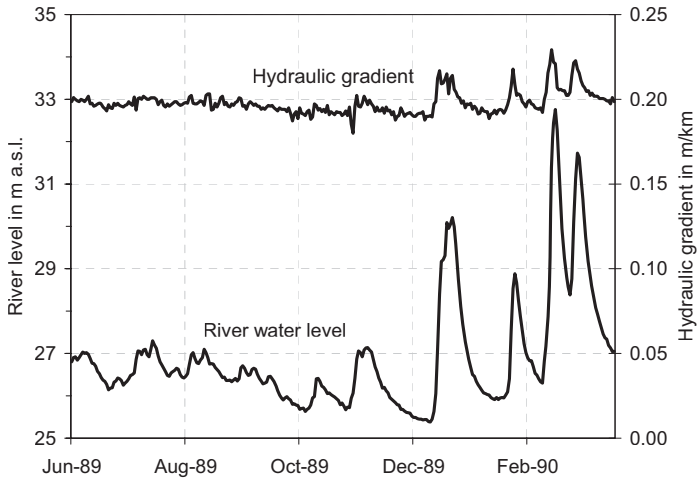

Figure 14. Stage hydrograph at km 744.2 and variation of river surface hydraulic gradient.

Along this river section there are two level stations, which are read out exactly at the same clock time (WP at km 722,3 and DP at km 744,2). Using

these data the variation of the hydraulic gradient, based on a river length of 22 km, can be determined. The steady-state value of the hydraulic gradient is 0.198 m/km; during the passage of a flood wave a maximum value of 0.230 m/km (+ 16%) is reached. During those unsteady flow conditions internal friction and friction along the riverbed is intensified due to the timely surplus on potential and kinetic energy, and erosion and bed load transport may occur.

Field studies were carried out between 1 June 1989 and 23 March 1990 with an average pumping rate between 1000 and 1100 m^3/h. The water level of the River Rhine (RH) at km 723.55 (PW III) and the water table at sampling wells C, B, and A along the cross section are shown in Fig. 15. The sampling wells C, B, and A are not equipped with automatic gauges due to frequent flooding. Therefore, there are several gaps in the data during flood events.

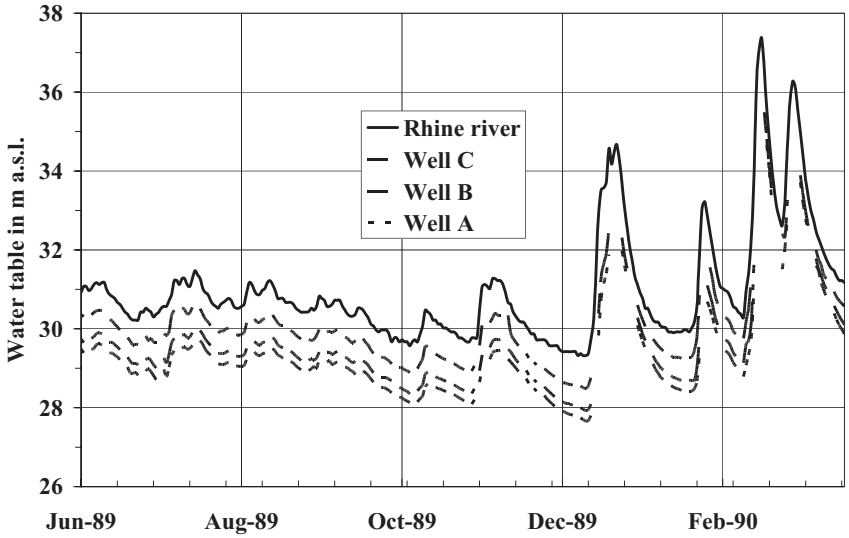

Figure 15. Water level of the Rhine River (RH) and water tables at the sampling wells C, B and A at km 723,55.

Contrary to the results of the investigation at Flehe waterworks (Fig. 9) no significant variation in the driving head between the river water level and the groundwater table in sampling well C indicates severe clogging during the passage of flood waves. This will be very explicit with Fig. 16, which shows the variations in driving head over a period of 42 weeks. These variations in driving head are caused by fluctuations in filter velocity only.

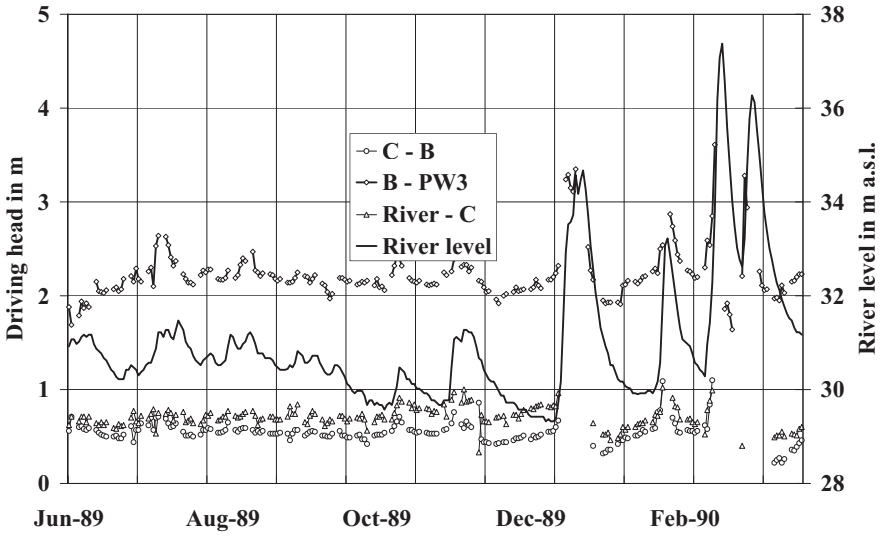

Figure 16. Variations in driving head at cross section km 723.55.

This result is an impressive confirmation of stream processes along the inside border of river channels with movable riverbed. Flow conditions cause alternating sedimentation and erosion of sandy matter, cleaning clogged areas

6. CONCLUSIONS

The permeability of clogged areas varies with the dynamic hydrology and cannot be regarded as constant. This is still an uncertainty, not only for projects of riverbank filtration plants but also for perfecting modelling. The clogging process is governed by the runoff dynamics of the river, the resulting stream processes (erosion, transport, sedimentation), and the quality of river water and depends on the location of the wells correlated to the river geometry (e.g. bends). The distance of the wells from the riverbank and the pumping rate create the depression cone beneath the riverbed. The clogging process can be understood as a perpetual search for balance correlated to the fluctuating river – aquifer interactions. Investigation of the clogging process needs time-series of relevant data over periods of several months.

In existing RBF plants with problems caused by severe clogging two counter measures may help to improve the situation: Reduction of the pumping rate and over time improving the quality of the river water.

REFERENCES

Breitung, V., 1999. Organische Schadstoffbelastung in Schwebstoffen des Rheins während Hochwasserwellen. Hydrologie und Wasserwirtschaft 43 (1), 17 -22.

Friege, H., 2001. Incentives for the improvement of the quality of river water. Proceedings of the International Riverbank Filtration Conference, Düsseldorf, Germany, November 2-4, 2000, IAWR - Rheinthemen 4, Amsterdam, pp. 13-29.

Gölz, E., Schubert, J., Liebich, D., 1991. Sohlenkolmation und Uferfiltration im Bereich des Wasserwerks Flehe (Düsseldorf). gwf-Wasser/Abwasser 132. Jahrgang, Heft 2, S. 69-76.

Gotthardt, J., 2001. 3-D Transport model to simulate peak pollution. Proceedings of the International Riverbank Filtration Conference, Düsseldorf, Germany, November 2-4, 2000, IAWR - Rheinthemen 4, Amsterdam, pp. 251 - 257.

Medema, G. J., Juhasz-Holterman, M.H.A., Luijten, J.A., 2001. Removal of micro-organisms by bank filtration in a gravel-sand soil. Proceedings of the International Riverbank Filtration Conference, Düsseldorf, Germany, November 2-4, 2000, IAWR - Rheinthemen 4, Amsterdam, pp. 161-168,

Riesen, S. van, 1975. Uferfiltratverminderung durch Selbstdichtung an Gewässersohlen. Dissertation, Universität Karlsruhe, Fakultät für Bauingenieur- und Vermessungswesen.

Schubert, J., 1984. Auswirkungen der Niedrigwasserperiode 1983 auf die Beschaffenheit des Mischgrundwassers. ARW-Jahresbericht 41, 191 - 220.

Schubert, J., 1993. Safeguarding the potable water supply in the case of accidents on rivers - experience gained from the Sandoz accident on the Rhine. 19th IWSA Congress, Budapest 1993, Technical Papers, SS 12-16.

Schubert, J., 1996. Monitoring strategy to safeguard the water supply in the case of accident-related river pollution. Monitoring Tailor-made II, Proceedings, Nunspeet, The Netherlands, September 1996, pp. 467 - 468.

Schubert, J., 2004. Significance of hydrologic aspects on RBF performance. (same issue)

HEAT AS A GROUND-WATER TRACER AT THE RUSSIAN RIVER RBF FACILITY, SONOMA COUNTY, CALIFORNIA

Jim Constantz[1], Grace W. Su[2], and Christine Hatch[3]

[1]U.S. Geological Survey, Menlo Park, CA 94025; [2]Lawrence Berkeley National Laboratory, Berkeley, CA 94720; [3]University of California, Santa Cruz, CA 95064

Abstract: Temperature is routinely collected as a water quality parameter, but only recently utilized as an environmental tracer of stream exchanges with ground water (Stonestrom and Constantz, 2003). In this paper, water levels and seasonal temperatures were used to estimate streambed hydraulic conductivities and water fluxes. Temperatures and water levels were analyzed from 3 observation wells near the Russian River RBF facility, north of Forestville, Sonoma County, CA. In addition, 9 shallow piezometers were installed in 3 cross-sections across the stream near a pair of collector wells at the RBF facility. Hydraulic conductivities and fluxes were estimated by matching simulated ground-water temperatures to the observed ground-water temperatures with an inverse modeling approach. Using temperature measurements in the shallow piezometers from 0.1 to 1.0 m below the channel, estimates of infiltration indicated a distinct area of streambed clogging near one of the RBF collector wells. For the deeper observation wells, temperature probes were located at depths between 3.5 m to 7.1 m below the channel. Estimated conductivities varied over an order of magnitude, with anisotropies of 5 (horizontal to vertical hydraulic conductivity) generally providing the best fit to observed temperatures.

Key words: Heat, temperature, water levels, hydraulic conductivity, infiltration, streambed clogging.

Stephen A. Hubbs (ed.), Riverbank Filtration Hydrology, 243–258.

1. INTRODUCTION

Quantifying stream exchanges with ground water has emerged as an important component of water resources management, partially due to increase in the conjunctive use of water. Reducing uncertainty in models used to select an optimal operation management alternative requires proper identification of the spatial and temporal variations in physical parameters, such as the hydraulic conductivity of the streambed and aquifer. Recently, heat as a tracer has been demonstrated to be a robust method for quantifying surface/ground water exchanges in a range of environments, from perennial streams in humid regions (e.g. Lapham, 1989; Silliman and Booth, 1993) to ephemeral channels in arid locations (e.g. Constantz and Thomas, 1996; Constantz et al., 2001; Constantz et al., 2002; Stonestrom and Constantz, 2003). Diurnal temperature profiles are measured and analyzed to quantify streambed fluxes and hydraulic conductivities in shallow streambed sediments (e.g., Ronan et al., 1996; Constantz, 1998; Constantz et al. 2003); while seasonal temperature variations are utilized to estimate deeper hydraulic conductivities and ground-water fluxes (e.g., Boyle and Saleem, 1979; Lapham, 1989; Taniguchi, 1993; Bartolino and Niswonger, 1999; Mihevc et al. 2001; Bravo et al., 2002; Ferguson et al., 2003; Su et al., 2004).

In observation wells, ground-water temperatures are frequently monitored along with water levels in observation wells (due to the need to monitor temperature for pressure-transducer calibrations), but these temperature values are rarely used in tandem with co-collected water-level values for assessment of the hydraulic setting. In general, ground-water temperature is evaluated with respect to water quality, but ignored as an environmental tracer. In this study, a transient ground water flow and transient heat transport model is utilized that incorporates the measured variability in water levels. These temperature and water level values are also used in this study to estimate the temporal changes in streambed-sediment hydraulic conductivity, to monitor for the presence of seasonal streambed clogging due to ground-water pumping.

The objective of this study is to demonstrate that diurnal and seasonal ground water temperature patterns combined with well water levels can be used to estimate the spatial and temporal variations in streambed hydraulic conductivities near a RBF facility. The Russian River in Sonoma County, CA was selected as an example study site to demonstrate the application of heat as tracer of ground-water movement near a pair of RBF collector wells. Temperature was monitored in 9 shallow piezometers installed in 3 cross-sections across the stream near a pair of collector wells. In addition, temperature and water-level were collected from 6 observation wells along

an extended reach of the Russian River near the RBF facility. Data from the 3 observation wells in either close proximity to the collector wells or an inflatable dam (described below) are discussed in this work. Two-dimensional ground-water flow and heat transport simulations of the region from the river to each observation well are conducted based on the measured field data. Estimates of hydraulic conductivities are obtained by fitting simulated ground water temperatures to the observed temperatures in the aquifer. The effects of formation anisotropy, layering near the streambed, river stage level, and ground water level on the temperature profiles are also investigated in the simulations.

2. RUSSIAN RIVER, SONOMA COUNTY, CA

The Russian River is located in northern California, originating in central Mendocino County, CA and flowing into the Pacific Ocean in western Sonoma County, CA. The main channel of the Russian River is about 110 miles long and flows southward from its headwaters until Mirabel Park, where the flow direction changes to predominantly westward (Figure 1).

The Russian River provides a major source of municipal water supply for Mendocino, Sonoma, and Marin Counties. For example, the Sonoma County Water Agency (SCWA) operates several collector wells along the Russian River with a maximum production capacity of 3×10^5 m^3/day (80 million gallons per day) that utilize natural filtration processes to provide water supply for over 500,000 people in Sonoma and Marin Counties. The Russian River is underlain primarily by alluvium and river channel deposits, which consist mainly of unconsolidated sands and gravels, interbedded with thin layers of silt and clay. For the area pertaining to this study, the alluvial aquifer is bounded by metamorphic bedrock (e.g., Franciscan Formation) and is considered impermeable relative to the alluvial materials (California Department of Water Resources, 1983).

To enhance water production capacity, the SCWA raises an inflatable dam typically from the spring through fall seasons, to increase the river stage and passively recharge the alluvial aquifer. In addition, the elevated stage permits diversion of river water to a series of recharge ponds located near the dam along the river. Operation of the inflatable dam creates a backwater that produces lower velocities and higher temperatures in the river compared with stream temperatures immediately upstream of the influence of the dam. This low-energy environment promotes the formation of a layer of fine-grained, biologically active material along the bottom of the river, which reduces the conductance of the riverbed.

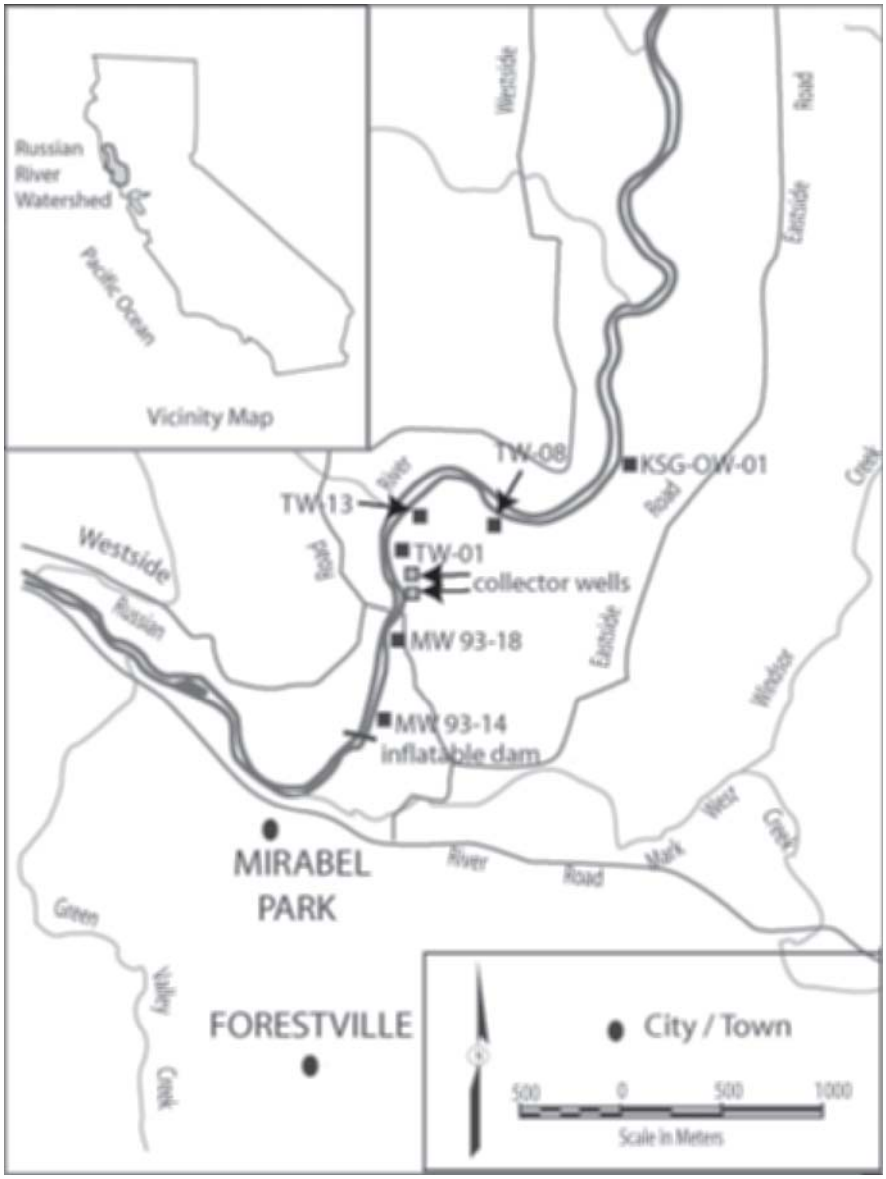

Figure 1. The location of the Russian River in northern California, and the location of the RBF collector, wells observations wells, and inflatable dam along the river in western Sonoma County.

3. PROCEDURE

3.1 Field Data

The 3 shallow piezometer cross-sections were completed in the river between MW93-18 and TW-01 (as shown in Figure 1). Each cross-section consisted of 3 two-inch diameter PVC pipes extending approximately 1 meter into the streambed at 3 locations near the left, middle, and right banks of the stream (resulting in a total of 9 shallow piezometers in 3 cross-sections). Each piezometer was instrumented with 3 single-channel temperature loggers at a shallow, middle, and deep location. One surface water temperature location was monitored at each cross-section. Water levels were determined quarterly by removing the piezometer cap and allowing the water level in the pipe to stabilize. Temperature and water-level values were used as input into 1-D inverse modeling determination of hydraulic conductivities and water fluxes.

Field values were derived from a series of deep observation wells along the river, and a set of three shallow piezometers cross-sections in the river. The locations of the observation wells along the Russian River where water levels and ground water temperatures were recorded and analyzed in this study are shown in Figure 1. The observation wells were constructed of two-inch diameter PVC well casing and a natural filter pack was used. Vented pressure transducer/temperature probes were installed inside the well casing and collected pressure head and temperature every hour. Vented pressure transducers allowed for automatic compensation of barometric pressure changes. The probes have a temperature accuracy of $\pm$ 0.25 ^{o}C and a pressure accuracy of $\pm$ 0.05 m. The location of the probes inside the well casing was determined by the length of cable used to suspend them inside the well casing, which ranged from 15-20 m. As a result, the probes were not always located within the screened interval of the observation wells. We assumed that the temperatures inside the well casing were representative of the surrounding ground water temperatures. Constantz et al. (2002) compared temperatures measured inside and outside of a PVC piezometer, demonstrating that the temperature difference was minimal during active infiltration.

3.2 Numerical Simulations

Two-dimensional simulations of ground water flow and heat transport in a near-stream environment were conducted in this study using VS2DHI (Hsieh et al., 2000), a graphical software package based on VS2DH (Healy

and Ronan, 1996). VS2DH has been successfully used to describe heat transport in variably saturated material at several sites near streams (e.g. Ronan et al., 1998; Constantz et al., 2002). In this study, measured well water levels, stream stage, and stream temperatures were used in simulations, and estimates of the hydraulic conductivities were obtained by fitting simulated ground-water temperatures to the observed temperatures from the 9 shallow piezometers, and the 6 observation wells along the Russian River. Simple 1-D simulations were used for the shallow simulations, and more complex 2-D simulations were used for the deeper simulations (see Figure 2). A porosity of 0.37 was chosen as representative of a medium sand. The heat capacities and thermal conductivity values were based on literature values for sand (Healy and Ronan, 1996). The thermal dispersivity value is usually close to zero for small spatial scales, but heterogeneities at greater scales can cause dispersivities to become significant. Longitudinal thermal dispersivity estimated in several field studies ranged from 0 - 3 m (de Marsily, 1986). A longitudinal thermal dispersivity of 0.5 m was selected in the present study. A comparison of simulated temperature profiles using longitudinal thermal dispersivities of 0.01 m and 0.5 m demonstrated that a superior fit to the observed temperatures was obtained when a dispersivity of 0.5 m was used. The horizontal scale in this study was equal to the 3 m horizontal grid spacing. In a study conducted along the Santa Clara River in Southern California (Constantz et al, 2003), a smaller scale (< 1 m) was simulated, and a thermal dispersivity of 0.01 m gave a better fit to the observed temperature profiles compared to a dispersivity of 0.5 m. The larger dispersivity value accounted for sediment heterogeneity. Since the transverse thermal dispersivity is typically about 1/10 of the longitudinal one (de Marsily, 1986), a value of 0.05 m was used in our simulations. For details of 1-D simulations modeling, see Constantz et al. (2003); and for details of 2-D simulation modeling under these conditions, see Su et al. (2004).

4. RESULTS AND DISCUSSION

Hydraulic conductivity and water flux estimates for the shallow piezometers relied on diurnal variations in temperature to estimate higher frequency changes in streambed hydraulic parameters. Figure 3 provides an example from July 2003 values of a thermograph that includes comparisons of observed values to simulated results using 1-D VS2DI inverse modeling. The best-fit match of simulated to observed streambed-sediment temperatures yielded a hydraulic conductivity of 4.17×10^{-4} m/s. The

sensitivity of sediment temperature to changes in hydraulic conductivity (and thus water flux)

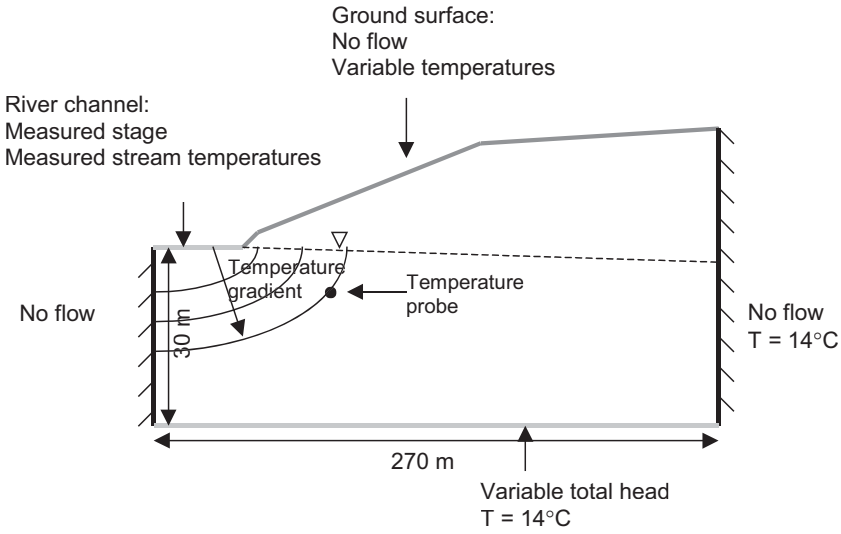

Figure 2. The cross-sectional simulation model reference frame, with the general location of the temperature-probe location in observation wells. Individual locations of temperature probes ranged from approximately 3 to 7 m below the channel.

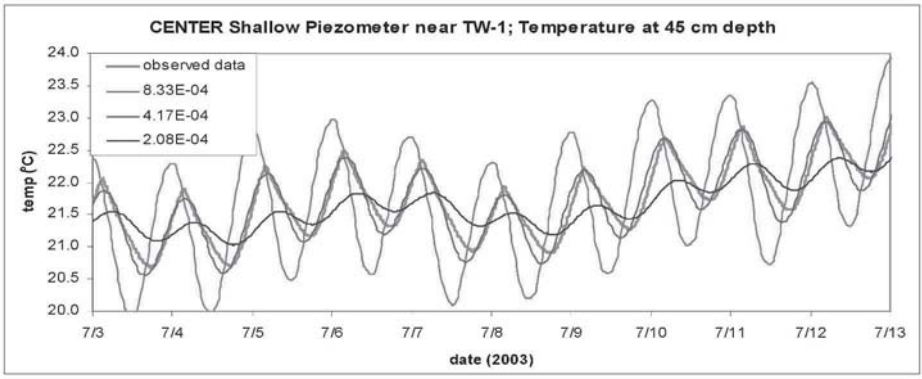

Figure 3. An example of simulated temperature matches to observed sediment-temperature values collected at 0.45 m below the channel in a shallow piezometer during July 2003. Note that best fit of simulated to observed temperatures was achieved for a hydraulic conductivity of 4.17×10^{-4} m/s.

is clearly evident when comparing the three separate fits to the observed values. Best-fit results for all 9 shallow piezometers over the entire month of June 2003 provided an average conductivity and flux values for the 9 shallow piezometers. A condensed summary of these results are depicted in Figure 4. As shown in the figure, piezometers were capped off during operation, and a riser pipe was installed quarterly (not shown) for values

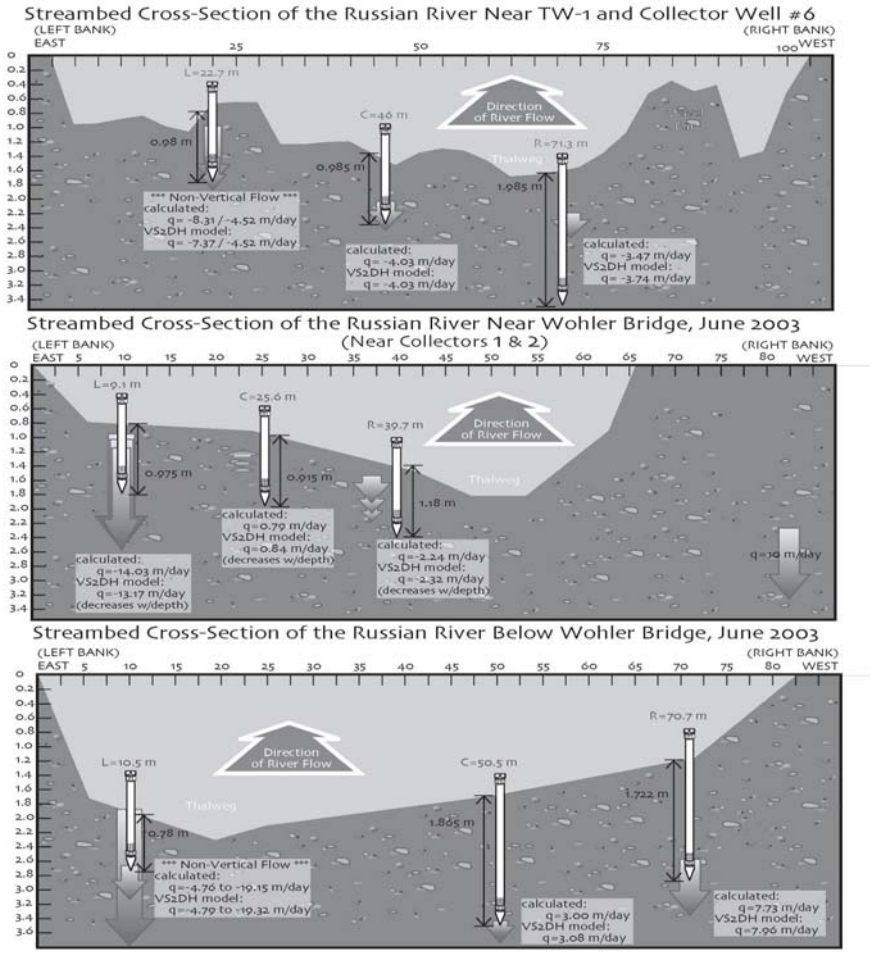

Figure 4. Temperature-based estimates of streambed fluxes, q, for each shallow piezometer. Values for q were determined by the product of measured hydraulic gradients and best-fit hydraulic conductivity values (calculated) or as a model output parameter. C is the distance from the left-bank benchmark.

retrieval to determine water levels. The figure gives a pair of temperature-based estimates of streambed fluxes, q, for each shallow piezometer. Values for q were determined by the product of measured hydraulic gradients and best-fit hydraulic conductivity values (calculated) or as a model output parameter. Independent agreement between the two methods verifies that the model output is giving comparable values for q as those based on the water levels. As expected at a RBF site, fluxes are strongly downward for most of the streambed being monitored. An exception is apparent for the location of the middle piezometer in the middle cross-section. This location appears to have an extensive low conductivity layer, which inhibits downward water movement. The slight upward movement is most likely shallow water discharging from the sediment above the imbedding layer. This evidence of streambed clogging is particularly important to track in a RBF site, because its development and potential expansion could be caused by the RBF operations and have direct impact on future RFB production.

Hydraulic conductivities near the 3 observation wells were estimated by matching simulated temperatures to the observed temperature values. Different values for the hydraulic conductivity (K) were used in the simulations, and the K value that resulted in the smallest difference between the simulated and observed temperatures for the time period analyzed was considered the best estimate of K. VS2DHI accounts for the change in K with temperature, and K values presented as results are normalized to a temperature of 20°C. Results for the 3 observation wells in close proximity to the RBF facility are presented here. For comparison, results for the other 3 wells are presented in Su et al. (2004). The simulated results at the different anisotropies (K_h/K_v = 1,2,5) in observation TW-13 are shown in Figure 5. The best fit K decreases as the anisotropy increases. The fit of the simulated temperature profiles to the observed ones for TW-13 at the different anisotropy values is nearly the same. Figure 5b depicts the sensitivity of the simulated temperature profile in well TW-13 to hydraulic conductivities an order of magnitude larger and smaller than the best-fit value (K = 4.1×10^{-4} m/s). A large hydraulic conductivity results in a temperature profile that follows the measured stream temperature, while a small K results in a nearly constant temperature profile.

The simulated results for well TW-01 are shown in Figure 6a. A good fit between the simulated and the measured temperature profiles is obtained at the different anisotropy values before August, but the fit becomes worse after August. The simulated results oscillate more than the observed temperatures at later times, indicating that a lower conductivity is needed for a better fit. Using a lower conductivity after August results in a much better

match to the observed values, as shown in Figure 6b for K_h/K_v = 5. The streambed conductivity may decrease over the summer due to the use of the

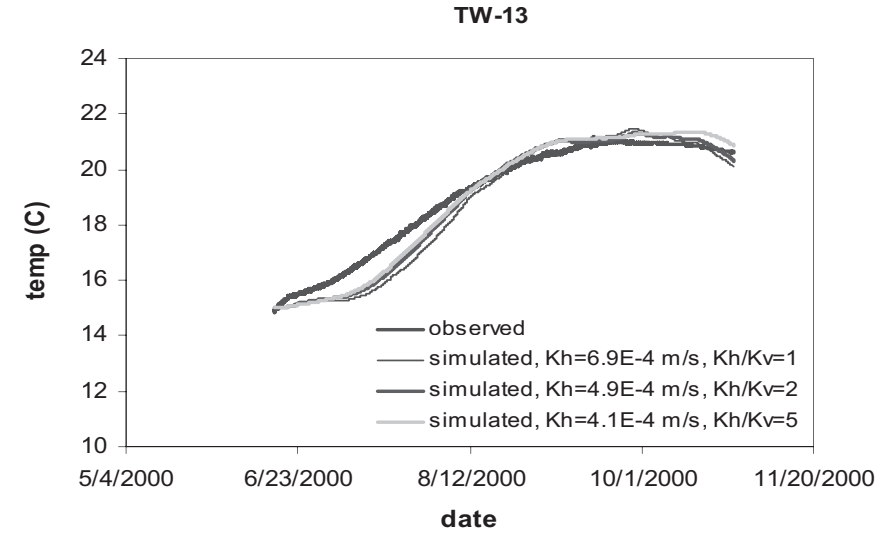

(a)

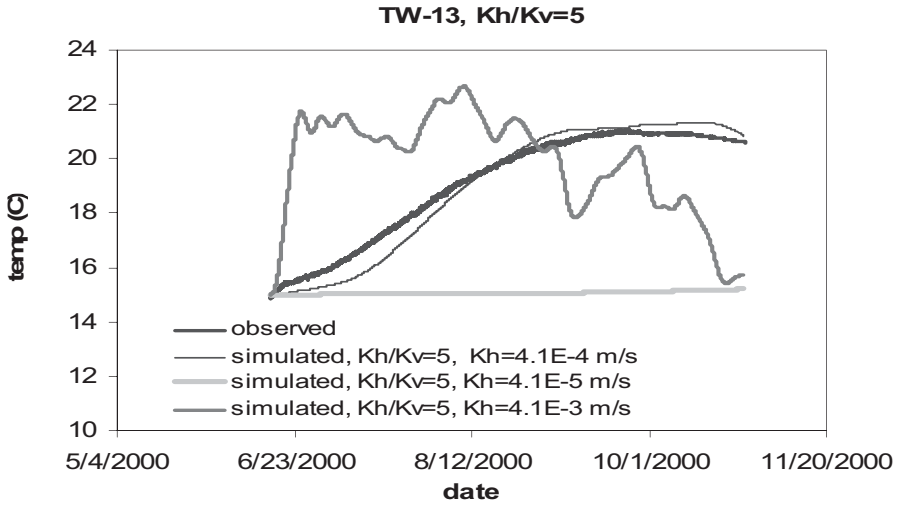

(b)

Figure 5. For observation well TW-13, (a) The best-fit sediment temperatures to observed temperatures for a range of hydraulic conductivities with horizontal to vertical anisotropic values. (b) The sensitive to large changes in K values is shown for a constant value of anisotropy.

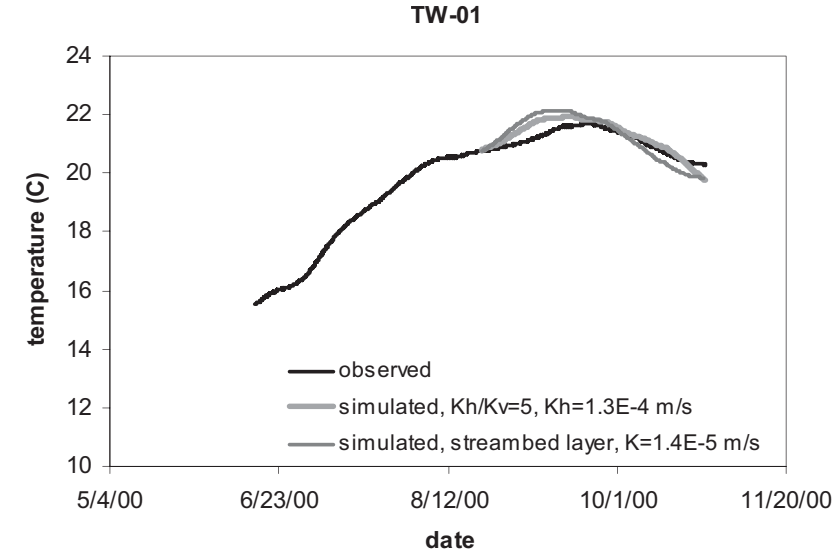

(a)

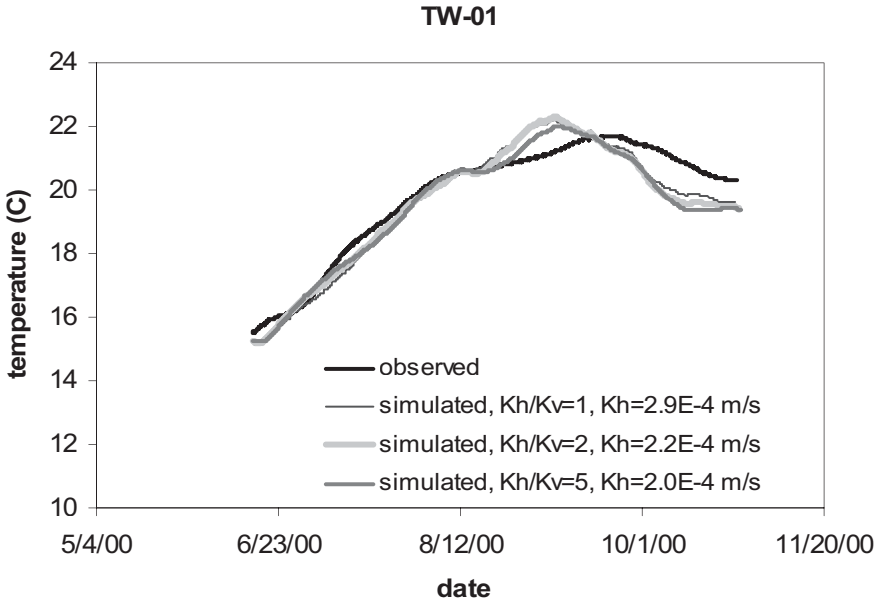

(b)

Figure 6. For observation well TW-01, (a) simulated to observed sediment temperatures are compared to show the effect of a streambed clogging layer is shown. (b) Simulated to observed sediment temperatures are compared to depict the difficulties in matching temperatures over the entire season.

inflatable dam, which increases the deposition of fine-grained sediment and organic matter plugging the streambed.

The results for well MW93-14 are shown in Figure 7a. Visual comparison of the simulated results indicates that the best fit to the observed temperatures occurs at an anisotropy of 5 before mid-August. After mid-August, the simulated temperature profile at an anisotropy of 5 is much lower and oscillates more than the observed values. A hydraulic conductivity over 35% less than the best fit value before mid-August (1.9×10^{-4} m/s) is necessary to obtain a good fit to the measured profile after mid-August for $K_h/K_v = 5$ (Figure 7b). Well MW93-14 is located just behind the inflatable dam, so the decrease in K is probably due to the accumulation of fine-grained sediments and organic matter behind the inflatable dam. Ground water temperatures and the effective hydraulic conductivity are sensitive to the changes in the hydraulic conductivity along the streambed. The root-mean square error (RMSE) was used to quantify the goodness-of-fit between the simulated and observed results at the different anisotropies. For TW-01, $K_h/K_v = 2$ and 5 give better fits to the values than $K_h/K_v = 1$ before mid-August. For well TW-13, $K_h/K_v = 5$ gives a better fit than $K_h/K_v = 1$ and 2. The RMSE for wells MW93-14 decreases significantly as the anisotropy increases. Based on these results, anisotropies of 5 generally give the best match to the observed temperatures. For a detailed discussion of model sensitivity to sediment heterogeneity and river stage, see Su et al. (2004). Note that results suggest that river discharge is more important than river stage in determining fluxes, as a result of enhanced scour created at higher discharge.

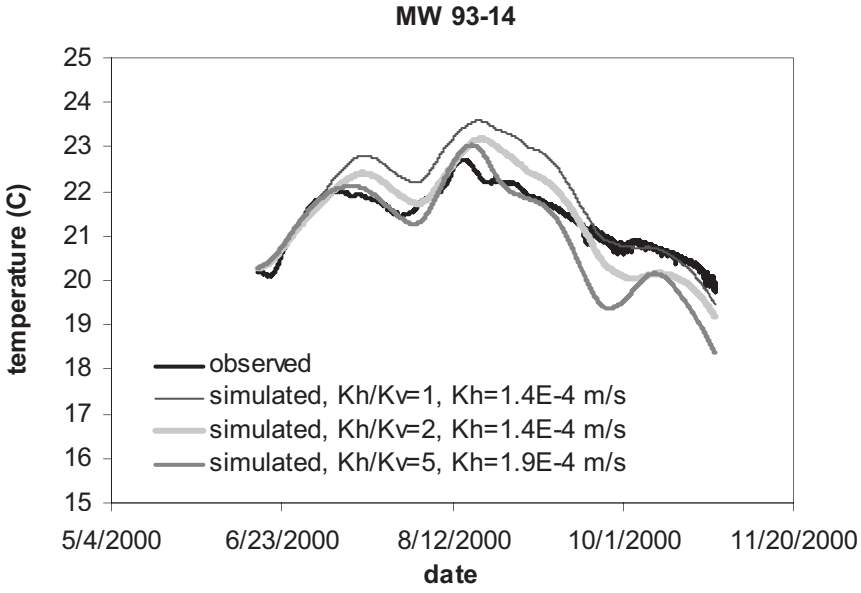

(a)

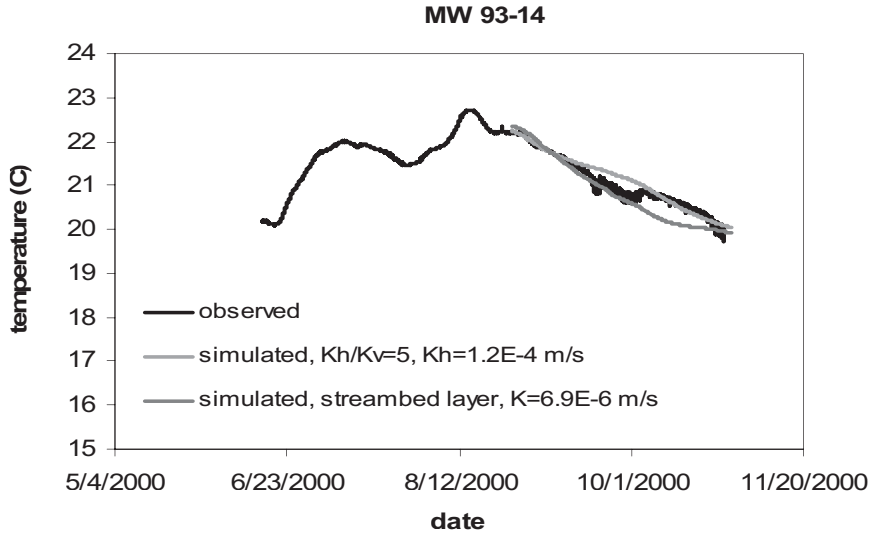

(b)

Figure 7. For observation well MW93-14, (a) simulated to observed sediment temperatures are compared to depict the difficulties in matching temperatures over the entire season. (b) Simulated to observed sediment temperatures are shown when best-fit hydraulic conductivities are matched for the late season values only.

5. SUMMARY AND CONCLUSIONS

Both diurnal and seasonal ground water temperature profiles and water levels were used to estimate alluvial aquifer hydraulic conductivities at our example study site, the Russian River in Sonoma County, CA. The seasonal ground water temperatures in the 6 wells analyzed along this site varied by less than 0.2 ^{o}C in 2 wells to nearly 8 ^{o}C in the other 4 wells. The range in observed temperature fluctuations was primarily attributed to the proximity of the RBF facility. Based on these temperature variations, the estimated conductivities varied up to two orders of magnitude over these 6 locations. The simulated temperature profiles generally fit the observed ones best for an anisotropic value of 5.

In some locations, a change in the observed temperature profile occurred through the summer and fall, most likely due to deposition of fine-grained sediment and organic matter plugging the streambed. A reasonable fit to this change in temperature profile was obtained by decreasing the effective hydraulic conductivity in the simulations. Other factors, such as changes in the ground water level and river stage were demonstrated not to be the cause of the change in the temperature profile. Simulations were also conducted where a thin low conductivity layer was placed below the streambed to represent the plugging that had occurred, and a reasonable fit to the change in the observed temperature profiles was also obtained. The most significant decrease in conductivity occurred in the region closest to the dam.

The shallow piezometer cross-sections relied on the diurnal temperature variations to give a shorter frequency estimate of conductivity changes. Results for June 2003 were given as an example to depict the spatial variability apparent near the RBF facility. A surficial region within which clogging may be spreading, was implied from the temperature-based estimates of water fluxes. Continued thermal monitoring should aid in tracking future patterns of clogging in the shallow streambed near the RBF facility

REFERENCES

Bartolino, J.R. and Niswonger, R.G, 1999, Numerical simulation of vertical ground-water flux of the Rio Grande from ground-water temperature profiles, central New Mexico, U.S. Geological Survey Water-Resources Investigations Report 99-4212, pp. 4-24.

Boyle, J.M. and Saleem, Z.A., 1979. Determination of recharge rates using temperature-depth profiles in wells, Water Resources Research, 15(6): 1616-1622.

Bravo, H. R., Feng, J., and Hunt, R. J., 2002, Using groundwater temperature data to constrain parameter estimation in a groundwater flow model of a wetland system. Water Resources Research, 38(8), 10.1029/2000WR000172: 28-1-28-14.

California Department of Water Resources, 1983, Evaluation of ground water resources: Sonoma County, Volume 5, Alexander Valley and Healdsburg Area.

Constantz, J. and Thomas, C.L., 1996, The use of streambed temperature profiles to estimate the depth, duration, and rate of percolation beneath arroyos, Water Resources Research, 32(12): 3597-3602.

Constantz, J. 1998, Interaction between stream temperature, streamflow, and groundwater exchanges in alpine streams, Water Resour. Res., vol. 34(7), 1609-1615.

Constantz, J., Stonestrom, D. A., Stewart, A.E., Niswonger, R., and Smith. T.R., 2001, Analysis of streambed temperatures in ephemeral channels to determine streamflow frequency and duration, Water Resources Research, 37(2): 317-328.

Constantz, J., Stewart, A.E., Niswonger, R., and Sarma, L., 2002, Analysis of temperature profiles for investigating stream losses beneath ephemeral channels, Water Resources Research, 38(12) 52-1 – 52-13

Constantz, J., Cox, M.H., and Su, G.W., 2003, Comparison of heat and bromide as ground water tracers near streams, Ground Water, 41(5), 647-656.

de Marsily, G. 1986. Quantitative hydrogeology: Groundwater hydrology for engineers. Academic Press, San Diego, CA, 440 pp.

Ferguson, G., Woodbury, A.D., and Matile, G.L.D., 2003, Estimating Deep Recharge Rates Beneath an Interlobate Moraine Using Temperature Logs, Ground Water, 41(5), 640-646.

Healy, R.W., and Ronan, A.D., 1996, Documentation of computer program VS2DH for simulation of energy transport in variably saturated porous media. U.S. Geological Survey Water-Resources Investigations Report 96-4230.

Hsieh, P.A., Wingle, W., and Healy, R.W., 2000, VS2DI--A graphical software package for simulating fluid flow and solute or energy transport in variably saturated porous media. U.S. Geological Survey Water-Resources Investigations Report 99-4130.

Lapham, W.W. 1989. Use of temperature profiles beneath streams to determine rates of vertical ground water flow and vertical hydraulic conductivity. U.S. Geol. Survey Water Supply Paper 2337.

Mihevc, T., Pohll, G., Niswonger, R., and Stevick, E., 2001, Truckee canal seepage analysis in the Fernley/Wadsworth area. Desert Research Institute Publication No. 41176.

Ronan, A.D., Prudic, D.E., Thodal, C.E., and Constantz, J., 1998, Field study and simulation of diurnal temperature effects on infiltration and variably saturated flow beneath an ephemeral stream, Water Resour. Res., vol.34(9), 2197-2153.

Silliman, S.E. and Booth, D.F., 1993, Analysis of time-series measurements of sediment temperature for identification of gaining vs. losing portions of Judy Creek, Indiana, Journal of Hydrology, 146(1): 131-148.

Stonestrom, D. A. and Constantz, J., 2003. Heat as a tool for studying the movement of ground water near streams. U.S. Geological Survey Circular 1260, 96 p.

Su, G.W., Jasperse, J., Seymour, D., and Constantz, J, 2004, Estimates of hydraulic conductivity in an alluvial system using temperature, Ground Water, 42(6), 890-901.

Taniguchi, M., 1993, Evaluation of vertical groundwater fluxes and thermal properties of aquifers based on transient temperature-depth profiles, Water Resources Research, 29(7), 2021-2026.

MONITORING CLOGGING OF A RBF-SYSTEM AT THE RIVER ENNS, AUSTRIA

B. Wett
Institute of Environmental Engineering, University of Innsbruck, Austria

Abstract: This presentation comprises hydraulic aspects of a research project at a bank filtration site at the oligotrophic alpine river Enns in Austria. The project was started in order to deepen the understanding of filtration and transformation processes which take place, where they take place and how stable they are throughout the year. Extensive monitoring equipment has been installed in the river bank focusing on the first meter of the flow-path from the river to the well. During the start-up period of well production the built-up of a clogging layer is monitored. Due to the dynamic interrelation between infiltration rate and hydraulic conductivity of the riverbed, clogging shows a balancing effect on infiltration along the bank stretch.

Key words: River bank filtration, clogging, conductivity, infiltration rate, flow-path

1. METHODOLOGY AND SITE DESCRIPTION

The River Enns drains an average annual amount of 6.6 million m^3 water from an area of 6.080 km^2 to the Danube. The 254 km long river crosses three main geological zones, from the limestone mountains in the south to the flysch zone upstream of the city of Steyr, where the investigated filtration site is situated, to the foothills of the Alps. During the last two glacial periods a huge amount of gravel was transported from the Alps and formed terraces on both sides of the river. In the area of the considered bank filtration site the river has completely cut through the gravel layer and the impermeable flysch layer forms the river bottom (Hasenleithner et al., 1999).

Stephen A. Hubbs (ed.), Riverbank Filtration Hydrology, 259–280.

The Ennskraft, an Austrian power supply enterprise which is in charge of the research project reported here, operates 10 hydropower stations along the River Enns. The investigated bank filtration well is situated about 50 m from the river bank, 750 m downstream of a hydro power plant (HPP Rosenau) and at the beginning of the 5 km long reservoir of the next power plant (HPP Garsten). No measures had been taken to seal the bank of the reservoir in the area of the study site. At this particular location the river stage is determined by the dam at a level of 302.0 m a.s.l. and the measured cross-section area of the river is 280 m^2. The minimum discharge of 70 m^3/s results in a mean flow velocity of 0.25 m/s. The mean flow velocity achieves the maximum annual value of 1.5 m/s at a discharge of 540 m^3/s and a cross-sectional area of 350 m^2 (maximum discharge during a one year monitoring period reaching the annual high-water level of 302.8 m a.s.l.). About 400,000 m^3 of sediment per year settles in the Enns reservoirs and a measured suspended solids concentration of only 8 mg/l on average passes the reservoirs. The concentration of suspended solids and discharge show hardly any correlation with the exception of significant high-water events. Since the river bed is cut into the dense flysch zone the river water infiltrates almost exclusively through the bank and not the bottom. Between river and well the aquifer thickness is about 5 m and the total thickness of the gravel layer is 15 m (Ingerle et al., 1999, Wett et al., 2002).

Organic loading is very low (the DOC concentration varies between 1 and 2 mg/L), and river water is saturated with oxygen (greater than 10 mg/L). Groundwater quality reflects the trends of land use and intensity of agriculture along the river. The further downstream the river, the higher the nitrate and pesticides concentrations are in the groundwater. In the region of the filtration site, groundwater shows nitrate concentrations of about 50 mg/L. The enrichment of the groundwater by river filtrate (less than 5 mg/L nitrate) offers a solution to obtain nitrate concentrations in agreement with drinking-water standards.

A high-grade steel box with windows for visual observation and video recording of river bed clogging was installed in the riverbank. One set of five probes was arranged at the upstream side of the box in natural sediment (multi-level Probe MLF) and two sets of five probes (MLD and MLE) were installed downstream in specified filter sand (0 to 4 mm) to measure hydraulic heads and obtain water samples. Two further probes were installed between the river and the well (PLE 6 m and PLF 18 m off the river) and one probe (KHB01) 7 m on the landward side of the well (KHB02) (Fig.1). Water quality has been monitored during a one year period at all these probes along the flow-path (Fig.2). A sodium-chloride tracer test was conducted in order to investigate the migration time.

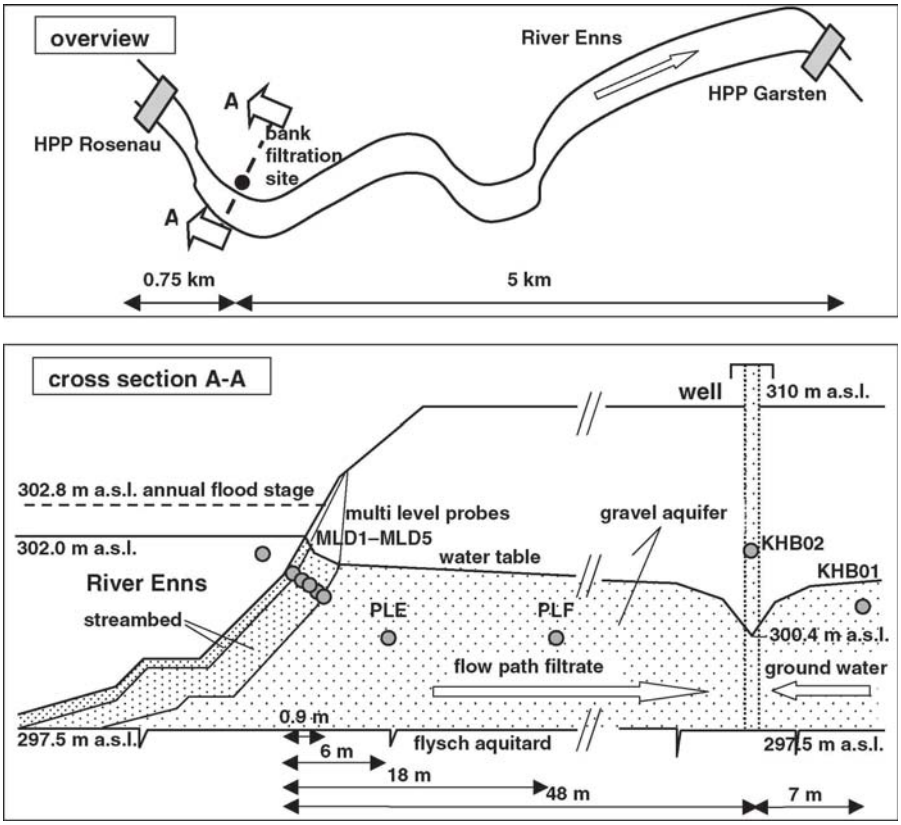

Figure 1. Schematic overview and cross-section of the bank filtration site on the Enns River, a tributary of the Danube River

Multilevel probes MLD, MLE and MLF are arranged at depths of 0.15, 0.30, 0.50, 0.70 and 0.90 m beneath riverbed surface. Water levels in the probes correspond with the levels of graduated glass pipes within the steel box (Fig.3). An analysis of hydraulic head data and relative variations of head differences allows for filter velocity calculations.

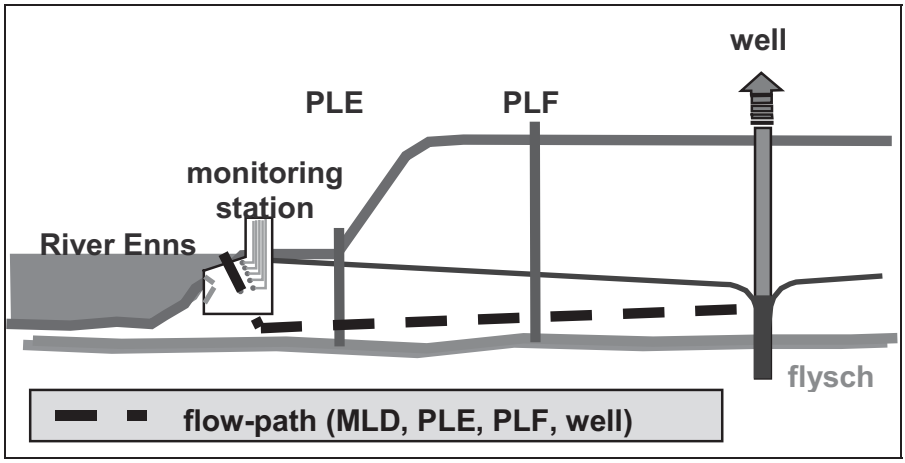

Figure 2. Installed monitoring infrastructure along the flow-path from the river to the well

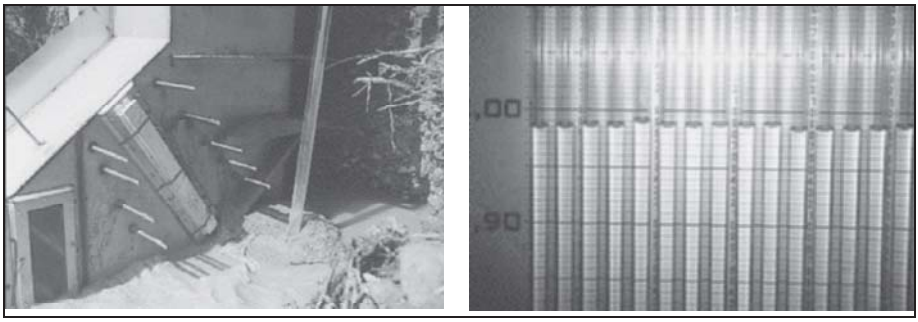

Figure 3. Outside and inside views of the monitoring station: a) Multilevel probes MLD and MLF at the downstream side before refilling of filter sand (left picture); b) Piezometric glass-pipes connected to the multilevel probes before start-up of well production (right picture)

2. RESULTS

2.1 River Bed Clogging and Hydraulic Slope along the Flow-Path

Fig.4 shows the data from the multilevel probe MLD in the riverbed. Before the well was put into operation the levels of ground- and surface

water had been balanced and no in- or exfiltration could be observed (compare Fig.3b: no head losses between MLD1 and MLD5). Then in October 1997 the pump was switched on delivering a constant 20 l/s. The relevant head losses developed at the surface of the riverbed, in the first 15 cm respectively (i.e. the water level difference in the probes represented by the vertical distance between profile Enns and profile MLD1 in Fig.4). Obviously the riverbed clogged in this zone which led to a major loss of the potential for infiltration flow. Hence the seepage rate reduces and as a further consequence the head losses in the deeper zones decrease (Fig.4). The continuous development of increasing water level differences at the surface and reduced differences in deeper zones was interrupted by high-water.

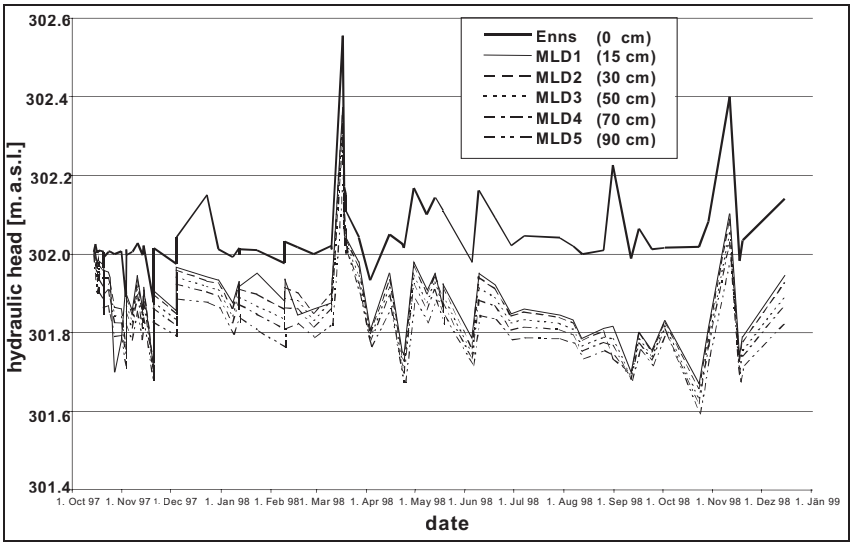

Figure 4. Hydraulic head profiles at 5 different zones in the riverbed (weekly measurement)

The most significant flood during the observation period occurred in March 1998 which is represented by the peak of the Enns water level in Fig.4. During the flood the water level difference between River Enns and probe MLD5 increased from 0.2 m to 0.3 m. Under the assumption of a constant hydraulic conductivity the infiltration rate increased by 50%. Reduced water level differences after the high water indicate an abrupt decrease of the potential losses. At first inspection, the measured profiles imply that during the flood the hydraulic conductivity of the surface layer of the riverbed was reset to the state at the beginning of the operation period. In fact, the dense surface layer was not eroded but the infiltration velocity was reduced. This fact is confirmed by the observation that the water level

differences of the 90 cm deep zone also decreased: a zone that is hardly affected by particle intrusion. Consequently the hypothesis is stated that the measured head losses vary due to two different influences: under average discharge conditions water level differences increase because of riverbed clogging (decreasing *kf* in equation 1). After flooding the water level differences are reduced at rather constant hydraulic conductivity because of a lower seepage rate *v* due to bank storage effects.

$$\frac{dH}{ds} = \frac{v}{kf} \qquad \ldots(1)$$

dH - water level difference in m
ds - distance in m
ν - Darcy flow velocity in m/s
kf - hydraulic conductivity in m/s

A discussion of measured head gradients requires a clear distinction of both impact factors – conductivity and flow velocity. Hydraulic conductivity refers to flow resistance generated by the filter medium (riverbed characteristics at a stable riverbank varies only in zones very close to the surface of the bed) and the filtrate medium (viscosity of the water shows seasonal variations due to temperature changes). Time variant development of hydraulic slope along the flow-path displays not only short-term interactions between seepage and conductivity during high water periods but also the long-term built-up of a clogging layer.

Another approach sorts out the three corresponding variables of equation 1) by a comparison of head losses, velocity and conductivity at the first 6 m and the consecutive 12 m of the flow-path. During the monitoring period the potential loss of the filtrate flow in the aquifer represented by the section PLE-PLF decreased to half of its initial value ΔH_{start} (Fig.5). Assuming constant conductivity (no clogging) more than 6 m off the river equation 1) is applied and results in a 50 % drop down of the flow velocity:

$$\frac{v_{end}}{v_{start}} = \frac{kf * \Delta H_{end} / \Delta s}{kf * \Delta H_{start} / \Delta s} = \frac{\Delta H_{end}}{\Delta H_{start}} = \frac{2.5}{5} = 0.5 \qquad \ldots (2)$$

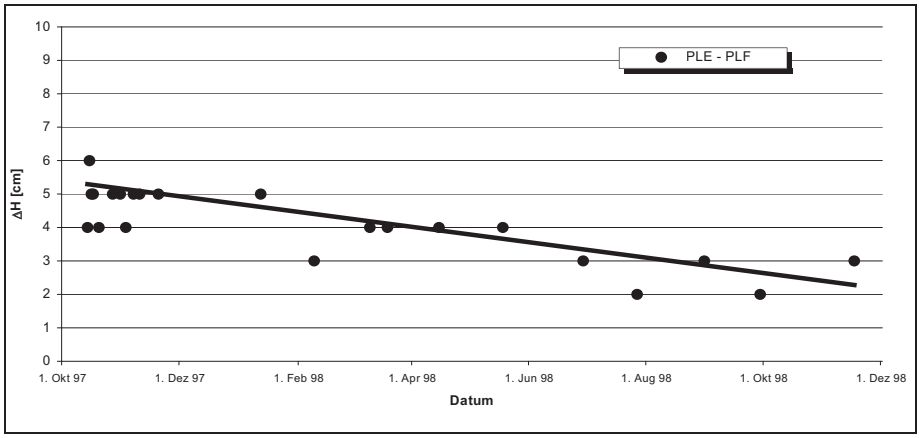

Figure 5. Plot of decreasing head losses between Probe PLE and Probe PLF against time

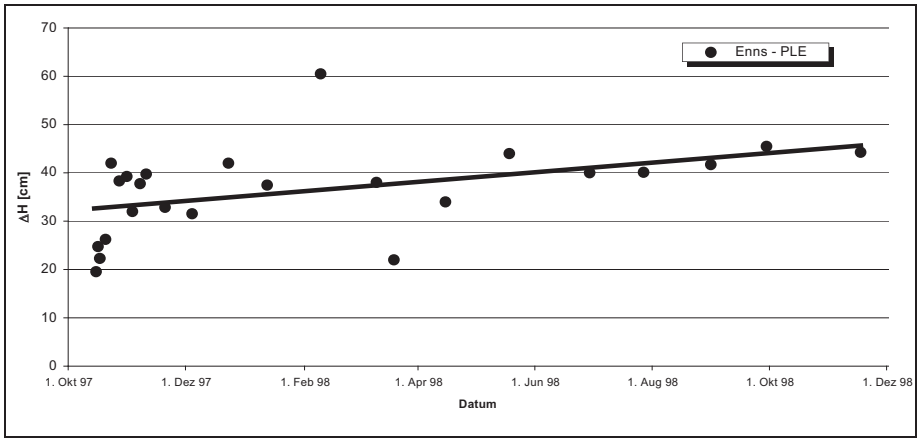

Figure 6. Plot of increasing head losses between River Enns and Probe PLE against time

Different from the assumption above, a change in conductivity is expected in the river bed due to clogging. But the ratio between initial and final velocity stays the same as above according to continuity. One more application of equation 1) in this case study indicates a decrease of conductivity of more than 50 % (Fig.6):

$$\frac{v_{end}}{v_{start}} = \frac{kf_{end} * \Delta H_{end} / \Delta s}{kf_{start} * \Delta H_{start} / \Delta s} = \frac{kf_{end} * \Delta H_{end}}{kf_{start} * \Delta H_{start}} = \frac{kf_{end} * 44}{kf_{start} * 33} = 0.5 \qquad ...(3)$$

$$kf_{end} = kf_{start} * 0.5 * \frac{33}{44} = kf_{start} * \frac{3}{8}$$

The relationship of head losses to the flow distance – i.e. the hydraulic slope – gives even more evidence to the fact that clogging takes effect at the surface of the river bed. The slope in the top layer with 15 cm thickness increases steeply in comparison to the minor and rather constant slope in deeper zones (Fig.7). Significant variations of the slope in the clogging layer are mainly caused by stream stage fluctuations.

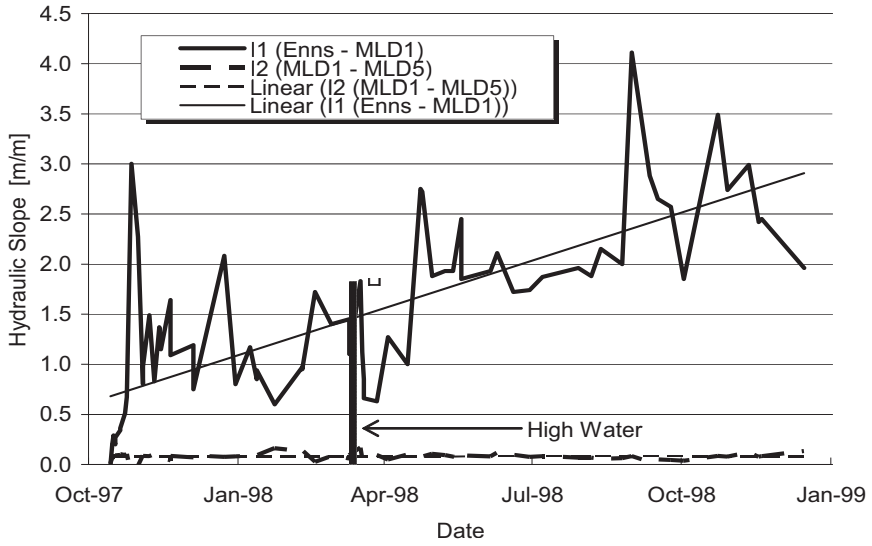

Figure 7. Hydraulic slope at the surface of the river bed (Enns – MLD1; 15cm) and in deeper zones (MLD1 – MLD5; 75 cm)

2.2 River Bed Clogging and Hydraulic Conductivity

It is common practice to quantify hydraulic conductivity of aquifers by field tests. At specified well production rates the conductivity is calculated from the drawdown of the water table measured in neighbouring probes. The same procedure has been applied to small scale pumping tests in the multi level probes at the monitoring stations. Steady state water table in the river bed (i.e. piezometric head in the probes; compare Fig.3) was considered as a

reference level. Then the sampling valve of one probe was opened and water flow rate and drawdown of the pressure head in the other probes was measured. This test was repeated at all levels of the probe and resulting *kf* values were averaged under consideration of the temperature influence (kf_2 in Fig.8). The conductivity in the top layer kf_1 is related to kf_2 according to equation 3) and the measured hydraulic slopes.

Table 1. Data form of a small scale pumping test in Probe MLD for the calculation of hydraulic conductivities in different river bed zones; grey cells indicate probes with water extraction (Ingerle et al., 1999)

Probe	Head	1	2	3	4	5	ml	sec	**l/sec**
Reference		302	302	302	302	302			
MLD1	301.874	0.41	0.14	0.13	0.145	0.175	390	30.25	**0.0129**
MLD2	301.865	0.145	0.42	0.145	0.15	0.18	500	28.38	**0.0176**
MLD3	301.85	0.065	0.09	0.515	0.175	0.185	760	29.13	**0.0261**
MLD4	301.83	0.112	0.013	0.167	0.58	0.2	880	29.93	**0.0294**
MLD5	301.795	0.102	0.117	0.137	0.17	0.735	1010	29.26	**0.0345**

The resulting profiles of river bed conductivity against time allow a comparison of clogging mechanisms in natural sediment and filter sand layers. The conductivity of the top layer in the area with natural sediment backfill (kf_1, MLF) is relatively high at the beginning of the monitoring period and decreases quickly. Despite different initial values, the conductivities kf_1 of the clogging layers at the surface after one year of pumping are in a close range, about one order of magnitude lower than at the beginning. Obviously the final conductivity of the top layer shows dependency of the bank material and the initial conductivity.

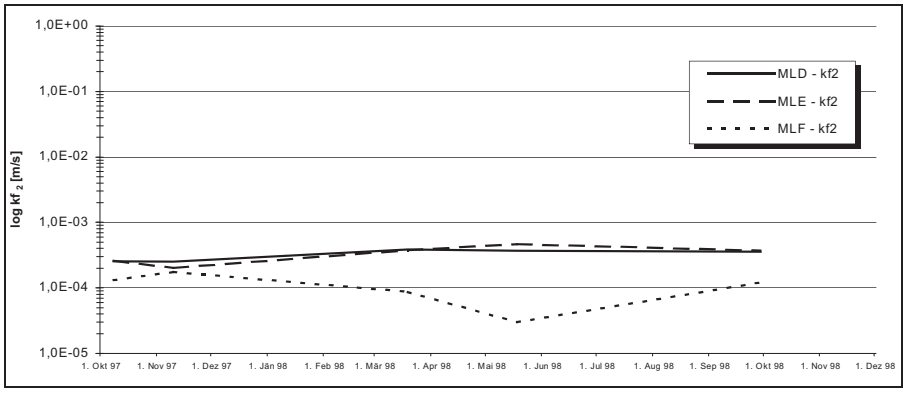

Figure 8. Profiles of hydraulic conductivity kf2 of the river bed zone between 15 and 90 cm

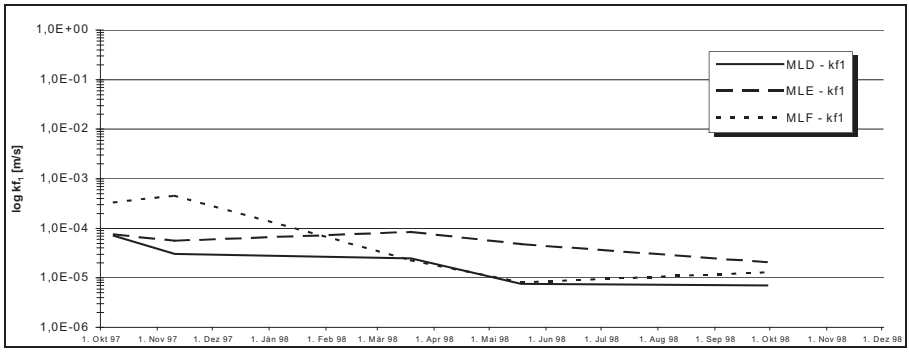

Figure 9. Profiles of hydraulic conductivity kf1 at the first 10 cm of the flow-path

Conductivities kf_1 of the top layer reach a stable state after 7 months of operation. This indicates a stagnation of the surface clogging process. Counter to this observation, measured head losses indicate continued clogging. The discrepancy is attributed to decreasing temperature and viscosity of water at the end of the monitoring period.

Conductivity kf_2 in deeper zones is rather constant but significantly higher in the uniform sand layer. Obviously the build-up of the clogging layer at the surface with decreasing conductivity kf_1 efficiently prevents intrusion of particles and limits the range of clogging effects. Higher hydraulic conductivity in the filter sand causes a significantly higher filter velocity than in natural sediment (the mean filter velocity is 1.99×10^{-5} m/s and 0.83×10^{-5} m/s, respectively).

2.3 Applicability of the Conventional Filtration Theory to River Bed Clogging

The Conventional Filtration Theory deals with the development of a flow resistance during the filtration or dewatering of a suspension. The filter medium induces the initial flow resistance and prevents a wash-out of solids. Then the retained particles generate an additional flow resistance and physical properties of the filter cake and the operating pressure can be related to the filtrate flow. Temperature dependences of physical properties such as density and viscosity can be considered.

On the basis of the two-resistance theory and the power-law type constitutive equations, researchers such as Cleveland *et al.* (1996), Sorensen et al. (1996) and Tiller and Kwon (1998) investigated the behaviour of highly compactable filter cakes (Lee et Wang, 2000). The two-resistance model based on the cake filtration theory is a well established mathematical model. In this model, the particles that are too large to enter filter pores are assumed to form a cake layer on the medium surface, thus providing additional resistance to filtration (Fig.10).

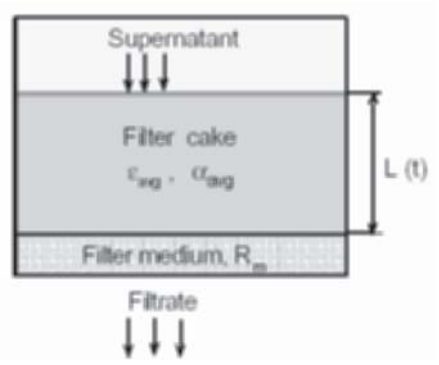

Figure 10. Scheme of the two-resistance approach

$$\frac{t}{V(t)} = \frac{\alpha_{avg}(t) \cdot c(t) \cdot \mu}{2 \cdot \Delta p(t)} \cdot V(t) + \frac{R_m \cdot \mu}{\Delta p(t)} \qquad \ldots (4)$$

where V represents the cumulative specific filtrate volume, Δp pressure loss, μ viscosity and c involves the porosity ε and densities ρ of solids and water. The medium resistance R_m is assumed as constant throughout the filtration process. At each time step the properties of the newly formed cake layer (porosity $\varepsilon(t)$ and specific cake resistance $\alpha(t)$) are characterised by average filter cake properties (homogeneous filter cake). The assumption implicit in

the derivation of equation (4) is that as the sludge slurry is filtered, each increment of slurry deposits its solids in the cake and the associated water passes through the filter medium as filtrate. The cake thickness increases up to the point where all the solids are deposited or until unsaturated conditions are reached and filtration ends. In modelling cake filtration processes, it is necessary to know the behaviour of the cake's compressibility and permeability (Das et Ramarao, 2001).

The parameters used in the filtration theory to describe the cake characteristics during the process are the specific cake resistance α_{avg} and the cake porosity ε_{avg}. The variation of these parameters is described by equations that are frequently referred to as constitutive relationships. Constitutive equations describe the deformation behaviour of the solids in a cake and can only be determined experimentally. Tiller proposed the following constitutive equations:

$$\alpha_{avg}(t) = \alpha_0 \left(1 + \frac{\Delta P(t)}{P_a} \right)^n \quad \ldots (5)$$

$$\left(1 - \varepsilon_{avg}(t)\right) = \left(1 - \varepsilon_0\right) \left(1 + \frac{\Delta P(t)}{P_a} \right)^{\beta} \quad \ldots (6)$$

where α_0 and ε_0 are specific filtration resistance and porosity at zero compacting pressure; P_a is an arbitrary normalising pressure; β and n are material specific parameters. n is called coefficient of compressibility, and a commonly determined value of n for highly organic sludge suspensions is 1 (e.g. for activated sludge, Sorensen and Hansen, 1993). It indicates a high degree of compressibility. Generally, the constitutive relations are determined by independent experiments in an apparatus known as the compression-permeability cell (C-P-cell). Another route is to obtain the parameters from experimental filtration data.

Average specific filtration resistance α_{avg} and porosity ε_{avg} (included in the density parameter $c(t)$) can be determined from the plot of t/V versus V based on the conventional filtration equation (4). The average specific cake resistance α_{avg} can be calculated from the slope of this plot, while the medium resistance R_m corresponds to the value of the y-intercept of the line. In the course of the filtration process the flow resistance of the cake dominates the overall filtration performance. It has to be considered that the filter medium resistance (river bed) is not negligible vs. the cake resistance (clogging layer) during the initial period, because at the beginning of the process the filter medium offers the major resistance to liquid flow and induces the built-up of the cake. The river bed forms the structural base of the cake.

Cake filtration theory is confirmed by the empirical findings presented above (section 2.3) that the final conductivity of the clogging-layer is not depending on the flow resistance of the filter medium or the river bed material respectively. The driving pressure of the filtration process (river stage) shows a proportional influence on the filtrate production in case no clogging layer has developed. If the river bed is covered by a clogging layer (filter cake) increased pressure significantly enhances the flow resistance of the cake. This effect occurs especially at high compressibility of the solids, i.e. at high organic content of the sludge.

2.4 River Bed Clogging and Temperature

Water temperature represents another significant influence on the hydraulic conductivity. This relation can be described by the formula of Poisenille-Chardabellas:

$$kf(T°) = fT(T°) * kf(10°) = \\ = \frac{1 + 0.0337 * T + 0{,}00022 * T^2}{1{,}359} * kf(10°) \qquad ...(7)$$

fT(T°) - temperature coefficient transforming hydraulic conductivity at 10 °C to T°C

kf(T°) - hydraulic conductivity in m/s at a temperature of T°C

Applied to the temperature conditions of the River Enns (seasonal temperature variations of 13 °C) the maximum hydraulic conductivity of the river bank during summer is 50 % higher than the minimum value during winter (Fig.11). Decreasing water temperatures in the autumn cause higher potential losses during infiltration. Therefore the water level profiles in Fig.4 imply continued clogging during the fall, but the temperature change is the main reason for increased water level differences.

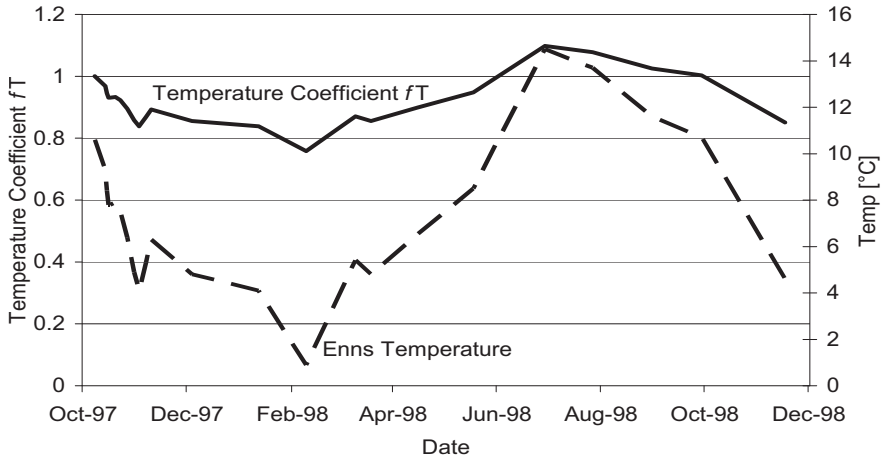

Figure 11. Temperature of the River Enns and its influence on the hydraulic conductivity of the river bed

2.5 River Bed Clogging and Infiltration Rates

Clogging significantly affects infiltration rates and vice versa infiltration promotes clogging. This interrelation can be depicted in a simplified manner by the application of analytical approaches. The following basic assumptions are taken into account:

- Plane water table (without filtrate abstraction, groundwater table = surface water level); well and river bottom reach the aquitard
- Radial flow to the well neglecting tangential velocity components (straight horizontal streamlines)
- Potential loss equals hydraulic slope (straight vertical equipotential lines)

An initial simplification neglects any clogging of the river bed leading to a k_A/k_{BF} ratio of 1. Following this assumption the boundary head $H(R)$ at the river-aquifer interface is constant along the bank at increasing radial distance R to the well (Figure 12). Based on continuity and Darcy's law, infiltration velocity $v(R)$ can be derived:

Continuity:

$$v(r) = v(R) * \frac{R * H(R)}{r * H(r)} \qquad ...(8)$$

Darcy (Dupuit's approach):

$$v(r) = kf * \frac{d\Phi}{dr} \cong kf * \frac{dH}{dr} \qquad ...(9)$$

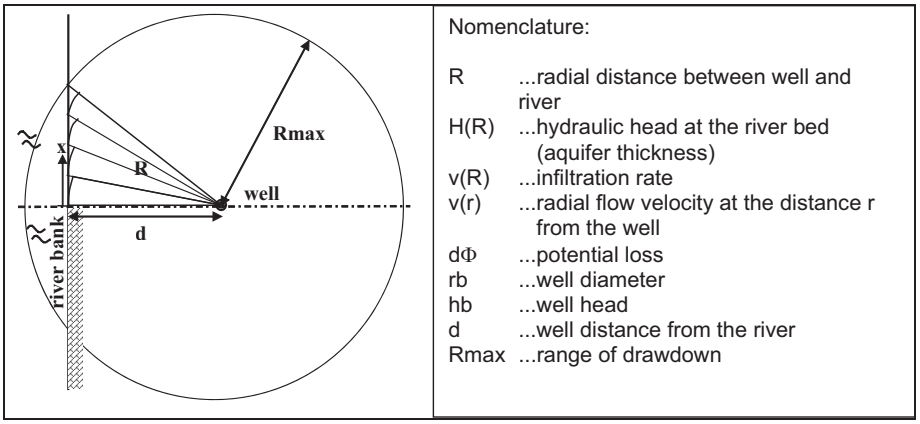

Figure 12. Discretisation of the considered infiltration area of a production well

The infiltration rate results from coupling equation 8) and 9), and from integration of hydraulic head *H(r)* and radial distance *r* along the flow path (from *R* to *rb*):

$$v(R) = \frac{(H(R)^2 - hb^2) * kf}{2 * R * H(R) * (\ln(R) - \ln(rb))} \qquad ...(10)$$

The analytical approach 7) results in a velocity distribution showing a significant peak in the central infiltration area (Fig. 13). According to the presented findings about the correlation between infiltration rate and reduction potential, a break-through of poorly filtered river water might be expected. But high infiltration rates and joint intrusion of fine particles cause a built-up of an additional clogging layer during the initial operation phase of the production well. Measurements of the potential loss in the river bed at the end of the 1-year monitoring period confirm the balancing interrelation of infiltration and clogging. Measured profiles of hydraulic head

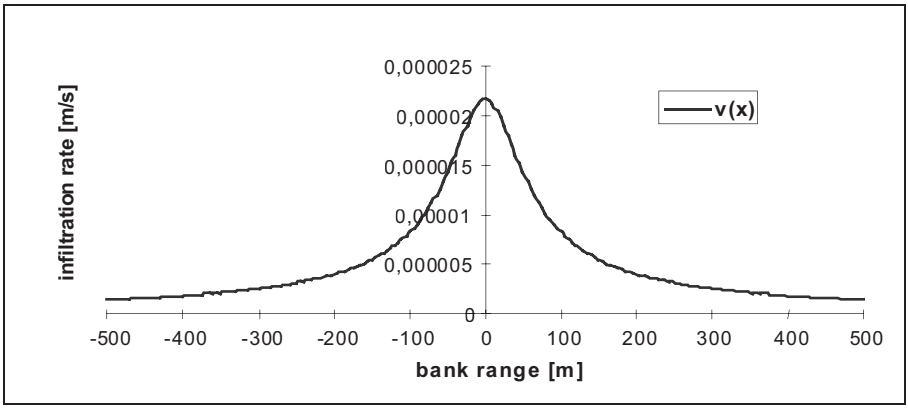

Figure 13. Analytically determined distribution of infiltration rates along the down- and upstream stretches of the bank (no clogging assumed; bank range x =(R2-d2)0.5).

differences *dH/dr* along the river show a clear plateau in the central infiltration area (Fig.14).

Decreasing infiltration of surface water in the central area was almost compensated by an expansion of the infiltration area. According to results in Table 2, filtrate production shows significantly lower sensitivity to riverbed conductivity than the infiltration velocity. Flow dependent clogging instead of a uniform decrease of riverbed conductivity (as assumed in the course of sensitivity analyses), increases the compensatory filtrate production.

2.6 Numerical Description of River Bed Clogging

The hydraulic conditions at the study site were modelled using the US Geological Survey code MODFLOW (McDonald and Harbaugh 1988). Hydraulic head data were employed to calibrate the 3D flow model under the assumption of a homogenous aquifer (horizontal hydraulic conductivity k_h = 3.8 x 10^{-3} m/s, anisotropic ratio of vertical to horizontal hydraulic conductivity k_v/k_h = 0.1, porosity μ = 0.2) and a riverbed leakance via a vertical boundary layer of 1 m thickness with reduced hydraulic conductivity. The hydraulic conductivity of this river bed layer was fitted to 3.8 x 10^{-5} m/s. For calibration of the transport model (MT3D; Zheng, 1990) a natural tracer effect was considered. Due to the large difference between nitrate concentrations in the river and the groundwater, nitrate was chosen as

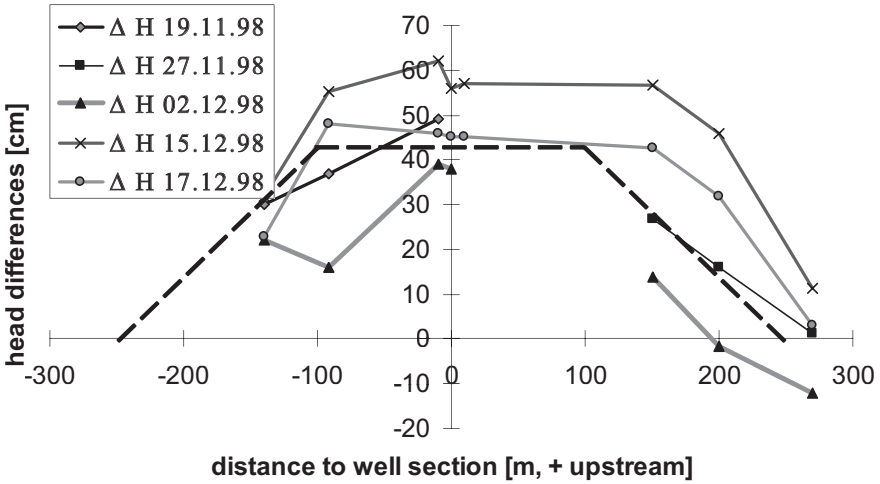

Figure 14. Measured potential losses in the river bed.

a calibration variable in an unsteady state simulation of the start up phase of the well operation. Obtained migration parameters matched well with values from the literature (Käss, 1992).

In the following section, the calibrated model of the presented site serves as the initial situation (plot and cross section in Fig.15) of a systematic parameter investigation. The linear sensitivity analysis uses a function, $\delta_{v,p}$, to quantify the sensitivity of the model response to a unit change in parameter value:

$$\delta_{v,p} = \frac{dv / v}{dp / p}$$

where p = parameter, v = output variable (model response).

The larger the value of the function, the more significant the specific parameter is for model behaviour. The applicability of this form is limited to linear cause-and-effect relationships or small parameter variations. The results in Table 2 outline the major influence of river bed clogging (conductivity ration of aquifer and riverbed k_A/k_{BF}) on the maximum infiltration rate v_{max}. A 10 % increase of k_A/k_{BF} results in a 4.4 % decrease

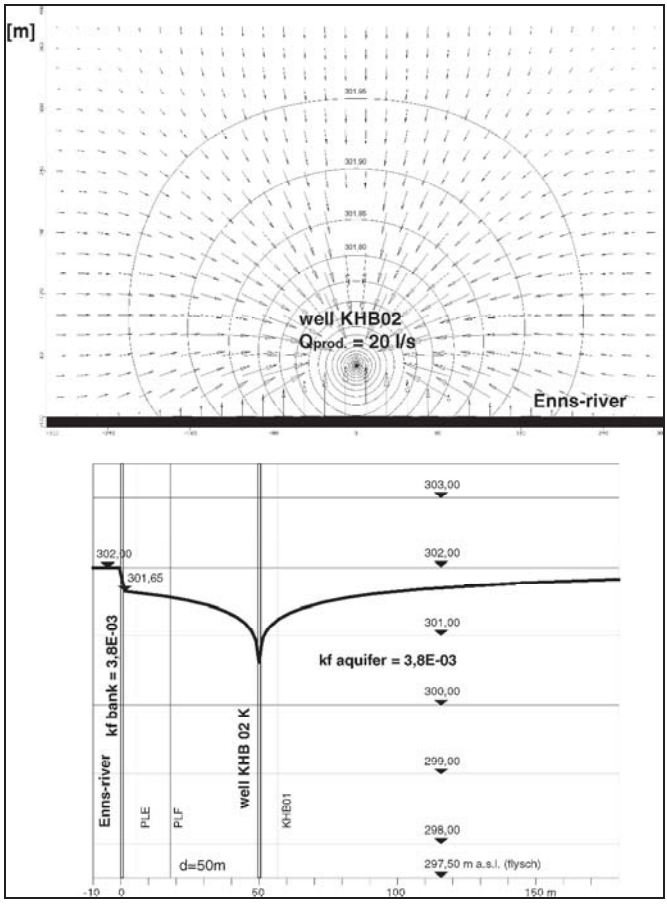

Figure 15. Initial conditions of numerical sensitivity analyses (MODFLOW software).

Table 2. Comparison of parameter sensitivities to hydraulic properties (hydraulic retention time HRT, filtrate portion QBF, maximum infiltration rate v_{max}) of the considered bank filtration site.

$\delta_{v,p}$	k_A / k_{BF}	k_A	$Q_{Prod.}$	d	H
HRT [d]	0.24	0.33	-1.01	1.89	1.20
QBF [%]	-0.25	-0.15	0.03	-0.18	0.17
v_{max} [m/h]	-0.44	-0.44	0.89	-0.76	-0.89

of the maximum infiltration rate v_{max} but only in a 2.5 % drop of the filtrate portion Q_{BF} (confirming compensatory flow via outer infiltration areas). A 10 % increase of the well distance *d* extends total migration time *HRT* by 18.9 % while the filtrate portion Q_{BF} is much less affected (- 1.8 %).

To validate the flow and transport model a separate tracer test was conducted. 200 l of a saturated sodium chloride solution were dosed into the riverbed via a multi-level probe and on-line measurement of the electrical conductivity in the probes PLE and PLF and in the well recorded the migration of the tracer. The peak of the simulated breakthrough curve reached the well after 4.5 days and showed a good agreement with measurements. This test was conducted at the end of the monitoring period and therefore the clogging issue had to taken into account. The hydraulic conductivity of the river bed (vertical boundary layer of 1 m thickness) in the central infiltration area 100 m up- and downstream of the well was set to half of the initial value (K_h = 1.9 x 10^{-5} m/s). The simulated status of the site (Fig.16) showed a satisfying fit with hydraulic head and tracer test data.

Comparing the plots in Fig.12 (analytical approach), Fig.15 and Fig.16, the obviously reduced conductivity in the central area flattens the distribution of infiltration rates. The numerically calculated maximum infiltration rate decreased from 1.32*10^{-5} m/s to 0.89*10^{-5} m/s in good agreement with the flow velocity in natural sediment layers.

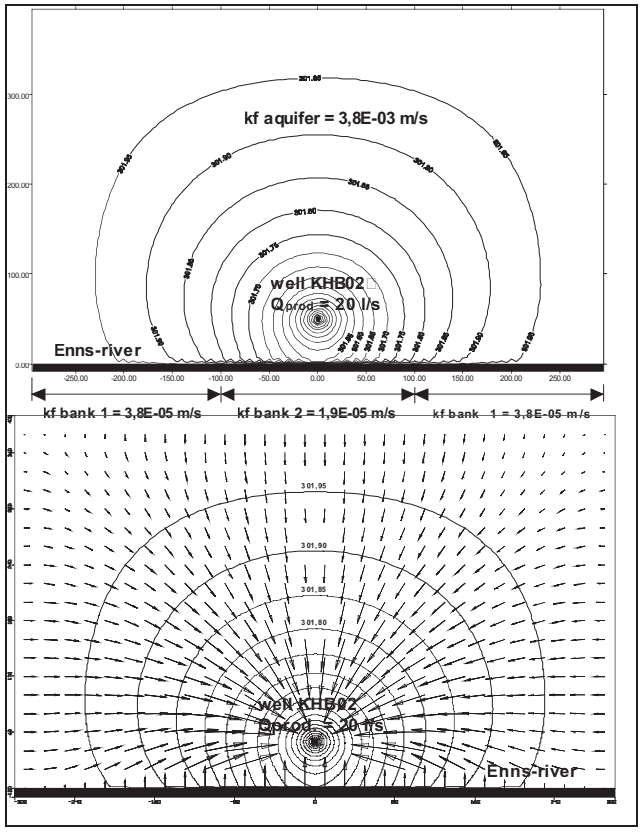

Figure 16. Simulated groundwater table and flow velocity distribution of the investigated RBF site considering reduced conductivity in the central infiltration area (clogging after one year of well production)

2.7 Visualisation of River Bed Clogging

Sedimentation and intrusion of suspended solids have been observed and documented at the front window of the monitoring station (Fig.17). Settled organic matter was covered with sand materials forming an increasingly homogenous sediment layer. It is a known fact that particulate organic matter deposited in the river bed represents an important carbon pool (e.g. Bretschko and Moser, 1993). This organic upper sediment layer represents a very active biological zone inducing relevant degradation processes (Brunke and Gonser, 1997). A comparison between hyporheic respiration rates at the installed multilevel probes clearly indicated higher carbon respiration in natural sediment zones than in the filter sand zones (Brugger et al., 2001).

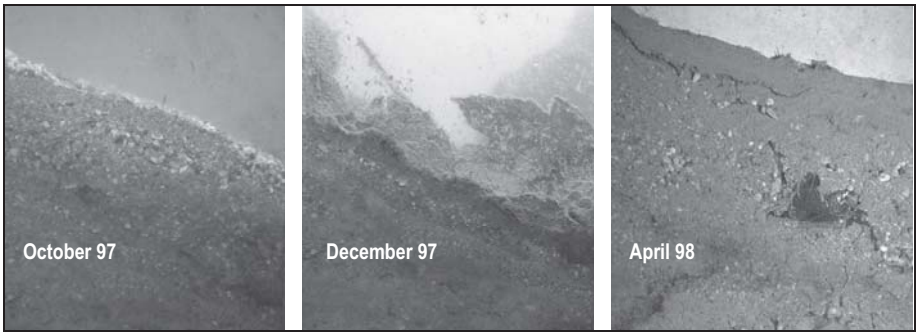

Figure 17. Built-up of a clogging layer and deposition of organic sediments

3. CONCLUSIONS

In this particular case study observed clogging processes achieved a rather stable status within a monitoring period of one year. During this period the hydraulic conductivity in the top layer (15 cm thickness) at the river bed surface decreased one order of magnitude (Fig.9) and the infiltration rate dropped to the half of the original value. The final conductivity value of this top layer was independent of the riverbed material (comparing natural sediment and specified filter sand). Dynamics of flow-related clogging appear as self-adjusting protection mechanisms against local flow peaks and channelling of the infiltration flow.

ACKNOWLEDGEMENTS

Basic results presented in this paper have been achieved by close interdisciplinary cooperation in the course of a research project co-ordinated (Ch. Hasenleithner) and funded by the Ennskraft Company.

REFERENCES

Brettschko, G., Moser, H., 1993. Transport and retention of matter in riparian ecotones. Hydrobiologia, 251, 95-102

Brugger, A., Wett, B., Kolar, I., Reitner, B., Herndl, G.J., 2001. Immobilisation and bacterial utilisation of dissolved organic carbon entering the riparian zone of the alpine Enns River, Austria. Aquatic Microbial Ecology, 24(2), 129-142.

Brunke, M., Gonser, T., 1997. The ecological significance of exchange processes between rivers and groundwater. Freshwater Biology 37, 1-33.

Cleveland T.G., Tiller F.M., Lee J.B. 1996. Theory of filtration of highly compactable biosolids. Wat. Sci. Tech., 34, 299-306

Das S., Ramarao B. V. 2002. Inversion of lime mud and papermaking pulp filtration data to determine compressibility and permeability relationships. Separation and purification techn., 28, 149-160

Hasenleithner, Ch., Brugger, A., Wett, B., 1999. Investigating the seepage rate in the reservoir of an alpine Austrian river with high water quality. Proc. 28. IAHR congress, Graz, A3, 16

Ingerle, K., Blaschke, A.P., Brugger, A., Hasenleithner, Ch., Herndl, G.J., Jarosch, H., Kolar, I., Lensing, H.J., Pöschl, S., Quéric, N., Reitner, B., Schöller, F., Sommer, R., Wett, B., 1999. Forschungsprojekt Uferfiltrat (Research project bank filtration). Research Initiative Verbund, Vienna, 60, 43-78.

Käss, W., 1992. Geohydraulische Markierungstechnik (Geohydraulic tracer technique), Hydrogeology 9, Gebrüder Borntraeger, Berlin-Stuttgart, 330-331.

Lee D. J., Wang C. H. 2000. Theories of cake filtration and consolidation and implications to sludge dewatering. Wat. Res., 34(1), 1-20

McDonald, M.G., Harbaugh, A.W., 1988. A modular three dimensional finite difference groundwater flow model. Technique of water resource investigations, 06-A1, US Geol. Surv., USA, 575 pp.

Sorensen P.B., Hansen J.Aa. 1993. Extreme compressibility in biological sludge dewatering. Wat. Sci. Tech., 28, 133-143

Sorensen P. B., Moldrup P., Hansen J. 1996. Filtration and expression of compressible cakes. Chemical Engin. Science, 51, 967-979

Tiller F.M., Kwon J.H. (1998). The role of porosity in filtration: XIII. Unexpected behaviour of highly compactible cakes. AIChE J., 44, 2159-2167

Wett, B., Jarosch, H., Ingerle, K., 2002. Flood induced infiltration affecting a bank filtrate well at the River Enns, Austria. J. of Hydrology, 266/3-4, 222-234.

Zheng, C., 1990. MT3D – A modular three-dimensional transport model for simulation of advection, dispersion and chemical reactions of contaminants in groundwater systems. S.S. Papadopulos & Assoc. Inc, Rockville, Maryland

MANAGING RESOURCES IN AN EUROPEAN SEMI-ARID ENVIRONMENT: COMBINED USE OF SURFACE AND GROUNDWATER FOR DRINKING WATER PRODUCTION IN THE BARCELONA METROPOLITAN AREA

Jordi Martín-Alonso
Head of the Laboratory of the Sant Joan Despí Waterworks Barcelona's Water Company (Agbar) Passeig de Sant Joan, 39. E-08009 Barcelona (Spain)
Tel. (+34) - 93.342.36.16, Fax (+34) – 93.342.36.66
Email: jma@agbar.es

Abstract: Barcelona's public water supply depends on surface water, groundwater, riverbank filtration, and artificial recharge. The semi-arid climate provides challenges to supplying water, and methods have been developed to manage the riverbed/aquifer interface at the point of infiltration of the riverbank filtration site. The hydrogeology, water quality, and operational elements of the Barcelona water supply are presented

Key words: river bank filtration, artificial recharge, water supply, Barcelona

1. BACKGROUND

Water supply for the districts of the Baix Llobregat and most of the districts in the Barcelona Metropolitan area (Northeast Spain) depends on the water resources of the Llobregat River (Figure 1). It drains an area of 4948.2 Km^2, and is 156.6 Km long having an average slope of 8.1 ‰. It has three main tributaries: the Cardener, Anoia and Rubí Rivers; having slopes

Stephen A. Hubbs (ed.), Riverbank Filtration Hydrology, 281–298.

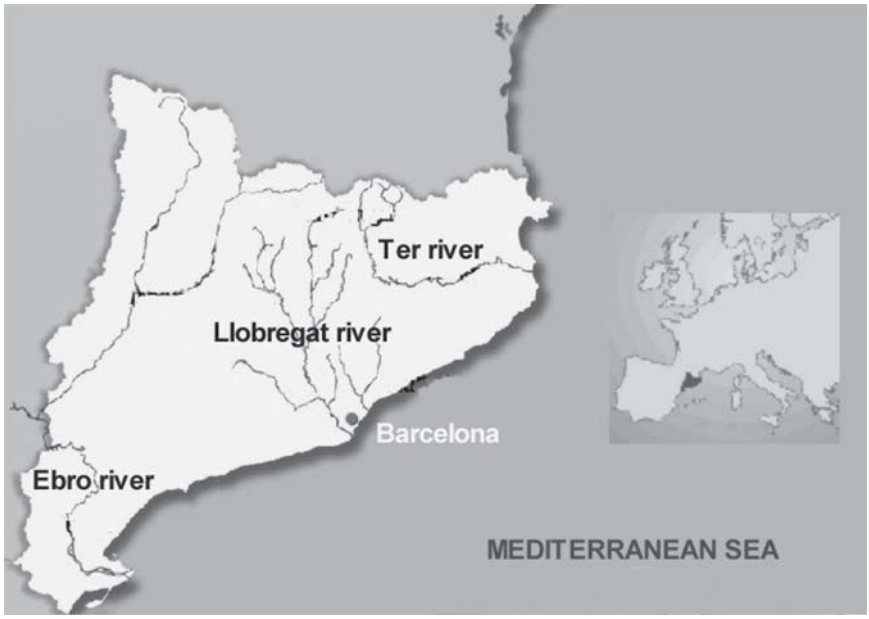

Figure 1. Geographical situation

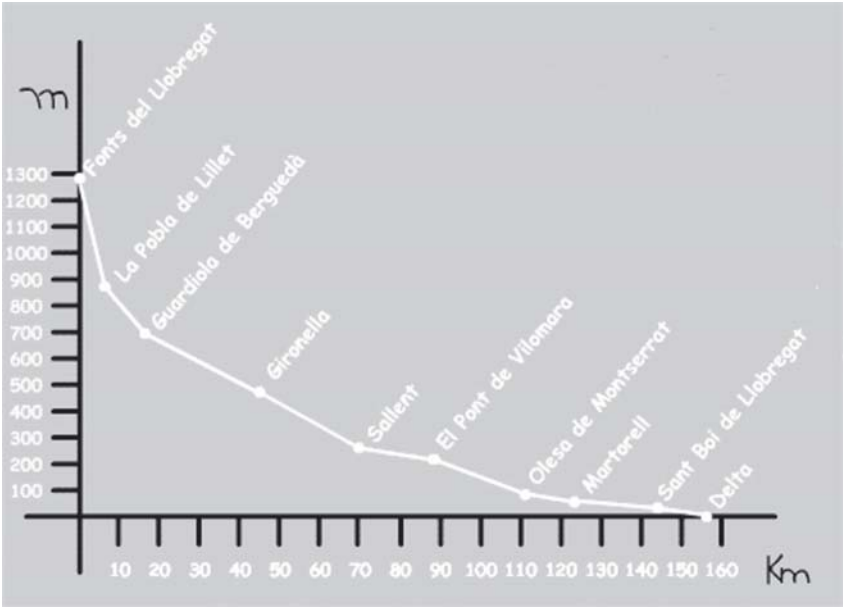

Figure 2. Longitudinal profile of the Llobregat river

of 11.1‰, 8.2 ‰ and 22.8 ‰, respectively (Catalán et al., 1971). The longitudinal profile on the main watercourse is shown in Figure 2.

The hydraulic regime of the Llobregat River is of the Mediterranean type: low flows during normal conditions with peak events of flooding. The water flow range is extremely wide: from absolute dryness up to 2000 m^3/s, with the "most probably found" flow of about 5 m^3/s and the average discharge – including floodings – of about 15 m^3/s. The yearly average flow in the period 1960-2003 is represented in Figure 3, along with the daily flows from three different years: 1996 (very wet with heavy floodings), 1998 (quite dry) and 2003 (average).

Heavy rainfall is not uncommon. An example of how intense precipitation may be is the episode of June 10th 2000, that caused an important flooding event in the lower Llobregat basin. Figure 4 shows the rainfall distribution with its most intense area situated in the Montserrat mountain, just 20 km upstream of the Sant Joan Despí Waterworks (Llasat et al, 2003):

Regarding its chemical quality, the headwaters of both the Llobregat River and the Cardener River (a tributary of the Llobregat) are located in a rather unpolluted area of the Eastern Pyrenees. The mid-waters of the rivers flow through a densely populated and industrialised area, where three potash mines are very active and strongly increase the salinity of the water resources. The lower course flows through one of the most densely populated areas of the Mediterranean region, as a consequence the Llobregat basin receives large inputs from industry and/or urban origin. (Otero et al., 2003; Soler et al., 2002).

Although limited in extension, the presence of halides in a limited expanse in the upper part of the basin has had a dramatic impact on water quality since the establishment of three salt mines in the 1920's (Caso, 1949; CESALL, 1932). The halides and the organic matter in the river lead to a surplus of chlorinated and brominated compounds when treated (Ventura et al, 1985, 1986). The Brine Collector of the Llobregat River (Figure 5) collects the polluted water from the Cardener River in the upper part of the basin and by-passes the surface water intake on the Llobregat River. This has minimized the influence of the pollution of the headwaters since 1989 (Martín-Alonso, 1994), although it is still the main problem from the ecological and sanitary points of view (Martín-Alonso et al., 1995).

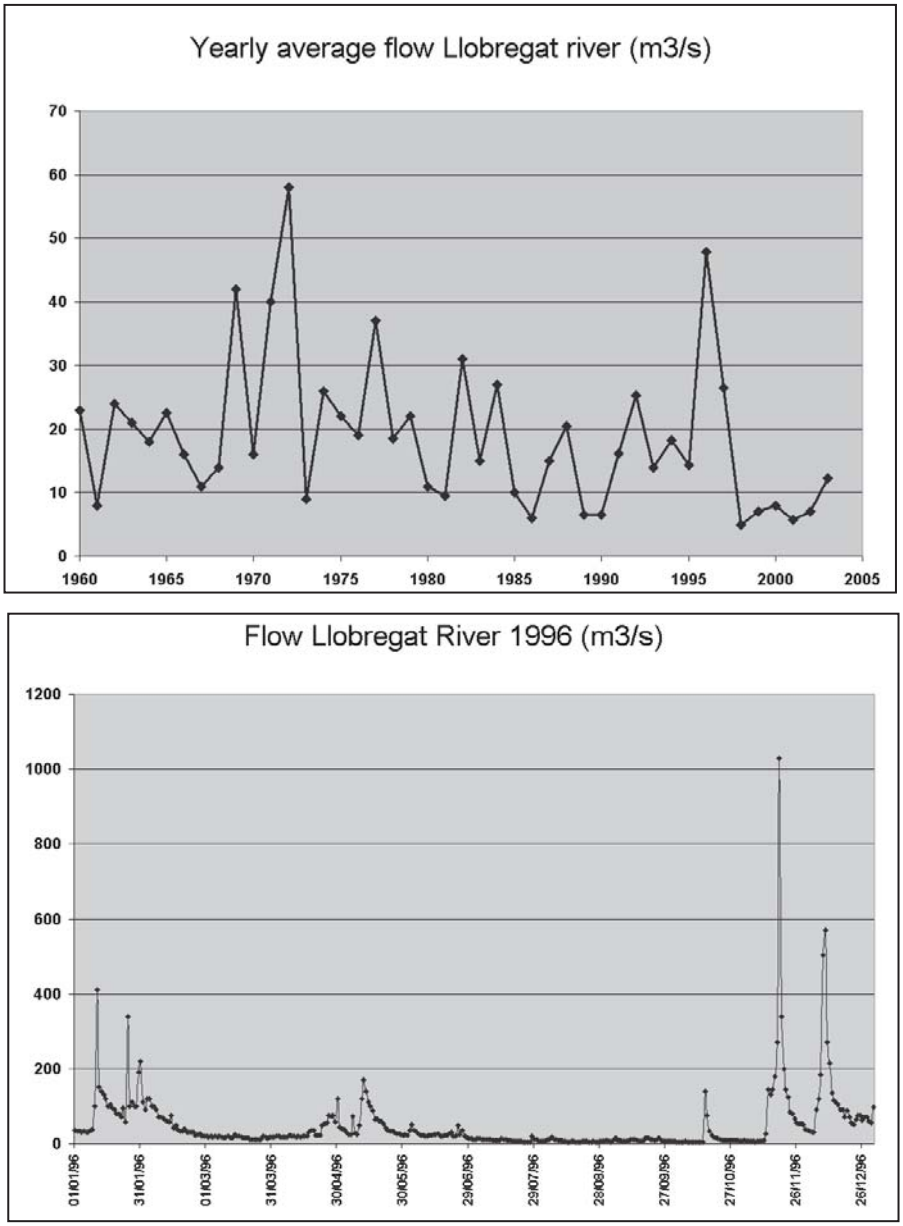

Figure 3. Flow of the Llobregat river at Sant Joan Despí (continued on next page)

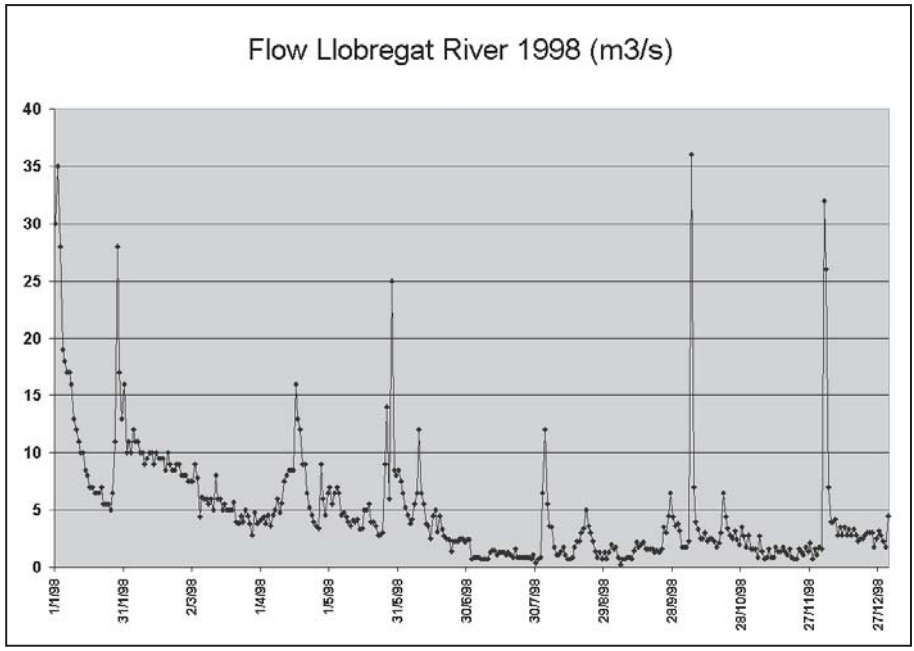

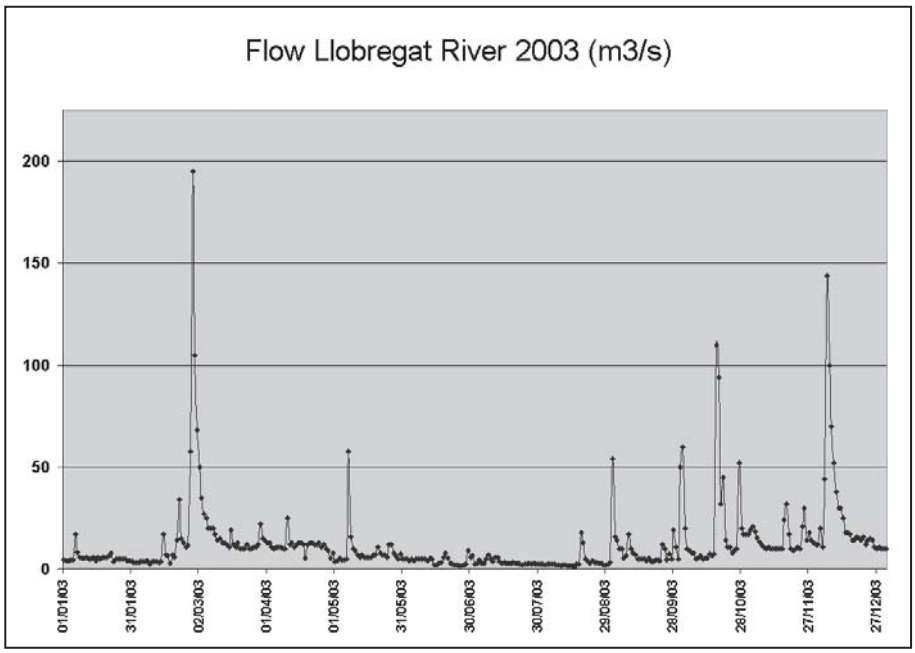

Figure 3. Continued.

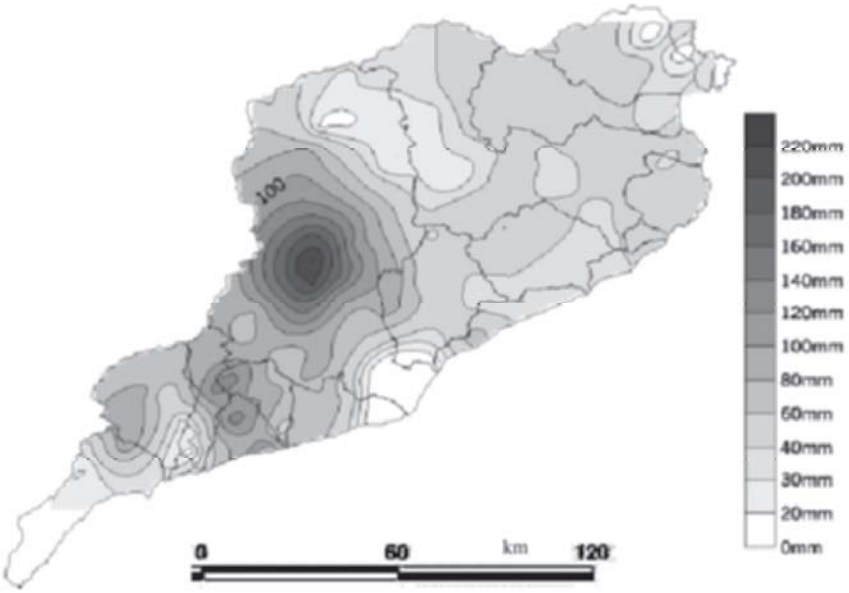

Figure 4. Distribution of accumulated rainfall between 21:00 UTC of 9th June 2000 and 21:00 UTC of 10th June 2000

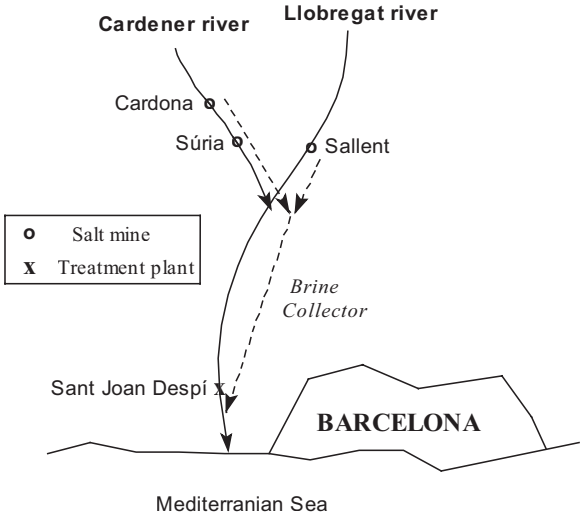

Figure 5. Schematic diagram of the Brine Collector of the Llobregat River

AQUIFER CHARACTERISTICS

1.1 Geology

An overview of the geology of the Llobregat River is presented in Figure 6. Quaternary alluvial sediments consisting of sands and gravels intercalated with silts and clay have a combined thickness of 40 m (Manzano, 1991). The alluvial sediments are overlain by a layer of silts and clays which are recent flood plain deposits of the river. Beyond Cornellà to the Southeast the alluvial sediments are separated into two distinct hydraulic units by an intervening layer of silt and clay which becomes thicker towards the coast. The lower alluvial aquifer is extensively exploited in the coastal zone. Alluvial sediments in the vicinity and to the Northwest of Cornellà form the unconfined zone of this important aquifer. The alluvial sediments are incised into a Miocene/Pliocene sedimentary sequence which forms part of the plain of Barcelona. The plain sediments form the side of the valley at Cornellà.

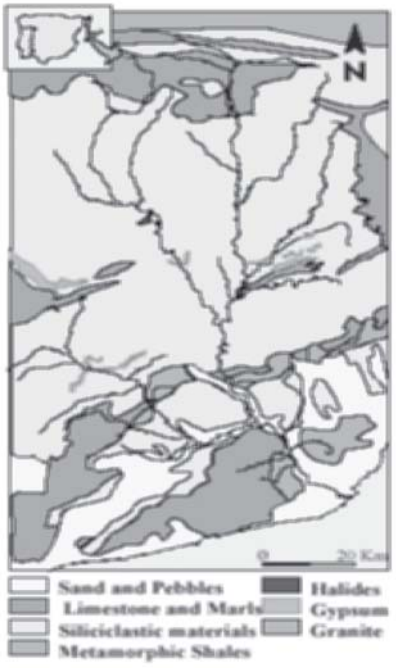

Figure 6. Geological map of the Llobregat basin

They consist of Miocene conglomerates and quartz sands with intercalations of loams and sandy marls, and Pliocene clays, sandy clays and minor interbebbed sands. The Pliocene includes a unit of sands, 5 to 10 m thick with occasional gravel, used locally as an aquifer for industrial supply. Quaternary continental red clays and beige silts overlie the Pliocene sediments.

These sediments are basically made up of highly permeable and porous gravels and granulated sand, although there are also some layers of nonporous materials. The gravels correspond to two or three quaternary terraces superimposed upon each other and the less permeable material could correspond to loams and clays from the flood plain or also to lateral or Eolithic contributions. With the only exception of the riverbed, the valley is almost completely covered by a layer of loams less than 5 m thick until a short distance before the main extraction area of Cornellà. As previously described, the aquifer is single and free in this entire zone. From Cornellà onwards, substantial layers of not very permeable materials begin to appear and the aquifer branches into two: an upper free branch and a lower, confined one.

The deep and confined aquifer that begins at Cornellà is, indubitably, the most important one and occupies the entire central zone of the delta, consisting of quaternary gravels and sands, stretching from Pallejà to the Mediterranean Sea, progressively widening into a total extension of about 110 km^2 with the fluvial levels being rather thick due to the large variations of sea level during the quaternary period. This stretch constitutes a hydrogeological unit that, in broad terms, has the features shown in Figure 7 (Miralles et al, 1989). The impermeable ceiling of the confined aquifer is formed by a wedge of clayish loams that increase in thickness towards the

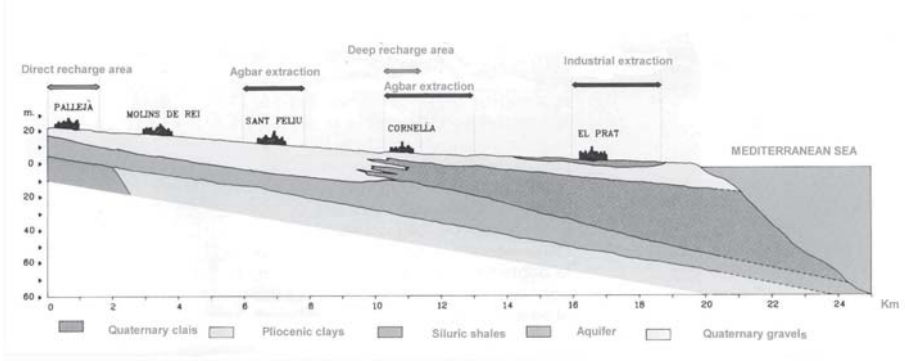

Figure 7. Structure of the Delta Aquifer of the Llobregat River

sea, where it is 40 m thick. The depth of this confined aquifer fluctuates between 30 m and 45 m thick and its maximum useful reserve throughout its length is estimated to be 114 hm^3.

The Agbar main pumping area is close to the contact between the Llobregat alluvium and the plain of Barcelona's sediments. Beyond the surface expression of the contact, the topographic break at the edge of the Llobregat flood plain, it is proposed that the sand and gravel aquifers of the two formations become juxtaposed in places (see Figure 6). At one point this juxtaposition occurs only 300 m from the Agbar pumping area. The hydrogeological expression of this geological contact is one of the features controlling contaminant movement at Cornellà. The main characteristics of the aquifer may be summarised as follows:

Surface:	110 km^2
Capacity:	114 hm^3
Length free aquifer:	11 Km
Minimum width free aquifer:	0,25 Km
Maximum width free aquifer:	2,1 Km
Length confined aquifer:	9 Km
Maximum width confined aquifer:	17 Km

1.2 Hydrogeology

The Llobregat river gravels have a saturated thickness of approximately 20 m and a hydraulic conductivity as high as 2500 m/d, resulting in a transmissivity up to 50,000 m^2/d. In contrast the plain sands are thinner and less permeable (Badiella and Custodio, 1991); their maximum transmissivity is in the order of 500 m/d. The contrast is reflected in the hydraulic gradients within the two aquifers. The gradient in the plain aquifer is markedly steeper than the gradient in the alluvial gravels.

Results of a pumping test conducted on one of the Agbar boreholes illustrate the restricted hydraulic communication between the alluvial aquifer and the plain aquifer. The large contrast in hydraulic conductivity between the two aquifers results in a partial barrier boundary at a distance of 300 m from the pumping borehole, coincident with the geological contact proposed in Figure 7.

The river itself is not in direct hydraulic continuity with the alluvial aquifer. The water level in the alluvial gravels is normally several metres below the riverbed. However, as it will be explained later, Agbar operates a system of artificial recharge using excess capacity of a river water treatment plant and employing some of their pumping boreholes as recharge wells during times of surplus. The alternating discharge/recharge regime

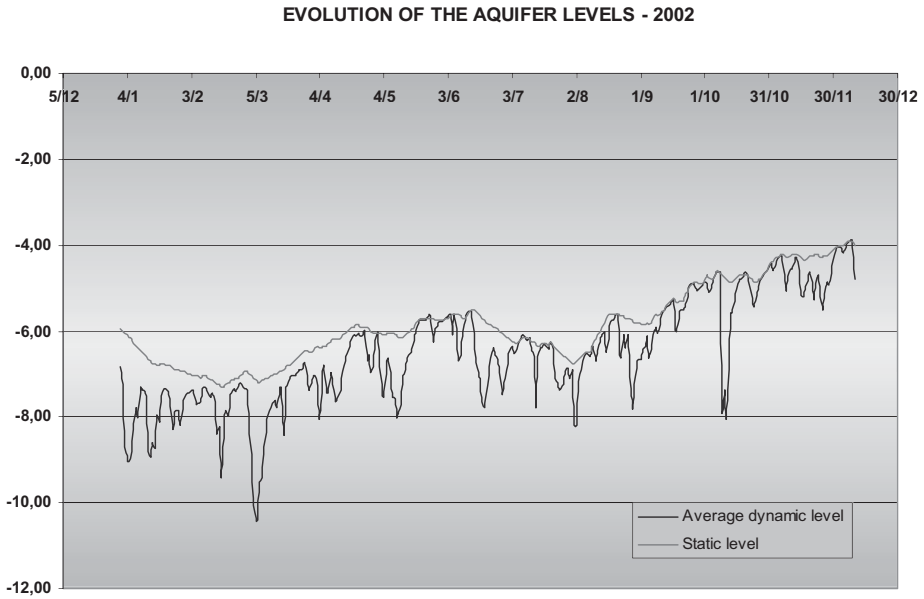

Figure 8. Static and Dynamic levels at Cornellà

operated by Agbar, and additional abstractions from the aquifer by industrial users, result in a complicated and dynamic groundwater regime. Figure 8 shows the average of all the dynamic levels measured in the pumping area and the level in an undisturbed location.

Since 1965 the water level measured in a piezometer at the Agbar pumping station has ranged between a maximum of +1 m (in 1997) to a minimum of –17 m (in 1990), as illustrated in Figure 9. This variation reflects the meteorological conditions and the consequent abstraction/ recharge operations by Agbar at Cornellà. The range of variation may be compared with the effect of short pumping periods which result in a cumulative drawdown of 3 m at the piezometer site.

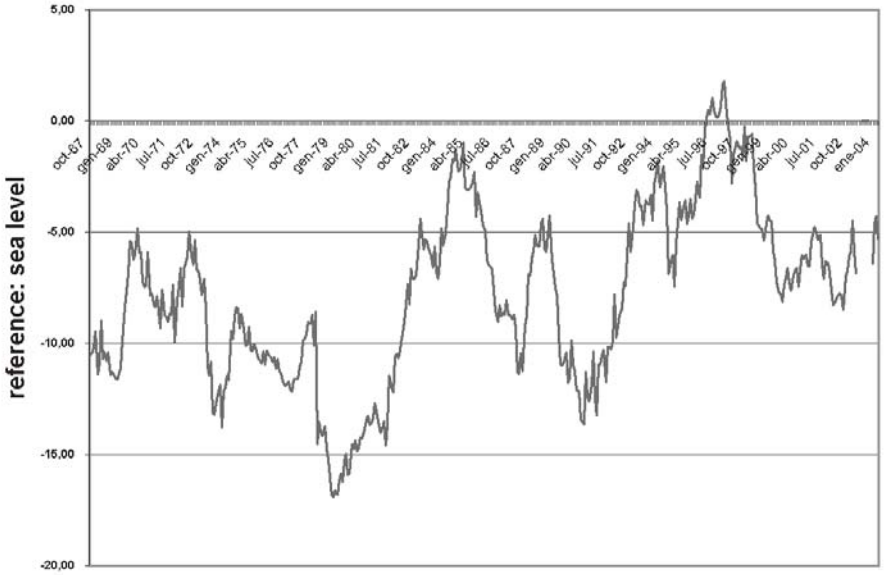

Figure 9. Piezometric level in the main extraction area (Cornellà) 1967-2004

1.3 Hydrochemistry

Both the plain aquifer and the alluvial gravel aquifer have a similar Total Dissolved Solids (TDS) concentration, approximately 1300 mg/L, but there exist a clear distinction in their chemical characteristics. The distinction lies in their cation composition. The alluvial groundwater has a lower relative concentration of Mg^{2+} and a higher relative concentration of Na^{+} and K^{+} than the plain groundwater. Furthermore, the alluvial groundwater has a lower Na^{+}/K^{+} ratio (about 10) than the plain sands (Na^{+}/K^{+} ratio range 30 to 90). These chemical distinctions support the geological interpretation of the position of the boundary between the two aquifers.

Possible sources for the elevated Mg^{2+} in the plain groundwater are the minerals smectite and chlorite, which have been detected by X-ray diffraction on samples of the plain sands. The higher concentration of K^{+} in the alluvial groundwater demonstrates the contribution of drainage from potash mines upstream of Cornellà on the quality of river water as a source of both natural and artificial recharge to the aquifer.

All groundwater samples from both aquifers are saturated with respect to calcite. Calcite has the important effect of buffering the pH of the groundwater within the observed range 6.80 to 7.73.

2. THE NEED FOR A COMBINED USE OF SURFACE AND GROUNDWATER

Until 1954, when the first treatment plant for surface water was built in Sant Joan Despí, all the resources used in the above mentioned zone were of subterranean origin and came from the aquifers in the lower valley and the delta of the Llobregat River. The growing demand for water in the zone of the delta of the Llobregat River, much greater than the resources of the aquifer, resulted in the levels being progressively lowered. In 1950, the Sociedad General de Aguas de Barcelona considered the possibility of increasing the infiltration of the river water in an artificial way, through the riverbed. Deep artificial recharging in 1969 complemented this step. Despite this effort, the aquifer is still overexploited: as it is shown if Figure 9, the piezometric level is in Cornellà (10 km far from the coastal line and 15 m of altitude) is usually below sea level.

Due to human activities, frequent pollution episodes of the aquifer have been reported: trichloroethylene (Isamat et al., 1977), hexavalent chromium (Custodio et al., 1991), gasoline (Godé et al., 1993) and polychlorinated naphtalenes (Ventura et al., 1997).

3. THE AIMS OF ARTIFICIAL RECHARGING.

Working any aquifer constitutes a dynamic process requiring a balance between the flows of waters that feed it and the flows pumped from all the wells that are supplied from subterranean water sources, as well as by the drainage of any springs in the zone.

The process of artificial recharging has a series of direct or indirect advantages that can be specified as follows:

a) **Increasing the water reserves:**
By diminishing the deficit of necessary water, the aquifer serves as high capacity reservoir; in the case of the Llobregat delta an increase in the level of 3 m makes it possible to store almost 1 hm^3 of water for every km^2 of surface area.

b) **Facilitating transport of the water:**
Given the fact that the delta of the Llobregat River's aquifer extends over a surface of about 110 km^2 and it has quite a uniform shape, water can be extracted from any place close to the points where it is used although they are a long way from the points of natural or artificial recharging, thus making building pipelines unnecessary.

c) **Improving the quality of the water:**
Both in the case of direct infiltration of the river water and recharging with treated surface water, the aquifer acts as a slow filter that retains suspended matter in the zones of infiltration, so the resulting groundwater has an improved and more constant quality.

d) **Increasing the phreatic level:**

If the contribution of water is sufficient to overcome the deficit, it will lead to a general increase in the levels of groundwater, having two obviously important consequences: saving the energy necessary for pumping the water and diminishing the possibility of intrusions of salty water into the aquifer in the coastal zone.

4. DIRECT ARTIFICIAL RECHARGING FROM THE SURFACE

In order to artificially recharge an aquifer from the surface it is necessary to choose a point in the river itself or close to it, where the aquifer comes out next to the river or is only covered by permeable materials. In this zone, natural recharging will obviously take place, either by the river water itself, or by the rain water that falls in this area. This natural recharging can be artificially aided by either preparing the riverbed or constructing shallow pools or ditches that are filled with the water to be recharged.

Rivers usually have muddied waters that, when the aquifers are directly recharged, cause progressive colmations of the permeable riverbed as the materials in suspension are retained in the pores of the gravels that make up the riverbed. This process will result in the clogging of the riverbed if the fluvial currents -during periodic floods- are not strong enough to resuspend the trapped sediment. If this natural process does not occur, it may be necessary to do it artificially. There is no doubt that the colmation process is the most delicate aspect of artificially recharging aquifers.

As previously mentioned, since 1950 the Sociedad General de Aguas de Barcelona has been recharging directly from the surface by scarifying the riverbed of the Llobregat river in the zone where the aquifer is free and in contact with the river. The scarifying operation is carried out always in the same zone, near the city of Pallejà. The procedure has been unchanged for years. Most of the difficulties encountered are not caused by the technique itself but rather by morphological variations in the river bed and modifications to the banks, caused by periodic floods of the river and sometimes by the holes left by abusive extraction of gravels.

The technique used can be divided into the following steps:

a) Preparation of the riverbed:

The riverbed has to be conditioned in order for the scarifying to be effective. The accumulations of sludge, mud and waste have to be cleared away, especially at the bottom of the holes left by the above-mentioned extractions of gravels which must be filled by clean gravels that have piled up in the back-waters of the river. In this way, one achieves an even riverbed that can be safely entered by the tractor used for this kind of work.

b) Scarification in practice:

The tractor has a bucket (for taking out the mud and moving the gravels) and a ripper for working the riverbed. The ripper must not penetrate the riverbed by more than 50 cm to ensure that suspended matter doesn't penetrate deeper zones, as these zones are difficult to recuperate later and, undoubtedly, would end up clogging up the riverbed and making it difficult for the water to enter the aquifer.

It is always necessary to scarify in the same direction as the current (from upstream towards downstream) so that the water that filtrates into the aquifer is flowing surface water and not the mud or crust that the ripper throws up into the water column.

c) Operational limits for optimal performance:

There are parameters of control that experience has shown to be worth bearing in mind in order not to deteriorate the quality of the water stored in the aquifer and ensure that the colmation process does not become irreversible:

- **Flow:** The river is only scarified when the flow at Pallejà is between 10 and 35 m^3/s. As the Sant Joan Despí Waterworks treats only up to 5.5 m^3/s, when dealing with this range of flow the water that is fed into the aquifer (about a cubic metre per second) would not affect the capacity of the waterworks. With flows higher than 35 m^3/s it is dangerous to enter the river with the tractor, apart from the fact that as we are dealing with extraordinary flows the process of natural recharging increases substantially.

- **Turbidity:** Care must be taken not to scarify the riverbed if the water that has to be filtered has an excess of suspended matter. The established limit allows us to work only when the turbidity of the river water at Pallejà is less than 100 N.T.U., usually infiltrating waters with a considerably lower level.

- **Chemical quality:** At the same time, care is taken to ensure the suitability of some indexes of general quality of surface water: ammonia content must be less than 1 mg/L, and chloride must not surpass the level

of 350 mg Cl/L. Additional parameters allow for the scarifying process to be postponed if a quality problem is detected in the recharging water.

5. ARTIFICIAL RECHARGING AT DEPTH

When the aquifers are separated from the surface by impermeable, fairly thick layers, it would be very expensive or almost impossible to recharge them directly using infiltration ditches or pools. For this reason an attempt has been made to carry out the operation by recharging through the pumping wells themselves.

The obstacle that has to be overcome when recharging by means of wells is the fact that they clog up, as is the case when dealing with direct recharging. However, the difference is that the phenomenon occurs at great depth, possibly resulting in an increase in the number and magnitude of the difficulties, to such a point that it is impossible to solve them, sometimes resulting in important and expensive facilities becoming inoperative. Therefore, the possibility of carrying out the artificial recharging at depth depends on the ability to carry out an efficient "unclogging" operation of the zone of the relevant aquifer, if, as usually occurs in practice, the water that is infiltrated has particles in suspension.

As of 1966, when Barcelona and the surrounding area received the additional waters of the Ter river for the purpose of providing water, the Water Treatment Plant of surface water of the Llobregat river at Sant Joan Despí often stopped operating at its full capacity although the discharge of the river was sufficient. As a result, the idea of taking advantage of the mentioned excesses of treated drinking water for artificially recharging the aquifer in the Cornellà pumping zone (as previously mentioned the aquifer is captive at this point) was considered.

The project began in 1969 and uses seven of the existing pumping wells for the purpose of both pumping and recharging, and five additional wells that were constructed for the sole purpose of artificial recharging. However as this water still has some suspended matter, the infiltration zone of the aquifer near the drilling shafts clogs up progressively. This makes it necessary to limit the infiltrated flow and to periodically unclog the area. As experience has shown, this is effectively carried out by means of vigorous pumping with a flow of the order of four times greater than that of the recharging flow.

6. FEATURES OF THE RECHARGING WELLS

The seven existing wells are all similar and are constructed by means of a cased shaft with a diameter of 950 mm and are 35 - 40 m deep, with a section of 10 m of well screen located in the zone of the aquifer. Each one of the sets of pumping equipment installed has a pump with a capacity of about 200 L/s, with a manometric height of 22 m, driven by a 125 horsepower electric engine. Given the fact that these wells were already equipped, the only thing that had to be done was to fit them with a pipe, making possible to introduce the recharge flow of about 50 L/s. A water gauge with a nominal diameter of 200 mm and a regulating valve made possible to maintain the flow within very strict limits.

The installation also has the necessary pipes and valves in order to discard the water during cleaning operations; this must be done periodically in order to unclog the aquifer in the infiltration zone next to the well screen of the drill shaft. In the five new wells constructed specifically for the purpose of recharging, the zone of the well screen was increased up to 15 - 20 m, and as a result of this greater area the recharged flow increased up to 100 L/s; in this case the control gauges have a nominal diameter of 250 mm. The pumping equipment in each one of the five new wells consists of 180 horsepower pumps with a capacity of 400 L/s and a manometric height of 18.5 m.

Practically all of the thirteen recharging wells are located in a transversal section of the aquifer. This layout means that the flow recharged into the aquifer is near the optimal.

7. OPERATING THE SYSTEM

The seven extracting/recharging wells (each with a capacity of 50 L/s), make it possible to recharge the aquifer with an approximate volume of 4000 m^3 per day. Experience has shown that it is worth unclogging the area when 60,000 m^3 of water have been infiltrated per well, that is to say, after being in operation continuously for 15 days. For cleaning purposes, a flow of 200 l/s is pumped for 10 minutes, resulting in losses of about 0.2%.

Similar criteria have been adopted for the wells with a recharging capacity of 100 L/s, proceeding to clean by pumping 400 L/s every 120,000 m^3 of water that is infiltrated per well, that is to say, after being in operation continuously for 15 days. The duration of the cleaning pumping is slightly longer (15 - 20 minutes) and as a result, the losses are of an order of 0.4%. The total infiltration capacity of the system reaches levels of 75,000 m^3 a day. The infiltration cones of each one of the recharging wells are checked in

order to clean them more efficiently if the permeability of the aquifer in the zone next to the drilling well screen decreases.

Although the water that is infiltrated comes from the excesses of the water treated at the Sant Joan Despí Water Treatment Plant, in order not to substantially worsen the quality of the subterranean water stored in the aquifer, the treated water is required to have a maximum content of 100 µg Total THM/L.

8. CONCLUSIONS

The combined use of surface and ground water is a key point to ensure the continuity of the drinking water supplied in the Barcelona's Metropolitan Area. The artificial infiltration of surface river water through the riverbed and the deep recharge of treated water into the aquifer were the strategies chosen to ensure the availability of water at any time, and have been successfully applied since the 1950's. Unfortunately, the overexploitation of the aquifer is still so important that the water table is consistently under sea level, leading an almost irreversible salinisation. Possible solutions for this situation are reduction of total abstraction from the aquifer, water importation from France (Rhône River), or sea water desalination.

REFERENCES

ACA (2004), taken from www.edu365.com

Caso, A (1949).Salinidad comunicada a las aguas del Llobregat, por las minas y fábricas de potasa de Cataluña. Ed. Direccion General de Minas y Combustibles, Madrid, 75 pages

Catalán, J.G, Oliver, B, and Alonso, J.J. (1971) Estudio Hidrológico del río Llobregat. CAEAAB and CEIAA Eds, Barcelona.

CESALL (1932). Memoria de la Comisión para el Estudio de la Salinidad de las Aguas del río Llobregat. Ed. Hidrográfica del Pirineo Oriental, Barcelona, 119 pages.

Custodio, E, Badiella, P. (1991) Informe acerca de las características, evolución y estado actual de la contaminación por Cromo detectada en 1896 en las captaciones del área de Cornellà (Barcelona). Curso Internacional de Hidrología Subterránea, progress report.

Godé, L.X, Serena, C, Ferrer, J.L.. and Valdés, J.L. (1993) Contaminación por gasolina del acuífero del Baix Llobregat. Medidas de descontaminación adoptadas. Resultados obtenidos. Int. Conf. Environ. Pollution, Sigtes (Spain).

Isamat, F.J., Sala, L., Cantó, J. and Miralles, J.M. (1977) Contaminación del acuífero del río Llobregat a la altura de Sant Feliu, por vertidos de residuos industriales en hoyos producidos por extracción de áridos. Intercolegial del Medio Ambiente Ed., Barcelona.

Llasat, M.C.; Rigo, T.,Barriendos, M.(2003) The 'Montserrat-2000' flash-flood event in comparison with spring floods in the Northeast of the Iberian Peninsula since the 14th century. International Journal of Climatology; 23; 453-469

Manzano, M. (1991) Síntesis histórica y estado actual de los trabajos sobre la hidrogeología del delta y valle bajo del río Llobregat (Barcelona) CIHS, internal document.

Martín-Alonso, J. (1994) Barcelona's water supply improvement: the brine collector of the Llobregat River. Water Sci.Technol. 30 (10), 221–227.

Martín-Alonso, J., Günther, F (1995) Influence of a salt dumping site in the surface water quality of the river Cardener (Spain)" Proc. Int. IAWQ Conf. Copenhagen

Miralles, J.M; and Cantó, J (1989) Aquifer refilling at the delta of the Llobregat River. Wat. Supply 7, R10, 11-1/4.

Otero, N, Tolosana-Delgado, R, and Soler, A. (2003) Proc. Compositional Data Analysis Workshop
15-17. Girona (Spain)

Soler, A., A. Canals, S. Goldstein, N. Otero, N. Antich, and J. Spangenberg, 2002. Sulphur and strontium. isotope composition of the Llobregat River (NE Spain): Tracers of natural and anthropogenic chemicals in stream waters. Water, Air and Soil Pollution 136, 207–224.

Ventura, F. and Martí, I (1997) Polychlorinated naphtalenes in groundwater samples from the Llobregat aquifer (Spain). J. Chrom. A, 786, 135-144

Ventura, F., Rivera, J. (1985). Factors influencing the high content of brominated trihalomethanes in Barcelona's water supply (Spain). Bull. Environ. Contam. Toxicol., 35, 73-81.

Ventura, F., Rivera, J. (1986). Potential formation of bromophenols in Barcelona's tap water due to the daily salt mine discharges and occasional phenol spills. Bull. Environ. Contam. Toxicol., 36, 219-225.

PRESENTATION OF DATA FOR FACTORS SIGNIFICANT TO YIELD FROM SEVERAL RIVERBANK FILTRATION SYSTEMS IN THE U.S. AND EUROPE

Tiffany G. Caldwell
University of Louisville/ Louisville Water Company, Louisville, KY, USA

Abstract: Yield in riverbank filtration (RBF) systems is affected by a variety of factors including the geology, hydraulics, site layout, and operational characteristics of each site. This paper identifies key parameters that affect yield in riverbank filtration systems and presents data for these parameters from RBF sites in the U.S. and Europe.

Key words: Riverbank filtration, RBF, specific capacity

1. INTRODUCTION

Riverbank filtration (RBF) has been used for water supply in Europe for over a century (Tufenkji *et al.* 2002). Use of RBF has recently become more prevalent in the U.S. as more and more utilities seek to improve the quality of source waters used for water supply and respond to new and upcoming regulations including surface water treatment, ground water under the influence of surface water (GWUDI), and disinfectant by-products regulations. Studies have demonstrated the positive effect of RBF on raw water quality. Several different mechanisms act to improve the quality of water extracted from RBF wells. First of all, river water is naturally filtered as is passes through the riverbed and aquifer. Secondly, the bank filtrate is diluted by groundwater. Natural biological and chemical processes that occur in the riverbed and aquifer further improve the water quality. This results in a water source that has lower turbidity and fewer microbes than the

Stephen A. Hubbs (ed.), Riverbank Filtration Hydrology, 299–344.

river water itself. The improvement in raw water quality makes riverbank filtration a desirable alternative to the traditional use of river water directly as a source for water supply (Wang *et al.* 2002).

One problem with the implementation of riverbank filtration is the inability to accurately predict the long-term yield from individual sites. Traditionally, yield has been predicted using an estimate of aquifer transmissivity and riverbed conductance from a short-term pump test at the site (Hubbs, chapter 2). However, this prediction method fails to account for influences of site geometry, river hydraulics, and source water quality on long-term yield. As a result, systems often fail to produce in the long-term at the rate predicted from the pump test.

Many different water utilities have experience with bank filtration. However, differences in operating conditions and site characteristics make it difficult to apply experience from one location to another (Schubert, chapter 10). A vast amount of data has been generated from specific studies and general monitoring of individual RBF sites. If these data could be compiled into a format that is easily applied on a wide variety of sites, existing experience could be used to improve design practices. This chapter presents data obtained from various riverbank filtration systems in the U.S. and Europe so that existing experience can be applied to enhance the understanding of factors affecting yield.

2. SITE OVERVIEW

2.1 Site Locations

Sites that were selected for this study were chosen on the basis of the amount and quality of data available, the ease of obtaining data, and the level of support from the utilities operating the systems. The selected sites include six sites from the United States and five sites from Europe. Most of the U.S. sites were located in the central part of the country where conditions are favorable for riverbank filtration. Sites in the central U.S. included wellfields along the Platte River near Ashland, NE, the Missouri River in Kansas City, KS, and the Raccoon River in Des Moines, IA. Other sites selected from the U.S. included wellfields along the Ohio River in Louisville, KY, the Great Miami River near Cincinnati, OH, and the Russian River in Sonoma Co., CA. In Europe, sites were selected along the Rhine River at Düsseldorf, Germany, along the Enns River at Steyr, Austria, and along the Llobregat River at Cornellà, Spain. Site locations in the U.S. and in Europe are shown in Figures 1 and 2, respectively. An additional site near Albany, NY on the Hudson River is also discussed. However, the data needed to compare the Albany site to the other sites was not available.

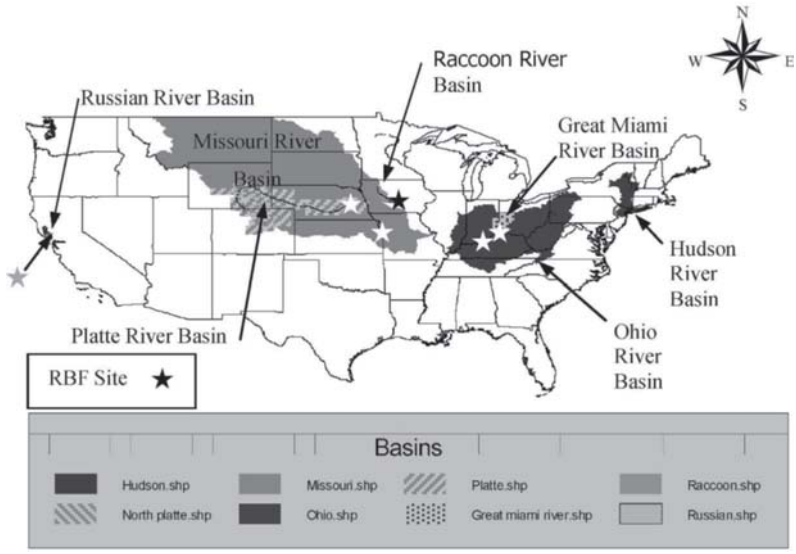

Figure 1. Map of Sites in the U.S.

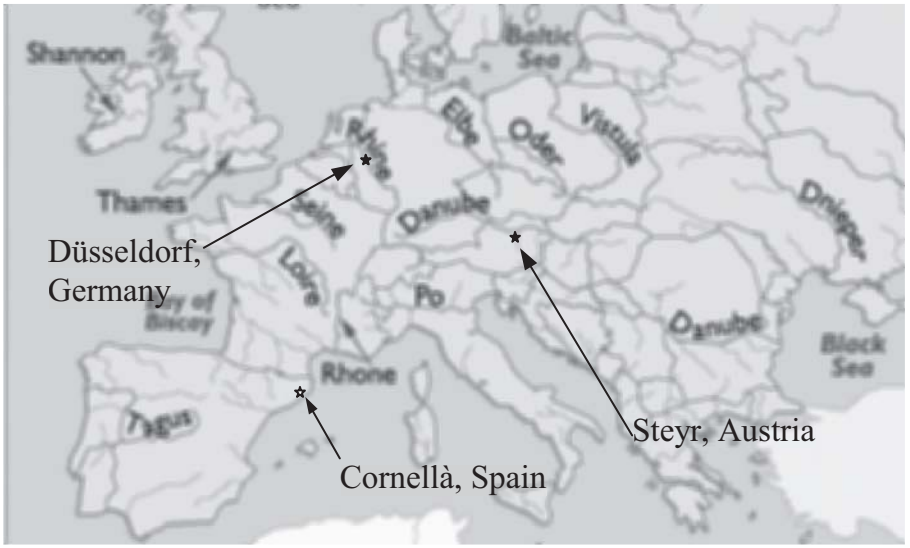

Adapted from WorldAtlas.com (2005).

Figure 2. Map of Sites in Europe

2.2 Site Summary

The selected sites represent RBF systems with different well field layouts (horizontal, vertical, and infiltration galleries) along a variety of river types including meandering, straight, and braided rivers. Capacities for U.S. sites ranged from approximately 11,000 m^3/day to 150,000 m^3/day. Capacities of the European sites ranged from 1700 m^3/day to 106,000 m^3/day. Site information for all sites is summarized in Table 1. The average production for each site is also shown graphically in Figure 3.

Table 1. Sites Selected for Study

United States				
Location	**Waterworks**	**Wellfield**	**Description**	**Average Production (m^3/day)**
Great Miami River near Cincinnati, OH	Greater Cincinnati Water Works	Charles M. Bolton	10 Vertical Wells	60,000
Missouri River in Kansas City, KS	Kansas City Board of Public Utilities	Nearman WTP	Single Radial Collector	120,000
Ohio River in Louisville, KY	Louisville Water Company	B.E. Payne WTP	Single Radial Collector	64,000
Platte River near Ashland, NE	City of Lincoln	Ashland	2 Radial Collectors	76,000
Raccoon River in Des Moines, IA	Des Moines Water Works	Platte River	5- Radial Collectors and 1-Horizontal Inclined Well	45,000 [(1)]
Russian River in Sonoma Co., CA	Sonoma County Water Agency	Wohler and Mirabel	5 - Radial Collectors	140,000
Europe				
Location	**Waterworks**	**Wellfield**	**Description**	**Average Production (m^3/day)**
River Enns in Austria	Ennskraft Company	KRB02	Single Vertical Well	1,700
Llobregat River in Spain	Barcelona's Water Company	Cornellà	26 Extracting Wells, 7 recharging wells	62,000
Rhine River in Germany	Flehe	Flehe, PW V	70 Vertical Filter Wells Connected by Siphon Pipe	33,000
Rhine River in Germany	Grind	Grind	7 Radial Collectors	106,000
Rhine River in Germany	Staad	Staad, PW I	25 Vertical Filter Wells Connected by Siphon Pipe	25,000

[(1)] Production data shown is for 5-radial collectors only. The single inclined horizontal well produces an average of 5,000 m^3/day.

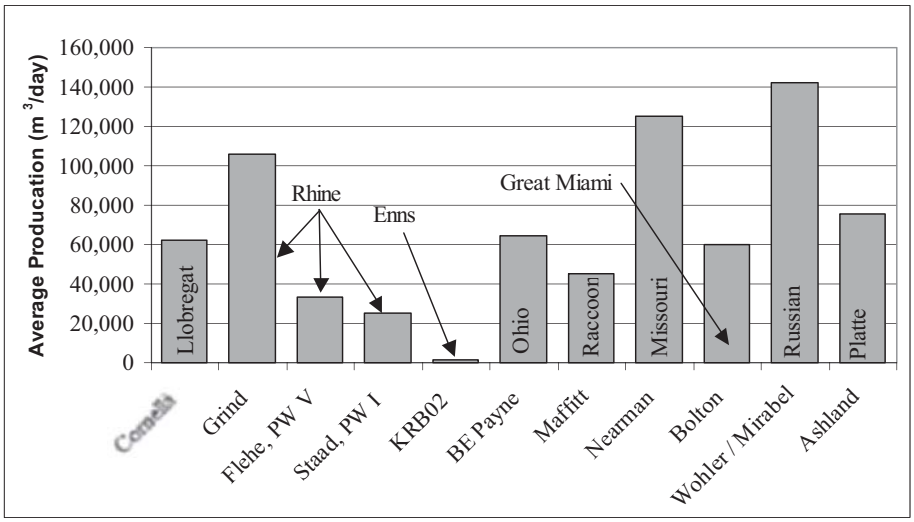

Figure 3. Average Production by Study Site

River profiles were generated for each selected site by plotting the surface elevation of the river at average flow versus distance along the river. These profiles show the slope of the river and the location of the RBF system along the river. From the profiles it can be seen, that the RBF sites are consistently located along the middle to lower reaches of the rivers. One of the most important distinctions among the rivers is the steepness of the profiles. The rivers range from long rivers with relatively flat slopes to short rivers with comparatively steep slopes. The slope is important because it determines the size of sediments that the river is capable of transporting in a given reach, which in turn influences the dominance of erosion or deposition (see Schubert, chapter 1). The profiles are presented in two categories for visual clarity. Rivers that are longer than 1000 km or higher in elevation than 500 m in elevation are shown in Figure 4a. The Platte River, a relatively short river, is included in this graph to show its confluence with the Missouri River. The remaining rivers are displayed in Figure 4b. A constant horizontal to vertical aspect ratio was used so that the slopes of the rivers shown on the two graphs can be visually compared.

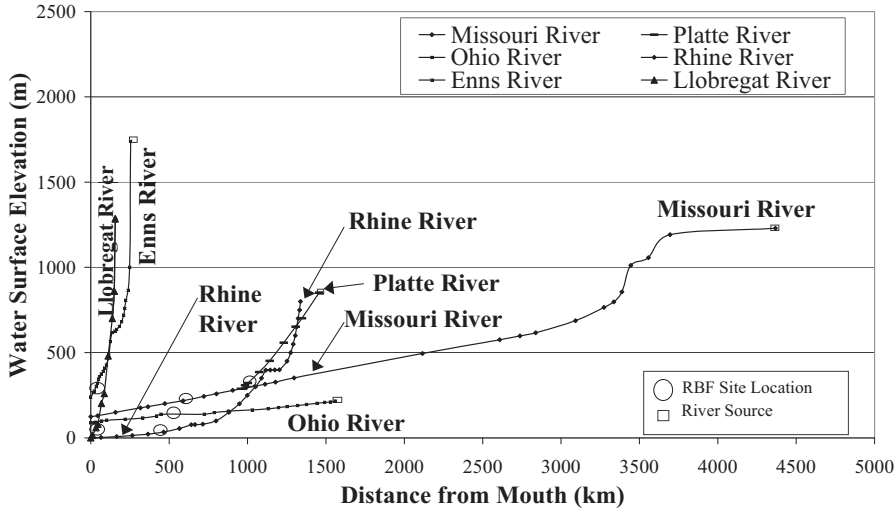

(a) Long River Profiles

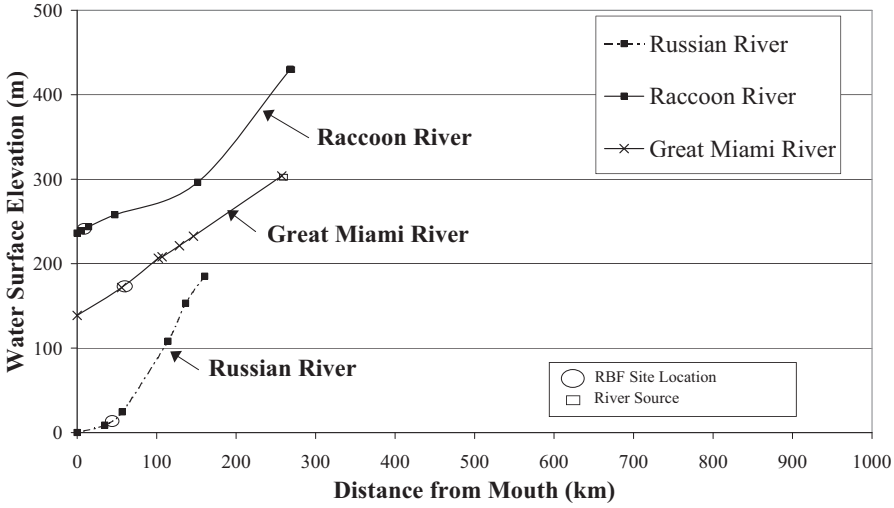

(b) Short River Profiles

Figure 4. River Profiles

3. SITE DESCRIPTIONS

This section includes short site summary for each location included in the study. The descriptions describe the location, the wellfield, and the river.

3.1 Ohio River at Louisville, KY

The Louisville Water Company began operating a single radial collector well in Louisville, KY in August of 1999. The well produces an average of 64,000 m^3/day. The wellfield is located adjacent to the Ohio River, which acts as a source of recharge. The Ohio can be characterized as one of the larger rivers included in the study. It is comparable in size to the Rhine River and is slightly larger than the Missouri River. It is approximately 10 m deep and 600 m wide at the wellfield location. The discharge of the Ohio River is affected by numerous dams located along its length. The Ohio River flows into the Mississippi River approximately 450 km downstream of the wellfield. See Hubbs (chapter 2) for more information on the riverbank filtration system in Louisville, KY.

3.2 Great Miami River near Cincinnati, OH

The Greater Cincinnati Water Works operates the Charles M. Bolton Wellfield in Southwestern Ohio near Cincinnati. The wellfield consists of 10 vertical wells spaced approximately 250 m apart adjacent to the Great Miami River. These wells draw water from the Great Miami River Buried Valley Aquifer, which is hydraulically connected to the Great Miami River (Gollnitz, *et al.* 2003). The 10 vertical wells are used in rotation and operated to meet demand (Gollnitz, *et al.* 2004). The wellfield produces an average of 12,000 m^3/day. The river itself is wide and shallow during normal flow and forms a series of pools and riffles along it length. It is similar in size and shape to the Russian River and Raccoon River. The bed consists of a poorly sorted mixture of cobbles, gravels, and finer material. The Great Miami River is a tributary to the Ohio River. It enters the Ohio River approximately 56 km downstream of the study site.

3.3 Raccoon River at Des Moines, IA

The Des Moines Water Works (DMWW) operates five radial collectors and one large inclined horizontal well adjacent to the Raccoon River in Des Moines, IA. According to data provided by DMWW, the five radial collectors produce an average of about 45,000 m^3/day combined while the

single horizontal well produces approximately 5,000 m^3/day. The wellfield is approximately 15 km upstream from the junction of the Raccoon and Des Moines Rivers. The Raccoon River is a relatively small river. It is wide and shallow like the Russian River and Great Miami River. It is a principal tributary to the Des Moines River.

3.4 Platte River near Ashland, NE

The City of Lincoln operates two radial collector wells on an island of the Platte River in Ashland, NE (Henson *et al*.). The two wells are spaced approximately 1000 m apart and produce a combined average of approximately 76,000 m^3/day (Lee 2004). The Platte River is a broad shallow stream. It becomes a braided channel during periods of low flow. It is similar in depth to the Raccoon, Russian, and Great Miami Rivers, but its width is approximately 10 times greater.

3.5 Russian River in Sonoma County, CA

The Sonoma County Water Agency operates two wellfields adjacent to the Russian River at Mirabel and at Wohler Bridge. The Mirabel wellfield is on an inside bend of the Russian River. It consists of three radial collector wells. The Wohler Bridge wellfield is upstream of the Mirabel wellfield and consists of two collector wells (Constantz 2004). The wells are spaced an average of 300 m apart. An inflatable dam is raised downstream of Wohler Bridge during periods of low flow to raise the river level and induce recharge to the aquifer through a series of infiltration ponds (Jasperse and Beach 2000). The Russian River itself is a wide shallow steam during normal flow and forms a series of pools and riffles along its length. It is similar in size and depth to the Raccoon River and Great Miami River. The Russian River becomes an estuary 37 km downstream of the wellfield at Jenner, CA. The Russian River Estuary flows into the Pacific Ocean. This study site is discussed further in the data collection section of this paper.

3.6 Missouri River at Kansas City, MO

Kansas City Board of Public Utilities began operating a radial collector well adjacent to the Missouri River in Kansas City, KS in August of 2000 (National Water Research Institute 2005). The well is the largest alluvial water well in the world (Collector Wells International, INC. 2005). It produces an average of 125,000 m^3/day and is capable of producing up to 170,000 m^3/day. The Missouri River is similar to the Ohio and Rhine Rivers, but slightly smaller. It is 4 m deep and 300 m wide under normal

flow conditions. The Missouri River flows into the Mississippi River approximately 590 km downstream of the site location. Like the Ohio River, the Missouri River is considered a principal tributary to the Mississippi River.

3.7 Llobregat River at Cornellà, Spain

Barcelona's Water Company (Aigües de Barcelona) operates a vertical wellfield near the Llobregat River in Cornellà, Spain. The wellfield consists of 33 vertical wells, including 26 extracting wells and 7 recharging wells (Martín-Alonso, 2004a). The wells are spaced approximately 200 m apart. The 26 extracting wells produce an average of 62,000 m^3/day. The Llobregat River is a small river with a width of approximately 25 m (Martín-Alonso 2004b). It enters the Mediterranean Sea downstream of the wellfield near Barcelona, Spain.

Many aspects of the site's location distinguish it from other sites. First of all, the RBF system differs from other systems in the way it is operated. The riverbed is fully clogged under normal flow conditions. Mechanical intervention is used to periodically renew clogged areas in the river through scarification of the riverbed. The Barcelona Water Company also uses recharge wells to improve recharge to the aquifer (Martín-Alonso 2004a).

The setting of the RBF system on the Llobregat River also distinguishes it from other systems. Because of its proximity to the Mediterranean Sea, drawdown from water withdrawal causes the intrusion of salt water into the aquifer. The river near the wellfield is not hydraulically connected to the aquifer (Martín-Alonso, 2004a). The infiltration only occurs after the riverbed has been scarified or in the case of flooding (Martín-Alonso 2005). In the first case, water infiltrates in the scarified area of the riverbed and then flows horizontally through the aquifer to the location of the wells. In the case of flooding, infiltration occurs all along the riverbed, resulting in significant recharge to the aquifer. Unique features of the RBF system on the Llobregat River are further discussed in the data collection section of this chapter. The RBF system is discussed in detail in Martín-Alonso (chapter 13).

3.8 Rhine River at Düsseldorf, Germany

Three-quarters of the water supply in Düsseldorf, Germany is supplied by riverbank filtration (Stadtwerke Düsseldorf, AG 2005). The Grind, Staad, and Flehe Waterworks all operate wellfields adjacent to the Rhine River at Düsseldorf, Germany. Because of their close proximity and similar characteristics, the three wellfields are discussed as a group. The Rhine River is one of the larger rivers included in this study. It is similar to

the Ohio and Missouri Rivers in size and shape, but it is slightly larger than the Missouri River. The Rhine River flows into the North Sea approximately 420 km downstream of Düsseldorf, Germany. For more information on RBF on the Rhine River see chapter 10 (Schubert).

The Grind wellfield is the furthest upstream of the three. The wellfield consists of 7 radial collector wells spaced approximately 500 m apart on an inside bend on the left side of the Rhine River (Schubert 2004). The 7 radial collector wells produce an average of 100,000 m^3/day combined.

The Flehe wellfield begins approximately 5 km downstream from the end of the Grind wellfield on an outside bend on the right side of the Rhine River. The wellfield consists of 70 vertical wells spaced approximately 20 m apart, which are connected by a siphon pipe (Schubert 2004). The well gallery produces an average of approximately 22,000 m^3/day.

The Staad wellfield begins approximately 16 km downstream from the end of the Flehe wellfield in a straight section on the right side of the Rhine River. The wellfield consists of 25 vertical wells spaced approximately 20 m apart, which are connected by a siphon pipe (Schubert 2004). The well gallery produces an average of approximately 19,000 m^3/day.

3.9 Enns River at Steyr, Austria

The Ennskraft Company operates a single experimental vertical well on the Enns River near Steyr, Austria (Wett 2004a). The well produces an average of 1700 m^3/day. Though the Enns River is very steep in its upper reaches, the slope at the study location is minimal because of the backwater effect of a reservoir near the wellfield. The Enns Rivers enters the Danube River approximately 35 km downstream.

4. FACTORS AFFECTING YIELD

Yield in bank filtration systems is a function of the volume of water available, the ease at which the water can be transmitted to the well from the aquifer, the ability of the river to recharge the aquifer, and the layout and type of wellfield. However, complex processes that vary from site to site can affect each of these factors. For example, the ability of the river to recharge the aquifer is important to the long-term sustainable yield in riverbank filtration systems. However, experience has shown that the mechanical clogging of the riverbed by fine particles that are suspended in the river water can significantly alter the hydraulic conductivity of the

riverbed and thus limit recharge to the aquifer (Hubbs and Caldwell 2004). The mechanical clogging process is controlled by the size and amount of suspended sediment, entrance velocities in the riverbed, and the riverbed medium. Upstream sediment erosion and deposition processes along with the velocities in the river control size and amount of suspended sediment. Experience has also shown that increased flow velocities and shear stress during a flood can act to resuspend the fine material in the riverbed, thus renewing the river's ability to recharge the aquifer. If adequate scouring events occur, the hydraulic conductivity lost to clogging will be balanced by the increase in conductivity after flood events (Schubert, chapter 1). Otherwise, clogging will result in loss of long-term yield.

The preceding example shows that yield can be affected by many characteristics that are unique to a site including **water quality** (size and amount and suspended sediment), **river hydrology** (because of impact to sediment transport and renewal capability of the river), and **riverbed characteristics** (medium affects susceptibility to clogging and riverbed conductance determines the ability of the river to recharge the aquifer). Yield is also affected other by factors including **site geometry** (layout of wellfield) and **aquifer characteristics** (transmissivity of the aquifer and volume of water available for extraction). **Operational data** (drawdown, driving head, etc.) indicate how well a RBF system is performing. Thus, these data enable the operational performance of the sites to be compared to site characteristics to aid in the understanding of how site conditions affect performance. The proceeding sections elaborate on the broad categories mentioned above and identifies commonly available factors within these categories that can be used to quantify the effects.

4.1 Aquifer characteristics

The aquifer's influence on yield in RBF systems can be characterized by the volume, transmissivity, storativity, and porosity of the aquifer. The volume of the aquifer is important because it determines the quantity of water available for abstraction from a well in the absence of recharge. The transmissivity of the aquifer characterizes the ease at which water flows through the aquifer to the well.

The volume of the aquifer is a function of the saturated thickness, width, and length of the aquifer. The length of the aquifer is not distinguishable in alluvial aquifers where the aquifer follows the river path. Therefore, the saturated thickness and width of the aquifer alone will be used to characterize the quantity of water available.

Transmissivity of the aquifer is a function of the conductivity of aquifer medium and the saturated thickness of the aquifer. Aquifer transmissivity

values are commonly available from pump tests at RBF sites. The transmissivity is the rate of flow per unit width of aquifer through the entire thickness of the aquifer due to a unit hydraulic gradient. Aquifer conductivity and saturated thickness can be used in lieu of transmissivity when it is not available. Transmissivity is the product of the conductivity and saturated thickness of the aquifer.

The storativity of an aquifer is the amount of water that is released per unit area for a unit drawdown in the phreatic surface in an unconfined aquifer. The storage coefficient is the amount of water released from a confined aquifer per unit area for a unit reduction in potentiometric level. The porosity is the ratio of the volume of voids to the total volume of the aquifer material. It influences the velocity at which water moves through an aquifer under a given hydraulic gradient.

Table 2. Aquifer Factors

Aquifer Characteristics
Width
Saturated Depth
Trasmissivity
Hydraulic Conductivity[1]
Storativity or Storage Coefficient
Porosity

[1] Hydraulic Conductivity to be used to calculate Transmissivity

4.2 River Hydrology/Hydraulics

River hydrology influences the ability of the river to recharge the aquifer in RBF systems through its effects on the hydrologic connection between the river and the aquifer. Important hydrologic and hydraulic parameters of the river include discharge, stage, and shear stress.

One of the most significant parameters is the bankfull discharge. Bankfull discharge is important because it can be used to approximate the dominant discharge (Knighton 1998), which is the flow responsible for the transport of the most sediment over time. If the bankfull discharge is responsible for the most sediment transport, it is reasonable to infer that it would likely be most responsible for renewal of clogged areas in RBF systems.

The runoff regime of a river affects yield in RBF systems by altering the riverbed through erosion, transport, and deposition thus determining the self-

cleaning potential of the river (Schubert, chapter 1). The runoff regime can be characterized by average parameters such as average discharge, average maximum yearly discharge, and average minimum yearly discharge near the RBF site. The maximum yearly discharge is computed by averaging the maximum yearly flows for all the years of record. Likewise, the minimum yearly discharge is computed by averaging the minimum yearly flows for all years of record. While these parameters enable rough comparison of flows from different rivers, actual flow measurements in a time series are needed to understand the flow dynamics in a river. A flow hydrograph for a typical year can be used illustrate the magnitude, frequency, and timing of runoff events.

A stage hydrograph is sometimes used in lieu of a flow hydrograph to characterize runoff dynamics. In natural rivers, the relationship between stage and flow is fairly consistent and can be characterized by a stage/discharge function. The stage/discharge relationship often is less defined in regulated rivers.

The stage of the river determines the direction of flow between the river and the aquifer (Schubert, chapter 1). When the elevation of the surface of the river is less than the elevation of the potentiometric surface in the aquifer, groundwater will flow from the aquifer into the river. When the surface of the river is above the potentiometric surface in the aquifer, the river will recharge the aquifer. In RBF, drawdown from pumping in the well lowers the water table to a level below the river surface resulting in recharge from the river to the aquifer.

The clogging and renewal processes in a river are controlled by the rivers ability to transport, deposit, and resuspend sediment. A clogged area is renewed when flow generates a shear stress on the riverbed that is capable of resuspending trapped sediment. Thus, the shear stress on the bottom of the river is a key factor that affects yield in riverbank filtration. One of the easiest methods for estimating shear stress utilizes the water surface profile of the river. The total energy in a stream is the sum of the velocity head, pressure head, and elevation head. If in a reach, most of the head loss is caused by friction along riverbed and other losses (bends, obstructions, wind effects, etc.) are negligible, the shear stress can be estimated through the change in energy between two adjacent cross sections (Schubert, chapter 1 and Hubbs, chapter 2). Assuming that the change in velocity head is small and the river has a uniform cross section, the head loss is approximately equal to the difference in elevation of the water surface. Thus, the water surface slope in a given reach is an indicator of the shear stress imposed on the riverbed.

Schubert (chapter 1) has indicated that most of the sediment transport in the riverbed occurs when the passing of a flood wave causes a temporary

increase in gradient and a temporary increase in discharge between two sections. Thus, the water surface slope and change in water surface slope with time over a very short reach during a flood event are the best indicators of the ability of a stream to transport sediment. However, data for the water surface slope over a very small reach and its variation with time are not readily available for most systems. It may be possible to compare systems by looking at the slope of the stage hydrograph during a high flow event. However, gross slope measured over an extended distance can be used to characterize the shear stress imposed on the riverbed under normal conditions.

The velocity of the river is another indicator of the shear stress imposed by a river and a river's ability to transport sediment. The shear stress on the riverbottom can be estimated from a velocity profile as described by Hubbs (chapter 2). However, since velocity profiles are not normally available, the mean velocity of the stream was substituted. The velocity changes with discharge. The velocity at bankfull and average discharge will be used to characterize the affect of velocity on the shear stress on the riverbed. The mean velocity was determined by dividing the discharge by the cross-sectional area of the stream.

The hydrologic and hydraulic factors that are relevant to yield in riverbank filtration systems are summarized below in Table 3. These factors were used to describe the river hydrology of RBF sites included in the study.

Table 3. River Hydrologic/Hydraulic Factors

River Hydrology/Hydraulic
Bankfull Stage/Discharge
Average Discharge
Average Maximum Yearly Discharge
Average Minimum Yearly Discharge
River Surface Slope at Average Discharge
Mean Velocity at Bankfull Discharge
Mean Velocity of Average Discharge
Cross-sectional Area at Bankfull Discharge[1]
Cross-sectional Area at Average Discharge[1]

[1] Cross-sectional area will be used to calculate Mean Velocity

4.3 Site Geometry

The site geometry of RBF facilities impacts the ability of the river to recharge the aquifer and influences severity of clogging. The location of a wellfield can be described by its distance from the river and proximity to river bends. The perpendicular distance from the center of the wellfield to the river determines the amount of river water that a given pumping scheme will cause to infiltrate the aquifer. Thus systems close to rivers would be expected to yield more water due to increased recharge. However, these systems are also more susceptible to clogging due to increased entrance velocities into the riverbed. RBF systems can be located in straight river sections or along the inside or outside of the river bend. The outside bend of a river experiences greater velocities and thus greater shear stress for a given discharge than the inside bend. Ironically, outside bends can be more susceptible to clogging. According the Schubert (chapter 10), large stones in outside bends may shield clogged layers from the renewal effects of shear stress during flood waves. Lower river velocities along inside bends result in the deposition of movable material that is not protected by an armor layer of large stones. Thus the clogging that occurs along the inside bend is more likely to be renewed by flood waves. Another advantage in locating wellfields at the inside bend is that the natural groundwater flow across such areas results in additional recharge to the aquifer (Schubert chapter 10). See Figure 5.

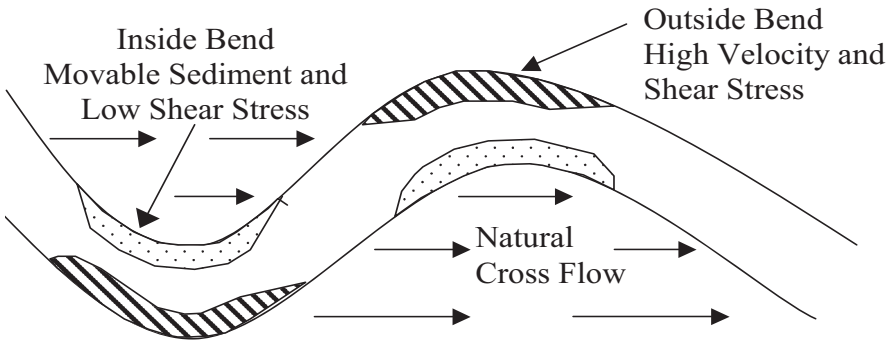

Figure 5. River Meander

The layout of the wellfield affects yield by controlling the flow paths of the river water through the riverbed to the aquifer and from the aquifer to the well. Wellfields with multiple wells spaced along the river impact a longer length of riverbank than single wells, and thus experience recharge from a longer reach in a river. The length of river impacted is expected to significantly influence yield. However, the limits of hydraulic influence are

difficult to quantify since a pumping well theoretically influences an infinite distance in all directions away from the well. Practical methods of estimating the length of river impacted will be discussed later.

Two types of RBF wells are vertical wells and radial collector wells. Typically, radial collector wells have greater capacities than vertical wells. The depth of the aquifer limits the length of wellscreen in a vertical well. In shallow aquifers, radial collector wells are preferable because more wellscreen can be utilized.

The geometry of the river itself also influences yield in RBF systems. The geometry can be characterized by the width and depth of the river. Particularly, in a river where clogging is problematic, the width of the river can act to compensate for lost capacity by enabling the infiltration area to spread across a wider area. In narrow rivers, the extent of the infiltration area can extend across the entire length of the river. In this situation, clogging has a more significant impact on yield, since the width of the infiltration area cannot increase to compensate for lost capacity. Conversely, when clogging occurs in RBF systems along a wide river, the width of the infiltration area grows to partially compensate for clogging. Hubbs documented this phenomenon during a pump test of a horizontal well in Louisville, KY (Hubbs and Caldwell 2004). Since both the depth and width of a river changes with stage, the depth and width of rivers at average discharge and bankfull discharge will be used to quantify the geometry of rivers at RBF sites.

The factors summarized below in Table 4 were used to describe the site geometry of RBF sites.

Table 4. Site Geometry Factors

Site Geometry
Distance from River to Center of Well
Location Relative to River Bends
Length of River Impacted
Type and number of Wells
Total Length of Wellscreen
Depth of River at Average Discharge
Depth of River at Bankfull Discharge
Width of River at Average Discharge
Width of River at Bankfull Discharge

4.4 Riverbed Characteristics

The riverbed is the interface between the river and the aquifer. Thus, it influences the ability of the river to recharge the aquifer. The ease at which water can flow through the riverbed can be quantified by its hydraulic conductivity. Medium composed of fine particles have lower conductivities than medium composed of coarser particles. Thus the grain size distribution of the riverbed can provide insight into hydraulic conductivity of the aquifer, when a direct measure of the hydraulic conductivity of the riverbed is not available. The grain size distribution can be quantified by estimating characteristic sizes such as the D_{10}, D_{50}, and D_{90}. The D_{10} size is important because it describes the size of the fine materials in the riverbed. A small D_{10} size would indicate the presence of very fine materials that could limit hydraulic conductivity and provide evidence of clogging. The D_{50} size indicates the average size of the particles. The D_{90} size describes the size of the larger fraction of particles. The D_{90} size can indicate the presence of an armor layer if it is large compared to the D_{10}, and the size of particles in transit are much smaller than this armor layer. The formation of an armor layer reduces capacity in RBF systems by protecting trapped sediment from resuspension during flood events. The presence of an armor layer can be confirmed by looking at the sediment size distribution as a function of depth in the first few feet of riverbed. If an armor coat is present, large sediment near the top of the riverbed will shield fine sediment in the layers below.

The significant riverbed characteristics are included below in Table 5.

Table 5. Riverbed Factors

Riverbed Characteristics
Vertical Hydraulic Conductivity
Particle Distribution of Sediment
D_{10}, D_{50}, and D_{90} Sizes
Presence or Absence of Armor Layer

4.5 Water Quality

River water quality affects yield by influencing clogging of the riverbed. Decreases in the hydraulic conductivity of the riverbed can result mechanical, biological, and chemical clogging. Therefore, the biological and chemical makeup of the water and size of suspended sediment can influence yield in RBF systems.

As described previously, mechanical clogging occurs when suspended sediment in the river becomes trapped in the riverbed as water passes from the river to the aquifer. The potential for mechanical clogging can be described by the size and amount of particles in suspension (Schubert 2002, pg 149). The size of suspended sediment can be described by a particle distribution or through the use of key sizes such as the D_{10}, D_{50}, or D_{90}. These sizes increase as the velocities in the stream increases. Thus, suspended sediment size and concentration is dependant upon discharge. The size distribution and concentration of suspended sediment at average discharge were chosen to represent the size quantity the suspended sediment in the river. The amount of suspended sediment can be represented by the total suspended solids or the turbidity of the water.

Biological clogging occurs when a biological film forms on the river bottom due to the accumulation of microbial bodies or their metabolic by-products (Baveye 2004). In order for biological clogging to occur there must be sufficient nutrients in the water to support biological activity (Engesgaard 2004). TOC, chlorophyll, and dissolved oxygen concentrations of the water are three factors that can be used to quantify the nutrient content of the water.

Chemical clogging is the loss of hydraulic conductivity of the riverbed due to clogging by chemical precipitants. Some factors thought to influence chemical clogging are the iron, ammonia, and nitrate concentrations, and the hardness of the water. Biological activity can lead to chemical clogging. This occurs when high levels of biodegradable material cause changes in the redox-potential and pH of the river water which in turn results in the precipitation of substances (Schubert 2002 pg 149). So, in addition to the factors identified above, the pH and redox potential of river water and extracted water should be considered when evaluating potential chemical clogging. Values at average discharge were chosen to represent the chemical quality the rivers. See Stuyfzand (chapter 6) for additional information on chemical clogging of RBF systems.

The water quality factors are summarized in Table 6.

Table 6. Water Quality Factors

River Water Quality
Suspended Sediment Size Distribution at Average Discharge
Suspended Sediment D_{10}, D_{50}, and D_{90} at Average Discharge
Average Total Suspended Solids
Average Turbidity
Average Phosphorous
Average Dissolved Oxygen
Average TOC level
Average Dissolved Oxygen in River and in Extracted Water
Chlorphyll Concentration
Average Iron Concentration
Average Nitrate Concentration
Average Ammonium Concentration
Average Hardness
Redox Potential of River and Extracted Water
Average pH

4.6 Operational Data

Operational data can be used to evaluate the performance of RBF facilities. Measurements of flowrate, drawdown, and temperature are often available from the utilities that operate RBF systems. The performance of a well is often evaluated using the specific capacity of the well, which is equal the discharge of the well divided by the corresponding drawdown and is assumed constant for a given temperature. Traditionally, specific capacity has been use to evaluate the performance of individual wells only. However, in the context of this research, specific capacity was used to evaluate the performance of the entire wellfield collectively. Thus, the term specific capacity, when used is this study, refers to the bulk specific capacity of the wellfield and takes into account the total discharge from the wellfield and the average drawdown in the wells. The maximum capacity of a system at a given temperature can be estimated by multiplying the specific capacity at that temperature expected by the available drawdown. When data that describe the variation of specific capacity with temperature are not available, the average discharge and drawdown can be used to generate a rough estimate of specific capacity.

Water temperature affects yield in RBF systems because it influences the viscosity of the water and thus the ease at which it moves through the

riverbed and the aquifer. Because of this, the amount of drawdown needed for a given flow fluctuates with water temperature. Therefore, water temperature measurements in the river and aquifer are needed to account for temperature affects on the specific capacity of a system. Temperature statistics such as the mean, minimum, and maximum temperatures are sufficient for rough comparisons of temperature variations between systems. Temperatures vary in annual cycles.

The operational factors that were used to evaluate the performance of RBF facilities are summarized in Table 7.

Table 7. RBF Performance Factors

Operation Data
Average Flowrate from Well
Average Drawdown in Well
Specific Capacity
Available Drawdown
Maximum Capacity
Min., Average, and Max. River Temperature for a Typical Year
Min., Average, and Max. Well Temperature for a Typical Year
Temperature Lag between River and Well

5. CONCEPTUAL MODEL OF RBF SYSTEM

The geometric conditions of the aquifer identified previously as aquifer characteristics important to yield were the aquifer width (W_A) and the saturated thickness of the aquifer (Th). The site conditions discussed in the site geometry section included: the perpendicular distance from the center a well to the river (D_w), the site locations relative to river bends, the length of river impacted (L), the types of well(s), the width of the river (W_R), and river depth of the river (y). A model was developed to help visualize some of these geometrical elements at a RBF facility. The model consisted of a wellfield adjacent to a river that is hydraulically connected to an alluvial aquifer. The basic layout of the model is shown below in Figure 5.

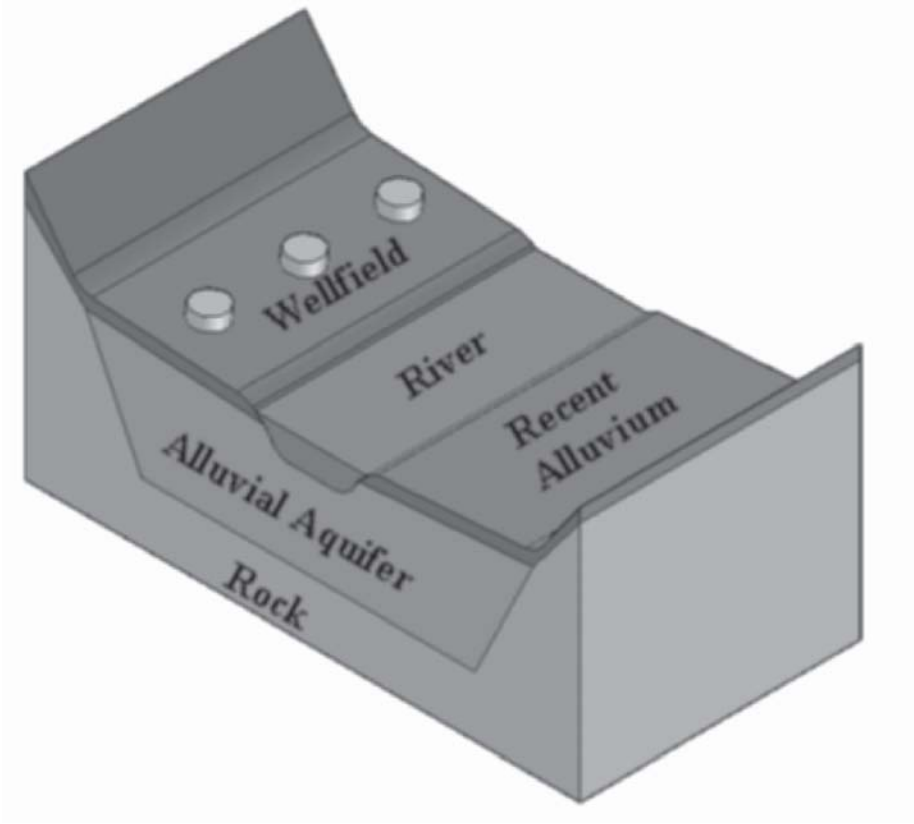

Figure 6. Conceptual Model of RBF System - Isometric View

The dimensions of geometric site characteristics were labeled in the top and front views of the conceptual model shown below in Figure 7 and Figure 8.

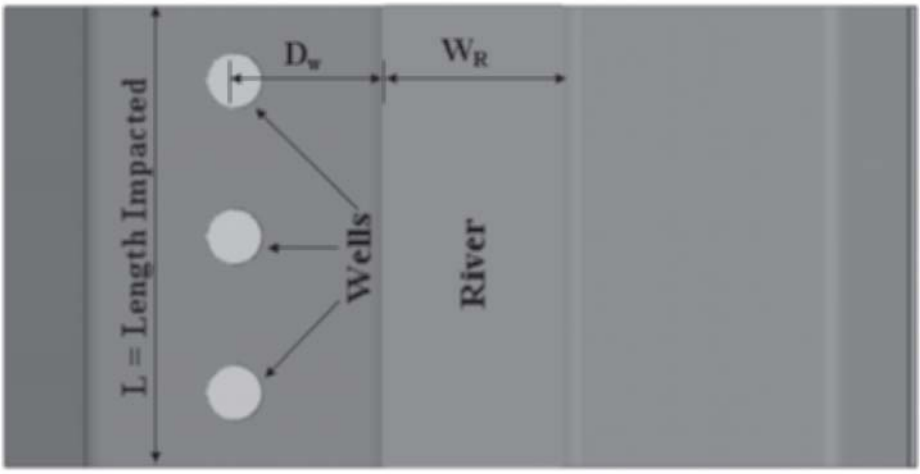

Figure 7. Top View of Conceptual Model

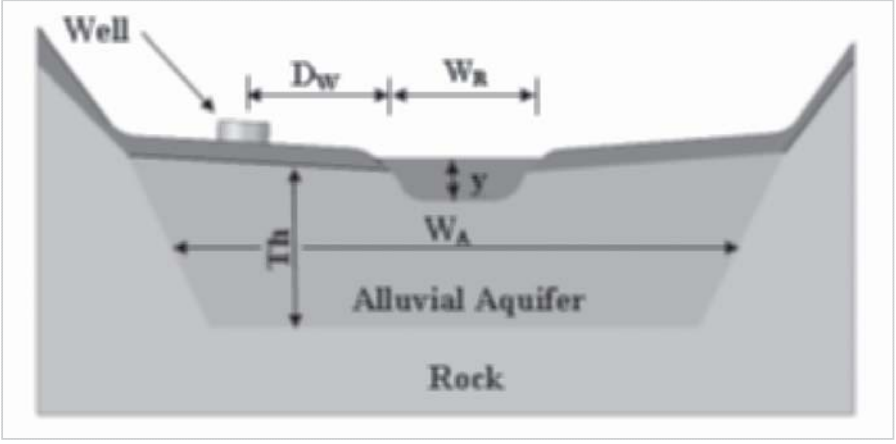

Figure 8. Front View of Conceptual Model

6. DATA COLLECTION

Each site included in the study was investigated to determine the values for the factors identified previously as significant to yield. Data was collected through literature searches, Internet searches, site visits, and email correspondence.

For sites in the United States, much of the required information came from United States Geographic Survey (USGS), the National Weather Service (NWS), literature searches, and sites visits. Data from the USGS were used extensively. For each site, stage measurements, streambed sediment analyses, and water quality data were collected from the USGS website for a gage station near the RBF site. Discharge measurements were used to calculate average discharge, yearly maximum discharge, and yearly minimum discharge. Stage measurements were used to determine stream elevations along each river. This information was combined with rivermile/kilometer information from USGS Water Data Reports to create water surface profiles for each river. When rivermile/kilometer information was not available from USGS, distances were estimated using river maps. The completed profiles were used to calculate stream surface slopes. Water quality data was used to estimate water quality parameters such as suspended solids concentration at important discharge rates. Streambed sediment data were used to evaluate D_{10}, D_{50}, and D_{90} sizes. In addition, river geometry and temperature measurements were available for certain sites.

Bankfull and flood discharges were available from the National Weather Service's Advanced Hydrologic Prediction Service and U.S. Army Corps of Engineers (USACE) for many of the sites. Plan and cross section views of RBF facilities were acquired from literature searches, site visits, and email correspondence. These drawings were used to determine the geometric site conditions, type of wellfield, location relative to riverbends, and various other measurements as defined in the conceptual model. However, because the conditions in some of the sites did not match the conceptual model, judgments had to be made to determine the best estimate of the required parameters.

Site visits proved valuable for verifying information previously collected and collecting new data. Sites that were visited included the Russian River in Sonoma County, California, the Great Miami River near Cincinnati, Ohio, and the Ohio River in Louisville, Kentucky. During the site visits, observations were made on the riverbed materials and with the materials that were being transported by the streams. Information from operating utilities was collected during the site visits and consisted of plan and cross sectional views of the sites, reports from studies performed, and raw operational data.

The information collected through the methods previously described was compiled into a table that summarized the data available for all the sites included in the study. Blanks cells were used to represent missing information. The table was then sent by email to the utilities that operated the sites, researchers who studied the sites, or other individuals who were otherwise knowledgeable of the RBF facility. Those individuals were asked to verify the information in the table and provide the information needed to complete the table. This process was especially useful for collecting data from European sites because literature and web searches provided little information for those sites. In fact, most of the information for European sites was acquired through email correspondence.

Much of the data acquired consisted of ranges of values. If a range of values was obtained for a particular factor, attempts were made to reduce the range into a representative value for easy comparison to the corresponding values from other sites included in the study. This was done using by using available information and choosing the most representative value or by averaging the maximum and minimum of the range when additional information was unavailable.

An important aspect to keep in mind when comparing the data is that the data points were colleted from many different sources. Ideally, the data for all sites included in the study would come from comparable sources and be reported in a standard way. However, some data points came from very specific tests while others were estimates by professionals familiar with the site. This procedure introduced some uncertainty into the analysis of the data.

6.1 Deviations from the Conceptual Model

Data collection for some of the sites was complicated by unique conditions that did not match the model. For example, some of the conditions in the RBF site adjacent to the Russian River in Sonoma County, California did not match the model. The site consisted of five collector wells, two of which were located on the left side of the river upstream of Wohler Bridge and three of which were further downstream on the right side of the river on an inside bend (Constantz 2004). Ideally, the two wellfields would have been separated into two sites to take into account the effects of the river bend on the three downstream wells. However, the performance of the sites could not be evaluated individually since the operators of the wellfields only monitored the total yield from the two sites combined. Since three of the five wells were on the inside bend, the site as a whole was designated as being on an inside bend. The length of riverbank impacted for the two wellfields was determined by estimating the length for each well and

calculating the sum. The estimation was revised after an engineer familiar with the site estimated that the length was two to three times the initial estimate. An average distance could be used to represent the distance from the center of the wells to the river. The operation of the wellfields further complicated the data collection for this site. A rubber dam downstream of the wellfields of the Wohler Bridge wellfield was raised in the summer to augment the river stage and divert flow into infiltration ponds that are used to provide additional recharge to the aquifer (Jasperse and Beach 2000). The dam is 35.4 km upstream from the mouth of the Russian River at the Estuary (Entrix 2004, Section 2, Pg. 10). The yield from the RBF wells during the period where the inflatable dam was raised were higher than yields in the winter periods when the dam and recharge ponds were not being used. Because the infiltration ponds and inflatable dam differed from the model, operational data from the winter period when the dam was lowered was used to describe the performance of the system.

The riverbank filtration site near Barcelona, Spain on the Llobregat River provided an example of a riverbank filtration system operated under extreme conditions. The riverbed is fully clogged under normal flow conditions. Mechanical intervention is used to periodically renew clogged areas in the river through scarification of the riverbed. The Barcelona Water Company also uses recharge wells to improve recharge to the aquifer (Martín-Alonso 2004a). Unlike the river in the conceptual model, the Llobregat River is not directly connected to the aquifer at the location of the riverbank filtration wells. Infiltration only occurs in the scarified area and in the case of flooding. In the first case, the water infiltrates vertically through the scarified area of the riverbed upstream of the RBF system and then flows horizontally through the aquifer downstream to the location where it is extracted using riverbank filtration wells (Martín-Alonso 2005). In the case of flooding, infiltration occurs all along the riverbed, resulting in significant recharge to the aquifer. The RBF system on Llobregat River is unique. The information for this location was included in the tables for informational purposes only. Parameters were estimated to be as representative as possible. However, the value of comparing the data from the Llobregat River RBF system to the others is limited because of the fundamental differences in the site characteristics and operation. This site is fully described by Martín-Alonso in chapter 13.

6.2 Method for Estimating Length of Riverbank Impacted

The length of riverbank impacted by a RBF system is difficult to estimate without detailed data from monitoring wells along the river. Therefore,

estimation by individuals experienced with the system was used where available. Otherwise, the length was estimated by observing the layout of the wellfield. For vertical wellfields, the length was assumed to be equal to the length of the wellfield plus half the distances between the outer wells and the nearest adjacent wells. A single radial collector well was assumed to impact 600 m of riverbank unless available information indicated otherwise. For multiple collector wells, the length was estimated using the same procedure as for the vertical wellfield. Though these procedures result in a crude estimation of length impacted, the results should be accurate enough for comparison between study sites. Ideally, the lengths would be estimated from standard values of negligible drawdown or certain percent of the total drawdown. This would ensure results that are more accurate and easier to compare.

7. ANALYSIS AND RESULTS

The data collected were divided into tables by category so that the sites could be compared by layout, river hydrology/hydraulics, aquifer characteristics, riverbed characteristics, river water quality, and operational performance. Information was not available for all factors for every site. Blank cells represent cases of missing information.

7.1 Comparison of Aquifer Characteristics

Data obtained for aquifer characteristics are presented in Table 8. Large, highly transmissive aquifers are expected to have positive influences on production in RBF systems. The aquifer at the Llobreget River had the highest transmissivity of all the sites. However, as mentioned previously, the RBF system on the Llobregat River is unique and difficult to compare with other systems. The systems with the larger aquifers included wellfields at the Great Miami and Rhine Rivers. The Enns River aquifer was the smallest of all the aquifers.

Table 8. Aquifer Characteristics

River	Wellfield	Aquifer Width (River Side) (km)	Aquifer Width Total (WA) (km)	Sat. Thick-ness (Th) (m)	Aquifer Area (m^2)	Trans-missivity (m^2/day)	Stora-tivity	Poro-sity
Llobregat	Cornellà		2.5[(1)]	40	100,000	18000		0.38
Rhine	Grind	5	10.0	15	150,000	3900		0.2
Rhine	Flehe, PW V	5	10.0	15	150,000	3900		0.2
Rhine	Staad, PW I	5	10.0	15	150,000	3900		0.2
Enns	KRB02	0.4	0.8	5	4,000	1600		0.2
Ohio	BEPAYNE	2	2.0	20	40,000	2500	0.0005	0.38
Raccoon	Maffitt							
Missouri	Nearman					9600		
Great Miami	Bolton	0.3	2.8	50	141,000	5700		0.25
Russian	Wohler / Mirabel			15		10600		
Platte	Ashland	1	2.6	20	53,000	3100	0.2	0.3

[(1)] Aquifer width shown for wellfield at Cornellà on the Llobregat River is given for location of RBF system. The aquifer with near the area of recharge from the river varies from 0.25 km to 2.1 km

7.2 Comparison of River Hydrology/Hydraulics

Hydrology and hydraulics data obtained for the study sites are presented in Table 9. As seen in the table, the rivers with the largest discharge are the Ohio River, the Rhine River, and the Missouri River. The river with the lowest slope is the Ohio River. See Figure 3a and 3b for river profiles for each river included in the study.

Table 9. River Hydrology/Hydraulics

River	Wellfield	River Discharge				Bankfull		Average Discharge		
		Avg. (m^3/s)	Bank-full (m^3/s)	Avg. Max. Yearly (m^3/s)	Avg. Min. Yearly (m^3/s)	Cross-sectional Area (m^2)	Mean Vel. (m/s)	Cross-sectional Area (m^2)	Mean Vel. (m/s)	River Surface Slope (m/km)
Llobregat	Cornellà	20		400	2			5 [1]	1.5 [1]	0.8
Rhine	Grind	2100		9400	810			2000	1.0	0.2
Rhine	Flehe, PW V	2100		9400	810			2000	1.0	0.2
Rhine	Staad, PW I	2100		9400	810			2000	1.0	0.2
Enns	KRB02	160		900	70			300	0.6	1.8
Ohio	BE-PAYNE	3300	8500	14000	240	6700	1.3	6000	0.5	0.04 [5]
Raccoon	Maffitt	50	300	500	4	200	1.7	60	1.0	0.5
Missouri	Nearman	1500	5100	4800	410	3000	1.8	1000	1.2	0.2
Great Miami	Bolton	100	900	1000	10	500	1.8	200	0.4	0.7
Russian	Wohler / Mirabel	40 [2]	500 [3]	800 [2]	5 [2]		2.0 [4]		0.6 [4]	0.8
Platte	Ashland	160	3700	1000	30	1000	2.6	200	0.8	0.2

[1] Data shown is for most frequent flow. The most frequent flow is 8 m^3/s

[2] Discharge measurements were computed by adding the daily flow data from USGS gage 11465350 at the mouth of Dry Creek to daily flows from USGS gage 1464000 near Healdsburg, approximately 19 km upstream of wellfield. Dry Creek flows were not measured for discharge values greater than 5.7 m^3/s. Missing flow records were filled in using flow values of 5.7 m^3/s. This should result in an underestimation of flows from Dry Creek. This will effect the average flow, average maximum yearly flow, and the average minimum yearly flow.

[3] Bankfull discharge given represents the bankfull condition of Russian River near Healdsburg 19 km upstream of the wellfield.

[4] Velocity at average and bankfull discharge was estimating using USGS measurement data from gage 1464000 near Healdsburg because discharge data for the wellfield location was unavailble. The condition likely differs from that of the wellfield.

[5] Wellifeld is located in pool upstream of a dam. Data given is the pool slope.

7.3 Comparison of Site Geometry

The wells included in the study displayed a variety of layouts. About half of the locations utilized vertical wells while the other half utilized radial collector wells. The well-to-river distances were between 35 m and 260 m for the majority of the sites. The well to river distance for the Llobregat River was more than 5 times larger than for the other locations. Well spacing varied from 20 m for the Staad and Flehe wellfields to 1000 m in the Platte River Wellfield. The Grind wellfield on the Rhine River had the largest total length of wellscreen. The Site Geometry information was split into two tables because of size limitations. The geometry data are presented in Tables 10 and 11.

Table 10. Site Characteristics -1

River	Wellfield	Distance from River to Wells (m)	Location Relative to River Bends	Length of River Impacted (m)	Number of Wells	Distance Between Wells (m)
Llobregat	Cornellà	1650	Unaffected	Negligible	26 Extracting Wells, 7 recharging wells	200
Rhine	Grind	260	Inside Bend	5000	7 Radial Collectors	500
Rhine	Flehe, PW V	50	Outside Bend	1400	70 Vertical Filter Wells Connected by Siphon Pipe	20
Rhine	Staad, PW I	35	Straight	500	25 Vertical Filter Wells Connected by Siphon Pipe	20
Enns	KRB02	48	Inside Bend	500	Single Vertical Well	N/A
Ohio	BEPAYNE	37	Straight	600	Single Radial Collector	N/A
Raccoon	Maffitt		Straight		5 Radial Collectors and 1 Horizontal Well	
Missouri	Nearman	61	Straight		Single Radial Collector Well	N/A
Great Miami	Bolton	100 (1)	Varies	2500	10 Vertical Wells	250
Russian River	Wohler Bridge and Mirabel		Straight/Inside (2) Bend	3000	5 -Radial Collectors	300
Platte	Ashland	130	Island in River	1500	2 - Radial Collectors	1000

(1) Distance provide for low flow condition

(2) The Wohler Bridge wellfield is on a straight section of the river. The Mirabel wellfield is on an inside bend.

Table 11. Site Characteristics-2

River	Wellfield	Average Length of Wellscreen (m)	Total Length of Wellscreen (m)	Depth of River at Average Discharge (m)	Depth of River at Bankfull Discharge (m)	Width of River at Average Discharge (m)	Width of River at Bankfull Discharge (m)
Llobregat	Cornellà	10	260	0.5 [1]		25	25
Rhine	Grind	670	4700	12	20	380	
Rhine	Flehe, PW V	19	1300	12	20	380	
Rhine	Staad, PW I	19	480	12	20	380	430
Enns	KRB02	2	2	5		80	90
Ohio	BEPAYNE	480	480	10	16	610	640
Raccoon	Maffitt	210 [2]	1100 [2]	1	3	60	90
Missouri	Nearman			4	8.2	305	351
Great Miami	Bolton	17	170	2	4	60	150
Russian River	Wohler Bridge and Mirabel			1	12	60	80
Platte	Ashland	400	800	1	5	300	400

[1] Depth given is for the most probable discharge.

[2] Wellscreen information displayed for the Maffitt Wellfield on the Raccoon River is for the 5 radial collector wells only. Data was not provided for the inclined horizontal well.

7.4 Comparison of Riverbed Characteristics

Riverbed characteristics data are presented in Table 12. The conductivity of the riverbed is important because it influences the quantity of water that passes from the river into the aquifer. The location with the highest riverbed conductivity was the wellfield adjacent to the Llobregat River. The D_{10}, D_{50}, and D_{90} sizes ranged from 0.2-0.4 mm, 0.5-20 mm, and 1.9 to 30 mm, respectively. An armor layer was reported at five of the study sites. Of these sites, the Russian River and the Great Miami River had armor layers that were moved regularly. This was expected since the sites reported higher velocities and lower D_{90} sizes than the other locations where armor layers had formed. Conversely, the armor layer on the Rhine River did not move frequently. This was expected since data indicated that the Flehe wellfield had the largest riverbed D_{90} size of the all the sites studies. The values for riverbed conductivity were extremely variable. Riverbed conductivity is

difficult to measure. The high variation can be attributed in part to differences in methods of defining and measuring riverbed conductivity.

Table 12. Riverbed Characteristics

River	Wellfield	Riverbed Hydrauilic Conductivity (m/day)	D_{10} (mm)	D_{50} (mm)	D_{90} (mm)	Armor Layer ?
Llobregat	Cornellà	0 [1]				Yes
Rhine	Grind	260 [2]		18		No
Rhine	Flehe, PW V	300 [2]	0.4	12	30	Yes
Rhine	Staad, PW I	300 [2]		20		Yes
Enns	KRB02	2 [3]	0.022	2		No
Ohio	BEPAYNE	15 [4]	0.25	2	8	No
Raccoon	Maffitt					
Missouri	Nearman		0.3	0.6	1.6	
Great Miami	Bolton	0.5 [5]				Yes[6]
Russian	Wohler Bridge and Mirabel		0.3	4.4	17	Yes [7]
Platte	Ashland	80	0.2	0.5	1.9	

[1] Under normal conditions a layer of silt completely blocks the infiltration of water and the riverbed is fully clogged. In the case of flooding, the silt layer is removed and for a short period of time the riverbed conductivity is similar to the aquifer conductivity.

[2] Riverbed conductivity values for the Rhine River were derived from particle size distribution for samples extracted from several borehead cores.

[3] Value refers to conductiviy of riverbank. The riverbed conductivity is 0 m/day. The value for the riverbank conductivity was estimating by calibrating a numerical model an assuming a 1-m thickness of riverbank.

[4] Estimate from "Evaluation of Riverbank Filtration as a Drinking Water Treatment Process" for the top 0.6 m of riverbed medium.

[5] Conductivity was calculated assuming uniform infiltration over the riverbed and using an average width

[6] An armor layer was observed during a site visit. However, there was evidence that the armor layer was frequently transported during flood events.

[7] There was evidence that the armor layer is moved frequently during flood events.

7.5 Comparison of River Water Quality

Water quality parameters are important in the chemical, biological, and mechanical clogging processes. The water quality data were split into two tables because of space constraints. These data are presented in Tables 13 and 14.

Table 13. Water Quality Characteristics -1

River	Wellfield	Suspended Sediment At Avg. Discharge			Turbidity at Average Discharge (NTU)	Total Suspended Solids at Average Discharge (mg/l)	Nutrients and Biological Activity at Average Discharge			
		D_{10} (mm)	D_{50} (mm)	D_{90} (mm)			Total Phos. (mg/l)	TOC (mg/l)	Dis. Oxygen (mg/l)	Chlorophyll Content (mg/l)
Llobregat	Cornellà				270			6	7.9	0.03
Rhine	Grind	<.5[(1)]	5 [(1)]	20 [(1)]	35		0.22	3	10.6	0.009
Rhine	Flehe, PW V	<.5[(1)]	5 [(1)]	20[(1)]	35		0.22	3	10.6	0.009
Rhine	Staad, PW I	<.5[(1)]	5 [(1)]	20[(1)]	35		0.22	3	10.6	0.009
Enns	KRB02					16	0.05	2	10-12	
Ohio	BEPAYNE	<0.002	0.005	0.03	60	40	0.2	3	10-12	0.005
Raccoon	Maffitt				50	180	0.3		9	
Missouri	Nearman				130	500		4	9.9	
Great Miami	Bolton				30	80	0.2	5	10	
Russian	Wohler / Mirabel		0.08	0.09	22		0.2	4	9	
Platte	Ashland		0.3	0.12	50	330	0.5	4	9.6	

[(1)] Data given is for bed load transfer size.

Table 14. Water Quality Characteristics –2

River	Wellfield	Chemical Clogging Parameters at Average Discharge						Quality of Extrated Water	
		Nitrate (mg/l as N)	Amm - onia (mg/l as N)	Hardness (mg/l as $CaCO_3$)	Iron (mg/l as Fe)	pH	Redox Potential mV	Dis. Oxygen (mg/l)	Redox Potential mV
Llobregat	Cornellà	9.8	1	400	0.06	8.5			
Rhine	Grind	3.6	0.2	250	1.2	7.9	300	0-6	
Rhine	Flehe, PW V	3.6	0.2	250	1.2	7.9	300	0-6	
Rhine	Staad, PW I	3.6	0.2	250	1.2	7.9	300	0-6	
Enns	KRB02	4	0.05	170	0.5	8.2	210	8	230
Ohio	BEPAYNE	1.4	0.07	140	0.9	7.9		0-2	
Raccoon	Maffitt	12	0.05	290	0.9				
Missouri	Nearman			230	4.5	8.0			
Great Miami	Bolton				0.02	8.1			
Russian	Wohler / Mirabel	0.2	0.05	100	2.5	7.6			
Platte	Ashland	0.9	0.1	190	10	8.2			

7.6 Comparison of Operational Performance

The operational data were split into two tables. The production and drawdown characteristics are presented in Table 15. The temperature characteristics are found in Table 16. There was a clear delineation between the available drawdown reported for study sites in the United States and study sites in Europe. The available drawdown at European sites ranged from 0 to 8 m. The available drawdown for the U.S. sites ranged from 14 to 19 m. Since the aquifers in the US and Europe were comparable, the difference in reported available drawdown can be attributed to differences of judgments of utilities in the U.S. and Europe about the amount of drawdown available for a given situation. Utilities in Europe were more conservative and less likely to fully utilize the aquifer than utilities in the U.S.

A similar discrepancy was evident in the temperature data. The magnitude of the variation of temperature in the wells at the U.S. sites matches more closely with the river temperature variation than does the variation in well temperature at sites in Europe. The maximum capacity was estimated by multiplying the average specific capacity by the available drawdown. The Platte River had the highest estimated maximum capacity.

Table 15. Operational Characteristics – 1

River	Wellfield	Average Pumping Rate (m^3/day)	Average Drawdown in Well (m)	Specific Capacity (m^2/day)	Available Drawdown (m)	Sustainable Capacity (m^3/day)
Llobregat	Cornellà	62,000	2.0	31,000	0[(1)]	0 [(2)]
Rhine	Grind	106,000	4.0	26,500	8	212,000
Rhine	Flehe, PW V	33,000	1.7	19,000	5	97,000
Rhine	Staad, PW I	25,000	2.0	12,500	5	63,000
Enns	KRB02	2,000	0.8	2,160		
Ohio	BE Payne	64,000	11.0	6,000	19	110,000
Raccoon	Maffitt	45,000	2.4	19,000	19	360,000
Missouri	Nearman	125,000	6.1	20,000	14	290,000
Great Miami	Bolton	60,000				
Russian River	Wohler / Mirabel	142,000[(3)]				
Platte	Ashland	76,000	3.0	26,000	19	480,000

[(1)] The water level in the aquifer is below sea level. The global abstraction from the system is causing severe saline intrusion (Martin, J., 2005).

[(2)] Current production practices overexploit the aquifer and are unsustainable (Martin, J., 2005).

[(3)] Data given is the average production in the river when the inflatable dam is not raised diversion ponds are not filled

Table 16. Operational Characteristics – 2

River	Wellfield	River Temperature for a Typical Year (deg C)			Well Temperature for a Typical Year (deg C)			Temperature [1] Lag between River and Well (days)
		Min.	Avg.	Max.	Min.	Avg.	Max.	
Llobregat	Cornellà	5	18	30	11	17	24	1460 [2]
Rhine	Grind	4	14	26	11	14	17	90
Rhine	Flehe, PW V	4	14	26	10	14	18	45
Rhine	Staad, PW I	4	14	26	10	14	18	35
Enns	KRB02	1		16				4
Ohio	BE Payne	3	17	29	12	18	26	60
Raccoon	Maffitt	1	14	25				
Missouri	Nearman	1	15	29	9	18	26	25
Great Miami	Bolton	1	16	31				
Russian River	Wohler / Mirabel							
Platte	Ashalnd	0	15	28	5	13	22	30

[1] Temperature lag was graphically estimated by visual comparison of time-series graphs of river and well temperature.

[2] Data given is the transient time between the scarification area and the abstraction area under normal conditions. The transient time differs when large amounts of water infiltrates from the river during periods of flooding. (Martin, J., 2005)

7.7 Identification of Factors Affecting Yield

The data were analyzed by a simple graphical comparison to identify the factors that have a strong impact on yield. Graphs of specific capacity and maximum capacity versus the factors studied were generated. Three factors were identified as having an on yield. As expected, capacity increased with transmissivity, though the data were somewhat sporadic. There was also a positive correlation between capacity and the length of riverbank impacted. An additional analysis revealed that the specific capacities varied in cycles that mirrored the annual temperature variations in the aquifer and river. This analysis is described in detail in the following section.

The impact of the remaining factors was difficult to identify by graphical comparison. The analysis revealed low correlation coefficients and trends opposite of those expected from theory. See the Discussion section for possible causes of the poor correlations between yield and the remaining factors.

7.8 Affect of Temperature Variation on Specific Capacity

The temperature of the water in the river and aquifer controls the viscosity of water as it passes from the river through the riverbed and aquifer to the

well. It is important to consider the effects of temperature on yield in RBF systems. Hubbs previously demonstrated the strong correlation between temperature and specific capacity at the study location in Louisville, KY adjacent to the Ohio River (2002). Water utilities at three of the study locations provided data necessary to repeat for those systems the analysis performed by Hubbs on the Louisville system. The data needed for the analysis included river level, well water level, production rates, and temperature data for the aquifer and/or river.

Hubbs used operational data from the Louisville Water Company for the period from the beginning of well operation in June 1999 to January 2003. The data showed nearly four years of annual temperature and specific capacity cyclic curves. The specific capacity data showed a strong correlation with temperature. The study also indicated a loss of specific capacity over the study period. Hubbs attributed the loss of specific capacity to clogging in the river. Experience from other systems had shown that the effects of clogging tend to stabilize over time. The results of his study are presented in Figure 14. As seen in the figure, well temperatures varied from 2 to 30 degrees Celsius and specific capacity varied from as high as 11,000 m^2/day at the beginning of the study to a low of 4,000 m^2/day at the end of the study.

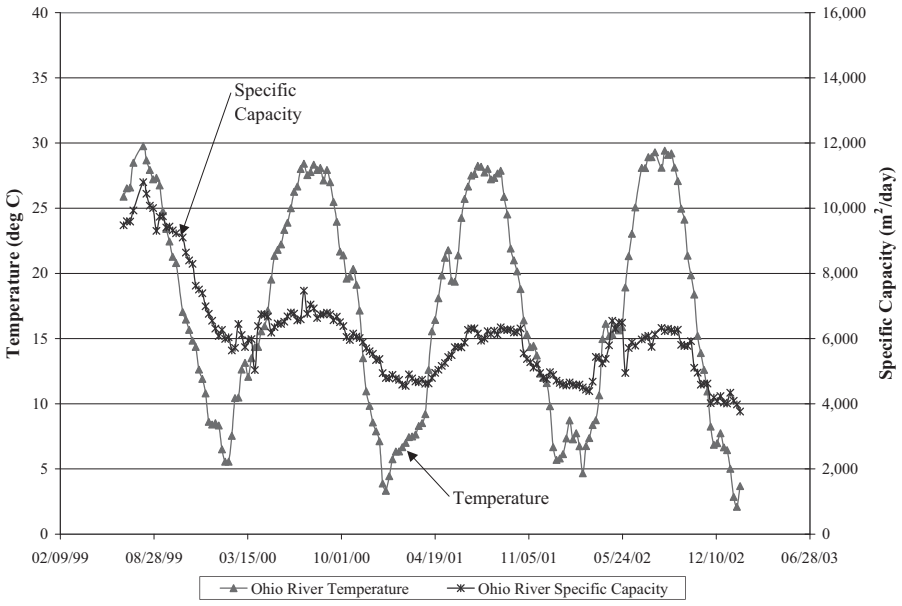

Figure 9. Ohio R. Specific Capacity and Temperature

The Des Moines Water Works (DMWW) provided data for the period from October 2001 to December 2002 for the five radial collector wells at the study site adjacent to the Raccoon River in Des Moines, IA. The data were taken less frequently than those used in Hubbs' study. Data were not provided for the horizontal well. Drawdown and production information was available for each of the five radial collector wells. The total production and average drawdown for the five wells was used to calculate a bulk specific capacity for the entire wellfield. The river temperature varied between 29 and 2 degrees Celsius. The bulk specific capacity ranged from 10,000 and 27,000 m^2/day. A strong correlation between specific capacity and temperature was evident even though the dataset was small. A regression analysis between bulk specific capacity and temperature yielded a regression coefficient (R^2) of 0.7. Specific capacity and temperature data for the Raccoon River are presented in Figure 10.

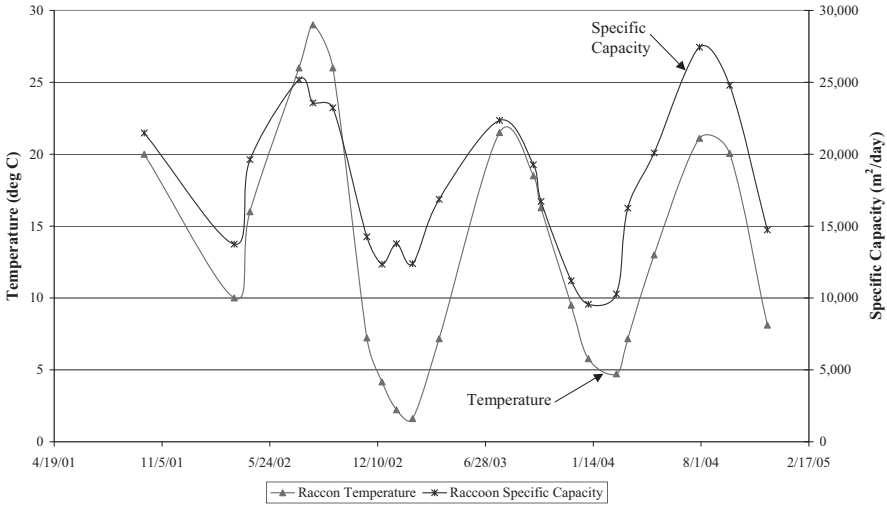

Figure 10. Raccoon R. Specific Capacity and Temperature

The City of Lincoln provided data for the two radial collector wells that are located on an island in the Platte River in Ashland, Nebraska. Data for the first well, well 90-1, consisted of 18 data points for the period from September 2003 to September 2004. Data for the second well, well 90-2, consisted of 12 data points for the period from December 2003 to September 2004. A regression analysis using the data from well 90-1 revealed a significant correlation between specific capacity and temperature with a regression coefficient (R^2) of 0.54. A similar analysis for well 90-2 yielded a regression coefficient near zero. The poor correlation between specific capacity and temperature at well 90-2 might have been the result of the

limited dataset or the influence of pumping from nearby wells. Specific capacity and temperature data for well 90-1 are presented in Figure 11.

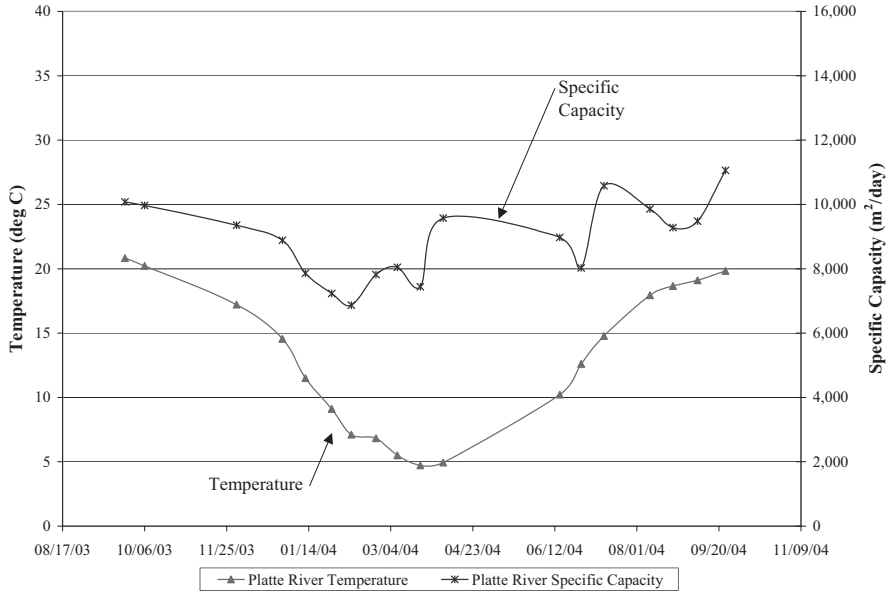

Figure 11 . Platte R. Specific Capacity and Temperature

The Kansas City Board of Public Utilities (KC BPU) provided data for the radial collector well adjacent to the Missouri River in Kansas City, Missouri. The dataset consisted of 29 data points for the period from October 2002 to November 2004. Well temperatures varied between 9 and 26 degrees Celsius while river temperatures varied from 0 to 29 degrees Celsius. The specific capacity ranged from 15,000 to 26,000 m^2/day. The influence of well temperature on specific capacity was more significant than the influence of river temperature. A regression analysis of the data produced a correlation coefficient of (R^2) 0.81 between well temperature and specific capacity. Specific capacity and well temperature data for the study site in Kansas City, Missouri is presented in Figure 12.

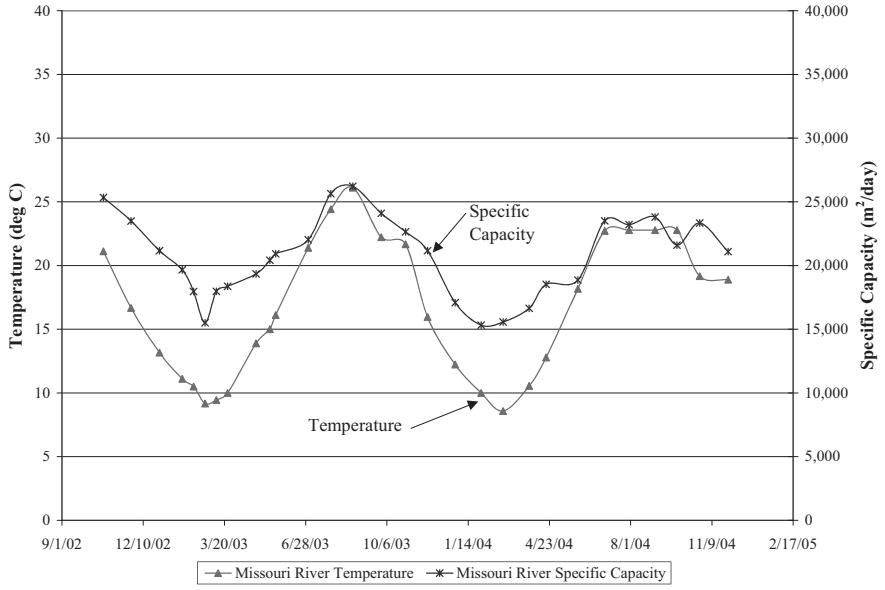

Figure 12. Missouri R. Specific Capacity and Temperature

The affect of temperature variation on specific capacity was evident for all four systems for which data needed to perform the analysis were available. The specific capacity varied in cycles that mimicked the annual temperature variations. The specific capacity was plotted versus temperature. This graph is shown as Figure 13. As seen in the figure, the specific capacity exhibited a nearly linear relationship with temperature. This confirms that water temperature has an important impact on yield in RBF systems.

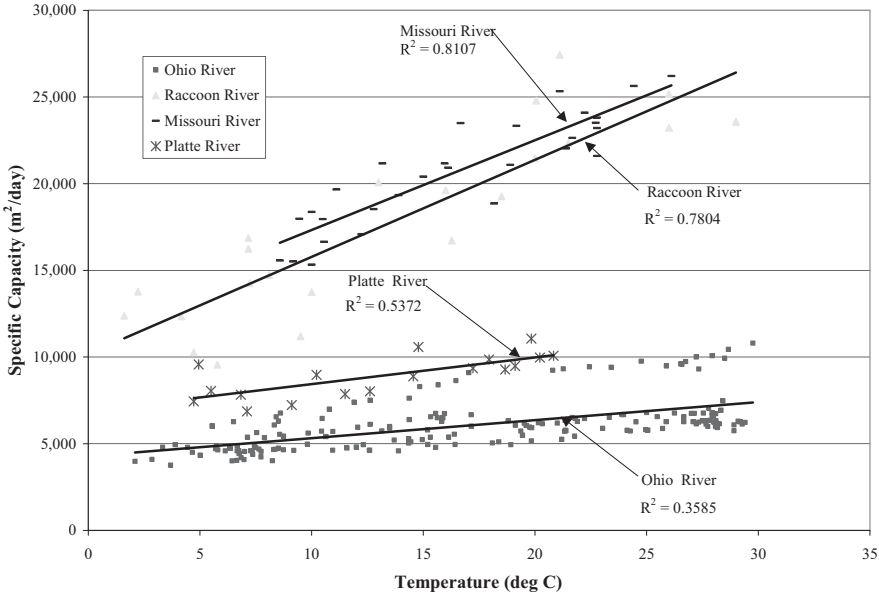

Figure 13. Specific Capacity and Temperature

8. DISCUSSION

The riverbank filtration systems included in this study were located in the middle to lower reaches of the rivers. These locations seemed to provide the right combination of aquifer size, river size, and river slope needed to support a riverbank filtration system. Locations in the upper reaches of rivers are normally not feasible locations for RBF wells because the aquifers at these locations tend to be too small to support the systems. Conversely, locations in the extreme lower reaches of rivers are sometimes infeasible for RBF because of near zero slopes and estuarine influences. The slope is considered a limiting factor because it characterizes the shear stress between the river and riverbed. When the shear stresses are too low to resuspend particles that clog the riverbed medium, high capacity riverbank filtration systems are typically not sustainable. However, successful applications of riverbank filtration in estuary reaches of rivers do exist.

A RBF system was constructed in the lower reaches of the Hudson River near Albany, NY. This system failed to produce near its design capacity. Though limited information was available, two obvious distinguishing factors between the system on the Hudson River and the

successful systems included in the study were the slope and the location relative to the Hudson River Estuary. The system was located in a section of the river with a near zero slope, just upstream of the limits of the saltwater influence from the estuary. The profile of the Hudson River was graphed together with the profiles of shorter rivers included in the study in Figure 14. As seen in the figure, there is a dramatic difference between the slope at the location of the RBF system on the Hudson River and the river slopes at the locations included in the study. Both the location of the RBF system that failed to produce near its design capacity and the location of a site downstream where RBF is being considered are shown on the graph. Since both locations are in extremely flat sections of the river, there is cause for concern that some of the problems that inhibited production at the upstream location might be encountered in the downstream location. The Hudson River example tends to support the hypothesis that a certain slope is needed to support RBF.

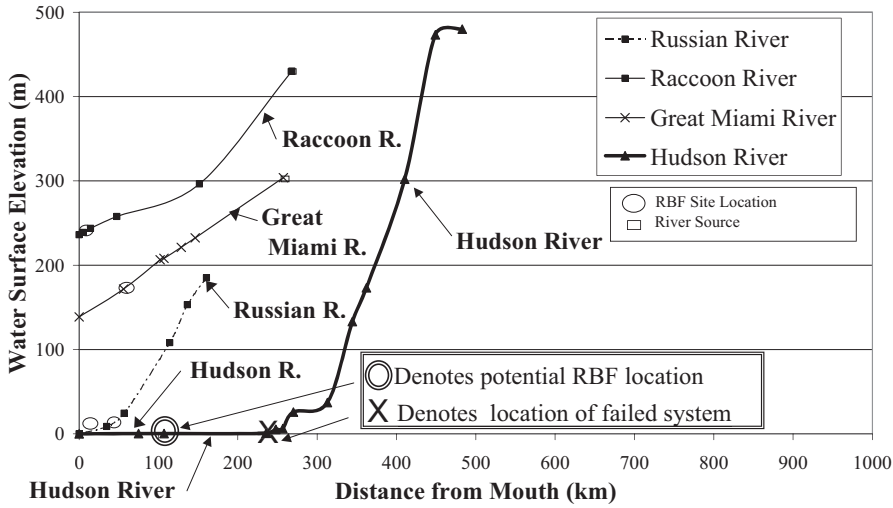

Figure 14. Water Surface Profile of the Hudson River

The analysis of data provided in this study represents one of the first attempts to characterize the factors that affect yield in RBF systems. The data from the systems show that RBF has been applied successfully in aquifers with cross-sectional areas ranging from 4000 m^2 to 140,000 m^2 and transmissivities ranging from 2,000 m^2/day to 18,000 m^2/day. The average river discharges ranged from 20 m^3/day to 3000 m^3/day and water surface slopes that ranged from 0.04 to 1.8 m/km. While these ranges provide some

insight into the variety of conditions in which RBF can be utilized, applications of these data are limited because of the sparse number of systems and the variety of data sources utilized for the study. All the sites studied were locations of successful application of RBF. Data from failed systems would provide valuable insights into the limiting values of aquifer parameters, river hydrology/hydraulics, water quality, system geometry, and riverbed characteristics. However, data from such systems are not readily available.

It was difficult to differentiate among the impacts that many of the factors had on yield. The ambiguity likely was due to the interdependence of the factors and the limited dataset that was analyzed. For example, capacity tended to increase as the distance from the river to the wellfield increased. This result was opposite to what was indicated by theory. However, the wellfields that were located far from the river were supported by highly transmissive aquifers. Thus, the high transmissivity probably masked the relationship between the distance to the aquifer and specific capacity.

The study was successful in demonstrating the influence of the transmissivity of the aquifer, the length of river impacted, and the temperature of the water in the river and well on yield from RBF systems. The impact of temperature on yield should be considered in the design and operation of all RBF systems. The specific capacities of the systems on the Ohio, Raccoon, Platte, and Missouri Rivers are shown for the minimum, average, and maximum temperatures in Table 16. All the systems analyzed showed a significant variation in specific capacity with temperature. The specific capacity of the system on the Raccoon River more than doubled as the temperature cycled from its minimum to maximum values. This doubling demonstrates the importance of considering the water temperature when evaluating a possible RBF location and choosing the dates of a pump test. A test performed when the infiltrating water temperature is highest could severely overestimate the average yield for a proposed system.

Table 17. Specific Capacity and Temperature

	Temperature (deg C)				Specific Capacity		
River	Min	Avg.	Max	Location	Min .	Avg.	Max
Ohio	2	17	30	River	4000	5000	6000
Raccoon	2	13	29	River	10000	18000	27000
Platte	5	13	21	Well	7000	8000	11000
Missouri	9	17	26	Well	15000	24000	26000

9. CONCLUSIONS

More and more utilities are implementing RBF for improved source water quality. Thus, the need for better methods of predicting yield in RBF systems is great. The processes that affect yield in riverbank filtration systems are too complex and variable to be completely understood using analyses based on theoretical considerations. The tables generated in this study were developed to demonstrate the differences among sites and to facilitate the transfer of experience. Though this study was limited to a small subset of the RBF systems in use, it demonstrated that RBF has been implemented successfully in a variety of complex conditions.

Traditionally, yield projections have been made based on short-term pumping tests (see Hubbs, Chapter 10). However, many systems operate as projected initially, and then experience a decline in yield during the first few years of operation before the systems stabilize. Thus, when projections are made from short-term pumping tests, the long-term yield should be expected to be significantly lower than the pumping tests indicates.

The data for each RBF system included in this study can be compared with the operational performance at each site to aid in the identification of factors affecting yield. This study demonstrated that yield in RBF systems is impacted by aquifer transmissivity, length of riverbank impacted, and temperatures in the aquifer and river. A strong correlation was developed between specific capacity and the temperature of water in the RBF aquifer. However, the affects of other parameters such as river discharge and river water quality measures were differentiated by means of simple correlations. This uncertainty probably was due to limitation in the number of sites studied and interdependencies among factors.

Further analysis is recommended to investigate how all the factors collectively affect the operational performance. The author hypothesizes that stochastic techniques can be applied to the data presented in this study to establish an empirical relationship among commonly available parameters and expected performance. Data from additional sites would be expected to improve the accuracy of the results. Such an analysis is recommended; it would enable the assessment of capacity and feasibility of RBF at individual sites by utilizing data unique to each site.

ACKNOWLEDGEMENTS

The research described in this document was completed through the cooperation of the Louisville Water Company, the University of Louisville, and the United States Geological Survey in a research project jointly funded by the Louisville Water Company, the United States Geological Survey, and the American Water Works Association Research Foundation.

The efforts of numerous individuals contributed to the completion of this study. The author would like to acknowledge the utilities, organizations, and individuals that provided the data that formed the basis for this study:

Louisville Water Company, Louisville, KY
Ohio River Valley Water Sanitation Commission, Louisville, KY
Greater Cincinnati Water Works, Cincinnati, OH
Sonoma County Water Agency, Sonoma Co., CA
United States Geological Survey, Louisville, KY
Kansas City Board of Public Utilities, Kansas City, KS
Kansas City Water Services, Kansas City, MO
Des Moines Water Work, Des Moines, IA
City of Lincoln, Lincoln, NE
Collector Wells International, INC.
Stephen Hubbs, Louisville, KY
Jim Constantz, Menlo Park, CA
Matthew Damos, Sonoma County, CA
Don Seymour, Sonoma County, CA
William Gollnitz, Cincinnati, OH
Bruce Whitteberry, Cincinnati, OH
Jurgen Schubert, Dusseldorf, Germany
Jordi Martín-Alonso, Barcelona, Spain
Bernhard Wett, Innsbruck, Austria
Durward Johnson, Kansas City, MO
Eric Lee, Lincoln, NE
Ted Corrigan, Des Moines, IA

The author would also like to acknowledge the guidance of Dr. Joseph Hagerty of the University of Louisville in Louisville, KY who served as the author's academic advisor and Stephen Hubbs of Louisville, KY, who participated in the research. The advice and input of Stephen Hubbs helped develop the ideas presented in this paper. He provided guidance throughout the research effort and aided in the completion of the study by visiting sites, establishing contacts, and planning research.

REFERENCES

Baveye P (2004) The bioclogging of porous media: Overview and relevance to riverbank filtration. Presented at NATO Advanced Research Workshop, Samorin, Slovakia. September 7-10, 2004.

Bouwer E, Weiss W, O'Melia C, and Ball, W (2003) Using Riverbank Filtration to Improve Water Quality. Presented at EPA/USGS Meeting on Cryptosporidium Removal by Bank Filtration. Reston, VA. September 9-10, 2003. [Online]. Avilable: <http://es.epa.gov/ncer/publications/meetings/9-9-2003/pdf/edward_bouwer.pdf>. [Cited March 1, 2005].

Beatsch D <donnab@orsanco.org> (2005) Water Quality Data Request for Louisville. Email to Tiffany Caldwell <tiffany.caldwell@gmail.com>.

Collector Wells International, INC (2005) Services-Specialty Expertise. [Online]. Available: <http://www.collectorwellsint.com/services.htm>. [Cited March 1 2005].

Collins M (2004). Comparing Experiences Between Slow Sand And Riverbank Filtration: The Role of the Schmutzdecke. Presented at NATO Advanced Research Workshop, Samorin, Slovakia. September 7-10, 2004.

Constantz J (2004) Use of Heat as a Tracer for Examining Streambed Conductance at the Russian River RBF Site, Sonoma County, California. Presented at NATO Advanced Research Workshop, Samorin, Slovakia. September 7-10, 2004.

Cox M, and Hatch C (2003) Water Temperature, Streamflow, and Ground-Water Elevation in and Adjacent to the Russian River between Hopland and Guerneville CA from 1998-2002. *USGS Open File Report 03-454.* Prepared in Cooperation with the Sonoma County Water Agency. [Online]. Available: <http://water.usgs.gov/pubs/of/2003/ofr03-454/ >. [Cited June 30, 2004]

Engesgaard P (2004) Bioclogging of Porous Media: Tracer Studies. Presented at NATO Advanced Research Workshop, Samorin, Slovakia. September 7-10, 2004.

Entrix, INC. (2004) Russian River Biological Assessment. [Online]. Available: <http://www.spn.usace.army.mil/ets/rrsection7>. [Cited March 1, 2005].

Gollnitz, W (2003) Induced Infiltration Rate Variability and Water Quality. Presented at EPA/USGS Meeting on Cryptosporidium Removal by Bank Filtration. Reston, VA. September 9-10, 2003. [Online]. Available: <http://es.epa.gov/ncer/publications/meetings/9-9-2003/pdf/william_gollnitz.pdf.> [Cited November 10, 2004].

Gollnitz W, Whitteberry B, and Vogt J (2004) Riverbank filtration: Induced Infiltration and Groundwater Quality. *Journal AWWA*. December 2004. 98-110.

Gollnitz W, Clancy J, Whitteberry B, and Vogt J (2003) RBF as a Microbial Treatment Process. *Journal AWWA*. December 2003. 56-66.

Grischek T (2004) Effects of Clogging on Groundwater Flow and Portion of Abstracted Bank Filtrate. Presented at NATO Advanced Research Workshop, Samorin, Slovakia. September 7-10, 2004.

Henson J, Obrist J, and Prior K (undated). Two Wells Yield 35 mgd: Lincoln's Wellfield Expansion.

Horizonal collectors wells for urban water supply. (1998. *Water Water and Environmental Engineering,* July 1998: 27-28.

Hubbs S (2004) Forces on the Riverbed. Presented at NATO Advanced Research Workshop, Samorin, Slovakia. September 7-10, 2004.

Hubbs, S (2002) Defining Sediment Transport in the Ohio River at Louisville In the Context of Impact of Yield from Bank Filtration Systems.

Hubbs S, (2004) Clogging in Louisville. Presented at NATO Advanced Research Workshop, Samorin, Slovakia. September 7-10, 2004.

Jasperse, J, and Beach, R (2000) An Analysis of the Water Production Capacity of the Sonoma County Water Agency Diversion Facilities Without the Diversion Dam. Prepared in Cooperation with the Sonoma County Water Agency. 09/2000.

Johnson D <DJohnson@bpu.com> (2005) RE: Horizontal Collector Well Information. Email to Tiffany Caldwell <tiffany.caldwell@gmail.com>.

Kansas City Board of Public Utilities. 2004. Water Quality Report. [Online]. Available: <http://www.bpu.com/documents/mineraldata/mineraldata2/water_report.pdf> [Accessed October 22, 2004].

Knighton D (1998) Fluvial Form & Processes. New York, NY: Oxford University Press, Inc.

László F (2004) The Hungarian Experience with Riverbank Filtration. Presented at NATO Advanced Research Workshop, Samorin, Slovakia. September 7-10, 2004.

Lee E<Elee@ci.lincon.ne.us> (2004) Data for RBF Project. Email to Tiffany Caldwell <tiffany.caldwell@louisville.edu>.

Lee E <Elee@ci.lincon.ne.us> (2005) Re: Riverbed conductivity data. Email to Tiffany Caldwell <tiffany.caldwell@gmail.com>.

Macheleidt W (2004) Determination of hydraulic conductivity of riverbeds. Presented at NATO Advanced Research Workshop, Samorin, Slovakia. September 7-10, 2004.

Martín-Alonso J < jma@agbar.es> (2005) Re: Riverbed Conductivity Data. E-mail to Tiffany Caldwell <tiffany.caldwell@louisville.edu>.

Martín-Alonso J (2004a) Managing Resources in an European Semi-arid Environment: Combined Use of Surface and Groundwater for Drinking Water Production in the Barcelona Metropolitan Area. Presented at NATO Advanced Research Workshop, Samorin, Slovakia. September 7-10, 2004.

Martín-Alonso J < jma@agbar.es> (2004b) Re: Data for RBF sites in Spain. E-mail to Tiffany Caldwell <tiffany.caldwell@louisville.edu>.

Martín-Alonso J <jma@agbar.es> (2004c) Re: Questions about Llobregat River site. E-mail to Tiffany Caldwell <tiffany.caldwell@louisville.edu>.

Martín-Alonso J < jma@agbar.es> (2004d) Re: Re: Data for RBF sites in Spain. E-mail to Tiffany Caldwell <tiffany.caldwell@louisville.edu>.

Martin M <Mmartin@ci.lincoln.ne.us> (2005) Additional data request. E-mail to Tiffany Caldwell <tiffany.caldwell@louisville.edu>.

Mucha R, Rodák D, Hlavatý Z, and Banský L (2004) Impact of riverbed clogging on ground water. Presented at NATO Advanced Research Workshop, Samorin, Slovakia. September 7-10, 2004.

National Water Research Institute (2005) The Third International Riverbank Filtration Conference. [Online]. Available: <http://216.133.236.158.asp.sp.asp?main=m3&sub=s4&id=3>. [Accessed January 15, 2005].

National Weather Service (2004) River Forecast Center. [Online]. Available: <http://www.crh.noaa.gov/ahps/rfc.php> [Accessed October 22, 2004].

Pearson Education (2004) Rivers of the United States (350 or more miles long). Available: <http://infoplease.com/ipa/a0001800.html> [Accessed October 22, 2004]

Ray C and Henning P (2004) Clogging-Induced Flow and Chemical Transport Simulation in RBF Systems. Presented at NATO Advanced Research Workshop, Samorin, Slovakia. September 7-10, 2004.

Schafer D (2004) Use of Aquifer Testing and Groundwater Modeling to Evaluate Aquifer/River Hydraulics at Louisville Water Company, Louisville, Kentucky, USA.

Presented at NATO Advanced Research Workshop, Samorin, Slovakia. September 7-10, 2004.

Schafer D (undated) Use of Aquifer Testing and Groundwater Modeling to Evaluate Aquifer/River Hydraulics at Louisville Water Company, Louisville, Kentucky, USA.

Schmidt C, Lange F, Brauch H, and Kuhn W. (2003) Experiences with riverbank filtration and infiltration in Germany. *Proceedings International Symposium of Artificial Recharge of Groundwater.* 11/14/2003, Daejon, Korea, 115-141. [Online]. Available: <http://www.tzw.de/pdf/bankfiltation.pdf>. [cited October 20, 2004]

Schubert J (2002) Hydraulic aspects of riverbank filtration – field studies. *Journal of Hydrology*. 266(2002) 145-161.

Schubert J <juschubert@mac.com> (2004) Re: Data for workshop chapter. E-mail to Tiffany Caldwell <tiffany.caldwell@louisville.edu>.

Sheets R, Darner R, and Whitteberry B (2002) Lag times of bank filtration at a well field, Cincinnati, Ohio, USA. 1998. *Journal of Hydrology,* 266 (2002): 162-174.

Schoenheinz D (2004) Water Quality Changes of the Elbe River and bank filtrate following extreme flooding. Presented at NATO Advanced Research Workshop, Samorin, Slovakia. September 7-10, 2004.

Sonoma County Permit and Resource Management Department and Sonoma County Water Agency (2001) Sonoma County Aggregate Resources Management Plan 1997 and 198 Monitoring Program Results: Russian River, Sonoma County, California.

Stadtwerke Düsseldorf, AG. (2005) Fresh Drinking Water Round the Clock. [Online]. Available: <http://www.swd-ag.de/download/broschueren/trinkwasser_frisch_engl.pdf>/ [cited February 24, 2005].

Stuyfzand P, Juhàsz-Holterman M and Lange, W (2004) Riverbank filtration in the Netherlands: well fields, clogging and geochemical reactions. Presented at NATO Advanced Research Workshop, Samorin, Slovakia. September 7-10, 2004.

Tufenkji N, Ryan J, and Elimelech M (2002) The Promise of Bank Filtration: A simple technology may inexpensively clean up poor raw quality surface water. *Environmental Science & Technology.* 11/1/2002 423-4028.

USACE (2004) Missouri River Region Yearly River Bulletin. Available: <http://www.nwd-mr.usace.army.mil/rcc/report/reports.html> [Accessed August 8, 2004]

USGS (2004) NWISWeb Data for a Nation. [Online]. Available: <http://waterdata.usgs.gov/nwis> [Accessed October 22, 2004].

Wang J, Hubbs S and Song R (2002) Evaluation of Riverbank Filtration as a Drinking Water Treatment Process. Louisville, Kentucky: AwwaRF and AWWA.

Wett B (2004a). Monitoring clogging after start-up of a RBF-system at the River Enns, Austria. Presented at NATO Advanced Research Workshop, Samorin, Slovakia. September 7-10, 2004.

Wett B <Bernhard.Wett@uibk.ac.at> (2004b) Re: A couple of questions about the RBF site on the River Enns. E-mail to Tiffany Caldwell <tiffany.caldwell@louisville.edu>.

Wett B <Bernhard.Wett@uibk.ac.at> (2005) Re: Riverbed conductivity data. Email to Tiffany Caldwell <tiffany.caldwell@gmail.com>.

Whitteberry B, and Gollnitz W (2003) Riverbank Filtration at the Charles M. Bolton Well Field Organic and Particle Reduction. Reston, VA. September 9-10, 2003. [Online]. Available: <http://es.epa.gov/ncer/publications/meetings/9-9-2003/pdf/bruce_whitteberry.pdf. [Cited January 14, 2005].

WorldAtlas.Com (2005) Major Rivers: Europe. [Online]. Available: <http://www.worldatlas.com/webimage/country/euriv.htm>. [Cited March 1, 2005].

Yongstrom G <gregy@orsanco.org.> (2005) Water Quality Data for Ohio River at Louisville. Email to <tiffany.caldwell@gmail.com>.